Brain connectivity and cognitive impairment in Parkinson's disease

Hugo César Baggio

Universitat de Barcelona

Brain connectivity and cognitive impairment in Parkinson's disease

Thesis presented by

Hugo César Baggio

to obtain the degree of doctor
from the University of Barcelona in accordance
with the requirements of the international
PhD diploma

Supervised by

Dr. Carme Junqué i Plaja

Faculty of Medicine, University of Barcelona
Medicine Doctoral Program

2014

The studies presented in this thesis were performed at the Neuropsychology Group, Department of Psychiatry and Clinical Psychobiology, University of Barcelona.

Funding for these studies was provided by a the Generalitat de Catalunya, by the Spanish Ministry of Science and Innovation, and CIBERNED.

Barcelona, 03 September 2014

Carme Junqué i Plaja, Professor at the University of Barcelona,

Certifies that she has guided and supervised the doctoral thesis entitled *Brain connectivity and cognitive impairment in Parkinson's disease* presented by Hugo César Baggio. She hereby asserts that this thesis fulfills the requirements to present his defense to be awarded the title of Doctor.

Signature,

Dr. Carme Junqué i Plaja

CONTENTS

FOREWORD

Sporadic Parkinson's disease (PD), an idiopathic chronic progressive neurological disease with several motor and non-motor features, is the second most common neurodegenerative disease after Alzheimer's disease.

The negative impact of PD is manifold. It represents a significant economic burden on health services and on individuals that is only expected to grow as the world population ages. Mortality in PD patients is uniformly described to be higher than in the general population. Importantly, the major impact of PD on quality of life reveals the relevance of its spectrum of manifestations. Motor, autonomic, psychiatric and cognitive symptoms place a heavy burden on both patients and their caregivers.

Considerable progress has been made in the symptomatic treatment of motor and some non-motor symptoms of PD since the introduction of levodopa in the late nineteen sixties. The same cannot be said about cognitive impairments. It is vital that we try to gain more knowledge about the pathophysiology of cognitive decline in PD so as to define potential future therapeutic targets and identify candidates for early, potentially disease-modifying treatments.

This thesis represents an attempt to characterize the mechanisms underlying cognitive impairments in PD through advanced neuroimaging techniques. The theoretical framework on which it is based is that the human brain is a complex network made up of functionally specialized regions, and that normal cognition relies on their coordinated activity. Normal coordinated activity, in turn, depends on the integrity of these functional subunits and of the lines of communication between them. Neuroimaging techniques based on this framework can help us gain insight into the disease process; additionally, by shedding light on the relationship between brain organization and function, they can help us learn more about the underpinnings of normal cognition.

This thesis is presented for the degree of Doctor by the University of Barcelona, and is the result of the work carried out over four years at the Department of Psychiatry and Clinical Psychobiology of the University of Barcelona. During this period, I have obtained the degree of Master of Neuroscience, linked to the Doctorate in Medicine Program (Quality Mention MCD2008-00023; Mention Towards Excellence MEE2011-0316) at the University of Barcelona.

This four-year work resulted in the production of the seven scientific papers listed below. Five of these papers have been published and one is accepted for publication in international indexed journals. The last paper is currently under review in an indexed journal.

- Baggio HC, Segura B, Sala-Llonch R, Marti MJ, Valldeoriola F, Compta Y, Tolosa E, Junqué C. *Cognitive impairment and resting-state network connectivity in Parkinson's disease*. Human Brain Mapping 2014 DOI: 10.1002/hbm.22622 (in press). IF (2013): 6.924. Q1.

- Segura B, Baggio HC, Marti MJ, Valldeoriola F, Compta Y, Garcia-Diaz AI, Vendrell P, Bargallo N, Tolosa E, Junqué C. *Cortical thinning associated with mild cognitive impairment in Parkinson's disease*. Movement Disorders 2014 DOI: 10.1002/mds.25982. IF (2013): 5.634. Q1.

- Baggio HC, Sala-Llonch R, Segura B, Marti MJ, Valldeoriola F, Compta Y, Tolosa E, Junqué C. *Functional brain networks and cognitive deficits in Parkinson's disease.* Human Brain Mapping 2014, 35:4620-34. IF (2013): 6.924. Q1.

- Segura B, Ibarretxe-Bilbao N, Sala-Llonch R, Baggio HC, Martí MJ, Valldeoriola F, Vendrell P, Bargalló N, Tolosa E, Junqué C. *Progressive changes in a recognition memory network in Parkinson's disease.* Journal of Neurology Neurosurgery and Psychiatry 2013, 84:370-8. IF (2013): 5.58. Q1.

- Ibarretxe-Bilbao N, Junqué C, Segura B, Baggio HC, Marti MJ, Valldeoriola F, Bargallo N, Tolosa E. *Progression of cortical thinning in early Parkinson's disease.* Movement Disorders 2012, 27:1746-53. IF (2012): 4.558. Q1.

- Baggio HC, Segura B, Ibarretxe-Bilbao N, Valldeoriola F, Marti MJ, Compta Y, Tolosa E, Junqué C. *Structural correlates of facial emotion recognition deficits in Parkinson's disease patients.* Neuropsychologia 2012, 50:2121-8. IF (2012): 3.477. Q1.

- Baggio HC, Segura B, Garrido-Millán JL, Marti MJ, Compta Y, Valldeoriola F, Tolosa E, Junqué C. *Resting-state frontostriatal functional connectivity in Parkinson's disease-related apathy*. Submitted.

GLOSSARY OF ABBREVIATIONS

ACC	anterior cingulate cortex
AD	Alzheimer's disease
AS	Starkstein's apathy scale
BDI	Beck Depression Inventory-II
BNT	Boston Naming Test
BOLD	blood-oxygen level-dependent
COMT	cathecol-O-methyltransferase inhibitor
CSF	cerebrospinal fluid
CTh	cortical thickness
DAN	dorsal attention network
DBS	deep-brain stimulation
DMN	default mode network
DTI	diffusion tensor imaging
EEG	electroencephalography
FA	fractional anisotropy
FDR	false-discovery rate
FER	facial emotion recognition
FLAIR	Fluid-attenuated inversion recovery
fMRI	functional magnetic resonance imaging
FPN	frontoparietal network
FWE	familywise error rate
FWHM	full width at half maximum
GM	gray matter
HC	healthy control
HY	Hoehn and Yahr scale
ICA	independent component analysis
ICDs	impulse control disorders
ICN	resting-state intrinsic connectivity network
JLO	Benton's Judgment of Line Orientation test
LB	Lewy body
LEDD	levodopa equivalent daily dose
LN	Lewy neurite
MAOI	monoamine oxidase B inhibitor
MCI	mild cognitive impairment
MD	mean diffusivity
MDS	Movement Disorder Society
MEG	magnetoencephalography
MNI	Montreal Neurological Institute MNI152 standard template
MRI	magnetic resonance imaging
NPI	Cumming's Neuropsychiatric Inventory
OFC	orbitofrontal cortex
PCC	posterior cingulate cortex
PD	Parkinson's disease
PD-A	Parkinson's disease patients with apathy
PDD	Parkinson's disease-related dementia
PD-MCI	Parkinson's disease patients with mild cognitive impairment
PD-NMCI	Parkinson's disease patients without mild cognitive impairment
PD-NA	Parkinson's disease patients without apathy
PET	positron emission tomography
PFC	prefrontal cortex
RAVLT	Rey's Auditory Verbal Learning Test
RBD	rapid-eye-movement behavior sleep disorder
ROI	region of interest
SD	standard deviation

SDMT	Symbol Digits Modalities Tests
SNR	signal-to-noise ratio
TE	echo time
TMT A-B parts	difference between Trail Making Test A and B
TMT-A	Trail-Making Test, part A
TMT-B	Trail-Making Test, part B
TR	repetition time
UPDRS	unified Parkinson's disease rating scale
VBM	voxel-based morphometry
VFD	Benton's Visual Form Discrimination test
VTA	ventral tegmental area
WM	white matter

chapter 1
GENERAL INTRODUCTION

PD NEUROPATHOLOGY

general aspects

Susceptible neurons in Parkinson's disease (PD) patients show eosinophilic perikaryal inclusions known as *Lewy bodies* (LB) and thread-like formations located in the neuronal processes, the *Lewy neurites* (LN) [Braak et al., 2003]. LB and LN are characterized by the accumulation of filamentous protein inclusions, the main component of which is phosphorylated, ubiquitinated and acetylated insoluble α-synuclein [Anderson et al., 2006]. The aggregation of abnormal α-synuclein is considered to precede the formation of these inclusions, and LN possibly antecede LB [Stefanis, 2012]. The factors that trigger the cascade of events that culminates with α-synuclein misfolding, loss of function and aggregation is not fully understood. Nonetheless, genetic mutations and animal models of α-synuclein overexpression suggest that, besides being a diagnostic marker as a component of these abnormal aggregates, this synaptic protein is primarily involved in neuronal dysfunction and death [Stefanis, 2012]. Indeed, even small elevations in wild-type α-synuclein appear to be sufficient to cause disease [Chartier-Harlin et al., 2004; Ikeuchi et al., 2008]. It is also hypothesized that it may, in its toxic misfolded forms, contribute to disease propagation in a *prion-like* fashion [Marques and Outeiro, 2012; Olanow and Brundin, 2013]. Giving strong support to these hypotheses, a recent study demonstrated that the intranigral/intrastriatal inoculation of LB-derived pathological α-synuclein – obtained from postmortem PD brains – was capable of triggering a PD-like pathological process in mice and monkeys [Recasens et al., 2014].

The mechanisms through which the aggregation of α-synuclein leads to cell dysfunction and death are not completely understood. α-synuclein is highly localized in the presynapses [Maroteaux et al., 1988], and its abnormal deposition begins and is most marked at the presynaptic terminals [Schulz-Schaeffer, 2010]. Presynaptic failure, with reduced neurotransmitter synthesis, storage, release and transporter binding, has been demonstrated in PD [Nikolaus et al., 2009], suggesting that disease-related deficits occur before neuronal death. Other findings give support to the notion that axonal pathology precedes soma degeneration [Dauer and Przedborski, 2003]. Distal axon loss in cardiac sympathetic neurons – affected early in the course of PD – has been shown to antecede cell death; additionally, α-synuclein deposition in these distal axons predicts these neurons' centripetal degeneration [Orimo et al., 2005; Orimo et al., 2008]. These findings have led some authors to propose that PD degeneration begins in the axons and includes impaired synaptic function and connectivity [Burke and O'Malley, 2013; O'Malley, 2010].

PD is not just dopamine

The vast majority of available data regarding the molecular mechanisms underlying cell dysfunction and death refer to dopaminergic neurons. The degenerative process doesn't begin or end in the dopaminergic system, and we cannot assume that the same pathophysiological processes therein observed apply to other cell types. As non-motor manifestations of PD receive progressively more clinical attention, so must their underlying cellular and molecular changes.

The hallmark of PD neuropathology is the progressive and marked degeneration of pigmented dopaminergic neurons in the substantia nigra pars compacta, associated with the presence of LB and LN. This is not, however, where the disease process begins. In their seminal works, Braak *et al.* and Del Tredici *et al.* [Braak et al., 2003; Del Tredici et al., 2002] have demonstrated that, in most cases of sporadic PD, LB and LN pathology progresses along a caudal-rostral path. According to these authors, the disease process usually begins in the dorsal vagal/glossopharyngeal motor nucleus or the anterior olfactory nucleus, followed by the intermediate reticular formation in the medulla oblongata (stage 1 in the Braak system). Next, pontine nuclei such as the coeruleus/subcoeruleus complex and caudal raphe nuclei are involved (stage 2). Only then is the substantia nigra in the midbrain affected, at stage 3, alongside the amygdala.

Early motor PD is not early PD pathology

This progression model is compatible with the occurrence of premotor symptoms in PD, which can be related to the degeneration of lower brain stem nuclei or olfactory regions at stages 1 and 2, even years before the onset of motor, dopamine deficiency-related symptoms [Tolosa et al., 2009]. Examples of such premotor manifestations are mood disorders, rapid eye movement sleep behavior disorder and dysautonomic symptoms, all of which can be associated with dysfunction of medullary or pontine nuclei, as well as olfactory dysfunction.

At stage 4, most nigral dopaminergic neurons have been lost and the pathologic process extends to the entorhinal cortex and allocortex (CA2-plexus); it also involves non-nigral pigmented mesencephalic nuclei, such as those in the ventral tegmental area (VTA), and the thalamus. Patients with early motor symptoms of PD usually have stage 3 or stage 4 disease [Halliday et al., 2006]. As the disease progresses, LB and LN pathology, extending from the mesocortex, reaches higher order sensory associative neocortical areas. The first regions to be affected, according to this staging system, are the anterior cingulate cortex (ACC), insula and prefrontal cortex (PFC). At stage 6, first order sensory association areas, followed by premotor and finally primary sensory and motor areas are involved, in such a way that nearly the entire neocortex is affected.

PD and the gut

Although pathologic studies point to the lower brainstem or olfactory nuclei as the usual epicenters of CNS α-synucleinopathy, the presence of α-synuclein-containing inclusions in peripheral tissues has been repeatedly demonstrated in PD [Jellinger, 2008]. Furthermore, Shannon *et al.* have recently described the presence of α-synuclein staining in postganglionic cholinergic neurons in the colonic submucosa obtained 2 to 5 years before the diagnosis of PD in 3 patients [Shannon et al., 2012]. Is PD is caused by a pathogenic agent that spreads from cell to cell, that enters the body through the gastrointestinal tract or the olfactory mucosa?

The Braak staging system briefly described above has been shown to be valid and useful [Dickson et al., 2010; Halliday et al., 2006; Parkkinen et al., 2008], although criticism has been made as the model does not explain the cases of advanced LN/LB pathology in the absence of neurological signs, or the lack of relationship between staging and clinical PD severity [Burke et al., 2008; Jellinger, 2009]. Halliday *et al.* found that a subgroup of PD patients, with disease of earlier onset and long duration, had LB distribution compatible with Braak stages. In older-onset patients, on the other hand, findings were not consistent with Braak staging and included higher LB load as well as more mixed pathology [Halliday et al., 2008].

cognitive impairment

The neuropathology of cognitive deficits in PD is currently a matter of debate. Braak *et al.* described that Mini-Mental State Examination (MMSE) scores correlated with Braak staging [Braak et al., 2005]. Along the same lines, Aarsland *et al.* found that LB scores correlated with annual MMSE decline; in this study, demented PD patients had limbic and neocortical LB disease [Aarsland et al., 2005]. Irwin *et al.* found that cortical LN/LB pathology was the most significant correlate of PDD [Irwin et al., 2012]. Ferrer *et al.*, on the other hand, concluded that abnormal α-synuclein at the synapses rather than LB or LN correlated with cognitive impairment [Ferrer, 2011]. Several other studies have found that cortical α-synuclein pathology is an important correlate of dementia in PD (PDD) [Apaydin et al., 2002; Compta et al., 2011; Harding and Halliday, 2001; Hurtig et al., 2000; Irwin et al., 2012].

The frequently described occurrence of a minority of subjects with extensive cortical α-synuclein pathology but no cognitive deficits [Parkkinen et al., 2005] and, conversely, the observation that some PDD patients have little cortical α-synucleinopathy [Braak et al., 2005; Irwin et al., 2012] indicate that this type of pathology may not be necessary or sufficient to cause PDD. In a recent study, Hall *et al.* found that demented PD patients had significantly more pronounced cholinergic neuron loss in the nucleus basalis and decreased cholinergic activity in the hippocampus, as well as more severe α-synuclein pathology in the basal forebrain and hippocampus [Hall et al., 2014]. Other findings also support the involvement of altered dopaminergic, noradrenergic, cholinergic and serotoninergic cortical innervation in cognitive impairment in PD [Ferrer, 2011].

Converging evidence from different studies suggests that another factor is highly relevant for the development of dementia in PD: concurrent Alzheimer's type pathology. The presence of Alzheimer's disease (AD)-type aggregates has been found to correlate with cognitive deficits in PDD [Compta et al., 2011; Jellinger and Attems, 2008]. PDD patients are described to have higher amyloid-β plaques and tau neurofibrillary tangles than non-demented patients [Compta et al., 2011; Irwin et al., 2012; Kempster et al., 2010; Tsuboi et al., 2007]. Recent studies have even suggested that AD-type pathology may be a stronger correlate of PDD than α-synuclein pathology [Compta et al., 2011; Irwin et al., 2012]. In the study by Compta *et al.*, cortical amyloid-β scores were seen to correlate with MMSE scores and with shorter time-to-dementia interval; it was also found that a combined model including amyloid-β, tau and cortical α-synuclein pathology was the most robust correlate of PDD [Compta et al., 2011]. The link between AD-type pathology and PDD is further strengthened by the observation that APOE and MAPT gene variants – respectively associated with amyloid-β aggregates [Ramanan et al., 2014] and tau pathology [Chen et al., 2010] – are associated with cognitive status and risk of dementia in PD patients [Goris et al., 2007; Morley et al., 2012; Williams-Gray et al., 2009]. More than an additive effect, *AD-related (amyloid-β and tau) and α-synuclein aggregates have been proposed to interact synergistically*, facilitating the accumulation of each other, thus contributing to cognitive decline in a subgroup of PD patients [Clinton et al., 2010; Lashley et al., 2008; Tsuboi et al., 2007].

While the relevance of different types of pathology continues to be a matter of debate, it seems possible to conclude that several factors concur in the heterogeneous genesis of PDD. Both synucleinopathy and AD-type disease, in what appears to be a synergistic interaction, contribute to different combinations of cortical and subcortical neuronal dysfunction and death, further complicated by damage to critical neurotransmitter systems.

CLINICAL ASPECTS OF PD

epidemiology

The average age of motor disease onset is around 60 years. Although it can be diagnosed at any age, PD is rare under the age of 40, and its incidence rises steeply after 60 years [de Lau and Breteler, 2006; Wolters and Baumann, 2014]. It is described to be more common in whites [de Lau and Breteler, 2006], and most series include a higher proportion of male than female patients [de Lau and Breteler, 2006; Ropper and Samuels, 2009].

Since the finding in 1983 that the toxin 1-methyl-4-phenyl-1,2,3,6-tetrahydropyridine (MPTP) can induce PD-like symptoms and lead to the selective death of dopaminergic substantia nigra neurons [Langston et al., 1983], studies have investigated the hypothesis that environmental toxins might increase the risk of PD. Exposure to pesticides has been found to increase the odds of developing the disease, although evidence is limited and based on insufficient data [Berry et al., 2010]. Likewise, the possible association of heavy metal exposure and risk of PD is currently inconclusive [de Lau and Breteler, 2006]. On the other hand, tobacco smoking, coffee consumption and use of nonsteroidal anti-inflammatory drugs appear to be protective factors against PD [Ascherio et al., 2001; Hernan et al., 2001; de Lau and Breteler, 2006; Noyce et al., 2012]. Additionally, a minority

of cases of PD is associated with specific mutations, such as the PARK (1, 2, 3, 5, 6, 7 and 8) and NR4A2 gene mutations. The greatest known genetic contributor to PD, however, is the leucine-rich repeat kinase (LRRK2) gene mutations, present in around 1% of cases of PD [Ropper and Samuels, 2009].

diagnosis

Although PD cannot be considered merely a motor disease, its clinical diagnosis depends on the presence of motor signs and symptoms, especially the four cardinal symptoms of *hypokinesia*, *bradykinesia*, *rest tremor* (usually in the 4-6 Hz range) and, at more advanced stages, *postural instability*. Collectively, these manifestations characterize a syndrome called *parkinsonism*, of which sporadic PD is just one of the possible causes. Other neurodegenerative diseases, such as multiple system atrophy, progressive supranuclear palsy and corticobasal degeneration, as well as vascular parkinsonism, repeated trauma, communicating hydrocephalus or certain drugs or toxins, can produce parkinsonian syndromes [Ropper and Samuels, 2009; Wolters and Baumann, 2014]. One important diagnostic factor is the improvement of motor signs and symptoms with levodopa therapy. Unlike idiopathic or genetic PD, other causes of parkinsonism respond poorly and temporarily or are refractory to dopaminergic treatment [Wolters and Baumann, 2014].

The most widely accepted clinical diagnostic criteria – the UK Parkinson's Disease Society Brain Bank Criteria [Daniel and Lees, 1993] – enable the diagnosis of PD in around 80% of the cases [Wolters and Baumann, 2014]. A significant proportion of patients need additional diagnostic procedures. Among them, dopamine transporter single photon emission computed tomography with ^{123}I ioflupane (DaTSCAN) is frequently used; its main role lies in the differentiation of parkinsonism and other causes of tremor, such as essential tremor [Bajaj et al., 2013], and may also help excluding conditions in which nigrostriatal dysfunction is absent, such as drug-induced, psychogenic and vascular parkinsonism [Kägi et al., 2010]. The demonstration of cardiac sympathetic denervation through ^{123}I-metaiodobenzylguanidine scintigraphy may also help in the differential diagnosis between PD or dementia with Lewy bodies and parkinsonian syndromes such as multiple system atrophy and progressive supranuclear palsy [Rascol and Schelosky, 2009].

disease severity – rating scales

To assess disease severity and for quantitative assessment of progression, multi-domain scales are typically used in patient follow-up as well as in research settings. Until recently, the Unified Parkinson's Disease Rating Scale (UPDRS) version 3, published in 1987, was the most commonly used scale [Wolters and Baumann, 2014]. It is composed of four subscales (Section I: mentation, behavior and mood; Section II: activities of daily living; Section III: motor examination; Section IV: complications). It also includes the Hoehn and Yahr scale (see below) and the Schwab and England scale, a measure of disability. The UPDRS shows good inter-rater and test-retest reliability and internal consistency [Siderowf et al., 2002; Wolters and Baumann, 2014].

In 2007, a revised version of the UPDRS sponsored by the *Movement* Disorder Society (MDS) was published in an attempt to overcome the limitations in the original scale [Goetz et al., 2007]. It maintains the original 4-section structure, although sections have been renamed (Section I: non-motor experiences of daily living; Section II: motor experiences of daily

living; Section III: motor examination; Section IV: motor complications). It was recently shown to have good clinimetric characteristics [Goetz et al., 2008].

The motor examination section (Part III) of the unified Parkinson's disease rating scale is the most frequently used measure to assess motor signs in PD [Goetz and Stebbins, 2004]. It comprises 27 scores (or 33 in the revised version) each with five possible scores (0: normal, 1: slight, 2: mild, 3: moderate, 4: severe).

The Hoehn and Yahr staging (HY) is the most widely used scale to classify the evolutionary course of PD [Wolters and Baumann, 2014]. The original version, published in 1965, consists of a 5-point scale: unilateral symptoms (stage 1), bilateral symptoms (stage 2), bilateral symptoms with balance impairment but independent physically (stage 3), severe disability but unassisted walking (stage 4), and confinement to bed or wheelchair if unassisted (stage 5) [Hoehn and Yahr, 1967]. A modified scale with two intermediate stages (1.5 – unilateral + axial symptoms; 2.5 – mild bilateral symptoms with recovery on pull test) is often used [Wolters and Baumann, 2014]. HY scale reliability testing has been limited, but it fulfils some criteria for validity and reliability; according to an MDS Task Force, in research settings it is useful primarily for inclusion/exclusion criteria, and for demographic presentation of patient groups [Goetz et al., 2004]

treatment of parkinsonism

PD is an inexorably progressive and incapacitating disease, although the rates of progression are highly variable [Wolters and Baumann, 2014]. Currently, there are no established disease-modifying or neuroprotective therapies [Connolly and Lang, 2014], let alone a cure. Nonetheless, available therapies can substantially improve signs, symptoms and quality of life [Hickey and Stacy, 2011]. Given the varied nature of motor and non-motor manifestations, a multidisciplinary approach combining neurologic, psychiatric, gerontologic and rehabilitative care is indicated for optimal-level treatment [Worth, 2013].

Pharmacological treatment for motor parkinsonism is complex and needs to be individualized [Wolters and Baumann, 2014]. As there is no strong evidence of available disease-modifying treatments, authors recommend postponing the initiation of drug therapy until the development of disabling or socially cumbersome symptoms [Connolly and Lang, 2014; Worth, 2013]. Monoamine oxidase type B inhibitors (MAOI) are often started early in the disease course, prior to dopamine agonists or levodopa. Some preliminary reports suggested that the MAOI rasagiline could have disease-modifying properties [Olanow et al., 2009; Rascol et al., 2011], a finding not confirmed by additional clinical trial evidence [Connolly and Lang, 2014]. The antiviral amantadine is also sometimes used as symptomatic monotherapy or adjunct therapy. A 2009 Cochrane review concluded, however, that there is insufficient evidence for its efficacy or safety due to the non-controlled nature of the studies supporting its use [Crosby et al., 2003].

When more significant motor symptoms develop, levodopa and/or dopamine agonists are usually started, both of which have proven symptomatic benefits and different side-effect profiles [Connolly and Lang, 2014]. Levodopa, combined with inhibitors of peripheral DOPA-decarboxylase, is still considered the most effective drug for the motor symptoms of PD [Fahn et al., 2004]. The marked initial *honeymoon-period* response to levodopa is

followed, after a variable period, by motor complications such as end-of-dose *wearing-off* and levodopa-induced *dyskinesias*. End-of-dose wearing-off can be reduced by fractionating the levodopa doses; by the introduction of drugs that reduce the degradation of dopamine, such as cathecol-O-methyl transferase (COMT) inhibitors and MAOI; by the introduction of dopamine agonists, or the use of subcutaneous apomorphine as needed [Pahwa et al., 2006; Worth, 2013].

Since dyskinesias are more common in patients with younger age at onset, dopamine agonists are often prescribed to patients under the ages of 50-60 years [Connolly and Lang, 2014; Warren Olanow et al., 2013; Worth, 2013]. The use of adjunctive dopamine agonist therapy, moreover, permits the use of lower doses of levodopa, thus minimizing or reducing the risk of both dyskinesias and wearing-off [Warren Olanow et al., 2013]. Dopamine agonists are not, however, devoid of side effects. Their use is associated with somnolence, hallucinations and impulse control disorders (ICD), among others [Perez-Lloret and Rascol, 2010]. Given that older PD patients have a higher risk of developing psychiatric and cognitive complications, levodopa is usually preferred in this age group [Connolly and Lang, 2014].

As the disease progresses, other treatment options usually become necessary. Therapeutic measures to reduce *off* periods (*i.e.*, periods in which parkinsonian symptoms are not controlled) include the use of continuous subcutaneous apomorphine infusion and continuous infusion of a levodopa/carbidopa gel via jejunostomy [Worth, 2013]. Patients who respond to levodopa but have motor fluctuations, dyskinesias or tremor that cannot be controlled with medical therapy can benefit from deep-brain stimulation (DBS) surgery [Wolters and Baumann, 2014; Worth, 2013]. Candidates for this procedure, who should have no significant cognitive decline or psychiatric symptoms, or any major comorbidities, are a small subgroup of cases, usually patients younger than 70 years, with early-onset PD [Hickey and Stacy, 2011; Morgante et al., 2007; Worth, 2013]. The subthalamic nucleus is the most common target for DBS, although in patients with severe dyskinesias the globus pallidus internus is sometimes selected [Hickey and Stacy, 2011]. DBS drastically improves overall motor function, but can produce motor (*e.g.*, dysarthria, freezing of gait, eyelid apraxia) and non-motor complications. Non-motor psychiatric complications include depression, apathy, or, paradoxically, mania or depression [Czernecki et al., 2008; Starkstein, 2012; Thobois et al., 2010]. Cognitive deficits, mainly related to selective impairments in phonemic and semantic verbal fluency and executive functions, can also be observed [Okun et al., 2009; Witt et al., 2008].

Novel non-dopaminergic treatment strategies are currently being developed, including drugs targeting adenosine, glutamate, adrenergic, and serotonin receptors, as well as calcium channel blockers, iron chelators, anti-inflammatories, neurotrophic factors, and gene therapies [Stayte and Vissel, 2014]. Hopefully, some of them will prove to offer better symptomatic control as well as reduce the rate of disease progression.

COGNITIVE DEFICITS IN PD

Interest in cognitive deficits in PD has grown considerably over the past few years, justified by their high prevalence and potentially devastating impact that contrast with the lack of effective treatments. The prevalence of cognitive deficits in untreated, newly-diagnosed patients has been described to be between 19 and 24% [Aarsland et al., 2009a; Muslimovic et al., 2005]. Despite considerable interindividual variation, the vast majority of PD patients develop cognitive impairments over time, and by 20 years of disease duration up to 90% of patients develop dementia, with a mean time from onset of PD to dementia of 10 years [Aarsland and Kurz, 2010; Hely et al., 1999]. A longitudinal study found that 10% of newly-diagnosed patients had developed dementia after a 5-year follow-up, with an annual dementia incidence of 30 per 1000 person-years [Williams-Gray et al., 2009].

Cognitive deficits in PD are heterogeneous and involve different neuropsychological functions [Tremblay et al., 2013]. The predominant patterns of cognitive impairment vary considerably across studies, probably due to the different tests used and the inclusion of patient samples with different demographic and clinical characteristics. In any case, most studies report on a high prevalence of deficits with putative frontostriatal bases, such as attention and executive functions [Elgh et al., 2009; Muslimovic et al., 2005; Owen, 2004; Williams-Gray et al., 2009], memory [Aarsland et al., 2009a; Muslimovic et al., 2005], psychomotor speed [Aarsland et al., 2009a; Muslimovic et al., 2005] and visuospatial/perceptual abilities [Aarsland et al., 2009a; Boller et al., 1984; Williams-Gray et al., 2009].

Some factors have been found to be associated with the risk of more severe cognitive deficits and dementia. Among them, age is described to be the strongest risk factor [Aarsland et al., 2007b]. Both later disease onset and advanced age are described as risk factors [Emre, 2003]. Indeed, PD patients have significantly faster cognitive decline after 70 years of age [Williams-Gray et al., 2009]. Additionally, age and severity of motor symptoms may have combined effects on the risk of dementia [Levy et al., 2002]. The risk of cognitive decline and dementia is also higher for patients with non-tremor-dominant motor presentation, axial/gait involvement, visual hallucinations, or associated depression or apathy [Aarsland and Kurz, 2010; Dujardin et al., 2009; Emre, 2003; Tremblay et al., 2013; Williams-Gray et al., 2009].

PD and age

Age and PD have a complex interrelation. Not only is the incidence of PD strongly associated with age: ageing is the single most significant factor influencing the clinical presentation, course and progression of PD and PD-related dementia [Aarsland et al., 2007b; Hindle, 2010]. It is hypothesized that, although neurodegenerative processes can begin at any age, suprathreshold dysfunction and faster degeneration would occur when age-related stressor tolerance fails to match the current load of disease-related stressors [Saxena and Caroni, 2011].

The presence of cognitive deficits is also a predictor of future risk of dementia, but the risk varies according to type of deficit: frontostriatal deficits are less related to future conversion to dementia than non-dopaminergic, cortical deficits [Williams-Gray et al., 2007; Williams-Gray et al., 2009].

The dual syndrome

As a neurodegenerative process that affects most of the brain, it is not surprising that PD-related cognitive deficits involve different neuropsychological functions. The analysis of clinical presentation, response to therapy and prognostic implications, however, indicates the existence of two overlapping cognitive syndromes in PD:

1. *Frontostriatal deficits*, mainly related to midbrain α-synuclein pathology and which can be improved or worsened by dopaminergic treatments [Gotham et al., 1986];

2. *Posterior cortical syndrome* involving memory, semantic fluency and visuospatial/visuoperceptual deficits and not related to dopamine imbalances. These impairments are possibly related to cortical synucleinopathy and/or AD-type pathology, cholinergic denervation and herald future conversion to dementia [Kehagia et al., 2010; Nombela et al., 2014; Robbins and Cools, 2014; Williams-Gray et al., 2009]. Neuroimaging is probably the best approach to try to disentangle the underpinnings of both syndromes, with potentially significant impact on risk stratification once disease-modifying treatments become a reality.

Frontostriatal deficits mainly refer to attention and executive abnormalities, including planning, working memory, attentional set-shifting, memory recall, verbal fluency, and attentional conflict resolution deficits [Robbins and Cools, 2014]. The observation that these deficits were similar to those displayed by patients with frontal lobe lesions led to the speculation that they were related to these regions [Owen et al., 1993]. The study of PD patients at various stages, including treatment-naïve, early-PD and more advanced, treated patients [Robbins and Cools, 2014] as well as the finding that some of these impairments responded to treatment with levodopa further suggested a dopaminergic, frontostriatal base [Downes et al., 1989; Lange et al., 1992].

Later observations appeared to indicate that some frontostriatal deficits, instead of improving, were made worse by the administration of levodopa. Cools *et al.* found that the medication impaired probabilistic reversal learning – considered to recruit the orbitofrontal cortex (OFC) and the ventral striatum, parts of the frontostriatal circuitry with relatively preserved dopaminergic input. Task-switching – with bigger reliance on the dorsal caudate nucleus, more affected by PD-related dopamine depletion – was improved [Cools et al., 2001]. Previous studies had demonstrated that there is an optimal level of dopamine for cognitive function, below and above which performance is impaired [Arnsten, 1998]. The effect of dopamine on cognition would therefore describe an *inverted-U shaped curve*, consistent with the Yerkes-Dodson model of arousal effects on cognitive performance

[Yerkes and Dodson, 1908]. Based on these results, the authors proposed that areas not affected by dopamine loss in PD underwent a *dopamine overdose* as a result of antiparkinsonian treatment [Cools et al., 2001].

Declarative memory deficits are frequently described in PD, even at early disease stages [Aarsland et al., 2009a; Brønnick et al., 2011; Muslimovic et al., 2005]. There is, however, a long history of controversy concerning which memory processes are affected. The traditional view that memory deficits in non-demented PD are secondary to executive dysfunction [Higginson et al., 2003] and associated with free-recall memory deficits, with little or no recognition or cued-retrieval impairments, has been more recently called into question [Higginson et al., 2005; Whittington et al., 2006]. Accordingly, Weintraub *et al.* found primary encoding as well as primary retrieval deficits in a sample of medicated PD subjects [Weintraub et al., 2004]. Moreover, two recent studies – including early, treatment-naïve [Brønnick et al., 2011] as well as medicated patients [Chiaravalloti et al., 2014] – find evidence of a learning/encoding-deficit over the retrieval hypothesis. These findings indicate that the search for the neuroanatomical bases of memory deficits in PD cannot be restricted to the frontostriatal circuits, but must include other areas such as the medial temporal lobe.

Visuospatial/visuoperceptual deficits are also commonly described in PD patients [Aarsland et al., 2009a; Boller et al., 1984; Williams-Gray et al., 2009]. These deficits do not respond to dopaminergic treatment or DBS [Israeli-Korn et al., 2013; Lange et al., 1992], suggesting that they are not related to dopaminergic, frontostriatal deficits. A relationship between these deficits and both disease duration and severe cognitive decline was already described by Levin *et al.* in 1991 [Levin et al., 1991]. Accordingly, the presence of such deficits in PD – assessed through the pentagon item in the MMSE – has been identified as a prognostic marker for dementia [Williams-Gray et al., 2009].

Contrasting with AD, praxis and language (except for verbal fluency) tend to be preserved [Emre, 2003].

mild cognitive impairment in PD

Alongside recent growing clinical and research interest in the cognitive manifestations of PD, some authors have begun applying the diagnosis of *mild cognitive impairment* (MCI) to PD patients who have cognitive decline beyond what would be expected for age, but who maintain normal functional activities [Litvan et al., 2011a]. The concept of MCI was initially used to characterize the presence of mild memory deficits in persons with preserved activities of daily living and a higher risk of subsequently developing AD [Petersen et al., 1997]. The rationale for this classification is that patients with MCI might be in a point of transition between normal cognition and dementia [Caviness et al., 2007]. Indeed, PD patients with MCI are at a higher risk of faster cognitive decline and dementia; a recent 3-year-follow-up longitudinal study found a relative risk of dementia of 39 for MCI patients compared with those without MCI [Pedersen et al., 2013]. The identification of adequate MCI criteria could therefore help identify patients at risk of worse cognitive outcomes, who would be candidates for early intervention.

Since until recently there were no standardized criteria to diagnose it, the prevalence of MCI in PD (PD-MCI) is difficult to estimate, but is described to lie between 20 and 55% [Aarsland et al., 2010; Goldman and Litvan, 2011; Litvan et al., 2011a] and to increase with age and disease duration [Litvan et al., 2011a]. Additionally, single-domain MCI is more common than multiple-domain; single-domain MCI cases are more frequently non-amnestic than amnestic, whereas multiple-domain MCI is more commonly amnestic than non-amnestic [Aarsland et al., 2010; Litvan et al., 2011a].

In an attempt to uniform the criteria used for diagnosing PD-MCI, an MDS task force has recently published its guidelines [Litvan et al., 2012]. Briefly, these criteria use a two-level scheme – depending on the comprehensiveness of the neuropsychological assessment – and assess 5 cognitive domains: attention, language, memory, visuospatial and executive functions. For the diagnosis of PD-MCI, the patient must have subjective or objective cognitive decline which does not interfere significantly with activities of daily life. *Level-I* criteria are used when less than two tests are available for each cognitive domain or when less than five domains are evaluated; a diagnosis of MCI is determined by impairment in at least two tests. *Level-II* criteria are used when two tests are included for each of the five domains, and MCI is defined as impairment in at least two tests in one domain or one test per domain in at least two domains. Both levels identify PD-MCI, but with different accuracy and extent of clinical characterization [Litvan et al., 2012]. Broeders *et al.* have found high inter and intra-rater reliability for Level II criteria [Broeders et al., 2013a].

There is no consensus, as yet, concerning the definition of an *abnormal test score* to define impairment. In the current MDS task force guidelines, an abnormal score would be determined by performance between 1 to 2 standard deviations (SD) below age-, education-, gender-, and culturally-appropriate norms; by significant decline on serial cognitive testing (*e.g.*, a change of at least 1 SD), or by significant decline from estimated premorbid levels [Litvan et al., 2012]. These criteria should ideally be standardized to ensure that studies are comparable, and two recent studies have addressed this issue. One such study suggested a cutoff score of 1.5 SD below appropriate norms [Dalrymple-Alford et al., 2011], whereas Goldman *et al.* concluded that a cutoff of 2 SD would have good sensitivity and specificity [Goldman et al., 2013].

PD-MCI and the dual syndrome

Despite growing evidence that different types of cognitive deficit in PD may be derived from two processes with different pathophysiological bases and prognostic implications, the currently proposed criteria for diagnosing MCI make no distinction between *frontostriatal* and *posterior cortical impairments*. Besides assessing the prognostic value of a diagnosis of PD-MCI, longitudinal studies should ideally investigate whether the involvement of specific cognitive domains influences the risk of subsequent dementia.

NEUROPSYCHIATRIC DEFICITS IN PD

Neuropsychiatric complications are common and potentially debilitating non-motor manifestations of PD, with important impact on quality of life, daily functioning and caregiver burden [Aarsland et al., 2009b; Leiknes et al., 2010]. Aarsland *et al.* found that 61% of PD patients had at least one psychiatric symptom, whereas Leroi *et al.* described a prevalence of 79% [Aarsland et al., 1999; Leroi et al., 2012b]. These symptoms are more common in PD patients with cognitive decline, being present in 89% of demented patients according to Aarsland *et al.* [Aarsland et al., 2007a; Leroi et al., 2012b]. The most common neuropsychiatric symptoms in PD are depression, apathy, psychosis, and impulse control or sleep disorders [Weintraub and Burn, 2011].

Depressive symptoms are frequently described as the most common psychiatric manifestation in PD. In a large systematic review, major depressive disorder was found to have a prevalence of 17%, minor depression 22%, dysthymia 13% and clinically significant depression 35% [Reijnders et al., 2008], whereas another study found an estimated prevalence of significant depressive symptoms of 30-40% [Aarsland et al., 2009b].

Depression in PD is not limited to a psychological reaction to a chronic debilitating illness; it is, at least partially, a component of the PD-related neurodegenerative process [Aarsland et al., 2009b]. PD patients appear to have higher rates of depression than subjects with comparable levels of disability form other causes [Ehmann et al., 1990]. Additionally, patients with depression have a higher risk of developing motor PD in the following years, indicating that depressive symptoms can sometimes be early, premotor manifestations of PD [Alonso et al., 2009; Fang et al., 2010; Ishihara and Brayne, 2006]. This observation is compatible with the fact that LB pathology in noradrenergic and serotonergic brainstem nuclei – such as the locus coeruleus and raphe nuclei – precedes nigral degeneration [Gallagher and Schrag, 2012]. Dopaminergic dysfunction is also considered to play a role [Remy et al., 2005]; besides conventional drugs such as tricyclic antidepressants or selective serotonin reuptake inhibitors, the dopamine agonist pramipexole was shown to be useful in the treatment of depression in PD [Weintraub and Burn, 2011].

Psychiatric impairments in PD include *apathy* and *impulse control disorders* (ICDs), opposite manifestations in the spectrum of disorders of reward and motivation. These disorders are thought to have similar neural substrates, namely, dopaminergic imbalances in frontostriatal circuits, specifically in the parts that compose the *reward/motivation pathways* – *i.e.*, ventral striatum and ventromedial PFC [Haber, 2011]. While apathy is thought to derive from a hypodopaminergic state, ICDs are considered to be associated with excessive dopamine stimulation in these circuits [Leroi et al., 2012a; Voon et al., 2014].

Apathy affects between 23 and 70% of patients [Cubo et al., 2012; Kirsch-Darrow et al., 2006; Pedersen et al., 2010]. It is characterized by reduced goal-directed behavior, flattened affect and lack of interest in new stimuli, and in one's own and others' problems [Kirsch-Darrow et al., 2006]. It often coexists with depression, and there is an overlap in the symptoms of both syndromes – specifically, depressive subjects frequently have symptoms of apathy [Kirsch-Darrow et al., 2011; Marin, 1990]. There is ample evidence, however, to support that apathy and depression exist as distinct nosological entities in PD [Aarsland et al., 1999; Dujardin et al., 2007; Isella et al., 2002; Kirsch-Darrow et al., 2011].

Apathy is a possible complication following subthalamic DBS [Czernecki et al., 2008; Thobois et al., 2010], at least in part due to the post-surgical reduction in dopaminergic medication dosage [Thobois et al., 2013]. Besides causing significant disability and caregiver burden and distress, apathy in PD is described to have a negative impact on cognition and increase the rate of cognitive decline [Butterfield et al., 2010; Dujardin et al., 2009].

ICDs in PD mainly comprise compulsive gambling, buying and eating as well as hypersexuality. They became relatively common complications in PD after the introduction of D2 receptor-selective dopamine agonists, especially in younger patients [Weintraub and Burn, 2011]. The prevalence of ICDs in patients treated with dopamine agonists has been described to be around 17%, against 7% in patients not taking these drugs, with an odds-ratio of 2-3.5 [Weintraub et al., 2010]. They are associated with other psychiatric and cognitive impairments, as well as with behaviors of punding (*i.e.*, abnormal repetitive non-goal oriented behaviors) and compulsive use of medication [Voon et al., 2007; Voon et al., 2011]. Furthermore, some authors have hypothesized a mechanistic overlap between ICDs and levodopa-induced dyskinesias [Voon et al., 2009].

Psychotic symptoms affect up to 60% of PD patients in the long-term, although prevalence rates depend on the cognitive status of the samples studied [Aarsland et al., 2014; Leroi et al., 2012b]. The most common psychotic symptoms in PD involve visuoperceptual disturbances. Complex visual hallucinations, often of animals or people, are the most typical manifestation [Aarsland et al., 2014]. Illusions, sensations of movement in the periphery (passage phenomena) and sensations of presence are also frequent [Aarsland et al., 2009b]. Other types of hallucination – auditory, tactile or olfactory – occur less commonly, and usually in association with visual ones [Aarsland et al., 2009b; Weintraub and Burn, 2011].

Although psychotic symptoms can be triggered by dopaminergic drugs, especially dopamine agonists, they have complex causes and are not restricted to drug side effects. These symptoms are more common in patients with older-onset PD, longer disease duration, and associated depression or REM-sleep behavior disorder [Aarsland et al., 2014]. Importantly, the occurrence of visual hallucinations is associated with a more *malignant disease course* and predicts faster cognitive decline, nursing home placement and mortality [Aarsland et al., 2014; Burn et al., 2006; Forsaa et al., 2010; Ramirez-Ruiz et al., 2007; Ramírez-Ruiz et al., 2006].

PD can be accompanied by several disorders of the sleep-awake cycle, such as insomnia and excessive daytime sleepiness; the most typical sleep-related manifestation, however, is *REM-sleep behavior disorder* (RBD), which affects between 30 and 50% of patients [Schrempf et al., 2014]. RBD is a parasomnia characterized by elaborate motor activity during REM sleep, frequently associated with the content of dreams, and related to loss of the normal muscle atonia during this sleep phase [Schenck and Mahowald, 2002]. One important aspect of RBD is that it can antecede the onset of motor PD by several decades [Aarsland et al., 2014]. Iranzo *et al.* found that 82% of patients with idiopathic RBD developed a Lewy body disorder – mainly PD or dementia with Lewy bodies – after approximately 14 years [Iranzo et al., 2013]. This aspect of RBD offers a unique opportunity for the study of the prodromal phases of PD and of potential disease-modifying treatments.

Emotional processing is also altered in PD patients. Several studies have reported the occurrence of impaired recognition of emotions – especially emotions with negative valence – in facial expression or in prosody [Ariatti et al., 2008; Dujardin et al., 2004; Kan et al., 2002; Yip et al., 2003].

COGNITION IN PD – STRUCTURAL NEUROIMAGING

In-vivo neuroimaging tools can provide invaluable data in the study of cognitive deficits associated with neurodegenerative diseases in general, including PD. The identification of clinically useful neuroimaging biomarkers with predictive power for the risk of future cognitive decline at the individual level would be the most immediate benefits from a clinical standpoint. Neuroimaging can also increase our knowledge regarding the pathological process itself. Identifying the neural substrates of cognitive deficits in PD can shed light on the patterns of disease progression and help establish whether different types of impairment are associated with different underlying brain changes – and whether these changes differ regarding their prognostic value.

Structural and functional MRI techniques have gone through significant advances in recent years, paralleling the increased interest in cognitive deficits in PD. As shown in Figure 1.1, the number of indexed Medline publications conforming to the keywords "Parkinson's disease" (title), "MRI" and "cognitive" in PubMed searches has been growing steadily since the late 1990's. Since around 2009, however, these publications have experienced a marked boom in the absolute number of publications as well as compared to the total number of indexed publications or to the total number of publications with the words "Parkinson's disease" in their title.

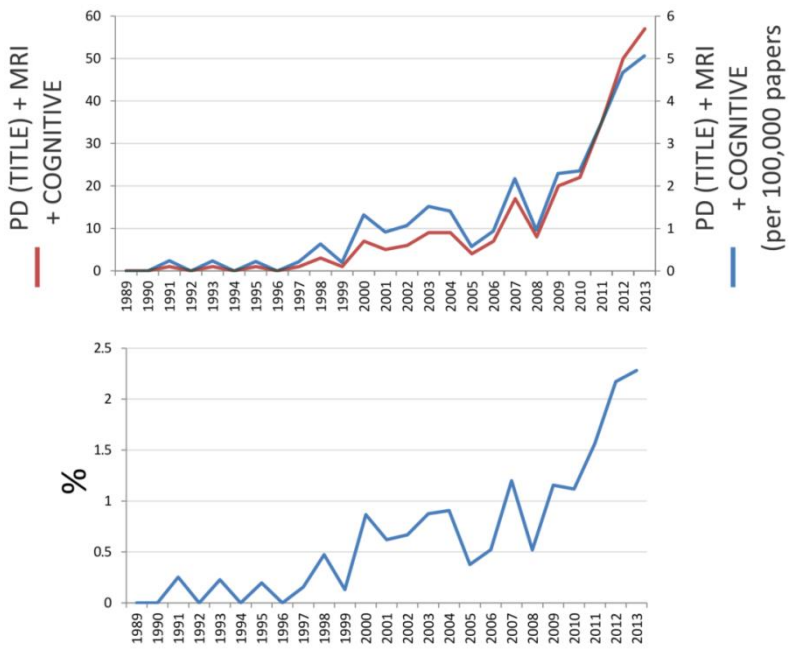

Figure 1.1. Trend of Medline publications addressing Parkinson's disease, magnetic resonance imaging and cognition. The top panel shows the number of Medline publications identified by the query *"parkinson's disease [TITLE] AND mri cognitive"* in PubMed. The red line indicates total number of such publications per year. The blue line indicates the number of such publications per 100,000 Medline papers published the same year. The bottom panel shows the number of publications with the aforementioned query for every 100 publications with the words "parkinson's disease" in their title.

GM structural neuroimaging - methods

The two most commonly used techniques to evaluate structural gray matter (GM) changes associated with cognitive decline in PD are *voxel-based morphometry* (VBM) and, more recently, *cortical thickness* (CTh) procedures.

Typically performed using structural T1-weighted images, VBM quantifies the amount of GM (either volume or density) inside each voxel. Initially, according to the optimized VBM protocol by Good *et al.*, brain voxels are identified as GM or non-GM based on their signal intensity [Good et al., 2001]. The structural images and corresponding GM images of all subjects are then registered to a common space (such as the MNI152 standard space) through non-linear transformation, so that a given voxel with coordinates *x, y, z* represents the same anatomical region in every subject. In the next step, all subjects' GM images are averaged, creating a study-specific GM template. Native-space GM images are then non-linearly registered to this template, and modulated to correct for local expansion or contraction produced in the non-linear transformation using the Jacobian determinants of the warps at each voxel [Good et al., 2001]. Finally, these registered, modulated images are smoothed; in this step, the intensity (*i.e.*, GM density or volume) of the smoothed voxel will be a locally weighted average of the intensity of the surrounding voxels, the size of the region being defined by the size of the smoothing kernel used [Ashburner and Friston, 2000]. The smoothing step helps to compensate for the inexact nature of the spatial normalization [Ashburner and Friston, 2000]. It also conditions the data to conform more closely to the Gaussian random field model underlying some types of statistical testing; some standard protocols, however, favor the use of permutation testing instead [Good et al., 2001; Nichols and Hayasaka, 2003; Winkler et al., 2014].

MRI and the multiple comparison (or multiple testing) problem

Statistical testing in advanced neuroimaging techniques is often performed at the *voxel* (or, for CTh analyses, *vertex*) level, resulting in as many statistical tests as there are voxels/vertices in the analysis. Simply applying a significance-level threshold (α) of 5% to each test (*i.e.*, each vertex or voxel) would result in an inordinately high number of false-positive tests (around 10,000 false rejections of the null hypothesis for a typical 2 mm-resolution VBM analysis, comprising around 200,000 GM voxels).

To reduce the occurrence of type I errors, multiple-comparison correction methods are required, but there is no consensus regarding the ideal one. The most frequently used methods apply *familywise error rate* (FWE) correction or the *false discovery rate* (FDR). In brief, for an α of 5%, FWE-corrected results have a 95% possibility of containing no false-positive tests. Or, put differently, there's an *'α%'* chance of any false-positive results in the whole *family* of tests, the family being comprised by all tests collectively. In FDR-corrected results, on the other hand, 5% of the positive tests are expected to be false positives.

FWE provides more strict control over type I errors, but is sometimes seen as too stringent

(cont.) [Nichols, 2012]. The goal of FDR correction, in turn, is not to eliminate false-positives, but to control how pervasive they are in the results [Bennett et al., 2009]. As Benjamini illustratively puts it, FDR has broken the dichotomy of the *don't-worry-be-happy* uncorrected approaches versus the *panic* FWE-correction methods, and is gradually gaining ground [Benjamini, 2010; Nichols, 2012; Nichols and Hayasaka, 2003]. No method can be expected to completely eliminate false-positive results; whether it be FWE-correction or FDR, it is important that the researcher informs about the type I error rate across the whole brain or the whole tested region [Bennett et al., 2009].

VBM has several limitations. In its early years, it suffered harsh criticism [Bookstein, 2001] that generated equally harsh rebuttal [Ashburner and Friston, 2001]. Sometimes it's not possible to differentiate GM atrophy from changes in folding or gyrification which may lead to suboptimal registration. Indeed, VBM is highly dependent on an adequate image registration (and therefore on the accuracy of the registration algorithms); specific patterns of abnormal anatomy may result in group-specific misregistration and, consequently, in falsely-positive GM volume/density differences [Bookstein, 2001; Mechelli et al., 2005].

As mentioned above, VBM provides a mixed measure of cortical grey matter including cortical surface area or cortical folding, as well as cortical thickness [Hutton et al., 2009]. If the pathological effect being studied on the cerebral cortex is hypothesized to be related primarily to changes in thickness, techniques that measure this variable directly can be expected to be more sensitive than VBM. In PD, although VBM is still the most frequently used method in structural MRI studies, the number of published papers that employ *cortical thickness* (CTh) techniques has been growing steadily since 2010 (see Figure 1.2).

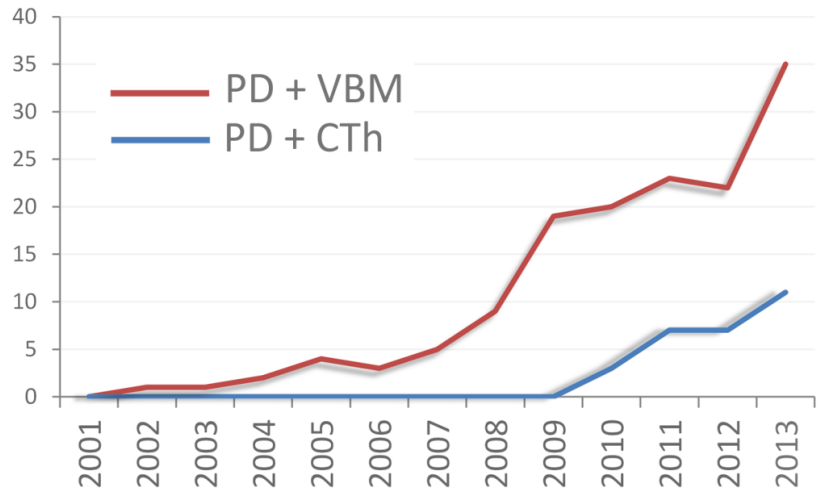

Figure 1.2. Trend of *voxel-based morphometry* and *cortical thickness* magnetic resonance imaging studies in Parkinson's disease. Number of Medline publications identified by the queries "*parkinson's disease voxel based morphometry*" (red line) or "*parkinson's disease 'cortical thickness'*" (blue line) in PubMed, per year.

As in VBM, CTh analyses typically use T1-weighted high-resolution structural images. FreeSurfer (http://surfer.nmr.mgh.harvard.edu) is the most widely used software in PD CTh studies, and follows the procedures described by Dale *et al.* and Fischl *et al.* [Dale et al., 1999; Fischl and Dale, 2000]. According to this approach, after correction for magnetic field inhomogeneities and registration to the Talairach atlas [Talairach and Tournoux, 1988], white matter (WM) voxels are identified according to their intensity and location. A triangular mesh is then built around the WM, representing the WM/GM boundary, and referred to as the *white surface*. To define the external GM boundary, the white surface is expanded outwards until a point of maximal contrast; this new outer mesh is called the *pial surface*. CTh at a given point is defined as the distance between corresponding vertices on the two surfaces. Intersubject registration can subsequently be performed using surface-based algorithms. Surface-based registration attempts to align the sulcal and gyral patterns of the cortex, with improved accuracy of registration in comparison with the volume-based methods typically used in VBM [Fischl et al., 1999; Ghosh et al., 2010].

GM structural neuroimaging in PD – previous studies

Following recent interest in the development of markers of dementia risk and the emerging concept of MCI in PD, several studies began stratifying PD samples into subgroups of patients with and without MCI. The majority of studies using either VBM or CTh have found limited or no evidence of GM structural deterioration in subjects without MCI [Hanganu et al., 2013; Mak et al., 2014b; Melzer et al., 2012; Pereira et al., 2014]. One exception is the study by Pagonabarraga *et al.*, in which PD patients without MCI (PD-NMCI) showed predominant parieto-occipito-temporal thinning compared with healthy controls (HC) [Pagonabarraga et al., 2013]. The GM structural findings in PDD patients likewise tend to reveal extended and widespread areas of cortical and subcortical GM atrophy [Beyer et al., 2007; Compta et al., 2012; Hwang et al., 2013; Melzer et al., 2012; Nagano-Saito et al., 2005; Song et al., 2011; Zarei et al., 2013].

PD-MCI subjects usually show evidence of significant cortical and subcortical GM atrophy compared with HC, but the pattern of degeneration is not consistent across studies. In a recent study, Pereira *et al.* assessed a multicentric cohort of 123 PD patients and 56 HC. Using a modified version of the MDS Task Force criteria, 33 patients were classified as PD-MCI. Subjects in this group showed significant cortical thinning in left lateral and medial parieto-occipital areas, in left frontal areas (including primary motor and premotor areas, as well as in lateral and medial parts of the superior frontal gyrus) and in the lateral temporal cortex bilaterally compared with HC. Compared with PD-NMCI, PD-MCI patients showed CTh reductions in left occipito-parietal areas [Pereira et al., 2014]. Also using CTh, Hanganu *et al.* analyzed a sample of 16 HC and 37 early-PD (19 PD-NMCI and 18 PD-MCI) subjects. The authors found that PD-MCI subjects, compared with HC, had thinning in limited bilateral medial occipito-temporal and left orbitofrontal regions [Hanganu et al., 2013]. More recently, the same group published a longitudinal study assessing progressive CTh changes in a sample of 18 HC and 32 early-PD (15 PD-NMCI and 17 PD-MCI) subjects. PD-MCI patients had a higher rate of thinning in temporo-occipito-parietal regions bilaterally and in the left OFC, as well as higher rate of volume loss in the amygdala and nucleus accumbens compared with HC [Hanganu et al., 2014]. Of note, in both studies by Hanganu *et al.*, patients were evaluated off their usual medication. It is possible that deficits caused by

dopamine deficits were overrepresented in the PD-MCI group, which in turn could reduce the sensitivity for GM structural changes in intergroup comparisons.

In a recent study mentioned above, Pagonabarraga *et al.* compared 18 HC, 26 PD-NMCI, 26 PD-MCI and 20 PDD subjects using CTh techniques. The authors identified a progressive pattern of severity in cortical thinning accompanying the severity of cognitive decline involving all cerebral lobes [Pagonabarraga et al., 2013]. Mak *et al.*, assessing mild-PD patients and also using CTh analyses, found no significant differences between 25 PD-MCI and 65 PD-NMCI subjects; the lack of a HC group and the somewhat atypical cognitive profile observed in the sample (no significant intergroup differences in episodic memory or visuospatial function) could partially explain the negative findings [Mak et al., 2014a]. In another study, the same group assessed mild-PD subjects (24 PD-MCI and 66 PD-NMCI) through VBM; using an uncorrected significance threshold of $p<.001$, the authors found that PD-MCI subjects had reduced GM volume in left insular, superior frontal and middle temporal cortical regions [Mak et al., 2014b]. Also using VBM and evaluating a sample of 34 HC, 57 PD-NMCI, 23 PD-MCI and 16 PDD subjects, Melzer *et al.* observed that PD-MCI had reduced GM volumes in fronto-temporo-parietal regions as well as in the hippocampi, amygdalae and putamina [Melzer et al., 2012].

An elusive pattern

There is considerable heterogeneity in the published literature regarding the structural correlates of MCI in PD, and a common pattern of degeneration hasn't been identified. This apparent inconsistency is probably due in part to the different methodological procedures used to define MCI and measure cognitive performance, to the inclusion of small patient samples with different clinical characteristics, and to the different analytical methods employed. Importantly, some authors have attempted to interpret their findings in light of the progression pattern predicted by the Braak staging, but it is far from clear that the GM substrates underlying cognitive changes in PD follow the ascending trajectory described for LN/LB pathology.

Another frequently-used approach in structural GM studies in PD is to investigate the anatomic correlates of deficits in specific cognitive functions. Hippocampal volume has been found to correlate with memory encoding performance [Weintraub et al., 2011]. Specifically, episodic memory performance correlated with volumes and radial distances of hippocampal subfields [Beyer et al., 2013; Pereira et al., 2013]. Some authors, however, failed to find associations between memory performance and hippocampal GM [Lee et al., 2010]. Visuospatial/visuoperceptual deficits, on the other hand, are described to correlate with temporo-parieto-occipital GM volume reductions [Pereira et al., 2009b]. Using the volumes of brain regions chosen *a priori*, Filoteo *et al.* also found that visuospatial performance correlated with volumes in the object-based system, whereas poorer visuoconstruction correlated with decreased frontal and object-based system volumes; additionally, these authors found that executive function impairments correlated with decreased frontostriatal volumes, and that memory deficits correlated with reduced volumes in medial temporal regions [Filoteo et al., 2014].

The studies mentioned above used either region-of-interest (ROI) analyses or assessed a limited range of cognitive functions; the regional/cognitive specificity or the results found, therefore, is difficult to establish. In the study by Pereira *et al.*, using a comprehensive neuropsychological assessment and whole-brain CTh analyses, the substrates of the cognitive domains that correlated significantly with thickness (visuospatial and executive) showed significant overlap in frontal, parietal and temporal regions [Pereira et al., 2014].

Structural neuroimaging approaches have also been used to assess the substrates of neuropsychiatric deficits in PD. Using VBM, depressed PD patients have been found to have GM density reductions in OFC regions [Feldmann et al., 2008] and WM reductions in frontal regions [Kostić et al., 2010]. In PD patients with apathy, VBM has revealed GM density reductions in frontal, insular and parietal regions [Reijnders et al., 2010]. Carriere *et al.*, on the other hand, found atrophy of the nuclei accumbens and head of the left caudate nucleus in apathetic PD patients using shape and volumetric analyses, while finding no differences in cortical thickness or WM FA [Carriere et al., 2014].

WM structural neuroimaging - methods

WM changes have also been assessed in the study of cognitive decline in PD, albeit less frequently than GM techniques. The most commonly used procedure is MRI diffusion tensor imaging (DTI), which uses the properties of diffusion-weighted MRI, sensitive to the microdiffusion of water molecules. Water diffusion inside and between cells is impeded by the presence of obstacles such as cell membranes, fibers and macromolecules [Le Bihan, 2003]. The coherent organization of axonal fibers in the WM results in a preferential direction of water diffusion (*i.e.*, *anisotropic diffusion*) [Beaulieu, 2002]. Indeed, diffusion parallel to WM tracts is 3 to 5 times higher than diffusion perpendicular to them [Le Bihan, 2003]. The exact contribution of the components of WM (such as myelin) to the highly anisotropic diffusion it displays is not known. Nonetheless, DTI offers an *in-vivo* indirect measure of microstructural WM properties that appears to be useful to the study of disease processes, and its use in the study of PD-related cognitive changes is growing (Figure 1.3).

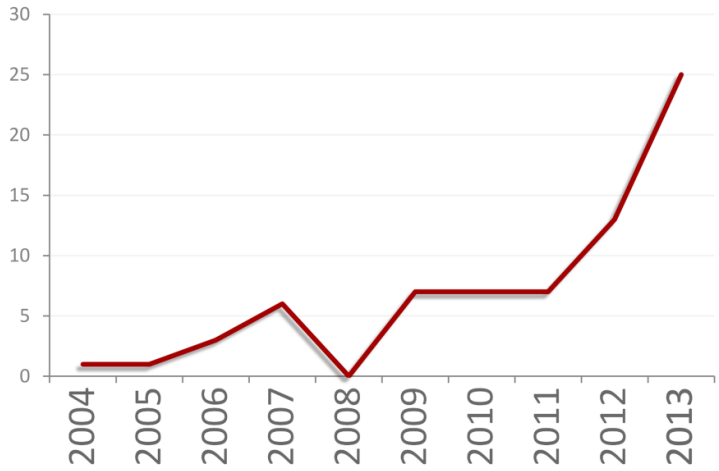

Figure 1.3. Trend of *diffusion tensor image* magnetic resonance imaging studies in Parkinson's disease. Number of Medline publications identified by the query "*parkinson's disease diffusion tensor*" in PubMed, per year.

In DTI, diffusion-weighted images obtained at different angles are fitted the diffusion-tensor model to produce the *diffusion tensor*, which can be visualized as an ellipsoid and represented by a matrix. The magnitude of water diffusion along the longest, middle and shortest orthogonal axes of the ellipsoid is represented by the matrix's *eigenvalues* (λ1, λ2, and λ3), *i.e.*, the length of the corresponding axes. The orientations of these axes – the *eigenvectors* of the matrix – are useful mainly for the reconstruction of WM bundles through *tractography*. Different metrics for the analysis of WM microstructure, in turn, can be derived from the eigenvalues. The most frequently used metric in WM imaging studies is the *fractional anisotropy* (FA), which indicates the degree of anisotropy in a scale of 0 (isotropic) to 1 (anisotropic). FA is hypothesized to be related to myelin integrity [Le Bihan, 2003], but is sensitive to other changes in WM organization as well [Jones et al., 2013]. FA is given by the formula:

$$FA = \sqrt{\frac{1}{2}} \frac{\sqrt{(\lambda 1 - \lambda 2)^2 - (\lambda 2 - \lambda 3)^2 - (\lambda 1 - \lambda 3)^2}}{\sqrt{\lambda 1^2 + \lambda 2^2 + \lambda 3^2}}$$

The *mean diffusivity* (MD) is another commonly used variable that measures the overall diffusion inside a voxel and is given by the arithmetic mean of the three eigenvalues. These metrics can be extracted from predefined ROIs or tracts obtained from tractography, or they can be evaluated globally in voxel-based analyses or tract-based statistics (TBSS) [Cochrane and Ebmeier, 2013].

WM structural neuroimaging in PD – previous studies

Based on the hypothesis that DTI metrics reflect microstructural WM properties, recent studies have applied these techniques in the assessment of several neurological diseases [Hattori et al., 2012]. In PD, WM changes have recently been recognized as an important substrate of its cognitive deficits [Agosta et al., 2013]. These changes have been reported even in non-demented PD, often involving diffuse brain areas [Hattori et al., 2012; Koshimori et al., 2014; Melzer et al., 2013; Theilmann et al., 2013; Zheng et al., 2014]. The frontal lobes are described as the most frequently involved region [Agosta et al., 2013; Gattellaro et al., 2009; Koshimori et al., 2014; Rae et al., 2012].

Agosta *et al.* recently assessed a sample of 33 HC, 13 PD-NMCI and 30 PD-MCI. The authors found widespread WM FA reductions in PD-MCI subjects compared with HC. No WM changes were detected in PD-NMCI subjects, and no GM changes as assessed by VBM were detected in either PD subgroup [Agosta et al., 2013]. In contrast, Melzer *et al.* found that PD-NMCI patients (n=63) had increased MD in the corpus callosum compared with HC (n=32); PD-MCI (n=28) and PDD (n=18) subjects, on the other hand, showed diffuse FA decrements and MD increments. Additionally, executive function, attention, memory, and a composite measure of global cognition were associated with MD, mainly in anterior WM tracts, and attention was associated with FA in right anterior and posterior regions [Melzer et al., 2013]. Zheng *et al.*, assessing a sample of 16 PD patients, found that executive functions and language correlated with FA and, inversely, with MD in frontal WM tracts; attention was associated with DTI measures in widespread regions [Zheng et al., 2014]. In another recent study, Koshimori *et al.* found diffuse increments in MD in a sample of 26 PD patients compared with 15 HC that correlated with executive and global cognitive impairment.

Additionally, PD patients showed cortical thinning in the dorsolateral PFC that correlated with the same cognitive measures [Koshimori et al., 2014].

Diffusion MRI and related techniques such as DTI have undergone considerable improvements over the last few years, as is reflected by the growing number of informative studies using these methodologies. Some limitations, however, must be taken into consideration when interpreting these studies' results, as they are sensitive not only to *microstructural integrity*, but also to the intra-voxel orientational coherence of axons [Beaulieu, 2002]. Furthermore, considering the different contribution of various microstructural features to the signal loss on which DTI is based, it is not appropriate to try to pinpoint a pathophysiological cause, such as reduced myelination [Jones et al., 2013]. Differences in anisotropy can also be due to differences in axon diameter, axon packing or increased membrane permeability [Jones et al., 2013]. Until the actual pathological underpinnings of the WM changes observed through diffusion MRI in PD are established, these results should be interpreted cautiously.

PD and early white matter damage

Recent neuroimaging work indicates that WM changes may precede GM degeneration in PD [Agosta et al., 2013; Hattori et al., 2012]. It may be difficult to determine this with certainty. Results are influenced not only by the chronological sequence of pathological events, but also by the sensitivity of the methods used to detect each type of change. Nonetheless, available research data from other fields suggests that PD-related neurodegeneration begins in the axon, and that axonal loss may antecede somatic death [Burke and O'Malley, 2013; Dauer and Przedborski, 2003; O'Malley, 2010; Orimo et al., 2008].

It is therefore biologically plausible that WM changes are an early marker of deterioration in PD, and current studies give support to their role in cognitive impairment in non-demented PD patients.

THE BRAIN AS A NETWORK

The study of the relationship between cognitive functions and the brain has historically been based on *'localizational'* approaches. These are still the basis of many current neuroimaging techniques that attempt to ascribe specific functions (or corresponding deficits) to functional or structural changes in specific brain areas. This type of approach has been very useful in providing information about the substrates of normal cognition and of pathological cognitive decline. In the past two decades, however, the study of cognition is increasingly focusing on an integrated model of brain function. Under this paradigm, cognitive functions are the by-product of the interactions within and between distributed and interconnected brain systems. Understanding the structure-function relations is thus critical for understanding the neural basis of cognition [Bressler and Menon, 2010]. As such, a *network perspective* of brain function accounting for the structural and dynamical functional interactions between regions offers a potentially useful framework for the

identification of new and relevant intermediate pathological phenotypes [Pievani et al., 2011].

large-scale functional networks

For any given task, a host of distributed, functionally specialized brain areas must work in concert to integrate sensorial inputs with previously stored information, as well as with executive and motor regions to effect an appropriate behavior. The collection of brain regions that interact in this manner to perform a given function make up a *large-scale functional network* [Bressler and Menon, 2010].

Functional MRI (fMRI) is a widely used technique to characterize the *dynamical activity couplings* between brain areas that give rise to the large-scale functional networks involved in cognitive processes. The coupling between regions, referred to as the *functional connectivity* between them, is estimated by the temporal correlation between these regions' blood-oxygen level-dependent (BOLD) signal (Figure 1.4).

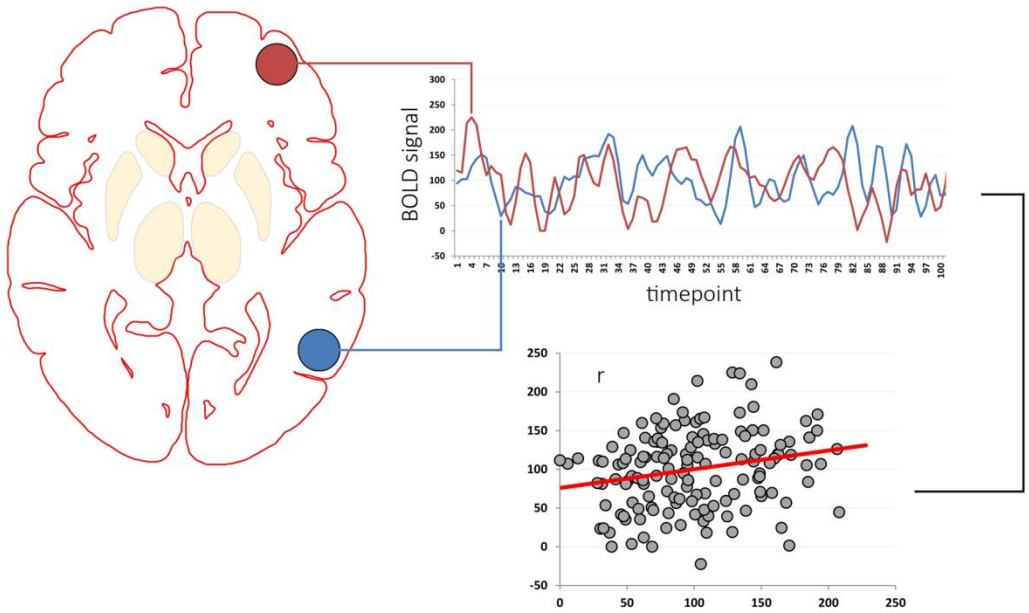

Figure 1.4. Estimation of functional connectivity. In its simplest form, the functional connectivity between two brain regions in fMRI is given by the correlation between their BOLD signal time series.

Following seminal studies by authors such as Biswal, Greicius, Fox and Raichle [Biswal et al., 1995; Fox et al., 2005; Greicius et al., 2003; Raichle et al., 2001], recent years have seen a major increase in the number of studies using task-free or *resting-state* fMRI (see Figure 1.5). During 'rest', coherent patterns of spontaneous BOLD signal oscillations are observed, revealing correlated and anti-correlated *resting-state intrinsic connectivity networks* (ICNs). ICNs display a highly robust pattern of connectivity across studies, with high test-retest reliability [Patriat et al., 2013; Shehzad et al., 2009; Thomason et al., 2011]. The correspondence between these networks and those described in task-based fMRI studies gives support to the idea that ICNs represent meaningful cognitive modules, and that

resting-state fMRI can be used to probe the brain's intrinsic connectivity architecture [Bressler and Tognoli, 2006].

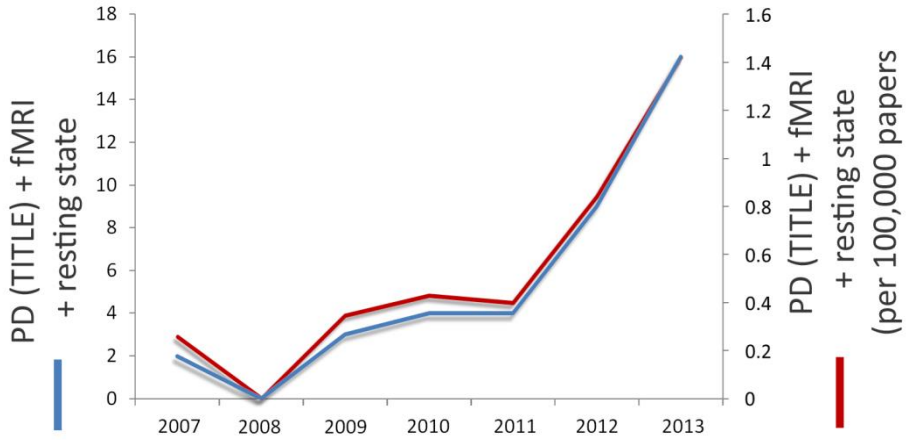

Figure 1.5. Trend of Medline publications addressing Parkinson's disease and resting-state functional MRI. The red line indicates the number of Medline publications identified by the query *"parkinson's disease [TITLE] AND fmri resting state"* in PubMed. The blue line indicates total number of such publications per year. The red line indicates the number of such publications per 100,000 Medline papers published the same year.

One specific ICN has received a great deal of attention – the *default mode network* (DMN), comprised of the precuneus/posterior cingulate, medial prefrontal, inferior parietal and medial and lateral temporal cortical regions, among other areas [Spreng et al., 2013]. Initially described by Shulman *et al.* as a group of areas that showed reduced activity during active tasks and increased activity during passive conditions in a series of positron emission tomography (PET) studies [Shulman et al., 1997], the DMN was subsequently described in fMRI studies [Raichle et al., 2001] and hypothesized to be related to self-referential processing [Gusnard and Raichle, 2001]. Importantly, DMN suppression is relevant for externally-directed attention and working-memory task performance; and the deactivation of DMN regions during encoding is related to subsequent retrieval of learned information [Anticevic et al., 2012].

The overlap between DMN anatomy and the regions of hypometabolism in AD led some authors to investigate pathological changes in this network – revealing that AD patients had altered patterns of DMN activation/deactivation and abnormal functional connectivity between this network's main nodes [Greicius et al., 2004; Mevel et al., 2011; Rombouts et al., 2005].

The analysis of resting-state fMRI data reveals the existence of other ICNs related to a broad range of neural functions, including basic sensory/motor and cognitive functions. Considerable attention has been given to cognitively relevant ICNs in recent studies; although the networks described tend to be similar across studies, a uniform nomenclature system hasn't yet been proposed. The *dorsal attention network* (DAN) is postulated to subserve externally-directed cognition – more specifically, *top-down allocation of attention* [Spreng et al., 2013; Vossel et al., 2012]. The DAN is formed by the dorsolateral PFC, frontal

eye fields, inferior precentral sulcus, superior occipital gyrus, middle temporal motion complex, and superior parietal lobule [Fox et al., 2005; Fox et al., 2006]. The *frontoparietal network* (FPN) – which includes the lateral prefrontal cortex, precuneus, inferior parietal lobule, medial superior prefrontal cortex and anterior insula – can flexibly connect to the DMN or the DAN depending on task nature, and is hypothesized to mediate the dynamic balance between these networks [Spreng et al., 2010; Spreng et al., 2013]. Another ICN, the *salience* or *cingulo-opercular network*, mainly located in anterior insular and dorsal anterior cingulate cortex (ACC) regions, as well as subcortical limbic structures, is related to reward/motivation. The anterior insula is hypothesized to detect salient external or internal inputs and mediate network-switching mechanisms through a *bottom-up process* [Bressler and Menon, 2010].

resting-state functional connectivity fMRI techniques – methods

image preprocessing

Different methodological strategies can be used for resting-state fMRI analysis. The noisy nature of the acquisition along with its susceptibility to artifacts – especially motion-related – and its data-driven nature warrant the use of a series of different preprocessing steps that can influence the estimated connectivity on which results are based [Liang et al., 2012].

The use of relatively long repetition times (TR) (usually 2-3s) and total acquisitions of 5-10 minutes in resting-state fMRI acquisitions limit the fluctuations that can be studied to frequencies between 0.001 and 0.25 Hz. Furthermore, the highest signal amplitudes in ICNs occur in frequencies <0.1 Hz [Boubela et al., 2013]. Resting-state fMRI data sets are usually bandpass-filtered so as to maintain frequencies between 0.01 and 0.1 Hz, assuming that fluctuations in other frequency bands are mainly related to noise. Frequencies corresponding to cardiac (around 1 Hz) and respiratory (around 0.3 Hz) cycles can be partially eliminated through this procedure, although the typical low sampling rate used may cause them to be aliased to the frequency range that is maintained [Murphy et al., 2013].

Preprocessing steps also typically include procedures to reduce the effects of head motion, which biases connectivity estimates [Van Dijk et al., 2012]. In the study of patients with movement disorders such as PD, this is a major issue as it can introduce spurious intergroup differences. During motion correction – a standard part of all fMRI preprocessing pipelines –, six motion parameters (3 translatory, 3 rotatory) are generally obtained; these parameters can then be regressed out of the BOLD time series using multiple linear regression [Murphy et al., 2013].

Additionally, in an attempt to remove the effects of signal fluctuations of non-neural origins – which include those related to head motion, respiration, vascular pulsation and scanner drift – the mean time series obtained from the WM and the CSF are frequently regressed out of the time series. This is based on the assumption that signal variation in these regions are unrelated to neural activity; this regression procedure improves the specificity of functional connectivity maps [Weissenbacher et al., 2009]. *Global signal regression* – the removal of the global mean signal across all brain voxels – used to be a standard preprocessing procedure, but has recently been brought into question due to the introduction of artifactual anti-correlations and the potentially meaningful nature of the discarded signal [Murphy et al., 2013; Schölvinck et al., 2010].

More recently, Power *et al.* proposed a procedure to detect timepoints with excessively different mean global signal (*i.e.*, outliers) – possibly corrupted by head motion. In this *scrubbing* procedure, outlier timepoints are regressed from the BOLD time series, eliminating their effect from connectivity calculations [Power et al., 2012].

Other methods to control for the effect of physiological and motion artifacts can be used, such as the regression of the first temporal derivatives of WM/CSF signal and motion parameters [Van Dijk et al., 2012], regression of the principal components obtained from WM/CSF [Behzadi et al., 2007] or independent component analysis-based denoising [Griffanti et al., 2014]. Cardiac/respiratory cycle and blood pressure recordings are useful methods to reduce physiological artifacts, but their used is limited by the availability of the corresponding equipment [Murphy et al., 2013].

seed-based techniques

Seed-based correlation techniques are straightforward and easily interpretable methods in functional connectivity analysis [Cole et al., 2010]. Briefly, the mean time courses of ROIs chosen *a priori* – representing structures or circuits of interest or the main nodes of ICNs – are extracted. These time courses are then used as regressors against the time courses of all voxels in the brain in a *seed-to-whole brain* approach. Whole-brain *r*-correlation maps – in which the value assigned to each voxel is given by the correlation coefficient between its time series and the time series of the ROI in question – are thus generated, corresponding to the functional connectivity maps of each ROI. Subsequently, Fisher's *r*-to-z transformation is typically applied to ensure that the correlation coefficients are approximately normally distributed. The resulting connectivity maps are then analyzed using voxelwise statistical testing.

Alternatively, in *seed-to-seed* (or node-to-node) techniques, the mean time course of each ROI is correlated with the mean time courses of every other ROI, limiting the analysis to the circuits of interest.

independent component analysis

Independent component analysis (ICA) identifies coherent spatial signal fluctuation patterns in the dataset, separating them into maximally independent components associated with the underlying signal sources – such as ICNs and spatially structured artifacts –, while avoiding the potential biases in the *a priori* selection of ROIs [Beckmann and Smith, 2004; Smith et al., 2014].

The number of components estimated in ICA – *i.e.*, its dimensionality reduction – is a possible source of variability in study results as there is no single best dimensionality reduction approach for characterizing the complex hierarchy of ICN neurobiology [Cole et al., 2010].

Performing between-subject ICA analysis is not a straightforward procedure, as it is difficult to establish a direct, one-to-one correspondence of ICNs identified at the individual level across subjects [Erhardt et al., 2011]. Most current approaches involve performing group-level ICA on the temporally-concatenated datasets of all subjects. This is followed by the creation of individual ICN maps through procedures such as *dual regression* [Cole et al., 2010; Erhardt et al., 2011; Filippini et al., 2009; Zuo et al., 2010]. This solves the problem of

intersubject ICN correspondence and takes advantage of the higher signal-to-noise ratio (SNR) offered by analyzing several subjects conjointly [Cole et al., 2010].

In dual regression, spatial maps corresponding to each independent component are used as spatial regressors against normalized individual datasets to obtain subject and component-specific time courses. These time courses are subsequently entered as temporal regressors in a second voxelwise multiple linear regression procedure against the individual datasets, thus generating individual spatial maps corresponding to each original group-level component [Cole et al., 2013; Filippini et al., 2009; Zuo et al., 2010] (Figure 1.6).

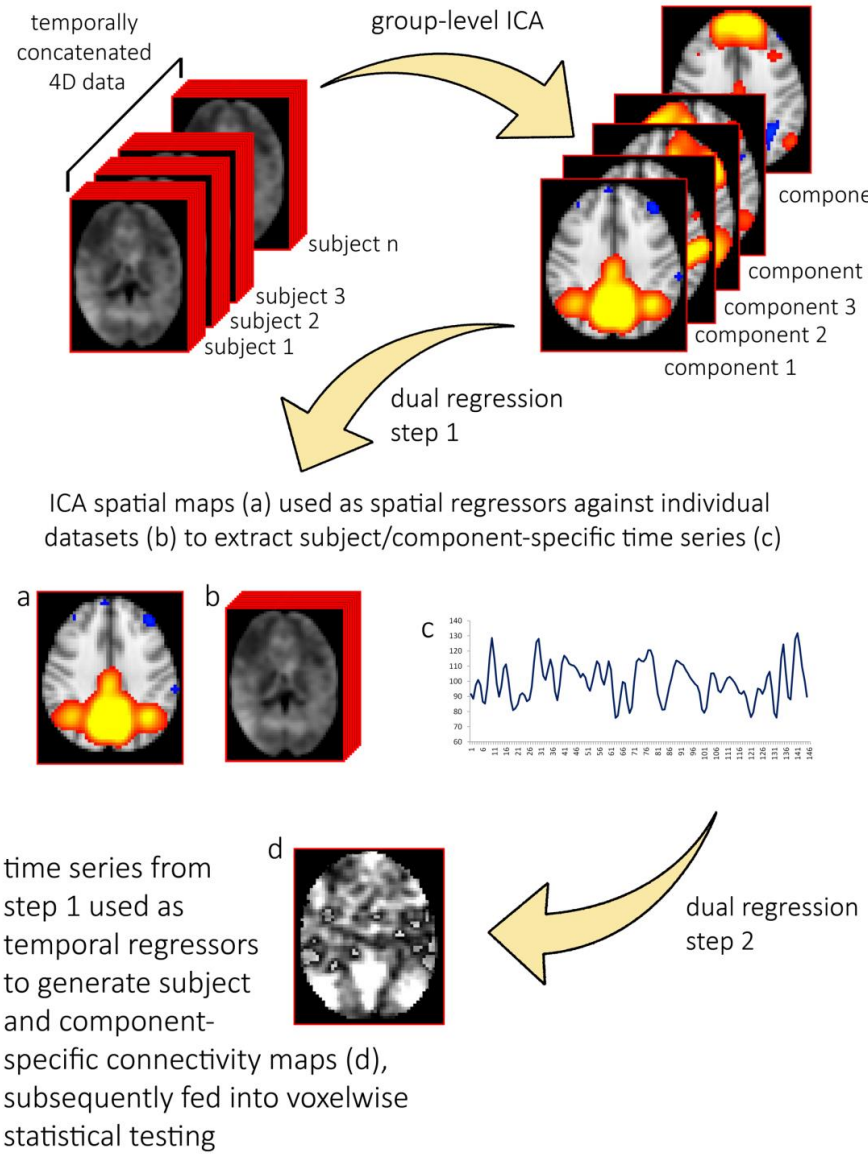

Figure 1.6. Simplified representation of independent component analysis followed by dual regression analysis.

graph theory

Connectomics is the scientific field concerned with generating and studying the *connectome*, *i.e.*, the full connectivity structure of brains [Sporns et al., 2005]. The comprehensive study of large, complex datasets such as the human neuroimaging connectome necessitates systematic analytical approaches that provide quantifiable, neurobiologically meaningful measures. In the context of complex network analysis, *graph theory* is a robust mathematical framework that can characterize the functional or structural properties of the brain by modelling it as a single network [Rubinov and Sporns, 2010].

In fMRI graph-theoretical analyses, neural networks – the *graphs* – are a collection of anatomical brain regions – the *nodes* –, linked by *edges*, usually consisting of the functional connectivity between nodes. Nodes are the basic elements of a network, assumed to represent its functional units. At the microscale, single neurons present themselves as ideal network nodes. Since only the macroscalar organization of the connectome is accessible to neuroimaging methods, network nodes should comprise regions as functionally homogeneous as possible, with a coherent pattern of functional connections [Rubinov and Sporns, 2010].

The problem of node definition

There is no consensual approach to the definition of brain nodes in neuroimaging studies. This is a relevant issue as different parcellation strategies can result in different network topological properties [Wang et al., 2009]; networks obtained with different schemes are therefore not quantitatively comparable [Rubinov and Sporns, 2010]. The most-frequently used parcellation scheme in fMRI studies divides the brain GM into 90 cortical and subcortical regions from the Automated Anatomical Labelling (AAL) atlas [Tijms et al., 2013; Tzourio-Mazoyer et al., 2002]. Several other approaches have been employed at varying resolutions, including the computationally expensive and noise-sensitive voxel-wise approaches, that reach the highest resolution permitted by the fMRI acquisition [Hayasaka and Laurienti, 2010; van den Heuvel et al., 2008].

Two nodes are said to be *neighbors* if a connection or edge is considered to exist between them; in functional networks, however, every pair of nodes will have a corresponding correlation coefficient (see Figure 1.7). Weak links possibly represent spurious connections and are often discarded through the use of arbitrary thresholds – either absolute (*i.e.*, setting a correlation-coefficient cutoff) or relative [Rubinov and Sporns, 2010]. Relative (or *sparsity*) thresholds maintain a given percentage of connections; applied to group analyses in which the number of nodes is frequently fixed, relative thresholding ensures that all subjects' resulting networks will have an equal number of edges and equal network density, making them more suitable for comparison [van Wijk et al., 2010]. One possible caveat of this approach in group analyses is the existence of subject networks with low overall connectivity alongside networks with higher connectivity. The former may have weak, possibly noise-related connections included in the thresholded network; in the latter, on the other hand, strong and significant connections might be discarded [van Wijk et al., 2010].

Careful data inspection is therefore warranted in order to avoid biasing the topology of the reconstructed networks.

Network metrics are frequently obtained across a range of thresholds to assess their consistency [Bullmore and Sporns, 2009]. After the thresholding procedure, the resulting correlation matrix can be binarized; alternatively, internodal correlation coefficients can be used as edge weights to obtain weighted graph measures [Bullmore and Sporns, 2009].

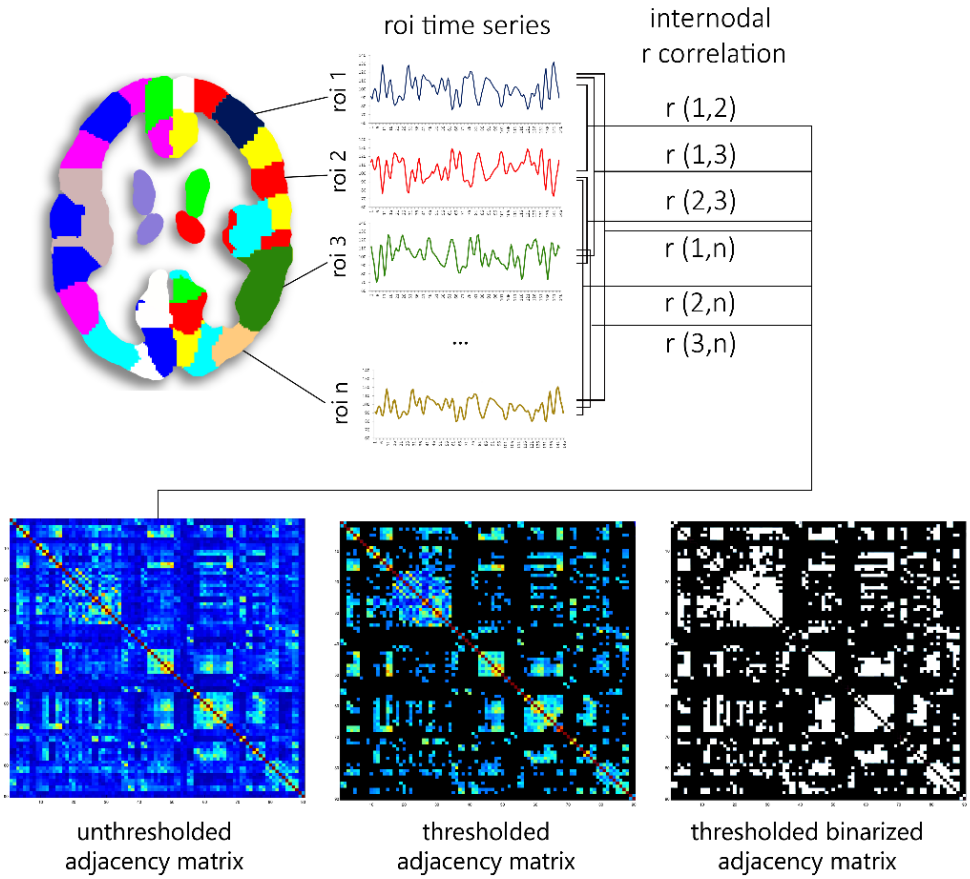

Figure 1.7. Schematic representation of the correlation procedure to define brain networks. In its simplest form, functional connectivity between a given pair of node is defined by the Pearson correlation between their respective time series. An adjacency matrix representing all internodal correlation coefficient is thus produced, and subsequently thresholded.

Graph theory metrics inform on different global and local topological network properties. The *characteristic path length* of a node informs about how closely this node is connected to all other network nodes. It is given by the average shortest distance between this node and every other node in the network, or, put differently, the average number of edges that need to be traversed in order to get from this node to any other node. *Network integration* is given by the *global characteristic path length*, which is the average of the characteristic path lengths of all network nodes. A related measure, the *global efficiency*, is inversely proportional to the

global characteristic path length. The *clustering coefficient* of a node, on the other hand, gives information about how interconnected this node's neighbors are. It is given by the ratio of the number of edges between this node's neighbors and the total number of possible such edges. For example, if node *a* has 3 neighbors, *b*, *c* and *d*, the maximum number of undirected edges between the latter is 3; if only one connection is present (*e.g.*, between *b* and *d*), the clustering coefficient of *a* is 1/3. The *global clustering coefficient*, given by the average of the clustering coefficients of all nodes in a network is a measure of local connectedness or *network segregation*. Networks that display a balance between global characteristic path length and clustering coefficients are considered to be *small-world networks*, characterized by high local specialization (high clustering) and some global *shortcuts* (low path length), allowing fast information transfer [Sporns and Honey, 2006; Watts and Strogatz, 1998] (Figure 1.8). The human connectome displays small-world topology in both functional and structural networks [Achard et al., 2006; Sporns and Honey, 2006].

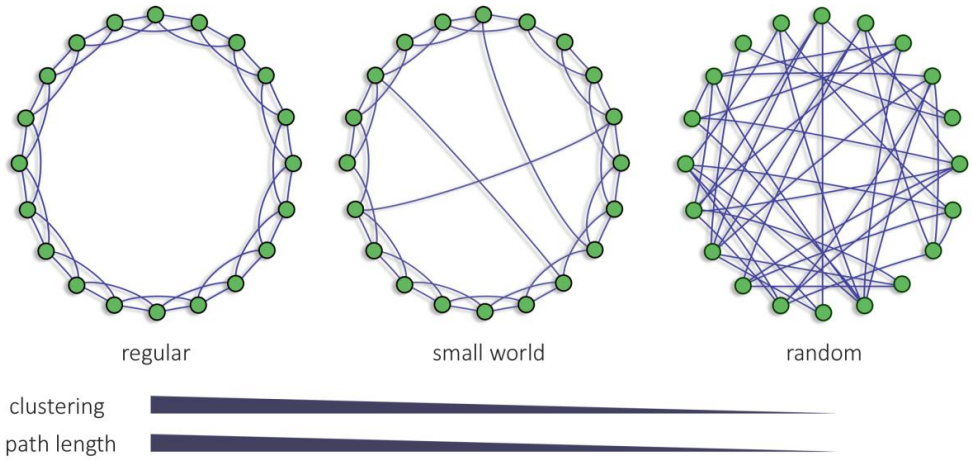

Figure 1.8. Small-world network topology. Small-world networks display topological characteristics that lie between prototypical regular (highly clustered, little integrated) and random (small internodal distances, low interconnectedness) networks of equal average degree (4).

The *degree* of a node, defined by the total number of input or output connections linked to it, gives information about this node's accessibility and influence inside the network. Degree in neural networks follows a heavy-tailed distribution, denoting the presence of a set of highly-connected nodes [van den Heuvel and Sporns, 2011]. These putative neural *hubs* are hypothesized to play a central role in overall network information transfer [van den Heuvel and Sporns, 2013]. Importantly, hub regions appear to be preferentially affected in several brain disorders [Crossley et al., 2014]

Finally, the *modularity* indicates how well a network can be subdivided into well-defined modules or *communities* made up of densely interconnected nodes with few intermodular connections, which may represent the network's functional subcomponents.

resting-state fMRI connectivity in PD – previous studies

Considering the prominent role played by dopamine deficits in nigrostriatal circuits, several studies in PD have focused on resting-state striatal connectivity using seed-based and ICA techniques. Perhaps as a result of patient samples with different clinical characteristics, as well as different methodological procedures, the observed results are not uniform. Studies using seed-to-whole brain approaches have found reduced connectivity between the striatum, especially the putamen, and diffuse cortical/mesolimbic areas in PD patients off medication [Agosta et al., 2014; Helmich et al., 2010; Luo et al., 2014]. In PD patients on medication, reduced connectivity between the striatum and thalamic/brainstem/cerebellar regions and increased connectivity between the striatum and motor/premotor cortical areas have been described [Agosta et al., 2014; Hacker et al., 2012; Yu et al., 2013]. Using ICA and dual regression, Szewczyk-Krolikowski described reduced connectivity of widespread frontal, temporal, parietal cortical as well as striatal and brainstem regions with the basal ganglia network in patients off medication compared with HC as well as compared with patients on medication [Szewczyk-Krolikowski et al., 2014]. Taken together, these study results indicate that dopamine deficits in PD lead to reduced functional corticostriatal connectivity, mainly involving the portions of the striatum most affected by dopaminergic nigrostriatal denervation, *i.e.*, the posterior putamen.

Baudrexel *et al.* used a seed-to-whole brain approach to assess basal ganglia connectivity changes in PD patients in the *off* state, but focused on the subthalamic nucleus. The authors found increased connectivity between this nucleus and primary sensorimotor cortical regions, mainly in the hand area [Baudrexel et al., 2011]. A recent study confirmed these findings in early, drug naïve as well as in *off*-state moderate-PD patients [Kurani et al., 2014].

There is, furthermore, evidence that PD patients have altered patterns of connectivity in other, cognitively relevant ICNs. As in other diseases, the most studied network is the DMN; changes in its patterns of activation and deactivation have been observed in task-based analyses [Eimeren and Monchi, 2009; Ibarretxe-Bilbao et al., 2011]. In resting-state fMRI studies, results are not always consistent, which may be related to the small study samples used, different methodologies and – importantly – insufficient reporting and controlling of head motion. Using ICA, Tessitore *et al.* found decreased intra-DMN resting-state connectivity in *on*-state PD patients with normal cognition, specifically in the medial temporal lobe and inferior parietal cortex. Additionally, connectivity in the medial temporal lobe correlated with memory performance, whereas connectivity in the parietal lobe correlated with visuospatial scores [Tessitore et al., 2012b]. Gorges *et al.*, in turn, used a seed-to-seed approach to DMN analysis and observed reduced functional connectivity between the medial PFC and the posterior cingulate cortex (PCC), as well as increased connectivity between left and right hippocampi [Gorges et al., 2013]. Comparing 24 PD patients in the *on* state (12 with visual hallucinations and 12 without) and 14 HC through an ICA-dual regression approach, Yao *et al*. found reduced intra-DMN resting-state functional connectivity in both PD groups. Additionally, patients with hallucinations were seen to have connectivity increases in the right frontal pole and in the precuneus/PCC, compared with patients without hallucinations [Yao et al., 2014].

Shine *et al.* also assessed a small group of PD patients in the *on* state according to the presence (n=9) or absence (n=13) of visual hallucinations, without a HC group. The authors used a seed-to-seed approach to evaluate the ventral attention/salience network, the DAN and the DMN, and found reduced connectivity between a DAN node (dorsal ACC) and a DMN node (anterior inferior parietal lobule) in patients with hallucinations [Shine et al., 2014].

Changes in FPN resting-state functional connectivity have also been reported. Tessitore *et al.* evaluated 15 HC and 29 PD patients in the *on* state – 16 of them with freezing of gait. The authors found reduced intra-right FPN connectivity in the subgroup with freezing of gait – which also had worse performance in attention/executive tests [Tessitore et al., 2012a].

To this date, very few studies have evaluated patterns of resting-state connectivity in PD using graph-theory approaches. Göttlich *et al.* compared 37 PD patients in the *on* state and 20 HC, using different parcellation schemes and applying a relative (sparsity) threshold range of 10-35% to construct binary networks. The authors found significantly higher clustering coefficients and characteristic path lengths in the PD group at 10 and 15% sparsity [Göttlich et al., 2013]. In a recent study, Lebedev *et al.* assessed a sample of 30 drug-naïve PD patients through a comprehensive neuropsychological battery and resting-state fMRI, as well as with DaTSCAN in a subsample. The authors observed that better performance in executive function tests was associated with higher nodal strength (sum of individual strengths of a node's links) in dorsal frontal and parietal regions; additionally, this pattern correlated positively with nigrostriatal dopaminergic function [Lebedev et al., 2014].

An underexplored field

Most published resting-state functional connectivity studies in PD haven't addressed the changes underlying cognitive impairment. And most studies that evaluated cognitive variables or cognitively-relevant networks suffer from methodological limitations, such as small sample sizes, absence of healthy control groups or insufficient control of motion artifacts. As a consequence, knowledge regarding the functional substrates of cognitive decline in PD is currently very limited.

Strong evidence from studies with healthy samples as well as with PD patients indicates that dopaminergic neurotransmission modulates resting-state functional connectivity as well as the dynamic balance between distinct ICNs. As exposed above, Szewczyk-Krolikowski *et al.* demonstrated that PD-related reductions in basal ganglia connectivity are reverted by dopaminergic medication [Szewczyk-Krolikowski et al., 2014]. Additionally, Cole *et al.* have shown that dopamine manipulation exerts linear and non-linear effects on corticostriatal connectivity, and linear effects on DMN connectivity in healthy subjects [Cole et al., 2013]. Dang *et al.*, in turn, found that subjects with higher dopamine synthesis capacity had higher resting-state functional connectivity between the DMN and the FPN, and reduced connectivity between the DMN and the DAN [Dang et al., 2012]. Finally, global resting-state brain connectivity has also been shown to be affected by dopamine

neurotransmission; Achard and Bullmore found that dopamine antagonism led to reduced global and local efficiency [Achard and Bullmore, 2007].

As such, and considering the functional substrates of cognitive deficits in PD under the perspective of the *dual syndrome* hypothesis discussed above, some connectivity changes in PD patients would be expected to be related to dopamine deficiency, whereas others would be independent from it.

Dopamine as a complex confounding factor

PD-related functional connectivity changes cannot be expected to manifest themselves as a linear global reduction in dopamine functional connectivity effects. Dopamine depletion in PD patients occurs unevenly across the dopaminergic system – midbrain dopaminergic neuron loss progresses heterogeneously [Damier et al., 1999; Hirsch et al., 1988]; affected areas thus coexist with spared areas. On the other hand, dopaminergic medication will exert its effects globally; in treated patients, therefore, areas of *dopaminergic overstimulation*, areas of relatively *normal neurotransmission* and *hypodopaminergic areas* will conceivably coexist.

Even discounting the possible effects of levodopa on non-dopaminergic neurons [Brown et al., 1999] and the theorized inverted U-shaped effect of dopamine on functional connectivity [Cole et al., 2013] – which might make hyper and hypodopaminergic states *look similar* –, the relationship between dopamine deficiency, dopaminergic treatment and functional connectivity changes in PD is a complex one. Assessing subjects in the *off* state can provide useful information; however, it doesn't solve the problem since the connectivity pattern observed will not reflect the actual substrates of dopamine-related cognitive deficits as they occur in patients' daily lives – *i.e.*, under the effect of their usual medication. Assessing patients in the *on* and *off* states would be the ideal study design, but differential state-related motion artifacts could bias the results.

REFERENCES

1. Aarsland D, Brønnick K, Ehrt U, De Deyn PP, Tekin S, Emre M, Cummings JL (2007a): Neuropsychiatric symptoms in patients with Parkinson's disease and dementia: frequency, profile and associated care giver stress. J Neurol Neurosurg Psychiatry 78:36–42.
2. Aarsland D, Brønnick K, Larsen JP, Tysnes OB, Alves G, Norwegian ParkWest Study Group (2009a): Cognitive impairment in incident, untreated Parkinson disease: the Norwegian ParkWest study. Neurology 72:1121–1126.
3. Aarsland D, Bronnick K, Williams-Gray C, Weintraub D, Marder K, Kulisevsky J, Burn D, Barone P, Pagonabarraga J, Allcock L, Santangelo G, Foltynie T, Janvin C, Larsen JP, Barker RA, Emre M (2010): Mild cognitive impairment in Parkinson disease: a multicenter pooled analysis. Neurology 75:1062–9.
4. Aarsland D, Kurz MW (2010): The epidemiology of dementia associated with Parkinson disease. J Neurol Sci 289:18–22.
5. Aarsland D, Kvaløy JT, Andersen K, Larsen JP, Tang MX, Lolk A, Kragh-Sørensen P, Marder K (2007b): The effect of age of onset of PD on risk of dementia. J Neurol 254:38–45.
6. Aarsland D, Larsen JP, Lim NG, Janvin C, Karlsen K, Tandberg E, Cummings JL (1999): Range of neuropsychiatric disturbances in patients with Parkinson's disease. J Neurol Neurosurg Psychiatry 67:492–6.
7. Aarsland D, Marsh L, Schrag A (2009b): Neuropsychiatric symptoms in Parkinson's disease. Mov Disord 24:2175–86.
8. Aarsland D, Perry R, Brown A, Larsen JP, Ballard C (2005): Neuropathology of dementia in Parkinson's disease: a prospective, community-based study. Ann Neurol 58:773–6.
9. Aarsland D, Taylor J-P, Weintraub D (2014): Psychiatric issues in cognitive impairment. Mov Disord 29:651–62.
10. Achard S, Bullmore E (2007): Efficiency and cost of economical brain functional networks. PLoS Comput Biol 3:e17.
11. Achard S, Salvador R, Whitcher B, Suckling J, Bullmore E (2006): A resilient, low-frequency, small-world human brain functional network with highly connected association cortical hubs. J Neurosci 26:63–72.
12. Agosta F, Canu E, Stefanova E, Sarro L, Tomić A, Spica V, Comi G, Kostić VS, Filippi M (2013): Mild cognitive impairment in Parkinson's disease is associated with a distributed pattern of brain white matter damage. Hum Brain Mapp 00.
13. Agosta F, Caso F, Stankovic I, Inuggi A, Petrovic I, Svetel M, Kostic VS, Filippi M (2014): Cortico-striatal-thalamic network functional connectivity in hemiparkinsonism. Neurobiol Aging.
14. Alonso A, Rodríguez LAG, Logroscino G, Hernán MA (2009): Use of antidepressants and the risk of Parkinson's disease: a prospective study. J Neurol Neurosurg Psychiatry 80:671–4.
15. Anderson JP, Walker DE, Goldstein JM, de Laat R, Banducci K, Caccavello RJ, Barbour R, Huang J, Kling K, Lee M, Diep L, Keim PS, Shen X, Chataway T, Schlossmacher MG, Seubert P, Schenk D, Sinha S, Gai WP, Chilcote TJ (2006): Phosphorylation of Ser-129 is the dominant pathological modification of alpha-synuclein in familial and sporadic Lewy body disease. J Biol Chem 281:29739–52.
16. Anticevic A, Cole MW, Murray JD, Corlett PR, Wang X-J, Krystal JH (2012): The role of default network deactivation in cognition and disease. Trends Cogn Sci 16:584–92.
17. Apaydin H, Ahlskog JE, Parisi JE, Boeve BF, Dickson DW (2002): Parkinson disease neuropathology: later-developing dementia and loss of the levodopa response. Arch Neurol 59:102–12.
18. Ariatti A, Benuzzi F, Nichelli P (2008): Recognition of emotions from visual and prosodic cues in Parkinson's disease. Neurol Sci 29:219–227.
19. Arnsten AF (1998): Catecholamine modulation of prefrontal cortical cognitive function. Trends Cogn Sci 2:436–47.
20. Ascherio A, Zhang SM, Hernán MA, Kawachi I, Colditz GA, Speizer FE, Willett WC (2001): Prospective study of caffeine consumption and risk of Parkinson's disease in men and women. Ann Neurol 50:56–63.
21. Ashburner J, Friston KJ (2000): Voxel-based morphometry--the methods. Neuroimage 11:805–21.
22. Ashburner J, Friston KJ (2001): Why voxel-based morphometry should be used. Neuroimage 14:1238–43.
23. Bajaj N, Hauser RA, Grachev ID (2013): Clinical utility of dopamine transporter single photon emission CT (DaT-SPECT) with (123I) ioflupane in diagnosis of parkinsonian syndromes. J Neurol Neurosurg Psychiatry 84:1288–95.
24. Baudrexel S, Witte T, Seifried C, von Wegner F, Beissner F, Klein JC, Steinmetz H, Deichmann R, Roeper J, Hilker R (2011): Resting state fMRI reveals increased subthalamic nucleus-motor cortex connectivity in Parkinson's disease. Neuroimage 55:1728–38.
25. Beaulieu C (2002): The basis of anisotropic water diffusion in the nervous system - a technical review. NMR Biomed 15:435–55.
26. Beckmann CF, Smith SM (2004): Probabilistic independent component analysis for functional magnetic resonance imaging. IEEE Trans Med Imaging 23:137–52.
27. Behzadi Y, Restom K, Liau J, Liu TT (2007): A component based noise correction method (CompCor) for BOLD and perfusion based fMRI. Neuroimage 37:90–101.
28. Benjamini Y (2010): Discovering the false discovery rate. J R Stat Soc Ser B (Statistical Methodol 72:405–416.
29. Bennett CM, Wolford GL, Miller MB (2009): The principled control of false positives in neuroimaging. Soc Cogn Affect Neurosci 4:417–22.
30. Berry C, La Vecchia C, Nicotera P (2010): Paraquat and Parkinson's disease. Cell Death Differ 17:1115–25.
31. Beyer MK, Bronnick KS, Hwang KS, Bergsland N, Tysnes OB, Larsen JP, Thompson PM, Somme JH, Apostolova LG (2013): Verbal memory is associated with structural hippocampal changes in newly diagnosed Parkinson's disease. J Neurol Neurosurg Psychiatry 84:23–8.

32. Beyer MK, Janvin CC, Larsen JP, Aarsland D (2007): A magnetic resonance imaging study of patients with Parkinson's disease with mild cognitive impairment and dementia using voxel-based morphometry. J Neurol Neurosurg Psychiatry 78:254–259.
33. Le Bihan D (2003): Looking into the functional architecture of the brain with diffusion MRI. Nat Rev Neurosci 4:469–80.
34. Biswal B, Yetkin FZ, Haughton VM, Hyde JS (1995): Functional connectivity in the motor cortex of resting human brain using echo-planar MRI. Magn Reson Med 34:537–41.
35. Boller F, Passafiume D, Keefe NC, Rogers K, Morrow L, Kim Y (1984): Visuospatial impairment in Parkinson's disease. Role of perceptual and motor factors. Arch Neurol 41:485–90.
36. Bookstein FL (2001): "Voxel-based morphometry" should not be used with imperfectly registered images. Neuroimage 14:1454–62.
37. Boubela RN, Kalcher K, Huf W, Kronnerwetter C, Filzmoser P, Moser E (2013): Beyond Noise: Using Temporal ICA to Extract Meaningful Information from High-Frequency fMRI Signal Fluctuations during Rest. Front Hum Neurosci 7:168.
38. Braak H, Rüb U, Jansen Steur ENH, Del Tredici K, de Vos RAI (2005): Cognitive status correlates with neuropathologic stage in Parkinson disease. Neurology 64:1404–10.
39. Braak H, Tredici K Del, Rüb U, de Vos R a. ., Jansen Steur EN., Braak E (2003): Staging of brain pathology related to sporadic Parkinson's disease. Neurobiol Aging 24:197–211.
40. Bressler SL, Menon V (2010): Large-scale brain networks in cognition: emerging methods and principles. Trends Cogn Sci 14:277–90.
41. Bressler SL, Tognoli E (2006): Operational principles of neurocognitive networks. Int J Psychophysiol 60:139–48.
42. Broeders M, de Bie RMA, Velseboer DC, Speelman JD, Muslimovic D, Schmand B (2013): Evolution of mild cognitive impairment in Parkinson disease. Neurology 81:346–52.
43. Brønnick K, Alves G, Aarsland D, Tysnes O-B, Larsen JP (2011): Verbal memory in drug-naive, newly diagnosed Parkinson's disease. The retrieval deficit hypothesis revisited. Neuropsychology 25:114–24.
44. Brown WD, Taylor MD, Roberts AD, Oakes TR, Schueller MJ, Holden JE, Malischke LM, DeJesus OT, Nickles RJ (1999): FluoroDOPA PET shows the nondopaminergic as well as dopaminergic destinations of levodopa. Neurology 53:1212–8.
45. Bullmore E, Sporns O (2009): Complex brain networks: graph theoretical analysis of structural and functional systems. Nat Rev Neurosci 10:186–98.
46. Burke RE, Dauer WT, Vonsattel JPG (2008): A critical evaluation of the Braak staging scheme for Parkinson's disease. Ann Neurol 64:485–91.
47. Burke RE, O'Malley K (2013): Axon degeneration in Parkinson's disease. Exp Neurol 246:72–83.
48. Burn D, Emre M, McKeith I, De Deyn PP, Aarsland D, Hsu C, Lane R (2006): Effects of rivastigmine in patients with and without visual hallucinations in dementia associated with Parkinson's disease. Mov Disord 21:1899–907.
49. Butterfield LC, Cimino CR, Oelke LE, Hauser R a, Sanchez-Ramos J (2010): The independent influence of apathy and depression on cognitive functioning in Parkinson's disease. Neuropsychology 24:721–30.
50. Carriere N, Besson P, Dujardin K, Duhamel A, Defebvre L, Delmaire C, Devos D (2014): Apathy in Parkinson's disease is associated with nucleus accumbens atrophy: A magnetic resonance imaging shape analysis. Mov Disord 00:1–7.
51. Caviness JN, Driver-Dunckley E, Connor DJ, Sabbagh MN, Hentz JG, Noble B, Evidente VGH, Shill HA, Adler CH (2007): Defining mild cognitive impairment in Parkinson's disease. Mov Disord 22:1272–7.
52. Chartier-Harlin M-C, Kachergus J, Roumier C, Mouroux V, Douay X, Lincoln S, Levecque C, Larvor L, Andrieux J, Hulihan M, Waucquier N, Defebvre L, Amouyel P, Farrer M, Destée A (2004): Alpha-synuclein locus duplication as a cause of familial Parkinson's disease. Lancet 364:1167–9.
53. Chen S, Townsend K, Goldberg TE, Davies P, Conejero-Goldberg C (2010): MAPT isoforms: differential transcriptional profiles related to 3R and 4R splice variants. J Alzheimers Dis 22:1313–29.
54. Chiaravalloti ND, Ibarretxe-Bilbao N, DeLuca J, Rusu O, Pena J, García-Gorostiaga I, Ojeda N (2014): The source of the memory impairment in Parkinson's disease: acquisition versus retrieval. Mov Disord 29:765–71.
55. Clinton LK, Blurton-Jones M, Myczek K, Trojanowski JQ, LaFerla FM (2010): Synergistic Interactions between Abeta, tau, and alpha-synuclein: acceleration of neuropathology and cognitive decline. J Neurosci 30:7281–9.
56. Cochrane CJ, Ebmeier KP (2013): Diffusion tensor imaging in parkinsonian syndromes: a systematic review and meta-analysis. Neurology 80:857–64.
57. Cole DM, Beckmann CF, Oei NYL, Both S, van Gerven JM a, Rombouts S a RB (2013): Differential and distributed effects of dopamine neuromodulations on resting-state network connectivity. Neuroimage 78:59–67.
58. Cole DM, Smith SM, Beckmann CF (2010): Advances and pitfalls in the analysis and interpretation of resting-state FMRI data. Front Syst Neurosci 4:8.
59. Compta Y, Ibarretxe-Bilbao N, Pereira JB, Junqué C, Bargalló N, Tolosa E, Valldeoriola F, Muñoz E, Camara A, Buongiorno M, Martí MJ (2012): Grey matter volume correlates of cerebrospinal markers of Alzheimer-pathology in Parkinson's disease and related dementia. Parkinsonism Relat Disord 18:941–7.
60. Compta Y, Parkkinen L, O'Sullivan SS, Vandrovcova J, Holton JL, Collins C, Lashley T, Kallis C, Williams DR, de Silva R, Lees AJ, Revesz T (2011): Lewy- and Alzheimer-type pathologies in Parkinson's disease dementia: which is more important? Brain 134:1493–505.
61. Connolly BS, Lang AE (2014): Pharmacological treatment of Parkinson disease: a review. JAMA 311:1670–83.
62. Cools R, Barker RA, Sahakian BJ, Robbins TW (2001): Enhanced or Impaired Cognitive Function in Parkinson ' s Disease as a Function of Dopaminergic Medication and Task Demands. Cereb cortex:1136–1143.
63. Crosby N, Deane KH, Clarke CE (2003): Amantadine in Parkinson's disease. Cochrane database Syst Rev:CD003468.

64. Crossley NA, Mechelli A, Scott J, Carletti F, Fox PT, McGuire P, Bullmore ET (2014): The hubs of the human connectome are generally implicated in the anatomy of brain disorders. Brain .
65. Cubo E, Benito-León J, Coronell C, Armesto D (2012): Clinical correlates of apathy in patients recently diagnosed with Parkinson's disease: the ANIMO study. Neuroepidemiology 38:48–55.
66. Czernecki V, Schüpbach M, Yaici S, Lévy R, Bardinet E, Yelnik J, Dubois B, Agid Y (2008): Apathy following subthalamic stimulation in Parkinson disease: a dopamine responsive symptom. Mov Disord 23:964–9.
67. Dale AM, Fischl B, Sereno MI (1999): Cortical surface-based analysis. I. Segmentation and surface reconstruction. Neuroimage 9:179–94.
68. Dalrymple-Alford JC, Livingston L, MacAskill MR, Graham C, Melzer TR, Porter RJ, Watts R, Anderson TJ (2011): Characterizing mild cognitive impairment in Parkinson's disease. Mov Disord 26:629–36.
69. Damier P, Hirsch EC, Agid Y, Graybiel AM (1999): The substantia nigra of the human brain. II. Patterns of loss of dopamine-containing neurons in Parkinson's disease. Brain 122 (Pt 8:1437–48.
70. Dang LC, O'Neil JP, Jagust WJ (2012): Dopamine supports coupling of attention-related networks. J Neurosci 32:9582–7.
71. Daniel SE, Lees AJ (1993): Parkinson's Disease Society Brain Bank, London: overview and research. J Neural Transm Suppl 39:165–72.
72. Dauer W, Przedborski S (2003): Parkinson's disease: mechanisms and models. Neuron 39:889–909.
73. Dickson DW, Uchikado H, Fujishiro H, Tsuboi Y (2010): Evidence in favor of Braak staging of Parkinson's disease. Mov Disord 25 Suppl 1:S78–82.
74. Van Dijk KR a, Sabuncu MR, Buckner RL (2012): The influence of head motion on intrinsic functional connectivity MRI. Neuroimage 59:431–8.
75. Downes JJ, Roberts AC, Sahakian BJ, Evenden JL, Morris RG, Robbins TW (1989): Impaired extra-dimensional shift performance in medicated and unmedicated Parkinson's disease: evidence for a specific attentional dysfunction. Neuropsychologia 27:1329–43.
76. Dujardin K, Blairy S, Defebvre L, Duhem S, Noël Y, Hess U, Destée A (2004): Deficits in decoding emotional facial expressions in Parkinson's disease. Neuropsychologia 42:239–250.
77. Dujardin K, Sockeel P, Delliaux M, Destée A, Defebvre L (2009): Apathy may herald cognitive decline and dementia in Parkinson's disease. Mov Disord 24:2391–7.
78. Dujardin K, Sockeel P, Devos D, Delliaux M, Krystkowiak P, Destée A, Defebvre L (2007): Characteristics of apathy in Parkinson's disease. Mov Disord 22:778–84.
79. Ehmann TS, Beninger RJ, Gawel MJ, Riopelle RJ (1990): Depressive symptoms in Parkinson's disease: a comparison with disabled control subjects. J Geriatr Psychiatry Neurol 3:3–9.
80. Eimeren MT van, Monchi O (2009): Dysfunction of the Default Mode Network in Parkinson Disease. Arch Neurol 66:877–883.
81. Elgh E, Domellöf M, Linder J, Edström M, Stenlund H, Forsgren L (2009): Cognitive function in early Parkinson's disease: a population-based study. Eur J Neurol 16:1278–84.
82. Emre M (2003): Dementia associated with Parkinson's disease. Lancet Neurol 2:229–37.
83. Erhardt EB, Rachakonda S, Bedrick EJ, Allen EA, Adali T, Calhoun VD (2011): Comparison of multi-subject ICA methods for analysis of fMRI data. Hum Brain Mapp 32:2075–95.
84. Fahn S, Oakes D, Shoulson I, Kieburtz K, Rudolph A, Lang A, Olanow CW, Tanner C, Marek K (2004): Levodopa and the progression of Parkinson's disease. N Engl J Med 351:2498–508.
85. Fang F, Xu Q, Park Y, Huang X, Hollenbeck A, Blair A, Schatzkin A, Kamel F, Chen H (2010): Depression and the subsequent risk of Parkinson's disease in the NIH-AARP Diet and Health Study. Mov Disord 25:1157–62.
86. Feldmann A, Illes Z, Kosztolanyi P, Illes E, Mike A, Kover F, Balas I, Kovacs N, Nagy F (2008): Morphometric changes of gray matter in Parkinson's disease with depression: a voxel-based morphometry study. Mov Disord 23:42–6.
87. Ferrer I (2011): Neuropathology and neurochemistry of nonmotor symptoms in Parkinson's disease. Parkinsons Dis 2011:708404.
88. Filippini N, MacIntosh BJ, Hough MG, Goodwin GM, Frisoni GB, Smith SM, Matthews PM, Beckmann CF, Mackay CE (2009): Distinct patterns of brain activity in young carriers of the APOE-epsilon4 allele. Proc Natl Acad Sci U S A 106:7209–14.
89. Filoteo JV, Reed JD, Litvan I, Harrington DL (2014): Volumetric correlates of cognitive functioning in nondemented patients with Parkinson's disease. Mov Disord 29:360–7.
90. Fischl B, Dale AM (2000): Measuring the thickness of the human cerebral cortex from magnetic resonance images. Proc Natl Acad Sci U S A 97:11050–11055.
91. Fischl B, Sereno MI, Dale AM (1999): Cortical surface-based analysis. II: Inflation, flattening, and a surface-based coordinate system. Neuroimage 9:195–207.
92. Forsaa EB, Larsen JP, Wentzel-Larsen T, Goetz CG, Stebbins GT, Aarsland D, Alves G (2010): A 12-year population-based study of psychosis in Parkinson disease. Arch Neurol 67:996–1001.
93. Fox MD, Corbetta M, Snyder AZ, Vincent JL, Raichle ME (2006): Spontaneous neuronal activity distinguishes human dorsal and ventral attention systems. Proc Natl Acad Sci U S A 103:10046–51.
94. Fox MD, Snyder AZ, Vincent JL, Corbetta M, Van Essen DC, Raichle ME (2005): The human brain is intrinsically organized into dynamic, anticorrelated functional networks. Proc Natl Acad Sci U S A 102:9673–8.
95. Gallagher DA, Schrag A (2012): Psychosis, apathy, depression and anxiety in Parkinson's disease. Neurobiol Dis 46:581–9.
96. Gattellaro G, Minati L, Grisoli M, Mariani C, Carella F, Osio M, Ciceri E, Albanese A, Bruzzone MG (2009): White matter involvement in idiopathic Parkinson disease: a diffusion

tensor imaging study. AJNR Am J Neuroradiol 30:1222–1226.
97. Ghosh SS, Kakunoori S, Augustinack J, Nieto-Castanon A, Kovelman I, Gaab N, Christodoulou JA, Triantafyllou C, Gabrieli JDE, Fischl B (2010): Evaluating the validity of volume-based and surface-based brain image registration for developmental cognitive neuroscience studies in children 4 to 11 years of age. Neuroimage 53:85–93.
98. Goetz CG, Fahn S, Martinez-Martin P, Poewe W, Sampaio C, Stebbins GT, Stern MB, Tilley BC, Dodel R, Dubois B, Holloway R, Jankovic J, Kulisevsky J, Lang AE, Lees A, Leurgans S, LeWitt PA, Nyenhuis D, Olanow CW, Rascol O, Schrag A, Teresi JA, Van Hilten JJ, LaPelle N (2007): Movement Disorder Society-sponsored revision of the Unified Parkinson's Disease Rating Scale (MDS-UPDRS): Process, format, and clinimetric testing plan. Mov Disord 22:41–7.
99. Goetz CG, Poewe W, Rascol O, Sampaio C, Stebbins GT, Counsell C, Giladi N, Holloway RG, Moore CG, Wenning GK, Yahr MD, Seidl L (2004): Movement Disorder Society Task Force report on the Hoehn and Yahr staging scale: status and recommendations. Mov Disord 19:1020–8.
100. Goetz CG, Stebbins GT (2004): Assuring interrater reliability for the UPDRS motor section: utility of the UPDRS teaching tape. Mov Disord 19:1453–6.
101. Goetz CG, Tilley BC, Shaftman SR, Stebbins GT, Fahn S, Martinez-Martin P, Poewe W, Sampaio C, Stern MB, Dodel R, Dubois B, Holloway R, Jankovic J, Kulisevsky J, Lang AE, Lees A, Leurgans S, LeWitt PA, Nyenhuis D, Olanow CW, Rascol O, Schrag A, Teresi JA, van Hilten JJ, LaPelle N (2008): Movement Disorder Society-sponsored revision of the Unified Parkinson's Disease Rating Scale (MDS-UPDRS): scale presentation and clinimetric testing results. Mov Disord 23:2129–70.
102. Goldman JG, Holden S, Bernard B, Ouyang B, Goetz CG, Stebbins GT (2013): Defining optimal cutoff scores for cognitive impairment using Movement Disorder Society Task Force criteria for mild cognitive impairment in Parkinson's disease. Mov Disord 28:1972–9.
103. Goldman JG, Litvan I (2011): Mild cognitive impairment in Parkinson's disease. Minerva Med 102:441–59.
104. Good CD, Johnsrude IS, Ashburner J, Henson RN, Friston KJ, Frackowiak RS (2001): A voxel-based morphometric study of ageing in 465 normal adult human brains. Neuroimage 14:21–36.
105. Gorges M, Müller H-P, Lulé D, Ludolph AC, Pinkhardt EH, Kassubek J (2013): Functional connectivity within the default mode network is associated with saccadic accuracy in Parkinson's disease: a resting-state FMRI and videooculographic study. Brain Connect 3:265–72.
106. Goris A, Williams-Gray CH, Clark GR, Foltynie T, Lewis SJG, Brown J, Ban M, Spillantini MG, Compston A, Burn DJ, Chinnery PF, Barker RA, Sawcer SJ (2007): Tau and alpha-synuclein in susceptibility to, and dementia in, Parkinson's disease. Ann Neurol 62:145–53.
107. Gotham AM, Brown RG, Marsden CD (1986): Levodopa treatment may benefit or impair "frontal" function in Parkinson's disease. Lancet 2:970–1.
108. Göttlich M, Münte TF, Heldmann M, Kasten M, Hagenah J, Krämer UM (2013): Altered resting state brain networks in Parkinson's disease. PLoS One 8:e77336.
109. Greicius MD, Krasnow B, Reiss AL, Menon V (2003): Functional connectivity in the resting brain: a network analysis of the default mode hypothesis. Proc Natl Acad Sci U S A 100:253–258.
110. Greicius MD, Srivastava G, Reiss AL, Menon V (2004): Default-mode network activity distinguishes Alzheimer's disease from healthy aging: evidence from functional MRI. Proc Natl Acad Sci U S A 101:4637–42.
111. Griffanti L, Salimi-Khorshidi G, Beckmann CF, Auerbach EJ, Douaud G, Sexton CE, Zsoldos E, Ebmeier KP, Filippini N, Mackay CE, Moeller S, Xu J, Yacoub E, Baselli G, Ugurbil K, Miller KL, Smith SM (2014): ICA-based artefact removal and accelerated fMRI acquisition for improved resting state network imaging. Neuroimage 95:232–47.
112. Gusnard DA, Raichle ME (2001): Searching for a baseline: functional imaging and the resting human brain. Nat Rev Neurosci 2:685–94.
113. Haber SN (2011): Neuroanatomy of Reward: A View from the Ventral Striatum. In: Gottfried, J, editor. Neurobiology of Sensation and Reward. Boca Raton (FL): CRC Press.
114. Hacker CD, Perlmutter JS, Criswell SR, Ances BM, Snyder AZ (2012): Resting state functional connectivity of the striatum in Parkinson's disease. Brain 135:3699–711.
115. Hall H, Reyes S, Landeck N, Bye C, Leanza G, Double K, Thompson L, Halliday G, Kirik D (2014): Hippocampal Lewy pathology and cholinergic dysfunction are associated with dementia in Parkinson's disease. Brain.
116. Halliday GM, Hely M, Reid W, Morris J (2008): The progression of pathology in longitudinally followed patients with Parkinson's disease. Acta Neuropathol 115:409–15.
117. Halliday GM, Del Tredici K, Braak H (2006): Critical appraisal of brain pathology staging related to presymptomatic and symptomatic cases of sporadic Parkinson's disease. J Neural Transm Suppl:99–103.
118. Hanganu A, Bedetti C, Degroot C, Mejia-Constain B, Lafontaine A-L, Soland V, Chouinard S, Bruneau M-A, Mellah S, Belleville S, Monchi O (2014): Mild cognitive impairment is linked with faster rate of cortical thinning in patients with Parkinson's disease longitudinally. Brain 137:1120–9.
119. Hanganu A, Bedetti C, Jubault T, Gagnon J-F, Mejia-Constain B, Degroot C, Lafontaine A-L, Chouinard S, Monchi O (2013): Mild cognitive impairment in patients with Parkinson's disease is associated with increased cortical degeneration. Mov Disord 28:1360–9.
120. Harding AJ, Halliday GM (2001): Cortical Lewy body pathology in the diagnosis of dementia. Acta Neuropathol 102:355–63.
121. Hattori T, Orimo S, Aoki S, Ito K, Abe O, Amano A, Sato R, Sakai K, Mizusawa H (2012): Cognitive status correlates with white matter alteration in Parkinson's disease. Hum Brain Mapp 33:727–39.
122. Hayasaka S, Laurienti PJ (2010): Comparison of characteristics between region-and voxel-based network analyses in resting-state fMRI data. Neuroimage 50:499–508.

123. Helmich RC, Derikx LC, Bakker M, Scheeringa R, Bloem BR, Toni I (2010): Spatial remapping of cortico-striatal connectivity in Parkinson's disease. Cereb Cortex 20:1175–86.
124. Hely MA, Morris JG, Traficante R, Reid WG, O'Sullivan DJ, Williamson PM (1999): The sydney multicentre study of Parkinson's disease: progression and mortality at 10 years. J Neurol Neurosurg Psychiatry 67:300–7.
125. Hernan MA, Zhang SM, Rueda-DeCastro AM, Colditz GA, Speizer FE, Ascherio A (2001): Cigarette smoking and the incidence of Parkinson's disease in two prospective studies. Ann Neurol 50:780–786.
126. Van den Heuvel MP, Sporns O (2011): Rich-club organization of the human connectome. J Neurosci 31:15775–86.
127. Van den Heuvel MP, Sporns O (2013): Network hubs in the human brain. Trends Cogn Sci 17:683–96.
128. Van den Heuvel MP, Stam CJ, Boersma M, Hulshoff Pol HE (2008): Small-world and scale-free organization of voxel-based resting-state functional connectivity in the human brain. Neuroimage 43:528–39.
129. Hickey P, Stacy M (2011): Available and emerging treatments for Parkinson's disease: a review. Drug Des Devel Ther 5:241–54.
130. Higginson CI, King DS, Levine D, Wheelock VL, Khamphay NO, Sigvardt KA (2003): The relationship between executive function and verbal memory in Parkinson's disease. Brain Cogn 52:343–52.
131. Higginson CI, Wheelock VL, Carroll KE, Sigvardt KA (2005): Recognition memory in Parkinson's disease with and without dementia: evidence inconsistent with the retrieval deficit hypothesis. J Clin Exp Neuropsychol 27:516–28.
132. Hindle J V (2010): Ageing, neurodegeneration and Parkinson's disease. Age Ageing 39:156–61.
133. Hirsch E, Graybiel AM, Agid YA (1988): Melanized dopaminergic neurons are differentially susceptible to degeneration in Parkinson's disease. Nature 334:345–8.
134. Hoehn MM, Yahr MD (1967): Parkinsonism: onset, progression and mortality. Neurology 17:427–42.
135. Hurtig HI, Trojanowski JQ, Galvin J, Ewbank D, Schmidt ML, Lee VM, Clark CM, Glosser G, Stern MB, Gollomp SM, Arnold SE (2000): Alpha-synuclein cortical Lewy bodies correlate with dementia in Parkinson's disease. Neurology 54:1916–21.
136. Hutton C, Draganski B, Ashburner J, Weiskopf N (2009): A comparison between voxel-based cortical thickness and voxel-based morphometry in normal aging. Neuroimage 48:371–80.
137. Hwang KS, Beyer MK, Green AE, Chung C, Thompson PM, Janvin C, Larsen JP, Aarsland D, Apostolova LG (2013): Mapping cortical atrophy in Parkinson's disease patients with dementia. J Parkinsons Dis 3:69–76.
138. Ibarretxe-Bilbao N, Zarei M, Junque C, Marti MJ, Segura B, Vendrell P, Valldeoriola F, Bargallo N, Tolosa E (2011): Dysfunctions of cerebral networks precede recognition memory deficits in early Parkinson's disease. Neuroimage 57:589–97.
139. Ikeuchi T, Kakita A, Shiga A, Kasuga K, Kaneko H, Tan C-F, Idezuka J, Wakabayashi K, Onodera O, Iwatsubo T, Nishizawa M, Takahashi H, Ishikawa A (2008): Patients homozygous and heterozygous for SNCA duplication in a family with parkinsonism and dementia. Arch Neurol 65:514–9.
140. Iranzo A, Tolosa E, Gelpi E, Molinuevo JL, Valldeoriola F, Serradell M, Sanchez-Valle R, Vilaseca I, Lomeña F, Vilas D, Lladó A, Gaig C, Santamaria J (2013): Neurodegenerative disease status and post-mortem pathology in idiopathic rapid-eye-movement sleep behaviour disorder: an observational cohort study. Lancet Neurol 12:443–53.
141. Irwin DJ, White MT, Toledo JB, Xie SX, Robinson JL, Van Deerlin V, Lee VM-Y, Leverenz JB, Montine TJ, Duda JE, Hurtig HI, Trojanowski JQ (2012): Neuropathologic substrates of Parkinson disease dementia. Ann Neurol 72:587–98.
142. Isella V, Melzi P, Grimaldi M, Iurlaro S, Piolti R, Ferrarese C, Frattola L, Appollonio I (2002): Clinical, neuropsychological, and morphometric correlates of apathy in Parkinson's disease. Mov Disord 17:366–71.
143. Ishihara L, Brayne C (2006): A systematic review of depression and mental illness preceding Parkinson's disease. Acta Neurol Scand 113:211–20.
144. Israeli-Korn SD, Hocherman S, Hassin-Baer S, Cohen OS, Inzelberg R (2013): Subthalamic nucleus deep brain stimulation does not improve visuo-motor impairment in Parkinson's disease. PLoS One 8:e65270.
145. Jellinger KA (2008): A critical reappraisal of current staging of Lewy-related pathology in human brain. Acta Neuropathol 116:1–16.
146. Jellinger KA (2009): A critical evaluation of current staging of alpha-synuclein pathology in Lewy body disorders. Biochim Biophys Acta 1792:730–40.
147. Jellinger KA, Attems J (2008): Prevalence and impact of vascular and Alzheimer pathologies in Lewy body disease. Acta Neuropathol 115:427–36.
148. Jones DK, Knösche TR, Turner R (2013): White matter integrity, fiber count, and other fallacies: the do's and don'ts of diffusion MRI. Neuroimage 73:239–54.
149. Kägi G, Bhatia KP, Tolosa E (2010): The role of DAT-SPECT in movement disorders. J Neurol Neurosurg Psychiatry 81:5–12.
150. Kan Y, Kawamura M, Hasegawa Y, Mochizuki S, Nakamura K (2002): Recognition of emotion from facial, prosodic and written verbal stimuli in Parkinson's disease. Cortex 38:623–630.
151. Kehagia A a, Barker R a, Robbins TW (2010): Neuropsychological and clinical heterogeneity of cognitive impairment and dementia in patients with Parkinson's disease. Lancet Neurol 9:1200–13.
152. Kempster PA, O'Sullivan SS, Holton JL, Revesz T, Lees AJ (2010): Relationships between age and late progression of Parkinson's disease: a clinico-pathological study. Brain 133:1755–62.
153. Kirsch-Darrow L, Fernandez HH, Fernandez HF, Marsiske M, Okun MS, Bowers D (2006): Dissociating apathy and depression in Parkinson disease. Neurology 67:33–8.
154. Kirsch-Darrow L, Marsiske M, Okun MS, Bauer R, Bowers D (2011): Apathy and depression: separate factors in Parkinson's disease. J Int Neuropsychol Soc 17:1058–66.

155. Koshimori Y, Segura B, Christopher L, Lobaugh N, Duff-Canning S, Mizrahi R, Hamani C, Lang AE, Aminian K, Houle S, Strafella AP (2014): Imaging changes associated with cognitive abnormalities in Parkinson's disease. Brain Struct Funct.
156. Kostić VS, Agosta F, Petrović I, Galantucci S, Spica V, Jecmenica-Lukic M, Filippi M (2010): Regional patterns of brain tissue loss associated with depression in Parkinson disease. Neurology 75:857–63.
157. Kurani AS, Seidler RD, Burciu RG, Comella CL, Corcos DM, Okun MS, MacKinnon CD, Vaillancourt DE (2014): Subthalamic nucleus-sensorimotor cortex functional connectivity in de novo and moderate Parkinson's disease. Neurobiol Aging.
158. Lange KW, Robbins TW, Marsden CD, James M, Owen AM, Paul GM (1992): L-dopa withdrawal in Parkinson's disease selectively impairs cognitive performance in tests sensitive to frontal lobe dysfunction. Psychopharmacology (Berl) 107:394–404.
159. Langston JW, Ballard P, Tetrud JW, Irwin I (1983): Chronic Parkinsonism in humans due to a product of meperidine-analog synthesis. Science 219:979–80.
160. Lashley T, Holton JL, Gray E, Kirkham K, O'Sullivan SS, Hilbig A, Wood NW, Lees AJ, Revesz T (2008): Cortical alpha-synuclein load is associated with amyloid-beta plaque burden in a subset of Parkinson's disease patients. Acta Neuropathol 115:417–25.
161. De Lau LML, Breteler MMB (2006): Epidemiology of Parkinson's disease. Lancet Neurol 5:525–35.
162. Lebedev A V, Westman E, Simmons A, Lebedeva A, Siepel FJ, Pereira JB, Aarsland D (2014): Large-scale resting state network correlates of cognitive impairment in Parkinson's disease and related dopaminergic deficits. Front Syst Neurosci 8:45.
163. Lee JE, Park H-J, Song SK, Sohn YH, Lee JD, Lee PH (2010): Neuroanatomic basis of amnestic MCI differs in patients with and without Parkinson disease. Neurology 75:2009–16.
164. Leiknes I, Tysnes O-B, Aarsland D, Larsen JP (2010): Caregiver distress associated with neuropsychiatric problems in patients with early Parkinson's disease: the Norwegian ParkWest study. Acta Neurol Scand 122:418–24.
165. Leroi I, Andrews M, McDonald K, Harbishettar V, Elliott R, Byrne EJ, Burns A (2012a): Apathy and impulse control disorders in Parkinson's disease: a direct comparison. Parkinsonism Relat Disord 18:198–203.
166. Leroi I, Pantula H, McDonald K, Harbishettar V (2012b): Neuropsychiatric symptoms in Parkinson's disease with mild cognitive impairment and dementia. Parkinsons Dis 2012:308097.
167. Levin BE, Llabre MM, Reisman S, Weiner WJ, Sanchez-Ramos J, Singer C, Brown MC (1991): Visuospatial impairment in Parkinson's disease. Neurology 41:365–9.
168. Levy G, Schupf N, Tang M-X, Cote LJ, Louis ED, Mejia H, Stern Y, Marder K (2002): Combined effect of age and severity on the risk of dementia in Parkinson's disease. Ann Neurol 51:722–9.
169. Liang X, Wang J, Yan C, Shu N, Xu K, Gong G, He Y (2012): Effects of different correlation metrics and preprocessing factors on small-world brain functional networks: a resting-state functional MRI study. PLoS One 7:e32766.
170. Litvan I, Aarsland D, Adler CH, Goldman JG, Kulisevsky J, Mollenhauer B, Rodriguez-Oroz MC, Tröster AI, Weintraub D (2011): MDS Task Force on mild cognitive impairment in Parkinson's disease: critical review of PD-MCI. Mov Disord 26:1814–24.
171. Litvan I, Goldman JG, Tröster AI, Schmand B a, Weintraub D, Petersen RC, Mollenhauer B, Adler CH, Marder K, Williams-Gray CH, Aarsland D, Kulisevsky J, Rodriguez-Oroz MC, Burn DJ, Barker R a, Emre M (2012): Diagnostic criteria for mild cognitive impairment in Parkinson's disease: Movement Disorder Society Task Force guidelines. Mov Disord 27:349–56.
172. Luo C, Song W, Chen Q, Zheng Z, Chen K, Cao B, Yang J, Li J, Huang X, Gong Q, Shang H-F (2014): Reduced functional connectivity in early-stage drug-naive Parkinson's disease: a resting-state fMRI study. Neurobiol Aging 35:431–41.
173. Mak E, Bergsland N, Dwyer MG, Zivadinov R, Kandiah N (2014a): Subcortical Atrophy Is Associated with Cognitive Impairment in Mild Parkinson Disease: A Combined Investigation of Volumetric Changes, Cortical Thickness, and Vertex-Based Shape Analysis. AJNR Am J Neuroradiol.
174. Mak E, Zhou J, Tan LCS, Au WL, Sitoh YY, Kandiah N (2014b): Cognitive deficits in mild Parkinson's disease are associated with distinct areas of grey matter atrophy. J Neurol Neurosurg Psychiatry 85:576–80.
175. Marin RS (1990): Differential diagnosis and classification of apathy. Am J Psychiatry 147:22–30.
176. Maroteaux L, Campanelli JT, Scheller RH (1988): Synuclein: a neuron-specific protein localized to the nucleus and presynaptic nerve terminal. J Neurosci 8:2804–15.
177. Marques O, Outeiro TF (2012): Alpha-synuclein: from secretion to dysfunction and death. Cell Death Dis 3:e350.
178. Mechelli A, Price CJ, Friston KJ, Ashburner J (2005): Voxel-Based Morphometry of the Human Brain: Methods and Applications. Curr Med Imaging Rev 1:105–113.
179. Melzer TR, Watts R, MacAskill MR, Pitcher TL, Livingston L, Keenan RJ, Dalrymple-Alford JC, Anderson TJ (2012): Grey matter atrophy in cognitively impaired Parkinson's disease. J Neurol Neurosurg Psychiatry 83:188–94.
180. Melzer TR, Watts R, MacAskill MR, Pitcher TL, Livingston L, Keenan RJ, Dalrymple-Alford JC, Anderson TJ (2013): White matter microstructure deteriorates across cognitive stages in Parkinson disease. Neurology 80:1841–9.
181. Mevel K, Chételat G, Eustache F, Desgranges B (2011): The default mode network in healthy aging and Alzheimer's disease. Int J Alzheimers Dis 2011:535816.
182. Morgante L, Morgante F, Moro E, Epifanio A, Girlanda P, Ragonese P, Antonini A, Barone P, Bonuccelli U, Contarino MF, Capus L, Ceravolo MG, Marconi R, Ceravolo R, D'Amelio M, Savettieri G (2007): How many parkinsonian patients are suitable candidates for deep brain stimulation of subthalamic nucleus? Results of a questionnaire. Parkinsonism Relat Disord 13:528–31.
183. Morley JF, Xie SX, Hurtig HI, Stern MB, Colcher A, Horn S, Dahodwala N, Duda JE, Weintraub D, Chen-Plotkin AS, Van

Deerlin V, Falcone D, Siderowf A (2012): Genetic influences on cognitive decline in Parkinson's disease. Mov Disord 27:512–8.
184. Murphy K, Birn RM, Bandettini PA (2013): Resting-state fMRI confounds and cleanup. Neuroimage 80:349–59.
185. Muslimovic D, Post B, Speelman JD, Schmand B (2005): Cognitive profile of patients with newly diagnosed Parkinson disease. Neurology 65:1239–45.
186. Nagano-Saito A, Washimi Y, Arahata Y, Kachi T, Lerch JP, Evans AC, Dagher A, Ito K (2005): Cerebral atrophy and its relation to cognitive impairment in Parkinson disease. Neurology 64:224–9.
187. Nichols TE (2012): Multiple testing corrections, nonparametric methods, and random field theory. Neuroimage 62:811–5.
188. Nichols TE, Hayasaka S (2003): Controlling the familywise error rate in functional neuroimaging: a comparative review. Stat Methods Med Res 12:419–46.
189. Nikolaus S, Antke C, Müller H-W (2009): In vivo imaging of synaptic function in the central nervous system: I. Movement disorders and dementia. Behav Brain Res 204:1–31.
190. Nombela C, Rowe JB, Winder-Rhodes SE, Hampshire A, Owen AM, Breen DP, Duncan GW, Khoo TK, Yarnall AJ, Firbank MJ, Chinnery PF, Robbins TW, O'Brien JT, Brooks DJ, Burn DJ, Barker RA (2014): Genetic impact on cognition and brain function in newly diagnosed Parkinson's disease: ICICLE-PD study. Brain.
191. Noyce AJ, Bestwick JP, Silveira-Moriyama L, Hawkes CH, Giovannoni G, Lees AJ, Schrag A (2012): Meta-analysis of early nonmotor features and risk factors for Parkinson disease. Ann Neurol 72:893–901.
192. O'Malley KL (2010): The role of axonopathy in Parkinson's disease. Exp Neurobiol 19:115–9.
193. Okun MS, Fernandez HH, Wu SS, Kirsch-Darrow L, Bowers D, Bova F, Suelter M, Jacobson CE, Wang X, Gordon CW, Zeilman P, Romrell J, Martin P, Ward H, Rodriguez RL, Foote KD (2009): Cognition and mood in Parkinson's disease in subthalamic nucleus versus globus pallidus interna deep brain stimulation: the COMPARE trial. Ann Neurol 65:586–95.
194. Olanow CW, Brundin P (2013): Parkinson's disease and alpha synuclein: is Parkinson's disease a prion-like disorder? Mov Disord 28:31–40.
195. Olanow CW, Rascol O, Hauser R, Feigin PD, Jankovic J, Lang A, Langston W, Melamed E, Poewe W, Stocchi F, Tolosa E (2009): A double-blind, delayed-start trial of rasagiline in Parkinson's disease. N Engl J Med 361:1268–78.
196. Orimo S, Amino T, Itoh Y, Takahashi A, Kojo T, Uchihara T, Tsuchiya K, Mori F, Wakabayashi K, Takahashi H (2005): Cardiac sympathetic denervation precedes neuronal loss in the sympathetic ganglia in Lewy body disease. Acta Neuropathol 109:583–8.
197. Orimo S, Uchihara T, Nakamura A, Mori F, Kakita A, Wakabayashi K, Takahashi H (2008): Axonal alpha-synuclein aggregates herald centripetal degeneration of cardiac sympathetic nerve in Parkinson's disease. Brain 131:642–50.
198. Owen AM (2004): Cognitive dysfunction in Parkinson's disease: the role of frontostriatal circuitry. Neuroscientist 10:525–37.
199. Owen AM, Roberts AC, Hodges JR, Summers BA, Polkey CE, Robbins TW (1993): Contrasting mechanisms of impaired attentional set-shifting in patients with frontal lobe damage or Parkinson's disease. Brain 116 (Pt 5:1159–75.
200. Pagonabarraga J, Corcuera-Solano I, Vives-Gilabert Y, Llebaria G, García-Sánchez C, Pascual-Sedano B, Delfino M, Kulisevsky J, Gómez-Ansón B (2013): Pattern of regional cortical thinning associated with cognitive deterioration in Parkinson's disease. PLoS One 8:e54980.
201. Pahwa R, Factor SA, Lyons KE, Ondo WG, Gronseth G, Bronte-Stewart H, Hallett M, Miyasaki J, Stevens J, Weiner WJ (2006): Practice Parameter: treatment of Parkinson disease with motor fluctuations and dyskinesia (an evidence-based review): report of the Quality Standards Subcommittee of the American Academy of Neurology. Neurology 66:983–95.
202. Parkkinen L, Kauppinen T, Pirttilä T, Autere JM, Alafuzoff I (2005): Alpha-synuclein pathology does not predict extrapyramidal symptoms or dementia. Ann Neurol 57:82–91.
203. Parkkinen L, Pirttilä T, Alafuzoff I (2008): Applicability of current staging/categorization of alpha-synuclein pathology and their clinical relevance. Acta Neuropathol 115:399–407.
204. Patriat R, Molloy EK, Meier TB, Kirk GR, Nair VA, Meyerand ME, Prabhakaran V, Birn RM (2013): The effect of resting condition on resting-state fMRI reliability and consistency: a comparison between resting with eyes open, closed, and fixated. Neuroimage 78:463–73.
205. Pedersen KF, Alves G, Brønnick K, Aarsland D, Tysnes O-B, Larsen JP (2010): Apathy in drug-naïve patients with incident Parkinson's disease: the Norwegian ParkWest study. J Neurol 257:217–23.
206. Pedersen KF, Larsen JP, Tysnes O-B, Alves G (2013): Prognosis of mild cognitive impairment in early Parkinson disease: the Norwegian ParkWest study. JAMA Neurol 70:580–6.
207. Pereira JB, Junqué C, Bartrés-Faz D, Ramírez-Ruiz B, Marti M-J, Tolosa E (2013): Regional vulnerability of hippocampal subfields and memory deficits in Parkinson's disease. Hippocampus 23:720–8.
208. Pereira JB, Junqué C, Martí M-J, Ramirez-Ruiz B, Bargalló N, Tolosa E (2009): Neuroanatomical substrate of visuospatial and visuoperceptual impairment in Parkinson's disease. Mov Disord 24:1193–9.
209. Pereira JB, Svenningsson P, Weintraub D, Brønnick K, Lebedev A, Westman E, Aarsland D (2014): Initial cognitive decline is associated with cortical thinning in early Parkinson disease. Neurology 82:2017–25.
210. Perez-Lloret S, Rascol O (2010): Dopamine receptor agonists for the treatment of early or advanced Parkinson's disease. CNS Drugs 24:941–68.
211. Petersen RC, Smith GE, Waring SC, Ivnik RJ, Kokmen E, Tangelos EG (1997): Aging, memory, and mild cognitive impairment. Int Psychogeriatr 9 Suppl 1:65–9.

212. Pievani M, de Haan W, Wu T, Seeley WW, Frisoni GB (2011): Functional network disruption in the degenerative dementias. Lancet Neurol 10:829–43.
213. Power JD, Barnes KA, Snyder AZ, Schlaggar BL, Petersen SE (2012): Spurious but systematic correlations in functional connectivity MRI networks arise from subject motion. Neuroimage 59:2142–54.
214. Rae CL, Correia MM, Altena E, Hughes LE, Barker RA, Rowe JB (2012): White matter pathology in Parkinson's disease: the effect of imaging protocol differences and relevance to executive function. Neuroimage 62:1675–1684.
215. Raichle ME, MacLeod AM, Snyder AZ, Powers WJ, Gusnard DA, Shulman GL (2001): A default mode of brain function. Proc Natl Acad Sci U S A 98:676–682.
216. Ramanan VK, Risacher SL, Nho K, Kim S, Swaminathan S, Shen L, Foroud TM, Hakonarson H, Huentelman MJ, Aisen PS, Petersen RC, Green RC, Jack CR, Koeppe RA, Jagust WJ, Weiner MW, Saykin AJ (2014): APOE and BCHE as modulators of cerebral amyloid deposition: a florbetapir PET genome-wide association study. Mol Psychiatry 19:351–7.
217. Ramirez-Ruiz B, Junque C, Marti M-J, Valldeoriola F, Tolosa E (2007): Cognitive changes in Parkinson's disease patients with visual hallucinations. Dement Geriatr Cogn Disord 23:281–8.
218. Ramírez-Ruiz B, Junqué C, Martí M-J, Valldeoriola F, Tolosa E (2006): Neuropsychological deficits in Parkinson's disease patients with visual hallucinations. Mov Disord 21:1483–7.
219. Rascol O, Fitzer-Attas CJ, Hauser R, Jankovic J, Lang A, Langston JW, Melamed E, Poewe W, Stocchi F, Tolosa E, Eyal E, Weiss YM, Olanow CW (2011): A double-blind, delayed-start trial of rasagiline in Parkinson's disease (the ADAGIO study): prespecified and post-hoc analyses of the need for additional therapies, changes in UPDRS scores, and non-motor outcomes. Lancet Neurol 10:415–23.
220. Rascol O, Schelosky L (2009): 123I-metaiodobenzylguanidine scintigraphy in Parkinson's disease and related disorders. Mov Disord 24 Suppl 2:S732–41.
221. Recasens A, Dehay B, Bové J, Carballo-Carbajal I, Dovero S, Pérez-Villalba A, Fernagut P-O, Blesa J, Parent A, Perier C, Fariñas I, Obeso JA, Bezard E, Vila M (2014): Lewy body extracts from Parkinson disease brains trigger α-synuclein pathology and neurodegeneration in mice and monkeys. Ann Neurol 75:351–62.
222. Reijnders JSAM, Ehrt U, Weber WEJ, Aarsland D, Leentjens AFG (2008): A systematic review of prevalence studies of depression in Parkinson's disease. Mov Disord 23:183–9; quiz 313.
223. Reijnders JSAM, Scholtissen B, Weber WEJ, Aalten P, Verhey FRJ, Leentjens AFG (2010): Neuroanatomical correlates of apathy in Parkinson's disease: A magnetic resonance imaging study using voxel-based morphometry. Mov Disord 25:2318–25.
224. Remy P, Doder M, Lees A, Turjanski N, Brooks D (2005): Depression in Parkinson's disease: loss of dopamine and noradrenaline innervation in the limbic system. Brain 128:1314–22.
225. Robbins TW, Cools R (2014): Cognitive deficits in Parkinson's disease: a cognitive neuroscience perspective. Mov Disord 29:597–607.
226. Rombouts SARB, Barkhof F, Goekoop R, Stam CJ, Scheltens P (2005): Altered resting state networks in mild cognitive impairment and mild Alzheimer's disease: an fMRI study. Hum Brain Mapp 26:231–9.
227. Ropper AH, Samuels MA (2009): Adams and Victor's principles of neurology 9th ed. McGraw-Hill.
228. Rubinov M, Sporns O (2010): Complex network measures of brain connectivity: uses and interpretations. Neuroimage 52:1059–69.
229. Saxena S, Caroni P (2011): Selective neuronal vulnerability in neurodegenerative diseases: from stressor thresholds to degeneration. Neuron 71:35–48.
230. Schenck CH, Mahowald MW (2002): REM sleep behavior disorder: clinical, developmental, and neuroscience perspectives 16 years after its formal identification in SLEEP. Sleep 25:120–38.
231. Schölvinck ML, Maier A, Ye FQ, Duyn JH, Leopold DA (2010): Neural basis of global resting-state fMRI activity. Proc Natl Acad Sci U S A 107:10238–43.
232. Schrempf W, Brandt MD, Storch A, Reichmann H (2014): Sleep disorders in Parkinson's disease. J Parkinsons Dis 4:211–21.
233. Schulz-Schaeffer WJ (2010): The synaptic pathology of alpha-synuclein aggregation in dementia with Lewy bodies, Parkinson's disease and Parkinson's disease dementia. Acta Neuropathol 120:131–143.
234. Shannon KM, Keshavarzian A, Dodiya HB, Jakate S, Kordower JH (2012): Is alpha-synuclein in the colon a biomarker for premotor Parkinson's disease? Evidence from 3 cases. Mov Disord 27:716–9.
235. Shehzad Z, Kelly AMC, Reiss PT, Gee DG, Gotimer K, Uddin LQ, Lee SH, Margulies DS, Roy AK, Biswal BB, Petkova E, Castellanos FX, Milham MP (2009): The resting brain: unconstrained yet reliable. Cereb Cortex 19:2209–29.
236. Shine JM, Halliday GM, Gilat M, Matar E, Bolitho SJ, Carlos M, Naismith SL, Lewis SJG (2014): The role of dysfunctional attentional control networks in visual misperceptions in Parkinson's disease. Hum Brain Mapp 35:2206–19.
237. Shulman GL, Fiez JA, Corbetta M, Buckner RL, Miezin FM, Raichle ME, Petersen SE (1997): Common Blood Flow Changes across Visual Tasks: II. Decreases in Cerebral Cortex. J Cogn Neurosci 9:648–63.
238. Siderowf A, McDermott M, Kieburtz K, Blindauer K, Plumb S, Shoulson I (2002): Test-retest reliability of the unified Parkinson's disease rating scale in patients with early Parkinson's disease: results from a multicenter clinical trial. Mov Disord 17:758–63.
239. Smith D V, Utevsky A V, Bland AR, Clement N, Clithero JA, Harsch AEW, McKell Carter R, Huettel SA (2014): Characterizing individual differences in functional connectivity using dual-regression and seed-based approaches. Neuroimage 95:1–12.
240. Song SK, Lee JE, Park H-J, Sohn YH, Lee JD, Lee PH (2011): The pattern of cortical atrophy in patients with Parkinson's disease according to cognitive status. Mov Disord 26:289–96.

241. Sporns O, Honey CJ (2006): Small worlds inside big brains. Proc Natl Acad Sci U S A 103:19219–20.
242. Sporns O, Tononi G, Kötter R (2005): The human connectome: A structural description of the human brain. PLoS Comput Biol 1:e42.
243. Spreng RN, Sepulcre J, Turner GR, Stevens WD, Schacter DL (2013): Intrinsic architecture underlying the relations among the default, dorsal attention, and frontoparietal control networks of the human brain. J Cogn Neurosci 25:74–86.
244. Spreng RN, Stevens WD, Chamberlain JP, Gilmore AW, Schacter DL (2010): Default network activity, coupled with the frontoparietal control network, supports goal-directed cognition. Neuroimage 53:303–17.
245. Starkstein SE (2012): Apathy in Parkinson's disease: diagnostic and etiological dilemmas. Mov Disord 27:174–8.
246. Stayte S, Vissel B (2014): Advances in non-dopaminergic treatments for Parkinson's disease. Front Neurosci 8:113.
247. Stefanis L (2012): α-Synuclein in Parkinson's disease. Cold Spring Harb Perspect Med 2:a009399.
248. Szewczyk-Krolikowski K, Menke RAL, Rolinski M, Duff E, Salimi-Khorshidi G, Filippini N, Zamboni G, Hu MTM, Mackay CE (2014): Functional connectivity in the basal ganglia network differentiates PD patients from controls. Neurology 83:208–14.
249. Talairach J, Tournoux P (1988): Co-Planar Stereotaxic Atlas of the Human Brain: 3-D Proportional System: An Approach to Cerebral Imaging. Thieme, Germany.
250. Tessitore A, Amboni M, Esposito F, Russo A, Picillo M, Marcuccio L, Pellecchia MT, Vitale C, Cirillo M, Tedeschi G, Barone P (2012a): Resting-state brain connectivity in patients with Parkinson's disease and freezing of gait. Parkinsonism Relat Disord 18:781–7.
251. Tessitore A, Esposito F, Vitale C, Santangelo G, Amboni M, Russo A, Corbo D, Cirillo G, Barone P, Tedeschi G (2012b): Default-mode network connectivity in cognitively unimpaired patients with Parkinson disease. Neurology 79:2226–32.
252. Theilmann RJ, Reed JD, Song DD, Huang MX, Lee RR, Litvan I, Harrington DL (2013): White-matter changes correlate with cognitive functioning in Parkinson's disease. Front Neurol 4:37.
253. Thobois S, Ardouin C, Lhommée E, Klinger H, Lagrange C, Xie J, Fraix V, Coelho Braga MC, Hassani R, Kistner A, Juphard A, Seigneuret E, Chabardes S, Mertens P, Polo G, Reilhac A, Costes N, LeBars D, Savasta M, Tremblay L, Quesada J-L, Bosson J-L, Benabid A-L, Broussolle E, Pollak P, Krack P (2010): Non-motor dopamine withdrawal syndrome after surgery for Parkinson's disease: predictors and underlying mesolimbic denervation. Brain 133:1111–27.
254. Thobois S, Lhommée E, Klinger H, Ardouin C, Schmitt E, Bichon A, Kistner A, Castrioto A, Xie J, Fraix V, Pelissier P, Chabardes S, Mertens P, Quesada J-L, Bosson J-L, Pollak P, Broussolle E, Krack P (2013): Parkinsonian apathy responds to dopaminergic stimulation of D2/D3 receptors with piribedil. Brain 136:1568–77.
255. Thomason ME, Dennis EL, Joshi AA, Joshi SH, Dinov ID, Chang C, Henry ML, Johnson RF, Thompson PM, Toga AW, Glover GH, Van Horn JD, Gotlib IH (2011): Resting-state fMRI can reliably map neural networks in children. Neuroimage 55:165–75.
256. Tijms BM, Wink AM, de Haan W, van der Flier WM, Stam CJ, Scheltens P, Barkhof F (2013): Alzheimer's disease: connecting findings from graph theoretical studies of brain networks. Neurobiol Aging 34:2023–36.
257. Tolosa E, Gaig C, Santamaría J, Compta Y (2009): Diagnosis and the premotor phase of Parkinson disease. Neurology 72:S12–20.
258. Del Tredici K, Rüb U, De Vos RAI, Bohl JRE, Braak H (2002): Where does parkinson disease pathology begin in the brain? J Neuropathol Exp Neurol 61:413–26.
259. Tremblay C, Achim AM, Macoir J, Monetta L (2013): The heterogeneity of cognitive symptoms in Parkinson's disease: a meta-analysis. J Neurol Neurosurg Psychiatry 84:1265–72.
260. Tsuboi Y, Uchikado H, Dickson DW (2007): Neuropathology of Parkinson's disease dementia and dementia with Lewy bodies with reference to striatal pathology. Parkinsonism Relat Disord 13 Suppl 3:S221–4.
261. Tzourio-Mazoyer N, Landeau B, Papathanassiou D, Crivello F, Etard O, Delcroix N, Mazoyer B, Joliot M (2002): Automated anatomical labeling of activations in SPM using a macroscopic anatomical parcellation of the MNI MRI single-subject brain. Neuroimage 15:273–89.
262. Voon V, Fernagut P-O, Wickens J, Baunez C, Rodriguez M, Pavon N, Juncos JL, Obeso JA, Bezard E (2009): Chronic dopaminergic stimulation in Parkinson's disease: from dyskinesias to impulse control disorders. Lancet Neurol 8:1140–9.
263. Voon V, Potenza MN, Thomsen T (2007): Medication-related impulse control and repetitive behaviors in Parkinson's disease. Curr Opin Neurol 20:484–92.
264. Voon V, Rizos A, Chakravartty R, Mulholland N, Robinson S, Howell NA, Harrison N, Vivian G, Ray Chaudhuri K (2014): Impulse control disorders in Parkinson's disease: decreased striatal dopamine transporter levels. J Neurol Neurosurg Psychiatry 85:148–52.
265. Voon V, Sohr M, Lang AE, Potenza MN, Siderowf AD, Whetteckey J, Weintraub D, Wunderlich GR, Stacy M (2011): Impulse control disorders in Parkinson disease: a multicenter case--control study. Ann Neurol 69:986–96.
266. Vossel S, Weidner R, Driver J, Friston KJ, Fink GR (2012): Deconstructing the architecture of dorsal and ventral attention systems with dynamic causal modeling. J Neurosci 32:10637–48.
267. Wang J, Wang L, Zang Y, Yang H, Tang H, Gong Q, Chen Z, Zhu C, He Y (2009): Parcellation-dependent small-world brain functional networks: a resting-state fMRI study. Hum Brain Mapp 30:1511–23.
268. Warren Olanow C, Kieburtz K, Rascol O, Poewe W, Schapira AH, Emre M, Nissinen H, Leinonen M, Stocchi F (2013): Factors predictive of the development of Levodopa-induced dyskinesia and wearing-off in Parkinson's disease. Mov Disord 28:1064–71.
269. Watts DJ, Strogatz SH (1998): Collective dynamics of "small-world" networks. Nature 393:440–2.

270. Weintraub D, Burn DJ (2011): Parkinson's disease: the quintessential neuropsychiatric disorder. Mov Disord 26:1022–31.
271. Weintraub D, Doshi J, Koka D, Davatzikos C, Siderowf AD, Duda JE, Wolk DA, Moberg PJ, Xie SX, Clark CM (2011): Neurodegeneration across stages of cognitive decline in Parkinson disease. Arch Neurol 68:1562–8.
272. Weintraub D, Koester J, Potenza MN, Siderowf AD, Stacy M, Voon V, Whetteckey J, Wunderlich GR, Lang AE (2010): Impulse control disorders in Parkinson disease: a cross-sectional study of 3090 patients. Arch Neurol 67:589–95.
273. Weintraub D, Moberg PJ, Culbertson WC, Duda JE, Stern MB (2004): Evidence for impaired encoding and retrieval memory profiles in Parkinson disease. Cogn Behav Neurol 17:195–200.
274. Weissenbacher A, Kasess C, Gerstl F, Lanzenberger R, Moser E, Windischberger C (2009): Correlations and anticorrelations in resting-state functional connectivity MRI: a quantitative comparison of preprocessing strategies. Neuroimage 47:1408–16.
275. Whittington CJ, Podd J, Stewart-Williams S (2006): Memory deficits in Parkinson's disease. J Clin Exp Neuropsychol 28:738–54.
276. Van Wijk BCM, Stam CJ, Daffertshofer A (2010): Comparing brain networks of different size and connectivity density using graph theory. PLoS One 5:e13701.
277. Williams-Gray CH, Evans JR, Goris A, Foltynie T, Ban M, Robbins TW, Brayne C, Kolachana BS, Weinberger DR, Sawcer SJ, Barker RA (2009): The distinct cognitive syndromes of Parkinson's disease: 5 year follow-up of the CamPaIGN cohort. Brain 132:2958–2969.
278. Williams-Gray CH, Foltynie T, Brayne CEG, Robbins TW, Barker R a (2007): Evolution of cognitive dysfunction in an incident Parkinson's disease cohort. Brain 130:1787–98.
279. Winkler AM, Ridgway GR, Webster MA, Smith SM, Nichols TE (2014): Permutation inference for the general linear model. Neuroimage 92:381–97.
280. Witt K, Daniels C, Reiff J, Krack P, Volkmann J, Pinsker MO, Krause M, Tronnier V, Kloss M, Schnitzler A, Wojtecki L, Bötzel K, Danek A, Hilker R, Sturm V, Kupsch A, Karner E, Deuschl G (2008): Neuropsychological and psychiatric changes after deep brain stimulation for Parkinson's disease: a randomised, multicentre study. Lancet Neurol 7:605–14.
281. Wolters E, Baumann C (2014): Parkinson Disease and Other Movement Disorders. Ed. Erik Wolters, Christian Baumann 1st ed. Amsterdam.
282. Worth PF (2013): How to treat Parkinson's disease in 2013. Clin Med (Northfield Il) 13:93–96.
283. Yao N, Shek-Kwan Chang R, Cheung C, Pang S, Lau KK, Suckling J, Rowe J, Yu K, Ka-Fung Mak H, Chua S-E, Ho SL, McAlonan GM (2014): The default mode network is disrupted in parkinson's disease with visual hallucinations. Hum Brain Mapp.
284. Yerkes RM, Dodson JD (1908): The relation of strength of stimulus to rapidity of habit-formation. J Comp Neurol Psychol 18:459–482.
285. Yip JTH, Lee TMC, Ho S-L, Tsang K-L, Li LSW (2003): Emotion recognition in patients with idiopathic Parkinson's disease. Mov Disord 18:1115–22.
286. Yu R, Liu B, Wang L, Chen J, Liu X (2013): Enhanced functional connectivity between putamen and supplementary motor area in Parkinson's disease patients. PLoS One 8:e59717.
287. Zarei M, Ibarretxe-Bilbao N, Compta Y, Hough M, Junque C, Bargallo N, Tolosa E, Martí MJ (2013): Cortical thinning is associated with disease stages and dementia in Parkinson's disease. J Neurol Neurosurg Psychiatry 84:875–81.
288. Zheng Z, Shemmassian S, Wijekoon C, Kim W, Bookheimer SY, Pouratian N (2014): DTI correlates of distinct cognitive impairments in Parkinson's disease. Hum Brain Mapp 35:1325–33.
289. Zuo X-N, Kelly C, Adelstein JS, Klein DF, Castellanos FX, Milham MP (2010): Reliable intrinsic connectivity networks: test-retest evaluation using ICA and dual regression approach. Neuroimage 49:2163–77.

chapter 2

HYPOTHESES AND OBJECTIVES

GENERAL HYPOTHESIS AND OBJECTIVE

The main hypothesis on which this thesis is based is that changes in structural and resting-state functional connectivity between distinct brain regions contribute to the occurrence of cognitive and neuropsychiatric deficits in PD.

The main objective of this thesis is to characterize the pattern of connectivity changes and accompanying GM atrophy underlying the cognitive and neuropsychiatric impairments that take place in PD prior to the onset of dementia using state-of-the-art magnetic resonance neuroimaging techniques.

SPECIFIC HYPOTHESES

1. The analysis of resting-state functional connectivity through the perspective of large-scale ICNs would be capable of detecting changes associated with cognitive deficits in PD. Disruptions of intra- and internetwork connectivity in cognitively relevant ICNs such as the DMN, the DAN and the FPN are probably involved in the pathophysiology of cognitive deficits in PD.

2. The analysis of resting-state functional connectivity data through a graph-theoretical framework can reveal changes in global and local network parameters associated with cognitive impairments in PD.

3. Distinct types of cognitive impairment in non-demented PD patients could correspond to different and dissociable underlying functional and structural correlates.

    3.1 Deficits related to dopamine imbalances in frontostriatal circuits – such as attentional and executive impairments or apathy – will be more strongly associated with functional connectivity changes than with GM atrophy.
    3.2 The presence of deficits not related to dopamine imbalances – such as memory and visuospatial/visuoperceptual impairments – will be accompanied by functional and atrophic structural changes in posterior, occipito-temporo-parietal cortical regions.

3.3 Apathy in PD patients could be explained by dysfunctions in the frontostriatal circuitry, mainly involving the *limbic* circuit – *i.e.*, the ventral striatum and OFC.

4. Functional MRI connectivity studies may be more sensitive than neuropsychological testing in detecting subtle degenerative changes even in early disease stages.

5. Facial emotion recognition deficits in PD will be associated with atrophy in GM regions involved in emotional processing and with WM microstructural changes in the long-range associative WM tracts connecting them to sensory regions and to higher-order cortical regions.

SPECIFIC OBJECTIVES

1. To explore the potential of state-of-the-art resting-state functional connectivity analytic techniques – such as ICA and graph theory – in the study of cognitive impairment in PD.

2. To explore resting-state functional connectivity within and between cognitively-relevant ICNs changes in PD patients with and without MCI; and to explore the relationship between these connectivity changes and different types of cognitive deficit in PD.

3. To evaluate the presence of changes in global and regional graph-theory measures in the functional brain networks of PD patients with and without MCI; and to investigate the relationship between these measures and distinct types of cognitive deficit in PD.

4. To assess the pattern of cortical thinning associated with the presence of MCI in PD patients, and the relationship between CTh and cognitive performance in PD patients.

5. To investigate the relationship between resting-state functional connectivity changes in frontostriatal circuits and the presence of apathy in PD patients.

6. To assess the role of structural GM and WM changes underlying facial emotion recognition deficits in PD patients.

7. To investigate the progressive patterns of GM atrophy in early-stage PD patients.

8. To investigate the progressive patterns of functional connectivity changes in recognition memory networks in early-stage PD patients.

chapter 3
METHODS

STUDY SAMPLES

The studies presented in this thesis, listed below, were performed using two samples of healthy controls and PD patients. Studies 1, 2, 3 and 5 used subjects from *Sample 2*; studies 6 and seven were performed with subjects from *Sample 1*. Study 4, in turn, was performed while sample 2 was being recruited, and used subjects from both samples.

Study 1

Baggio HC, Segura B, Sala-Llonch R, Martí MJ, Valldeoriola F, Compta Y, Tolosa E, Junqué C. *Cognitive impairment and resting-state network connectivity in Parkinson's disease*. Human Brain Mapping 2014 DOI: 10.1002/hbm.22622 (in press).

Study 2

Baggio HC, Sala-Llonch R, Segura B, Martí MJ, Valldeoriola F, Compta Y, Tolosa E, Junqué C. *Functional brain networks and cognitive deficits in Parkinson's disease.* Human Brain Mapping 2014, 35:4620-34.

Study 3

Segura B, Baggio HC, Martí MJ, Valldeoriola F, Compta Y, Garcia-Diaz AI, Vendrell P, Bargallo N, Tolosa E, Junqué C. *Cortical thinning associated with mild cognitive impairment in Parkinson's disease*. Movement Disorders 2014 DOI: 10.1002/mds.25982.

Study 4

Baggio HC, Segura B, Ibarretxe-Bilbao N, Valldeoriola F, Martí MJ, Compta Y, Tolosa E, Junqué C. *Structural correlates of facial emotion recognition deficits in Parkinson's disease patients.* Neuropsychologia 2012, 50:2121-8.

Study 5

Baggio HC, Segura B, Garrido-Millán JL, Martí MJ, Compta Y, Valldeoriola F, Tolosa E, Junqué C. *Resting-state frontostriatal functional connectivity in Parkinson's disease-related apathy*. Submitted.

Study 6

Segura B, Ibarretxe-Bilbao N, Sala-Llonch R, Baggio HC, Martí MJ, Valldeoriola F, Vendrell P, Bargalló N, Tolosa E, Junqué C. *Progressive changes in a recognition memory network in Parkinson's disease.* Journal of Neurology Neurosurgery and Psychiatry 2013, 84:370-8.

Study 7

Ibarretxe-Bilbao N, Junqué C, Segura B, Baggio HC, Martí MJ, Valldeoriola F, Bargalló N, Tolosa E. *Progression of cortical thinning in early Parkinson's disease.* Movement Disorders 2012, 27:1746-53.

Sample 1

This study sample was assessed longitudinally. The baseline sample was composed of 24 early-stage PD patients and 24 HC. Patients were recruited from the Parkinson's disease and Movement Disorders Unit, Neurology Service, Hospital Clínic, Barcelona. Healthy controls matched for age, gender and years of education were recruited from patients' friends and spouses.

From the initial sample, two patients died, two moved to another province and three patients declined to participate. In the healthy control group, two subjects died, five subjects declined to participate and two could not be contacted. Finally, 17 PD patients and 15 healthy controls participated in the follow-up assessment after a mean period of 35.5 months.

The inclusion criteria at baseline for PD patients were: *fulfilment of the UK PD Society Brain Bank diagnostic criteria for PD* [Daniel and Lees, 1993]; *age: 40–65 years; HY stage ≤ II; disease duration ≤ 5 years; absence of motor fluctuations.*
Exclusion criteria for all subjects were: *presence of dementia; presence of (other) neurological or psychiatric disorders; presence of visual hallucinations.*

MRI acquisition

MRI data was acquired on a 3-Tesla MRI scanner (MAGNETOM Trio, Siemens, Germany) located at the Centre de Diagnòstic per la Imatge of the Hospital Clínic, Barcelona, using an 8-channel head coil. High-resolution, three-dimensional *structural T1-weighted images* were acquired in the sagittal plane with a magnetization prepared rapid gradient-echo (MPRAGE) sequence (repetition time (TR)/echo time (TE) 2,300/2.98 ms; inversion time (TI) 900 ms; 256 x 256 matrix, 1 mm isotropic voxel). Sagittal diffusion-weighted images were obtained using a single-shot EPI sequence (TR 7700 ms, TE 89 ms), with diffusion-encoding in 30 directions at *b*=0 and 1000 s/mm2; two identical diffusion-weighted sequences were acquired for each subject.

A multislice gradient echo, echo-planar imaging functional sequence was also acquired with the following parameters: TR=2000 ms; echo time TE=30 ms; 36x3 mm axial slices providing whole brain coverage. In this fMRI acquisition we used a recognition memory paradigm, in which participants first viewed 35 words (duration of 2 s per word and interword interval of 1 s) outside the scanner with instructions to remember them, and were later asked to recognize these 35 words during fMRI scanning from a list of 70 words (35 previously presented words and 35 new words). The words were four to six letters in length and of moderate frequency of use, and were obtained from the Lexesp-Corco database. These words were presented inside the scanner with VisualStim digital MRI-compatible high-resolution stereo 3D glasses (Resonance Technology, Inc.) and Presentation® version 10.1 (Neurobehavioral Systems). The whole experiment consisted of a 20-block paradigm with alternating activation and control conditions (10 blocks each) and a total duration of 400 s (20 s per block). In the activation blocks participants viewed seven words, of which three had been previously presented, and pressed a button on a MR-compatible response box using their right hands to indicate whether they remembered having read the word in the list before scanning. They were encouraged to respond while the word was on the screen (2 s). Responses given outside this interval were excluded from analysis. In the control blocks, participants were presented with seven concatenations of letters (simulating the length of a word) of which three were the letters *AAAAAA* and the other four were

random letters. Again, using their right hands, participants were asked to press the button on the response box to indicate that the item was *AAAAAA* and did not have to press when other letter strings appeared.

Neuropsychological assessment

All subjects underwent a comprehensive neuropsychological assessment to evaluate the following functions:

- *Memory:* Rey's Auditory Verbal Learning Test (RAVLT);
- *Attention and working memory:* backward and forward digit spans from the Wechsler Adult Intelligence Scale-III Digits subtest;
- Verbal fluencies, including *phonemic fluency* (total of words starting with "p" produced in 1 min) and *semantic fluency* (number of names of animals produced in 1 min);
- *Visuospatial/visuoperceptual*: Visual Object and Space Perception Battery (only administered at follow-up).

Additionally, Cumming's Neuropsychiatric Inventory (NPI) [Cummings et al., 1994] was used to assess the presence of neuropsychiatric symptoms.

Sample 2

This sample consisted of 121 PD patients consecutively recruited from the Parkinson's Disease and Movement Disorders Unit, Department of Neurology, Hospital Clínic, Barcelona and 49 healthy controls, recruited from a group of persons who had volunteered to take part in studies addressing age-related processes at the Institut de l'Envelliment, Universitat Autònoma de Barcelona.

The inclusion criteria for PD patients was *fulfilling the UK PD Society Brain Bank diagnostic criteria for PD; no surgical treatment with deep brain stimulation*.

The exclusion criteria were: *history of DBS surgery; HY > 3; dementia according to the MDS criteria* [Emre, 2003]*; juvenile-onset PD; psychiatric or neurologic comorbidity other than depression; low global intelligence quotient estimated by the Vocabulary subtest of the Wechsler Adult Intelligence Vocabulary subtest of the Wechsler Adult Intelligence Scale, 3rd edition (scaled score < 7 points); MMSE score < 25; claustrophobia; pathological MRI findings other than mild white matter hyperintensities in long-TR sequences; MRI findings other than mild WM hyperintensities in long-TR sequences; MRI artifacts.*

Ninety-four PD patients and 32 healthy volunteers were finally selected. Twelve patients and eight controls were excluded because they fulfilled criteria for dementia or other neurological disease, six PD patients for psychiatric comorbidity, one PD patient who scored higher than 3 on the H&Y scale, one PD patient who presented young-onset PD, three PD patients and one control who presented low global intelligence quotient scores, two PD patients for claustrophobia, three healthy subjects who did not complete the neuropsychological assessment, and two controls and two PD patients because of MRI artifacts.

MRI acquisition

MRI data was acquired on the same scanner as Sample 1. A high-resolution, three-dimensional *structural T1-weighted* sequence and two *diffusion-weighted* sequences were acquired with the same protocol used in Sample 1. The scanning protocol also included a *resting-state*, 5-minute-long functional gradient-echo echo-planar imaging sequence (150 T2*-weighted volumes, TR=2 s, TE=19 ms, flip angle=90^0, slice thickness=3 mm, FOV=240 mm, in which subjects were instructed to keep their eyes closed, not to think of anything in particular and not to fall asleep), and a T2-weighted axial fluid-attenuated inversion recovery (FLAIR) sequence (TR=9 s, TE=96 ms).

Neuropsychological assessment

All subjects underwent a comprehensive neuropsychological assessment evaluating the following functions:

- *Memory:* Rey's Auditory Verbal Learning Test (RAVLT);
- *Attention and working memory:* backward and forward digit spans from the Wechsler Adult Intelligence Scale-III Digits subtest; Trail Making Test, parts A (TMT-A) and B (TMT-B); Stroop Color-Word Test and the Symbol Digits Modalities Tests (SDMT);
- *Executive functions*: verbal fluencies, including *phonemic fluency* (total of words starting with "p" produced in 1 min) and *semantic fluency* (number of names of animals produced in 1 min);
- *Language*: short version of the Boston Naming Test (BNT);
- *Visuospatial/visuoperceptual*: Benton's Judgment of Line Orientation (JLO) and Visual Form Discrimination (VFD) tests.

Additionally, Starkstein's Apathy Scale (AS) was used to assess the presence and severity of symptoms of apathy [Starkstein et al., 1992], and the Ekman 60 test was employed to evaluate facial emotion recognition (FER) performance [Ekman and Friesen, 1976]. Premorbid IQ was estimated using the *vocabulary* subtest of the Wechsler Adult Intelligence Scale, 3rd edition.

In both samples, motor symptoms were assessed with the UPDRS motor section and disease evolution was evaluated with the HY scale. The Beck Depression Inventory-II (BDI) was used to assess the presence and severity of depressive symptoms [Beck et al., 1996].

NEUROIMAGING TECHNIQUES

Resting-state image preprocessing: the preprocessing pipeline used in *studies 1, 2 and 5* was performed with FSL (http://www.fmrib.ox.ac.uk/fsl) and AFNI (http://afni.nimh.nih.gov/afni), and included removal of the first 5 volumes to allow for T1 saturation effects, skull stripping, grandmean scaling and temporal filtering (bandpass filtering of 0.01-0.1 Hz). To control for the effect of subject head movement, physiological artifacts (e.g., breathing and vascular) and other non-neural sources of signal variation on the estimation of connectivity, motion correction (using FSL's MCFLIRT) and regression of nuisance signals (six motion parameters, cerebrospinal fluid signal and WM signal) were performed. Cerebrospinal fluid and WM mean signals were determined by averaging the native-space functional time series of all voxels contained inside the corresponding masks obtained from the segmentation of the T1-weighted images using FSL's FAST.

In *studies 1 and 5*, in order to remove the effects of volumes corrupted by motion, a scrubbing procedure, similar to that suggested by [Power et al., 2012], was applied. Briefly, root mean square intensity differences between volumes m and m-1 (DVARS) were calculated, indicating how much the global intensity of a volume changed compared to the previous timepoint. Volumes with DVARS above the 75th percentile + 1.5 times the interquartile range were considered as outliers and added to the confound matrices alongside the nuisance factors described above, thus removing their effects from the analyses.

Independent component analysis and dual regression: in *study 1*, preprocessed images were analyzed with MELODIC, part of FSL, using a temporal-concatenation spatial ICA approach (see Chapter 1 – *THE BRAIN AS A NETWORK – resting-state functional connectivity fMRI techniques*) [Beckmann and Smith, 2004] and a predefined dimensionality of 25. The networks of interest (DAN, DMN, FPN) were identified out of the 25 extracted components through spatial cross-correlations and visual inspection and subsequently fed into a dual-regression analysis (see Chapter 1 – *THE BRAIN AS A NETWORK: resting-state functional connectivity fMRI techniques - methods*) [Filippini et al., 2009].

In *study 6*, analysis of the task-related fMRI images was carried out using tensorial ICA, as implemented in MELODIC [Beckmann and Smith, 2005]. The number of independent components was estimated by MELODIC using the Laplace approximation to the Bayesian evidence of the model order [Beckmann and Smith, 2004]. Five task-related components were then selected out of the 18 extracted components (two associated with the *task>control* and three to the *control>task contrast*) and correlated with the model-based activation map (*recognition memory task>control task*) (see below) to identify the main task-related independent component.

Model-based fMRI analysis: used in *study 6*, this approach was carried out using FEAT, part of FSL. At the individual level, we obtained an activation map for each subject (*recognition memory task>control task*).

Higher level analysis was then performed using FLAME to evaluate between-group differences and to obtain global average (one-sample *t* test) activation maps.

Seed-to-seed correlation: in order to calculate interregional functional connectivity in *studies 1, 2 and 6*, BOLD time series of all voxels included in the ROIs were averaged and correlated with the mean time series of all other ROIs included in the study. In *study 1*, 43 nodes (10 DAN, 18 DMN and 15 bilateral FPN nodes) were included using 10-mm radius circular masks and the MNI coordinates described previously [Spreng et al., 2013]. In *study 2*, the cerebral gray matter was parcellated into 45 ROIs per hemisphere AAL atlas [Tzourio-Mazoyer et al., 2002]; seed-to-seed correlation data was used to perform subsequent graph analyses. In *study 6*, eight spherical 8mm-ROIs, centered on the peak voxels of the most relevant clusters from the main task component obtained from the model-free analysis, were used.

Graph-theory analysis: This approach was used in *study 2*, using the Brain Connectivity Toolbox [Rubinov and Sporns, 2010]. Individual 90x90 adjacency matrices were produced through seed-to-seed correlation and subsequently thresholded using sparsity cutoffs (see Chapter 1 – *THE BRAIN AS A NETWORK: graph theory*). The obtained networks were analyzed in terms of their global (or whole-brain) characteristics (characteristic path length, clustering coefficient, *small-worldness*, global

efficiency, modularity), as well as regional (or nodal) measures (degree, betweenness centrality, clustering coefficient, local efficiency).

Seed-to-voxel correlation: in *study 5*, the frontal cortices were parcellated into 4 regions (limbic, executive, rostral motor and caudal motor), as described elsewhere [Tziortzi et al., 2014]; the striata were divided into 3 ROIs (limbic, executive and sensorimotor regions) using the Oxford-GSK-Imanova Striatal Connectivity Atlas, and the thalami were defined using the Harvard-Oxford subcortical structural atlas, both available from FSL. The mean time series of each ROI was correlated with the time series of every voxel inside the regions of interest, thus producing a correlation map for each ROI in which each voxel's value is given by the resulting Pearson's r coefficient.

Voxel-based morphometry: VBM analyses (see Chapter 1 – *COGNITION IN PD – STRUCTURAL NEUROIMAGING: GM structural neuroimaging in PD – methods)* were used in *studies 1, 4, 5 and 7* using FSL tools (http://fsl.fmrib.ox.ac.uk/fsl/fslwiki). To perform group-level statistical testing, voxelwise general linear model with non-parametric, permutation testing (5,000 permutations) was applied. Either FWE or FDR were used for multiple comparisons correction.

Cortical thickness analysis: CTh analyses (see Chapter 1 – *COGNITION IN PD – STRUCTURAL NEUROIMAGING: GM structural neuroimaging in PD – methods*) were used in *studies 1, 3 and 7* and were performed using FreeSurfer (http://surfer.nmr.harvard.edu). Statistical testing was performed using a vertex-by-vertex general linear model. All results were corrected for multiple comparisons using clusterwise Monte-Carlo simulation (10,000 iterations).

Shape analysis: subcortical structures of interest (nucleus accumbens, pallidum, caudate nucleus, putamen and thalamus) were segmented using FIRST as implemented in FSL. For shape analysis, surface meshes are fitted for each region of interest as a vertex distribution model, modelling its shape. Multivariate testing is then performed on the 3-dimensional coordinates of each vertex, followed by multiple-comparison correction, thus allowing the detection of localized structural changes [Patenaude et al., 2011].

Diffusion-tensor imaging: DTI analyses (see Chapter 1 – *COGNITION IN PD – STRUCTURAL NEUROIMAGING: WM structural neuroimaging in PD – methods*) were used in *study 3* using FSL tools. Voxelwise statistical analysis of the FA data was carried out using TBSS (Tract-Based Spatial Statistics [Smith et al., 2006]), part of FSL. In this technique, the mean FA image is created and thinned to create a mean FA skeleton which represents the centers of all tracts common to the group. Each subject's aligned FA data is then projected onto this skeleton; resulting data was fed into voxelwise cross-subject statistics using non-parametric, permutation testing, corrected for multiple comparisons across space using FWE.

NEUROPSYCHOLOGICAL ANALYSIS – MILD COGNITIVE IMPAIRMENT

Two different classification schemes were used to define the presence of MCI. In both schemes, z scores for each test and for each subject were calculated based on the control group's means and standard deviations. Expected z scores adjusted for age, sex and education for each test and each subject were calculated based on a multiple regression analysis performed in the healthy control group [Aarsland et al., 2009]. A given individual test score was considered abnormal if its z score was

at least 1.5 lower than the expected score. MCI was defined as the presence of at least two abnormal test scores in the same cognitive domain, or at least one abnormal test per domain in at least two domains.

In *studies 1 and 2*, three cognitive domains [Aarsland et al., 2009] were considered. The domains and corresponding neuropsychological tests used were:

Attention/executive: backward minus forward digit spans; TMT-A minus TMT-B scores; phonemic fluency scores, and Stroop Color-Word Test interference scores;
Visuospatial/visuoperceptual: JLO and VFD;
Memory: RAVLT total learning (sum of correct responses from trial I to trial V) and 20-minute free recall scores.

In *study 3*, the five following cognitive domains [Litvan et al., 2012] were taken into account, with the corresponding neuropsychological tests:

Attention and working memory: TMT-A, TMT-B, forward and backward digit span, Stroop Color-Word Test, SDMT;
Executive functions: phonemic and semantic fluencies;
Language: short version of the Boston Naming Test (BNT);
Memory: RAVLT total learning and 20-minute free recall scores.
Visuospatial and visuoperceptual: JLO and VFD.

Additionally, composite z-scores for each domain were calculated by averaging the z-scores of all tests within that domain.

REFERENCES

1. Beck AT, Steer RA, Brown GK (1996): Manual for the Beck Depression Inventory-II. San Antonio, TX: Psychological Corporation.
2. Beckmann CF, Smith SM (2005): Tensorial extensions of independent component analysis for multisubject FMRI analysis. Neuroimage 25:294–311.
3. Beckmann CF, Smith SM (2004): Probabilistic independent component analysis for functional magnetic resonance imaging. IEEE Trans Med Imaging 23:137–52.
4. Cummings JL, Mega M, Gray K, Rosenberg-Thompson S, Carusi DA, Gornbein J (1994): The Neuropsychiatric Inventory: comprehensive assessment of psychopathology in dementia. Neurology 44:2308–2314.
5. Daniel SE, Lees AJ (1993): Parkinson's Disease Society Brain Bank, London: overview and research. J Neural Transm Suppl 39:165–72.
6. Ekman P, Friesen W V (1976): Pictures of Facial Affect. Consult Psychol Press Paloalto.
7. Emre M (2003): Dementia associated with Parkinson's disease. Lancet Neurol 2:229–37.
8. Filippini N, MacIntosh BJ, Hough MG, Goodwin GM, Frisoni GB, Smith SM, Matthews PM, Beckmann CF, Mackay CE (2009): Distinct patterns of brain activity in young carriers of the APOE-epsilon4 allele. Proc Natl Acad Sci U S A 106:7209–14.
9. Litvan I, Goldman JG, Tröster AI, Schmand B a, Weintraub D, Petersen RC, Mollenhauer B, Adler CH, Marder K, Williams-Gray CH, Aarsland D, Kulisevsky J, Rodriguez-Oroz MC, Burn DJ, Barker R a, Emre M (2012): Diagnostic criteria for mild cognitive impairment in Parkinson's disease: Movement Disorder Society Task Force guidelines. Mov Disord 27:349–56.
10. Patenaude B, Smith SM, Kennedy DN, Jenkinson M (2011): A Bayesian model of shape and appearance for subcortical brain segmentation. Neuroimage 56:907–22.
11. Rubinov M, Sporns O (2010): Complex network measures of brain connectivity: uses and interpretations. Neuroimage 52:1059–69.
12. Smith SM, Jenkinson M, Johansen-Berg H, Rueckert D, Nichols TE, Mackay CE, Watkins KE, Ciccarelli O, Cader MZ, Matthews PM, Behrens TEJ (2006): Tract-based spatial statistics: voxelwise analysis of multi-subject diffusion data. Neuroimage 31:1487–505.
13. Starkstein SE, Mayberg HS, Preziosi TJ, Andrezejewski P, Leiguarda R, Robinson RG (1992): Reliability, validity, and clinical correlates of apathy in Parkinson's disease. J Neuropsychiatry Clin Neurosci 4:134–9.
14. Tziortzi AC, Haber SN, Searle GE, Tsoumpas C, Long CJ, Shotbolt P, Douaud G, Jbabdi S, Behrens TEJ, Rabiner E a, Jenkinson M, Gunn RN (2014): Connectivity-based functional analysis of dopamine release in the striatum using diffusion-weighted MRI and positron emission tomography. Cereb Cortex 24:1165–77.
15. Tzourio-Mazoyer N, Landeau B, Papathanassiou D, Crivello F, Etard O, Delcroix N, Mazoyer B, Joliot M (2002): Automated anatomical labeling of activations in SPM using a macroscopic anatomical parcellation of the MNI MRI single-subject brain. Neuroimage 15:273–89.

chapter 4

RESULTS

study 1

COGNITIVE IMPAIRMENT AND RESTING-STATE NETWORK CONNECTIVITY IN PARKINSON'S DISEASE

Human Brain Mapping 2014

Hugo César Baggio, Bàrbara Segura, Roser Sala Llonch, Maria José Martí, Francesc Valldeoriola, Yaroslau Compta, Eduardo Tolosa, Carme Junqué

◆ Human Brain Mapping 00:00–00 (2014) ◆

Cognitive Impairment and Resting-State Network Connectivity in Parkinson's Disease

Hugo-Cesar Baggio,[1] Bàrbara Segura,[1] Roser Sala-Llonch,[1] Maria-José Marti,[2,3] Francesc Valldeoriola,[2,3] Yaroslau Compta,[2,3] Eduardo Tolosa,[2,3,4] and Carme Junqué[1,3,4]*

[1]*Departament de Psiquiatria i Psicobiologia Clínica, Universitat de Barcelona, Barcelona, Catalonia, Spain*
[2]*Parkinson's Disease and Movement Disorders Unit, Neurology Service, Institut Clínic de Neurociències (ICN), Hospital Clínic de Barcelona, Barcelona, Catalonia, Spain*
[3]*Centro de Investigación Biomédica en Red sobre Enfermedades Neurodegenerativas (CIBERNED), Hospital Clínic de Barcelona, Barcelona, Catalonia, Spain*
[4]*Institut d'Investigacions Biomèdiques August Pi i Sunyer (IDIBAPS), Barcelona, Catalonia, Spain*

Abstract: The purpose of this work was to evaluate changes in the connectivity patterns of a set of cognitively relevant, dynamically interrelated brain networks in association with cognitive deficits in Parkinson's disease (PD) using resting-state functional MRI. Sixty-five nondemented PD patients and 36 matched healthy controls were included. Thirty-four percent of PD patients were classified as having mild cognitive impairment (MCI) based on performance in attention/executive, visuospatial/visuoperceptual (VS/VP) and memory functions. A data-driven approach using independent component analysis (ICA) was used to identify the default-mode network (DMN), the dorsal attention network (DAN) and the bilateral frontoparietal networks (FPN), which were compared between groups using a dual-regression approach controlling for gray matter atrophy. Additional seed-based analyses using a priori defined regions of interest were used to characterize local changes in intranetwork and internetwork connectivity. Structural group comparisons through voxel-based morphometry and cortical thickness were additionally performed to assess associated gray matter atrophy. ICA results revealed reduced connectivity between the DAN and right frontoinsular regions in MCI patients, associated with worse performance in attention/executive functions. The DMN displayed increased connectivity with medial and lateral occipito-parietal regions in MCI patients, associated with worse VS/VP performance, and with occipital reductions in cortical thickness. In line with data-driven results, seed-based analyses mainly revealed reduced within-DAN, within-DMN and DAN-FPN connectivity, as well as loss of normal DAN-DMN anticorrelation in MCI patients. Our findings demonstrate differential connectivity changes affecting the networks evaluated, which we hypothesize to be

Additional Supporting Information may be found in the online version of this article.

Contract grant sponsor: Spanish Ministry of Science and Innovation; Contract grant number: PSI2013- 41393 (to C.J.; H.C.B.; and B.S.); Contract grant sponsor: Generalitat de Catalunya; Contract grant number: 2014SGR98 (to C.J.) and 2011FI_B 00045 (to H.C.B.), Contract grant sponsor: CIBERNED

*Correspondence to: Prof. Carme Junqué, Department of Psychiatry and Clinical Psychobiology. University of Barcelona, Casanova 143 (08036) Barcelona, Spain. E-mail: cjunque@ub.edu

Received for publication 2 May 2014; Revised 29 July 2014; Accepted 20 August 2014.

DOI: 10.1002/hbm.22622

Published online 00 Month 2014 in Wiley Online Library (wileyonlinelibrary.com).

related to the pathophysiological bases of different types of cognitive impairment in PD. *Hum Brain Mapp 00:000–000, 2014.*

Key words: Parkinson's disease; mild cognitive impairment; fMRI; resting-state connectivity

INTRODUCTION

In the framework of an integrated model of brain function, neuroimaging studies have demonstrated the relevance of a set of dynamically interrelated brain intrinsic connectivity networks (ICNs) considered to play an important role in cognitive processing: the default-mode network (DMN), the dorsal attention network (DAN), and the frontoparietal networks (FPN) [Sala-Llonch et al., 2012; Seeley et al., 2007; Spreng et al., 2010]. These networks can be evaluated through resting-state functional techniques, and their role as part of the functional substrates of cognitive manifestations of neuropathological processes can be assessed [Smith et al., 2009; Spreng et al., 2010].

Cognitive impairment is an important cause of disability in Parkinson's disease (PD), and patients with mild cognitive impairment (MCI) are at a higher risk of subsequently developing dementia [Williams-Gray et al., 2007], which over time affects around 75% of patients (see [Aarsland and Kurz, 2010]). In a previous study with the same subject sample, we used a graph-theoretical approach to assess changes in global patterns of resting-state functional connectivity and found that MCI in PD was associated with widespread connectivity decrements as well as some increments [Baggio et al., 2014]. Since previous studies in PD have mainly focused on changes affecting the DMN [Eimeren and Monchi, 2009; Krajcovicova et al., 2012; Rektorova et al., 2012; Tessitore et al., 2012], little is known about how the disease affects other resting-state ICNs.

Our goal in this study was to evaluate connectivity changes in a set of brain networks—the DMN, the DAN, and the bilateral FPN [Spreng et al., 2013]. Specifically, our objective was, in a first step, to assess changes in overall ICN connectivity in the presence of MCI in a large sample of nondemented PD patients through a data-driven independent component analysis (ICA) resting-state functional MRI approach. We also aimed to assess the relationship between changes in patterns of network connectivity and performance in the cognitive functions most frequently affected in PD without dementia, that is, attention/executive (A/E), episodic memory, and visuospatial/visuoperceptual (VS/VP) [Aarsland et al., 2009; Elgh et al., 2009; Muslimovic et al., 2005]. In a second step, we aimed to evaluate the local patterns of ICN functional connectivity disruption associated with the presence of MCI in PD using an a priori seed-based analysis. Additionally, we have performed structural analyses to assess whether connectivity changes were accompanied by gray matter (GM) atrophy.

MATERIALS AND METHODS

Participants

Eighty-four nondemented PD patients and 38 healthy controls (HC) matched for age, sex, and years of education were recruited [Baggio et al., 2014]. The inclusion criterion for patients was the fulfillment of UK PD Society Brain Bank diagnostic criteria for PD. Exclusion criteria were: (i) MMSE $\leq$25 or dementia [Emre et al., 2007], (ii) Hoehn and Yahr (HY) score $>$ III, (iii) significant psychiatric, neurological or systemic comorbidity, (iv) significant pathological MRI findings other than mild white-matter (WM) hyperintensities in the FLAIR sequence, and (v) root-mean-square head motion $>$ 0.3 mm translation or 0.6° rotation. Four patients were excluded due to macroscopic movement, 14 due to head motion $>$ 0.3 mm translation or $>$ 0.6° rotation, and one for being an outlier in dual-regression analyses. Two HC were excluded due to microvascular WM changes, leaving a final sample of 65 PD patients and 36 HC. All patients except one were taking antiparkinsonian medication; all assessments were done in the *on* state. Levodopa equivalent daily dose (LEDD) was calculated as suggested by Tomlinson et al. [Tomlinson et al., 2010]. Motor disease severity was evaluated using HY staging and the Unified Parkinson's Disease Rating Scale motor section (UPDRS-III). The study was approved by the ethics committee of the University of Barcelona. All subjects provided written informed consent to participate.

Neuropsychological Assessment

Attention/executive (backward minus forward digit spans; Trail-Making Test part A minus part B scores; phonemic fluency scores (words beginning with "*P*" produced in 60 s), and Stroop Color-Word Test interference scores), VS/VP (Benton's Visual Form Discrimination and Judgment of Line Orientation tests) and memory (Rey's Auditory Verbal Learning Test total learning and 20-min free recall scores) functions were tested in all subjects. *Z*-scores for each test and subject were calculated based on the HC group's means and standard deviations. Expected *z*-scores adjusted for age, sex, and education for each test and subject were calculated based on a multiple regression analysis performed in the HC group [Aarsland et al., 2009]. Subjects were classified as having MCI if the actual *z*-score for a test was $\geq$1.5 lower than the expected score in at least two tests in one domain or in one test per domain in at least two domains. As expected [Muslimovic et al., 2005], most MCI subjects had

deficits in more than one function, precluding the creation of patient groups with single-domain impairments. Composite z-scores for each domain were calculated by averaging the age, sex, and education-corrected z-scores of all tests within that domain.

MRI Acquisition

Structural T1-weighted images, functional resting-state images and FLAIR images were acquired on a 3T Siemens MRI scanner as previously described [Baggio et al., 2014].

Processing of fMRI

The preprocessing of resting-state images was performed with FSL release 5.0.5 (http://www.fmrib.ox.ac.uk/fsl/) and AFNI (http://afni.nimh.nih.gov/afni). Briefly, it included removal of the first five volumes to allow for T1 saturation effects, skull stripping, grandmean scaling and temporal filtering (bandpass filtering of 0.01–0.1 Hz).

To control for the effect of subject head movement, physiological artifacts (e.g., breathing and vascular) and other non-neural sources of signal variation on the estimation of connectivity, motion correction (using FSL's MCFLIRT), and regression of nuisance signals (six motion parameters, cerebrospinal fluid signal and WM signal) were performed. Cerebrospinal fluid and WM mean signals were determined by averaging the native-space functional time series of all voxels contained inside the corresponding masks obtained from the segmentation of the T1-weighted images using FSL's FAST. To remove the effects of volumes corrupted by motion, a scrubbing procedure, similar to that suggested by [Power et al., 2012], was applied. Briefly, root-mean square intensity differences between (unpreprocessed) volumes m and $m-1$ (DVARS) were calculated, indicating how much the global intensity of a volume changed compared to the previous timepoint. Volumes with DVARS above the 75th percentile + 1.5 times the interquartile range were considered as outliers and added to the confound matrices alongside the nuisance factors described above, thus removing their effects from the analyses. Functional images were registered to their corresponding T1-weighted images and then registered to the MNI-152 template using linear transformations, and subsequently smoothed with a 6-mm full-width at half maximum Gaussian kernel.

Additionally, individual subject translatory and rotatory head movements were calculated according to the following formula:

$$\frac{1}{M-1}\sum_{i=2}^{M}\sqrt{|x_i-x_{i-1}|^2+|y_i-y_{i-1}|^2+|z_i-z_{i-1}|^2},$$

where x_i, y_i, and z_i are translations or rotations in the three axes at timepoint i, and M is the total number of timepoints (145) [Liu et al., 2008].

To detect and quantify global (periventricular + deep) WM hyperintensity load, we used an automated segmentation procedure [Ithapu et al., 2014] using the FLAIR and T1-weighted images. Results are given in normalized volumes taking brain volume into account.

Quality Control

Despite rigorous head-motion exclusion criteria, rotational head motion was significantly higher in non-MCI (PD-NMCI) patients than in HC ($P = 0.028$, post hoc Bonferroni test), with no significant differences between HC and PD-MCI patients or between patient subgroups. Head motion data were added as covariates of no interest in intergroup comparisons.

Data-Driven Connectivity Assessment: ICA and Dual Regression

Preprocessed images were analyzed with MELODIC using a temporal-concatenation spatial ICA approach [Beckmann and Smith, 2004]. In this step, temporally and spatially coherent patterns of signal variation were extracted from functional images with a predetermined dimensionality of 25. To identify the ICNs of interest, spatial cross-correlation was performed in a two-step procedure: (1) Between the 25 extracted components and 20 resting-state ICN templates published in [Smith et al., 2009], which describes the DMN, right FPN, and left FPN; (2) Between the 25 extracted components and the combined main nodes of the DAN (see below) described from [Spreng et al., 2013]. The correspondence between the components and the strongest correlations with the ICNs of interested was further confirmed by visual inspection based on the descriptions available from reference studies [Fox et al., 2006; Raichle, 2011; Smith et al., 2009; Spreng et al., 2013].

The selected components were subsequently fed into a dual-regression analysis [Filippini et al., 2009]. In this step, each group component is used as a mask to extract a subject and component-specific mean time course, describing the temporal dynamics of each ICN. The time courses are then used as voxelwise regressors in a linear model against the individual fMRI sets to obtain subject-specific spatial maps for each ICN. Voxelwise one-sample t-tests were used to establish each group's significant ICN maps through nonparametric, permutation testing (5,000 permutations). To perform intergroup connectivity analyses, subjects' regression maps for each ICN of interest were compared using a voxelwise general linear model also with permutation testing (5,000 permutations). A binary mask created from the sum of all groups' thresholded maps for all four networks was used as a search volume for intergroup analyses to assess intranetwork and internetwork connectivity differences. Individual subjects' GM volume maps (see below) were entered as voxelwise

TABLE I. Anatomical regions used as network nodes for seed-based connectivity analyses

	Left hemisphere/midline		Right hemisphere	
Region	Network	Abbreviation	Network	Abbreviation
Frontal eye fields	DAN	DA left FEF	DAN	DA right FEF
Inferior precentral sulcus	DAN	DA left iPCS	DAN	DA right iPCS
Middle temporal motion complex	DAN	DA left MT	DAN	DA right MT
Superior occipital gyrus	DAN	DA left SOG	DAN	DA right SOG
Superior parietal lobule	DAN	DA left SPL	DAN	DA right SPL
Anterior medial prefrontal cortex	DMN	DMN amPFC		
Dorsal medial prefrontal cortex	DMN	DMN dmPFC		
Posterior cingulate cortex	DMN	DMN pCC		
Precuneus	DMN	DMN PCu		
Ventral medial prefrontal cortex	DMN	DMN vmPFC		
Anterior temporal lobe	DMN	DMN left aTL	DMN	DMN right aTL
Hippocampal formation	DMN	DMN left HF	DMN	DMN right HF
Inferior frontal gyrus	DMN	DMN left IFG	DMN	DMN right IFG
Posterior inferior parietal lobule	DMN	DMN left pIPL	DMN	DMN right pIPL
Superior frontal gyrus	DMN	DMN left SFG	FPN	FP right SFG
Superior temporal sulcus	DMN	DMN left STS	DMN	DMN right STS
Temporal parietal junction	DMN	DMN left TPJ	DMN	DMN right TPJ
Dorsal anterior cingulate cortex	FPN	FP daCC		
Medial superior prefrontal cortex	FPN	FP msPFC		
Anterior inferior parietal lobule	FPN	FP left aIPL	FPN	FP right aIPL
Anterior insula	FPN	FP left aINS	FPN	FP right aINS
Dorsolateral prefrontal cortex	FPN	FP left dlPFC	FPN	FP right dlPFC
Middle frontal gyrus BA 6	FPN	FP left MFG BA6	FPN	FP right MFG BA6
Middle frontal gyrus BA 9	FPN	FP left MFG BA9	FPN	FP right MFG BA9
Rostrolateral prefrontal cortex	FPN	FP left rlPFC	FPN	FP right rlPFC

Resting-state networks to which each node belongs is indicated: DAN (dorsal attention network), DMN (default mode network) or FPN (frontoparietal network).

regressors in intergroup comparisons to control for the effect of structural atrophy on connectivity measures; results were similar to those using global GM volume obtained with voxel-based morphometry (VBM) and mean cortical thickness obtained with FreeSurfer (see below) as covariates of no interest. In accordance with previous studies [Agosta et al., 2012; Brier et al., 2012], false-discovery rate (FDR) correction was used for multiple comparisons correction in intergroup testing ($P < 0.05$); to further control the occurrence of false-positive intergroup results, a cluster-size threshold of 100 voxels was applied to intergroup analyses as in [Agosta et al., 2012].

To evaluate the relationship between connectivity changes and cognitive performance, mean regression coefficients extracted from the clusters of significant PD-MCI-versus-PD-NMCI differences were correlated with demographic/clinical variables (age, education, UPDRS, BDI, LEDD). Subsequently, they were correlated with each individual's cognitive function scores (A/E, memory, VS/VP) while controlling for the other two functions. LEDD significantly correlated with intergroup differences in DAN connectivity; results including this measure as a covariate of no interest were similar to those without controlling for it.

Seed-Based Functional Connectivity Analysis Using A Priori-Defined Regions of Interest

In total, 43 nodes (10 DAN, 18 DMN, and 15 bilateral FPN nodes; see Table I) were included using the MNI coordinates described in [Spreng et al., 2013] and 10-mm radius circular masks. Voxels shared by more than one mask were excluded. The time series of all voxels inside each region were averaged, and the connectivity between two nodes was estimated using Pearson's correlation between their mean time series.

Our previous work evaluating the same sample [Baggio et al., 2014] showed that interregional connectivity differences tended to be more pronounced between PD-MCI and HC, a tendency also observed in the mean internetwork and intranetwork connectivity results obtained with seed-based analysis (Supporting Information Figure 1). We used the Jonckheere–Terpstra (JT) test [Bewick et al., 2004], a nonparametric test for ordered differences in three or more samples ($HC \geq$ PD-NMCI $\geq$ PD-MCI or $HC \leq$ PD-NMCI $\leq$ PD-MCI, with at least one inequality being strict), to assess intergroup differences in functional connectivity. This analysis was done in two steps: (1) between mean intranetwork and

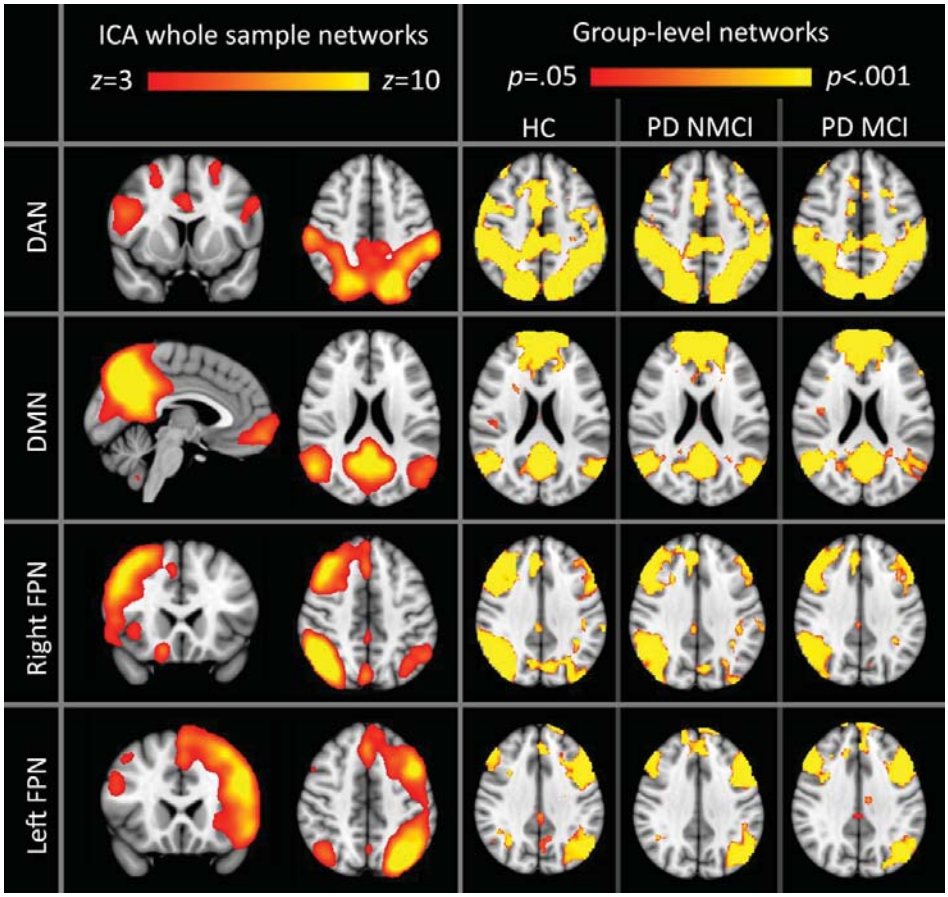

Figure 1.

Resting-state networks of interest. Left-sided images: maps obtained from independent component analyses (ICA) of the whole sample. Right-sided images: group-level maps obtained from dual-regression analyses ($P < 0.05$, FDR corrected). DAN: dorsal attention network; DMN: default-mode network; FPN: frontoparietal network. The right hemisphere is displayed on the left side of axial and coronal views.

internetwork connectivity values (average of the correlation coefficients between nodes according to network affiliation), and (2) between individual intranetwork and internetwork connectivity values (i.e., for connections between every pair of nodes). Permutation testing (10,000 permutations) generating random group affiliation was used to yield a null distribution against which the actual JT test statistics were compared to determine the statistical significance (set at $P < 0.05$) of each interregional connection analysis.

Processing of Structural Images

Structural analyses were done using two different and complementary techniques [Pereira et al., 2012]: VBM to assess GM volume, and cortical thickness (CTh).

VBM: Structural data was analyzed with FSL-VBM [Douaud et al., 2007], a VBM-style analysis. First, structural images were brain-extracted and GM-segmented before being registered to the MNI152 standard space. The resulting images were averaged to create a study-specific

TABLE II. Sociodemographic, clinical, head motion, and white-matter hyperintensity characteristics of participants

		PD		
	HC $n = 36$	Non-MCI $n = 43$	MCI $n = 22$	Test stats/P
Age (yrs.)	63.4 (10.5)	64.0 (9.8)	66.1 (12.2)	0.473/0.624
Sex (female:male)	17:19	20:23	8:14	0.431/0.806 χ
Years of education	10.3 (4.0)	10.8 (5.1)	8.8 (4.0)	2.178/0.119
MMSE	29.70 (.47)	29.35 (0.90)	28.50 (1.22)	**13.285/<0.001**
Hand dominance (*r:l*)	34:2	42:1	22:0	2.429/0.657 χ
BDI	5.81 (5.66)	8.9 (6.1)	11.5 (6.6)	**6.357/0.003**
Age at onset (yrs.)	–	57.8 (10.2)	56.8 (13.5)	0.340/0.735†
Disease duration	–	6.1 (4.4)	9.3 (5.5)	**2.523/0.014**‡
LEDD	–	646.7 (419.2)	951.9 (498.2)	**2.604/0.011**†
HY (1:2:3)	–	20:21:2	3:15:4	**8.315/0.016** χ
UPDRS-III	–	14.1 (7.5)	18.2 (8.7)	**1.927/0.059**†
Number of outlier timepoints	4.0 (2.6)	3.9 (2.6)	5.3 (3.4)	2.016/0.139
Head rotation (degrees)	0.03 (.01)	0.05 (.04)	0.04 (0.03)	**3.586/0.031**
Head translation (mm)	0.08 (.05)	0.07 (.04)	0.07 (0.05)	0.349/0.706
Normalized WM hyperintensity volume	792.4 (964.0)	792.7 (1278.8)	976.0 (1032.3)	0.230/0.795

Results are presented in means (SD). Statistically significant results ($P < 0.05$) are marked in bold. MMSE: mini-mental state examination. BDI: Beck's Depression Inventory-II scores. Disease duration: duration of motor symptoms, in years. LEDD: Levodopa equivalent daily dose, in mg. HY: Hoehn and Yahr scale. Test stats: *F*-statistics, Pearson's chi-squared (χ) or Student's t (‡). Post hoc analyses showed significant differences between MCI patients and HC for BDI, between MCI patients and both HC and non-MCI patients for MMSE scores, and between non-MCI patients and healthy controls for head rotation ($P < 0.05$, Bonferroni correction).

template, to which native GM images were nonlinearly re-registered. Second, native GM images were registered to this study-specific template and modulated to correct for local expansion or contraction due to the nonlinear component of the spatial transformation. To perform intergroup connectivity analyses, voxelwise general linear model with nonparametric, permutation testing (5,000 permutations) was applied. FDR was used for multiple comparisons correction ($q < 0.05$).

CTh was estimated using the automated FreeSurfer stream (version 5.1; http://surfer.nmr.harvard.edu). The procedures carried out include the removal of non-brain

TABLE III. Neuropsychological performance results for healthy controls and Parkinson's disease patients according to MCI status

	HC $n = 36$ mean (SD)	PD-NMCI $n = 43$ mean (SD)	PD-MCI $n = 22$ mean (SD)	F/P
VFD	29.61 (2.70)	29.09 (2.34)	26.50 (3.45)	9.550/<0.001
JLO	23.94 (3.99)	23.12 (3.93)	19.50 (5.23)	7.926/0.001
RAVLT total	44.67 (6.05)	44.47 (9.08)	33.55 (7.93)	16.866/0.001
RAVLT retrieval	9.08 (2.10)	8.58 (2.64)	6.05 (2.94)	10.645/<0.001
Digits backwards minus forwards	−1.69 (1.16)	−1.81 (1.03)	−1.23 (1.07)	2.663/0.075
Stroop interference	−2.42 (8.96)	−0.97 (9.92)	−3.31 (5.62)	0.553/0.577
TMT A−B	−50.17 (23.93)	−57.33 (29.58)	−142.35 (104.00)	22.340/<0.001
Phonemic fluency	16.57 (5.03)	16.40 (4.962)	11.82 (5.44)	7.183/0.001
VS/VP *z*-score	−0.012 (0.572)	−0.169 (0.601)	−0.989 (.880)	16.169/<0.001
Memory *z*-score	−0.010 (0.818)	−0.092 (1.028)	−1.365 (1.156)	15.157/<0.001
A/E *z*-score	0.027 (0.537)	−0.022 (0.519)	−0.776 (.996)	12.077/<0.001

Results are presented as means (SD). PD-NMCI: Parkinson's disease patients without MCI; PD-MCI: patients with MCI; VFD: visual form discrimination test; JLO: judgment of line orientation test; RAVLT: Rey's auditory verbal learning test; Digits backwards minus forwards: difference between backward and forward digit spans; TMT A-B: difference between Trail Making Test parts A and B; VS/VP: visuospatial/visuoperceptual; A/E: attention/executive. *Z*-scores for cognitive domains refer to the difference between actual *z*-scores and expected age, sex and education-adjusted *z*-scores, averaged throughout the tests within that domain. For all significant F-test comparisons, post hoc analyses showed that MCI patients' scores were significantly worse than non-MCI patients' and healthy controls', with no significant differences between the latter ($P < 0.05$, post hoc Bonferroni test).

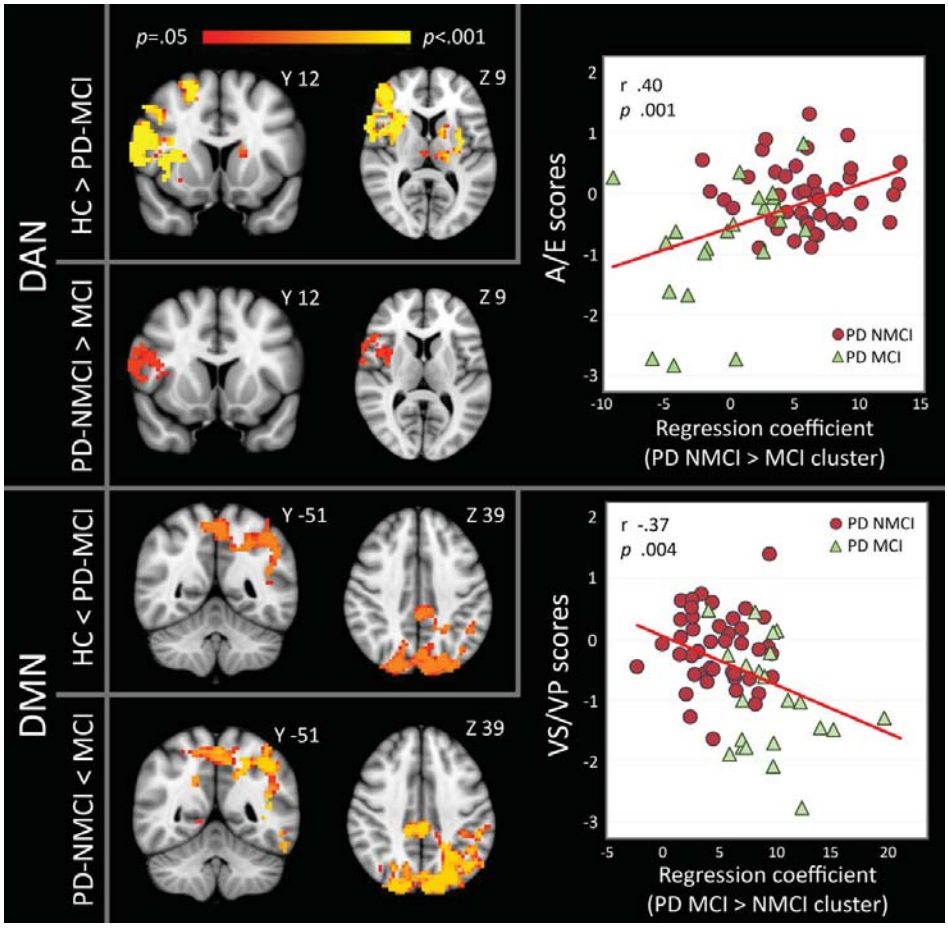

Figure 2.

Data-driven analysis intergroup connectivity comparisons. Left side: clusters of significant ($P < 0.05$, FDR-corrected; 100-voxel threshold) connectivity group differences for PD patients with mild cognitive impairment (PD-MCI) versus HC or patients without mild cognitive impairment (PD-NMCI) for the dorsal attention network (DAN) and the default-mode network (DMN). FDR-corrected *P* values are color-coded according to the bar at the top. MNI *Y* and *Z* coordinates of the slices shown are indicated. Right side: scatterplots showing the correlation between connectivity values (*regression coefficients obtained from the clusters of significant PD-MCI versus PD-NMCI differences) and age-, sex-, and education-corrected z-scores in attention/executive (A/E) and visuospatial/visuoperceptual (VS/VP) functions in the PD patient group. *r*: partial-correlation coefficient. The right hemisphere is displayed on the left side.

data, intensity normalization, tessellation of the GM/WM boundary, automated topology correction [Fischl et al., 2001; Ségonne et al., 2007], and accurate surface deformation to identify tissue borders [Dale et al., 1999; Fischl and Dale, 2000]. Cortical thickness is then calculated as the distance between the white and GM surfaces at each vertex of the reconstructed cortical mantle. Maps were smoothed with an across-surface 15-mm full-width at half maximum circularly symmetric Gaussian kernel.

Intergroup comparisons between groups were performed using a vertex-by-vertex general linear model. All results were corrected for multiple comparisons using

TABLE IV. Clusters of significant intergroup connectivity differences

	Region	MNI152 coordinates of maximum (*x y z*)	Cluster volume (mm^3)	Peak FDR-corrected *P*-value
DAN HC>PD-MCI	Superior frontal gyri, right middle/inferior frontal gyri, right precentral gyrus, right anterior/middle insula	21 36 −15	65,988	0.005
	Right middle temporal gyrus, temporo-occipital junction	60 −57 −6	4,158	0.005
	Left caudate nucleus, left putamen	−12 0 18	3,159	0.005
	Thalami	−6 −15 −3	3,105	0.009
DAN PD-NMCI> PD-MCI	Right inferior frontal gyrus, frontal operculum, anterior/middle insula	57 12 3	7,938	0.038
	Right middle temporal gyrus, temporo-occipital junction	60 −30 −27	3,294	0.038
DMN HC<PD-MCI	Bilateral dorsal precuneus, posterior cingulate gyrus, superior occipito-parietal junctions and superior occipital gyri, left superior parietal lobule	−33 −66 18	42,957	0.034
	Left temporo-occipital junction	−57 −69 −12	4,860	0.034
DMN PD-NMCI <PD-MCI	Bilateral dorsal precuneus, posterior cingulate gyrus, superior occipito-parietal junctions and superior occipital gyri, left superior parietal lobule, left temporo-occipital junction	−57 −21 −27	74,007	0.009

DAN: dorsal attention network; DMN: default mode network; HC: healthy controls; PD-MCI: Parkinson's disease patients with mild cognitive impairment; PD-NMCI: Parkinson's disease patients without mild cognitive impairment.

cluster-wise Monte-Carlo simulation (10,000 iterations). Significance level was set at $P < 0.05$.

To assess the relationship between changes in CTh and cognitive performance, mean thickness values extracted from the clusters of significant group differences were correlated with cognitive function scores (A/E, memory, VS/VP) while controlling for the other two functions and for age (which correlated with CTh values). In addition, to investigate the relationship between structural and functional changes, mean thickness extracted from clusters of significant CTh intergroup differences were correlated with connectivity values extracted from significant functional connectivity differences, controlling for age.

Sociodemographic/Clinical/WM Hyperintensity Data Statistical Analyses

Statistical significance threshold was set at $P < 0.05$. Pearson's chi-squared test was used to compare categorical variables (hand dominance, sex, HY). Student's *t*-test was used to compare head motion, clinical data means between PD patients, and HC. Three-level one-way ANOVAs were used to compare head motion, clinical, WM hyperintensity load, and sociodemographic data between HC and patient subgroups. Significance *P* values were adjusted using post hoc Bonferroni tests.

RESULTS

Table II shows sociodemographic, clinical, head motion, and WM hyperintensity load characteristics for the three groups (HC, non-MCI PD patients [PD-NMCI], MCI PD patients [PD-MCI]). Table III shows neuropsychological assessment results and group comparisons. As expected [Hoops et al., 2009], although subjects' MMSE scores were within the normal range, neuropsychological assessment focusing on specific cognitive functions was able to detect the presence of deficits in a high percentage of patients. Twenty-two patients (33.8%) fulfilled criteria for MCI. VS/VP scores did not correlate significantly with A/E or memory scores, with clinical/demographical variables such as age, education, LEDD, disease duration, or UPDRS-III or BDI scores. A/E scores significantly correlated with memory scores ($r = 0.31$, $P = 0.011$); the latter, in turn, also correlated significantly with LEDD ($r = -0.27$, $P = 0.027$).

Data-Driven Connectivity Analysis

The ICA components corresponding to the ICNs of interest, as well as the areas in all groups that showed to be significantly related to them (one-sample *t*-test, $P < 0.05$,

FDR-corrected) in dual-regression analyses, included, as main regions (see Fig. 1):

DAN: caudal anterior cingulate gyrus, frontal eye fields, dorsolateral prefrontal areas, temporooccipital junctions, and dorsal occipitoparietal regions.

DMN: posterior cingulate gyrus/precuneus, medial prefrontal region, angular gyri, and middle/superior frontal gyri.

Right and left FPN: ipsilateral inferior parietal lobule, lateral prefrontal cortex, insula and opercular region, as well as precuneus.

Intergroup comparisons: No significant differences were observed between HC and the collapsed PD patient group for any of the networks analyzed. Statistically significant group differences were observed when stratifying the PD sample into PD-MCI and PD-NMCI subgroups (see Fig. 2 and Table IV). Compared with HC, the DAN in PD-MCI showed reduced connectivity ($P < 0.05$, FDR-corrected) with widespread, predominantly right sided, frontal/insular areas, as well as with the thalami and left striatum. Connectivity reductions of the DAN in PD-MCI compared with PD-NMCI patients were similar, although less extensive, to those seen between PD-MCI and HC, and involved regions that are part of the DAN itself and of the right FPN (see Fig. 2 and Table IV).

Compared with HC and with PD-NMCI, PD-MCI showed significant connectivity increases ($P < 0.05$, FDR-corrected) between the DMN and posterior cortical regions (see Fig. 2 and Table IV). These regions corresponded to areas of the DAN and the left FPN. No significant connectivity differences were observed between HC and PD-NMCI for any of the ICNs analyzed.

Correlation analyses: Connectivity levels, assessed through the regression coefficients obtained from the clusters of significant differences between PD-MCI and PD-NMCI (DAN and DMN), did not correlate significantly with age, years of education, or BDI/UPDRS-III scores. Connectivity levels in the DAN clusters, conversely, correlated with LEDD ($r = -0.34$, $P = 0.006$).

Partial-correlation analyses evaluating the relationship between connectivity levels in the significant PD-MCI-versus-PD-NMCI comparison clusters and age-, education-, and sex-corrected neuropsychological data revealed:

- significant positive correlation between connectivity in the DAN clusters and A/E scores (partial-correlation coefficient = 0.40, $P = 0.001$).
- significant negative correlation between connectivity in the DMN clusters and VS/VP scores (partial-correlation coefficient= -0.37, $P = 0.004$) and MMSE (partial-correlation coefficient = -0.32, $P = 0.011$) scores.

There were no significant correlations between connectivity values in the clusters of significant intergroup differences and WM hyperintensity load.

Seed-Based A Priori-Defined Connectivity Analysis

Visual inspection confirmed that the a priori masks overlapped with the corresponding regions of the ICNs obtained from ICA. Comparing mean intranetwork and internetwork connectivity values, significant ordered reductions (HC ≥ PD-NMCI ≥ PD-MCI) were observed in intra-DAN connectivity ($P = 0.036$, 10,000 permutations), and there was suggestive evidence of increases in DAN-DMN internetwork connectivity ($P = 0.067$, 10,000 permutations; see Supporting Information Figure 1). The analysis of individual interregional connections showed that ordered connectivity reductions (HC ≥ PD-NMCI ≥ PD-MCI) were present both within and between networks (Fig. 3). Intranetwork reductions were found mainly in the DMN and the DAN and were characterized by reductions from positive correlation coefficients in HC to values closer to zero in PD-MCI. Most intra-DMN connectivity reductions involved this ICN's midline nodes and their connections with the left hippocampus, anterior temporal regions and posterior inferior parietal lobules. Intra-DAN reductions were mainly seen between frontal nodes and occipital/parietal nodes. Internetwork connectivity reductions were also observed, mainly affecting connections between the frontal and right insular FPN nodes and occipital/parietal DAN nodes. In HC, these nodes' time series were positively correlated, whereas in PD-MCI they tended to correlate negatively. Connectivity reductions were also seen in a few sparse connections between DAN and DMN nodes.

Connectivity increases (HC ≤ PD-NMCI ≤ PD-MCI) were also present, involving internetwork connections. Most such increases were found between midline and frontal/temporal DMN nodes and posterior DAN nodes. As expected, in HC these nodes' time series were negatively correlated. In PD-MCI, they tended to be close to zero (see Fig. 3).

See the Supporting Information Table I, for additional information regarding the interregional connections for which significant ordered connectivity effects were observed.

GM Structural Assessment

CTh analyses showed that, compared with HC, PD-MCI subjects had significant cortical thinning in lateral occipital, inferior parietal, and occipito-temporal areas bilaterally, as well as in the left precuneus. PD-NMCI, compared with HC, showed less extensive areas of reduced CTh, also involving lateral occipital regions bilaterally, and in the right middle/inferior temporal gyrus (see Fig. 4 and the Supporting Information Table II). No significant differences were observed between PD-MCI and PD-NMCI.

Partial-correlation analyses evaluating the relationship between mean cortical thickness in the significant HC-versus-PD-NMCI and HC-versus-PD-MCI comparison clusters and neuropsychological and connectivity values revealed (see Supporting Information Figure 2):

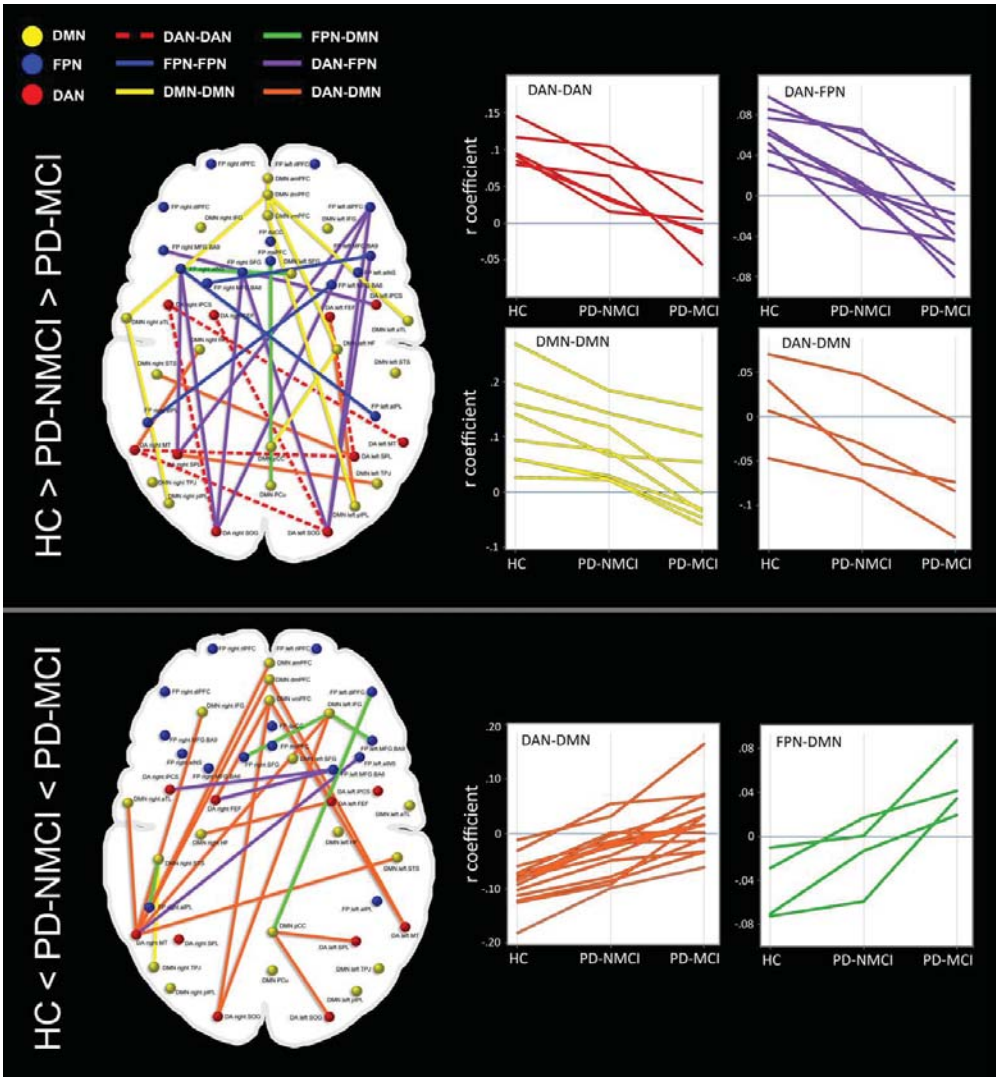

Figure 3.

Seed-based connectivity analysis results. Left side: schematic representation of the interregional connections where significant ($P < 0.05$) ordered connectivity changes were observed. Network affiliation of the nodes shown as well as of the internodal connections is indicated in the legend above. Abbreviations refer to those described in Table I. Right side: plots showing *r* coefficient levels according to group for the connections where significant effects were found, according to the network affiliation of the involved nodes. Only intranetwork or internetwork changes comprising more than three connections are plotted. DAN: dorsal attention network; DMN: default-mode network; FPN: frontoparietal network; HC: healthy controls; PD-NMCI: Parkinson's disease patients without mild cognitive impairment; PD-MCI: Parkinson's disease patients with mild cognitive impairment.

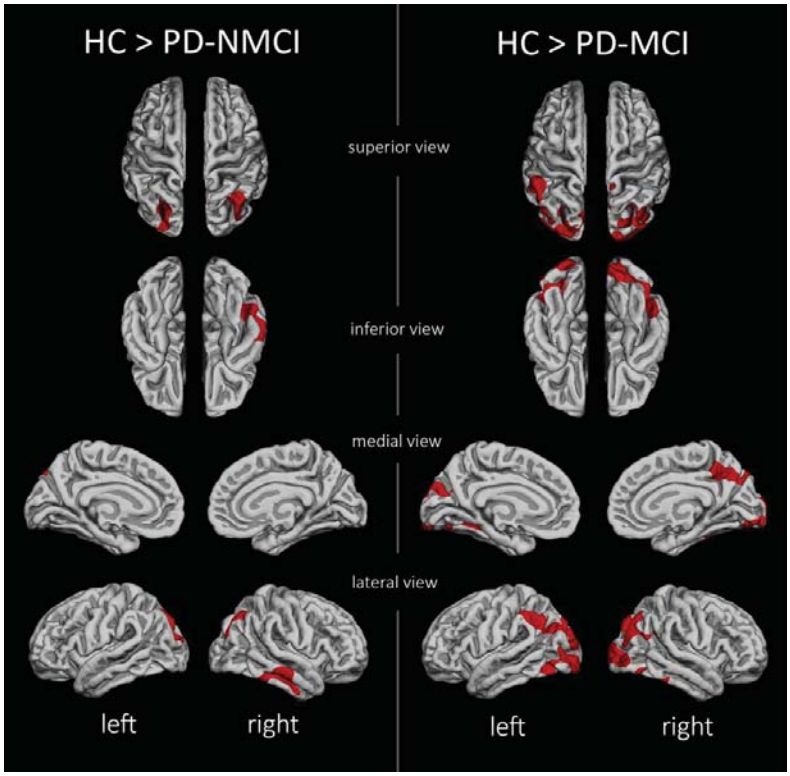

Figure 4.

Vertexwise comparison of cortical thickness between HC, Parkinson's disease patients without mild cognitive impairment (PD-NMCI), and Parkinson's disease patient with mild cognitive impairment (PD-MCI). Red clusters indicate areas of significantly reduced cortical thickness in PD-NMCI compared with HC (left) and in PD-MCI compared with HC (right; $P < 0.05$). [Color figure can be viewed in the online issue, which is available at wileyonlinelibrary.com.]

- positive correlation between CTh in the left-sided lateral occipital/temporo-occipital HC-versus-PD-MCI cluster and VS/VP scores (partial-correlation coefficient = 0.26, $P = 0.042$).
- negative correlation between CTh in the left-sided lateral occipital/temporo-occipital HC-versus-PD-MCI cluster and connectivity levels in the clusters of increased connectivity between the DMN and occipito-parietal regions in PD-MCI compared with PD-NMCI (partial-correlation coefficient $= -0.26$, $P = 0.038$) and in PD-MCI compared with controls (partial-correlation coefficient $= -0.28$, $P = 0.025$).

No significant intergroup differences or correlations with neuropsychological scores were found for mean CTh. In accordance with previous studies that described a higher sensitivity of CTh in the detection of PD-related structural atrophy, no significant intergroup GM volume differences were observed with VBM [Pereira et al., 2012].

DISCUSSION

In this study, we investigated the resting-state functional connectivity of brain ICNs in PD patients according to the presence or absence of MCI using two complementary techniques. As main findings, we observed that PD patients with MCI had a reduction in connectivity between right frontoinsular regions and the DAN, associated with A/E performance; and an increased connectivity between posterior cortical regions—where there was also evidence of structural degeneration—and the DMN, associated with VS/VP scores.

Previous studies have described an association between changes in DMN connectivity and neuropsychological performance in distinct neurological and psychiatric diseases (see [Mevel et al., 2011] and [Whitfield-Gabrieli and Ford, 2012]), but little is known about how changes in internetwork connectivity relate to cognitive decline. Previous fMRI studies show that, during externally-directed cognitive tasks, DAN activity increases whereas DMN activity is reduced; during "rest" or internally-directed/self-referential thoughts, the opposite is observed [Kelly et al., 2008]. The FPN, functionally and anatomically interposed between the main DMN and DAN nodes, has been postulated to flexibly connect to one network or the other depending on attentional task demands, mediating the transition between them [Spreng et al., 2013; Vincent et al., 2008]. This transition appears to be relevant for cognitive task performance [Kelly et al., 2008]. In this work, PD-MCI subjects displayed reduced connectivity between the DAN and the right anterior insula and adjacent frontal areas, which are regions of the DAN itself and of the right FPN—networks that are considered to play a role in attentional processes [Hellyer et al., 2014]. Furthermore, the relevance of the frontoinsular cortex in cognition has recently been demonstrated (see [Christopher et al., 2014a]). Importantly, this region has been shown to exert a critical and causal role in switching between DAN and DMN across tasks of different modalities, as well as in the resting state [Sridharan et al., 2008]. In PD patients with visual hallucinations, insular GM volume was seen to correlate with DAN activation during a visual task [Shine et al., 2014]. We have found that reduced connectivity—without detectable associated structural atrophy—between this area and the DAN in PD patients was associated with worse performance in A/E functions, suggesting that functional right frontoinsular cortical changes are involved in this type of deficit in PD. It could be speculated that this association is related to impaired network-switching mechanisms, a hypothesis that could be assessed by future, task-based fMRI studies.

In healthy persons, dopamine synthesis capacity has been shown to correlate with reduced DAN-FPN and increased FPN-DMN coupling, during the resting state [Dang et al., 2012]. Importantly, a recent study found that PD-MCI patients have reduced insular dopaminergic D2 receptors, and that this loss is associated with worse performance in executive functions [Christopher et al., 2014b]. Taken together with our findings, these data indicate that A/E deficits in PD—considered to be related to frontostriatal dopaminergic imbalances (see [Cools and D'Esposito, 2011])—may be mediated by dopaminergic effects on DAN connectivity.

In this study, PD-MCI subjects displayed increased connectivity between the DMN and occipito-parietal lateral and medial cortical regions that are components of the left FPN and the DAN. Seed-based analyses also revealed an increased connectivity between DMN and posterior DAN nodes in PD-MCI, characterized by the loss of the negative correlation normally observed between these regions. Despite variable findings regarding the DMN in PD, the most frequently described connectivity changes involve abnormal patterns of activation and deactivation of the precuneus/PCC during rest and cognitive tasks [Eimeren and Monchi, 2009]. In this study, connectivity increments between the DMN and occipito-parietal cortical areas were seen to be associated with worse VS/VP performance. Seed-based analyses revealed reduced within-DMN connectivity, a finding in line with a recent resting-state fMRI study that evaluated cognitively unimpaired PD patients [Tessitore et al., 2012]. As in this study, connectivity changes affecting posterior cortical regions correlated with performance in VS/VP tests. Interestingly, we also found cortical thinning in occipito-parietal regions in the PD patient group, more markedly in the PD-MCI subgroup, which also showed a relationship with VS/VP performance. These findings are in line with and complement previous structural neuroimaging studies addressing the neuroanatomical bases of VS/VP deficits in PD [Pereira et al., 2009]. Furthermore, previous evidence suggests that task-positive FPN and the DMN competitively connect with visual areas during visual tasks, and that the degree of decoupling of the DMN with these structures predicts task performance [Chadick and Gazzaley, 2011]. Our findings suggest that changes in connectivity between the DMN and posterior cortical areas belonging to the DAN and the FPN may be part of the substrates of VS/VP deficits in PD through a disruption of these dynamic coupling mechanisms.

Longitudinal studies have shown that, unlike dopamine-related deficits, impairments with posterior cortical bases are predictors of future dementia in PD [Williams-Gray et al., 2007; Williams-Gray et al., 2009]. Data from a longitudinal PET study found that reduced glucose metabolism in occipital and posterior cingulate regions heralded future conversion to dementia [Bohnen et al., 2011], emphasizing the importance of posterior cortical changes as predictors of dementia in PD. We hypothesize that the connectivity increases observed, as well as the structural atrophy seen to be associated with it, are related to the cortical dysfunctions that lead to progressive cognitive decline and, ultimately, dementia. As with current evidence this association is speculative, however, it remains to be studied whether these occipito-parieto-temporal connectivity and structural changes are related to the cortical pathology that appears to be critical for the development of dementia in PD, such as synucleinopathy or Alzheimer's-type pathology [Compta et al., 2011].

The finding of increased functional connectivity associated with worse cognitive status merits further discussion. Increased functional connectivity is a frequent finding in neurological diseases of different nature [Hillary et al., in press; Pievani et al., 2011]. In this study, however, connectivity increments were primarily observed in internetwork connections. Specifically, seed-based analyses showed that these connectivity increases predominantly involved the loss of the normal pattern of anti-correlation between

DMN nodes and parietal, occipital and temporal DAN nodes in PD-MCI; the latter nodes were also seen to be less connected to other DAN and FPN nodes. Instead of an actual direct increase in connectivity, at least part of the observed effect might be mediated by the reduced connectivity of DAN nodes with their parent network; being less connected to other DAN regions, these nodes may also lose the expected negative correlation this network displays with the DMN.

One possible limitation of our study is that, despite the rigorous head motion exclusion criteria and preprocessing steps aimed at minimizing the effect of motion artifacts, we cannot guarantee that our results were not influenced to some degree by them. Nonetheless, the identified connectivity effects were more pronounced in PD-MCI, which had less head motion than the PD-NMCI group. These observations suggest that our results have actual biological origins. Furthermore, patients in our study were assessed in the *on* state, that is, under the effect of dopaminergic medication, which influences ICN connectivity [Cole et al., 2013; Dang et al., 2012]. Although this may limit the assessment of PD-related effects on the studied ICNs, our goal was to evaluate the substrate of the cognitive deficits as they occur in patients' daily lives—under the influence of their usual medication. Furthermore, our results were maintained when adding LEDD as a covariate, suggesting that the connectivity changes observed go beyond the effects of dopaminergic medication. As this may not entirely control for the acute and chronic effects of dopaminergic therapy, however, future studies including both *on* and *off*-state assessments, as well as drug-naïve subjects, could provide useful additional information.

This study shows that cognitive decline in PD is associated with different patterns of connectivity changes affecting large-scale brain ICNs. These findings suggest that network changes, mainly characterized by the loss of intra-network connectivity and an increase in the connectivity between networks that normally display anti-correlated activities, are part of the neural substrate underlying cognitive deficits in PD. Moreover, our results give support to the hypothesis that the brain networks studied play a role in the neural processing of distinct neuropsychological functions. Future, longitudinal studies may help establish a potential role for ICN connectivity measures as predictors of cognitive decline in PD.

ACKNOWLEDGMENT

The authors M.J.M., R.S., F.V., and Y.C. report no disclosures.

REFERENCES

Aarsland D, Kurz MW (2010): The epidemiology of dementia associated with Parkinson disease. J Neurol Sci 289:18–22.

Aarsland D, Brønnick K, Larsen JP, Tysnes OB, Alves G (2009): Cognitive impairment in incident, untreated Parkinson disease: The Norwegian ParkWest study. Neurology 72:1121–1126.

Agosta F, Pievani M, Geroldi C, Copetti M, Frisoni GB, Filippi M (2012): Resting state fMRI in Alzheimer's disease: Beyond the default mode network. Neurobiol Aging 33:1564–1578.

Baggio H-C, Sala-Llonch R, Segura B, Marti M-J, Valldeoriola F, Compta Y, Tolosa E, Junqué C (2014): Functional brain networks and cognitive deficits in Parkinson's disease. Hum Brain Mapp 35:4620–4634.

Beckmann CF, Smith SM (2004): Probabilistic independent component analysis for functional magnetic resonance imaging. IEEE Trans Med Imaging 23:137–152.

Bewick V, Cheek L, Ball J (2004): Statistics review 10: Further nonparametric methods. Crit Care 8:196–199.

Bohnen NI, Koeppe RA, Minoshima S, Giordani B, Albin RL, Frey KA, Kuhl DE (2011): Cerebral glucose metabolic features of Parkinson disease and incident dementia: Longitudinal study. J Nucl Med 52:848–855.

Brier MR, Thomas JB, Snyder AZ, Benzinger TL, Zhang D, Raichle ME, Holtzman DM, Morris JC, Ances BM (2012): Loss of intranetwork and internetwork resting state functional connections with Alzheimer's disease progression. J Neurosci 32: 8890–8889.

Chadick JZ, Gazzaley A (2011): Differential coupling of visual cortex with default or frontal-parietal network based on goals. Nat Neurosci 14:830–832.

Christopher L, Koshimori Y, Lang AE, Criaud M, Strafella AP (2014a): Uncovering the role of the insula in non-motor symptoms of Parkinson's disease. Brain 137:2143–2154.

Christopher L, Marras C, Duff-Canning S, Koshimori Y, Chen R, Boileau I, Segura B, Monchi O, Lang AE, Rusjan P, Houle S, Strafella AP (2014b): Combined insular and striatal dopamine dysfunction are associated with executive deficits in Parkinson's disease with mild cognitive impairment. Brain 137:565–575.

Cole DM, Beckmann CF, Oei NYL, Both S, van Gerven JMA, Rombouts SA RB (2013): Differential and distributed effects of dopamine neuromodulations on resting-state network connectivity. Neuroimage 78:59–67.

Compta Y, Parkkinen L, O'Sullivan SS, Vandrovcova J, Holton JL, Collins C, Lashley T, Kallis C, Williams DR, de Silva R, Lees AJ, Revesz T (2011): Lewy- and Alzheimer-type pathologies in Parkinson's disease dementia: Which is more important? Brain 134:1493–1505.

Cools R, D'Esposito M (2011): Inverted-U-shaped dopamine actions on human working memory and cognitive control. Biol Psychiatry 69:e113–e125.

Dale AM, Fischl B, Sereno MI (1999): Cortical surface-based analysis. I. Segmentation and surface reconstruction. Neuroimage 9: 179–194.

Dang LC, O'Neil JP, Jagust WJ (2012): Dopamine supports coupling of attention-related networks. J Neurosci 32:9582–9587.

Douaud G, Smith S, Jenkinson M, Behrens T, Johansen-Berg H, Vickers J, James S, Voets N, Watkins K, Matthews PM, James A (2007): Anatomically related grey and white matter abnormalities in adolescent-onset schizophrenia. Brain 130:2375–2386.

Eimeren MT van, Monchi O (2009): Dysfunction of the Default Mode Network in Parkinson Disease. Arch Neurol 66:877–883.

Elgh E, Domellöf M, Linder J, Edström M, Stenlund H, Forsgren L (2009): Cognitive function in early Parkinson's disease: A population-based study. Eur J Neurol 16:1278–1284.

Emre M, Aarsland D, Brown R, Burn DJ, Duyckaerts C, Mizuno Y, Broe GA, Cummings J, Dickson DW, Gauthier S, Goldman

J, Goetz C, Korczyn A, Lees A, Levy R, Litvan I, McKeith I, Olanow W, Poewe W, Quinn N, Sampaio C, Tolosa E, Dubois B (2007): Clinical diagnostic criteria for dementia associated with Parkinson's disease. Mov Disord 22:1689–1707; quiz 1837.

Filippini N, MacIntosh BJ, Hough MG, Goodwin GM, Frisoni GB, Smith SM, Matthews PM, Beckmann CF, Mackay CE (2009): Distinct patterns of brain activity in young carriers of the APOE-epsilon4 allele. Proc Natl Acad Sci USA 106:7209–7214.

Fischl B, Dale AM (2000): Measuring the thickness of the human cerebral cortex from magnetic resonance images. Proc Natl Acad Sci USA 97:11050–11055.

Fischl B, Liu A, Dale AM (2001): Automated manifold surgery: Constructing geometrically accurate and topologically correct models of the human cerebral cortex. IEEE Trans Med Imaging 20:70–80.

Fox MD, Corbetta M, Snyder AZ, Vincent JL, Raichle ME (2006): Spontaneous neuronal activity distinguishes human dorsal and ventral attention systems. Proc Natl Acad Sci USA 103:10046–10051.

Hellyer PJ, Shanahan M, Scott G, Wise RJS, Sharp DJ, Leech R (2014): The control of global brain dynamics: Opposing actions of frontoparietal control and default mode networks on attention. J Neurosci 34:451–461.

Hillary FG, Roman CA, Venkatesan U, Rajtmajer SM, Bajo R, Castellanos ND: Hyperconnectivity is a Fundamental Response to Neurological Disruption (in press).

Hoops S, Nazem S, Siderowf AD, Duda JE, Xie SX, Stern MB, Weintraub D (2009): Validity of the MoCA and MMSE in the detection of MCI and dementia in Parkinson disease. Neurology 73:1738–1745.

Ithapu V, Singh V, Lindner C, Austin BP, Hinrichs C, Carlsson CM, Bendlin BB, Johnson SC (2014): Extracting and summarizing white matter hyperintensities using supervised segmentation methods in Alzheimer's disease risk and aging studies. Hum Brain Mapp 4235:4219–4235.

Kelly AMC, Uddin LQ, Biswal BB, Castellanos FX, Milham MP (2008): Competition between functional brain networks mediates behavioral variability. Neuroimage 39:527–537.

Krajcovicova L, Mikl M, Marecek R, Rektorova I (2012): The default mode network integrity in patients with Parkinson's disease is levodopa equivalent dose-dependent. J Neural Transm 119:443–454.

Liu Y, Liang M, Zhou Y, He Y, Hao Y, Song M, Yu C, Liu H, Liu Z, Jiang T (2008): Disrupted small-world networks in schizophrenia. Brain 131:945–961.

Mevel K, Chételat G, Eustache F, Desgranges B (2011): The default mode network in healthy aging and Alzheimer's disease. Int J Alzheimers Dis 2011:535816.

Muslimovic D, Post B, Speelman JD, Schmand B (2005): Cognitive profile of patients with newly diagnosed Parkinson disease. Neurology 65:1239–1245.

Pereira JB, Junqué C, MartÚ M-J, Ramirez-Ruiz B, Bargalló N, Tolosa E (2009): Neuroanatomical substrate of visuospatial and visuoperceptual impairment in Parkinson's disease. Mov Disord 24:1193–1199.

Pereira JB, Ibarretxe-Bilbao N, Marti M-J, Compta Y, Junqué C, Bargallo N, Tolosa E (2012): Assessment of cortical degeneration in patients with Parkinson's disease by voxel-based morphometry, cortical folding, and cortical thickness. Hum Brain Mapp 33:2521–2534.

Pievani M, de Haan W, Wu T, Seeley WW, Frisoni GB (2011): Functional network disruption in the degenerative dementias. Lancet Neurol 10:829–843.

Power JD, Barnes KA, Snyder AZ, Schlaggar BL, Petersen SE (2012): Spurious but systematic correlations in functional connectivity MRI networks arise from subject motion. Neuroimage 59:2142–2154.

Raichle ME (2011): The restless brain. Brain Connect 1:3–12.

Rektorova I, Krajcovicova L, Marecek R, Mikl M (2012): Default mode network and extrastriate visual resting state network in patients with Parkinson's disease dementia. Neurodegener Dis 10:232–237.

Sala-Llonch R, Arenaza-Urquijo EM, Valls-Pedret C, Vidal-Piñeiro D, Bargalló N, Junqué C, Bartrés-Faz D (2012): Dynamic functional reorganizations and relationship with working memory performance in healthy aging. Front Hum Neurosci 6:152.

Seeley WW, Menon V, Schatzberg AF, Keller J, Glover GH, Kenna H, Reiss AL, Greicius MD (2007): Dissociable intrinsic connectivity networks for salience processing and executive control. J Neurosci 27:2349–2356.

Ségonne F, Pacheco J, Fischl B (2007): Geometrically accurate topology-correction of cortical surfaces using nonseparating loops. IEEE Trans Med Imaging 26:518–529.

Shine JM, Halliday GM, Gilat M, Matar E, Bolitho SJ, Carlos M, Naismith SL, Lewis SJG (2014): The role of dysfunctional attentional control networks in visual misperceptions in Parkinson's disease. Hum Brain Mapp 35:2206–2219.

Smith SM, Fox PT, Miller KL, Glahn DC, Fox PM, Mackay CE, Filippini N, Watkins KE, Toro R, Laird AR, Beckmann CF (2009): Correspondence of the brain's functional architecture during activation and rest. Proc Natl Acad Sci USA 106:13040–13045.

Spreng RN, Stevens WD, Chamberlain JP, Gilmore AW, Schacter DL (2010): Default network activity, coupled with the frontoparietal control network, supports goal-directed cognition. Neuroimage 53:303–317.

Spreng RN, Sepulcre J, Turner GR, Stevens WD, Schacter DL (2013): Intrinsic architecture underlying the relations among the default, dorsal attention, and frontoparietal control networks of the human brain. J Cogn Neurosci 25:74–86.

Sridharan D, Levitin DJ, Menon V (2008): A critical role for the right fronto-insular cortex in switching between central-executive and default-mode networks. Proc Natl Acad Sci USA 105: 12569–12574.

Tessitore A, Esposito F, Vitale C, Santangelo G, Amboni M, Russo A, Corbo D, Cirillo G, Barone P, Tedeschi G (2012): Default-mode network connectivity in cognitively unimpaired patients with Parkinson disease. Neurology 79:2226–2232.

Tomlinson CL, Stowe R, Patel S, Rick C, Gray R, Clarke CE (2010): Systematic review of levodopa dose equivalency reporting in Parkinson's disease. Mov Disord 25:2649–2653.

Vincent JL, Kahn I, Snyder AZ, Raichle ME, Buckner RL (2008): Evidence for a frontoparietal control system revealed by intrinsic functional connectivity. J Neurophysiol 100:3328–3342.

Whitfield-Gabrieli S, Ford JM (2012): Default mode network activity and connectivity in psychopathology. Annu Rev Clin Psychol 8:49–76.

Williams-Gray CH, Foltynie T, Brayne CEG, Robbins TW, Barker RA (2007): Evolution of cognitive dysfunction in an incident Parkinson's disease cohort. Brain 130:1787–1798.

Williams-Gray CH, Evans JR, Goris A, Foltynie T, Ban M, Robbins TW, Brayne C, Kolachana BS, Weinberger DR, Sawcer SJ, Barker RA (2009): The distinct cognitive syndromes of Parkinson's disease: 5 year follow-up of the CamPaIGN cohort. Brain 132:2958–2969.

SUPPLEMENTARY MATERIALS

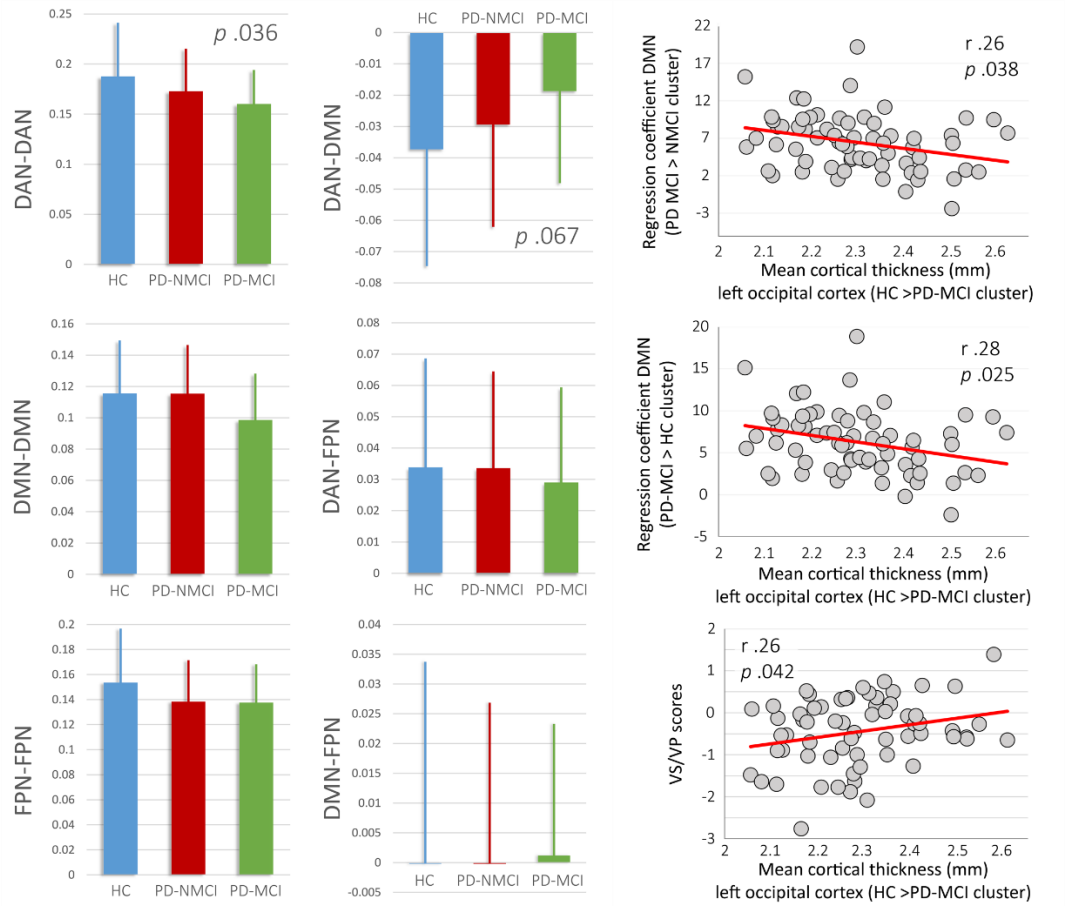

Supplementary Figure 1. *Left-side (bar graphs):* Mean intra and internetwork correlation values (y axis) according to group. HC: healthy controls; PD-NMCI: Parkinson's disease patients without mild cognitive impairment; PD-MCI: Parkinson's disease patients with MCI. DAN: dorsal attention network; DMN: default mode network; FPN: frontoparietal network. P values refer to the Jonckheere-Terpstra test results for ordered differences (HC > PD-NMCI > PD-MCI or PD-MCI > PD-NMCI > HC), obtained through permutation testing (10,000 permutations). *Right side (scatterplots):* Correlations in the PD group between mean cortical thickness in the cluster of significantly reduced thickness in PD-MCI compared with HC in left lateral occipital cortex/temporo-occipital junction and both connectivity levels and cognitive performance. In the top panel, these thickness values are plotted against connectivity levels in the clusters of significantly increased connectivity with the DMN in PD-MCI compared with PD-NMCI; in the middle panel, thickness values are plotted against connectivity values in the clusters of significantly increased connectivity with the DMN in PD-MCI compared with HC; in the bottom panel, thickness values are plotted against VS/VP scores (bottom panel).

Connection	r coefficient HC	PD-NMCI	PD-MCI	*p*
HC ≥ **PC-NMCI ≥ PD**-MCI				
DA l FEF-DA l SPL	.116 (.181)	.104 (.15)	.016 (.19)	.039
DA l SOG-DA r FEF	.145 (.202)	.083 (.141)	.055 (.214)	.049
DA l MT-DA r iPCS	.09 (.117)	.015 (.143)	.005 (.135)	.005
DA l SOG-DA r MT	.094 (.169)	.03 (.149)	-.011 (.161)	.008
DA l SPL-DA r MT	.084 (.18)	.034 (.177)	-.014 (.145)	.021
DA r iPCS-DA r SOG	.079 (.118)	.064 (.145)	-.056 (.143)	.001
DA l FEF-DMN l pIPL	-.047 (.177)	-.071 (.148)	-.135 (.117)	.033
DA r SPL-DMN l TPJ	.007 (.135)	-.031 (.12)	-.083 (.156)	.019
DA r MT-DMN r HF	.07 (.15)	.047 (.154)	-.005 (.136)	.047
DA l SPL-DMN r STS	.041 (.158)	-.053 (.155)	-.073 (.139)	.006
DA r SOG-FP l dlPFC	.077 (.13)	.066 (.198)	-.038 (.153)	.027
DA r SPL-FP l dlPFC	.086 (.141)	.062 (.149)	.006 (.154)	.031
DA l SOG-FP l MFG BA9	.065 (.149)	.005 (.168)	-.027 (.192)	.046
DA l SOG-FP l dlPFC	.098 (.157)	.048 (.172)	.012 (.169)	.029
DA l iPCS-FP r MFG BA9	.031 (.119)	.003 (.154)	-.067 (.14)	.009
DA r SOG-FP r aINS	.061 (.14)	.008 (.156)	-.018 (.143)	.028
DA r SPL-FP r aINS	.045 (.121)	.012 (.17)	-.044 (.192)	.046
DA l SOG-FP r SFG	.06 (.16)	.013 (.169)	-.08 (.188)	.004
DA r SOG-FP r SFG	.052 (.15)	-.032 (.151)	-.043 (.174)	.013
DMN dmPFC-DMN l aTL	.027 (.139)	.023 (.152)	-.058 (.129)	.037
DMN dmPFC-DMN l HF	.061 (.158)	.024 (.172)	-.045 (.135)	.023
DMN l HF-DMN pCC	.06 (.153)	.03 (.165)	-.03 (.195)	.046
DMN dmPFC-DMN r aTL	.094 (.15)	.075 (.179)	-.034 (.149)	.034
DMN r aTL-DMN r pIPL	.141 (.149)	.067 (.196)	.054 (.174)	.049
DMN amPFC-DMN vmPFC	.269 (.16)	.184 (.209)	.151 (.233)	.020
DMN dmPFC-DMN vmPFC	.161 (.16)	.119 (.145)	-.002 (.191)	.001
DMN l pIPL-DMN vmPFC	.197 (.189)	.143 (.164)	.102 (.154)	.042
DMN PCu-FP msPFC	.039 (.125)	-.034 (.189)	-.047 (.16)	.026
DMN l SFG-FP r aINS	.017 (.164)	-.035 (.139)	-.101 (.14)	.003
FP l aIPL-FP r aINS	.075 (.142)	.023 (.181)	-.014 (.155)	.046
FP l MFG BA6-FP r aIPL	.087 (.143)	.039 (.156)	-.01 (.162)	.030
FP l MFG BA9-FP r MFG BA6	.069 (.155)	.036 (.128)	-.02 (.202)	.036
DA r MT-DMN amPFC	-.123 (.15)	-.087 (.139)	-.034 (.193)	.037
HC ≤ PC-NMCI ≤ PD-MCI				
DA r MT-DMN amPFC	-.123 (.15)	-.087 (.139)	-.034 (.193)	.037
DA r MT-DMN dmPFC	-.114 (.135)	-.08 (.191)	-.009 (.148)	.032
DA r MT-DMN l IFG	-.084 (.168)	-.023 (.152)	.071 (.21)	.003
DA r SOG-DMN l IFG	-.182 (.16)	-.1 (.19)	-.063 (.179)	.015
DA r MT-DMN l STS	-.082 (.148)	-.041 (.157)	.032 (.177)	.010

DA l SOG-DMN pCC	-.087 (.177)	-.004 (.216)	.047 (.196)	.010
DA r MT-DMN r aTL	-.012 (.19)	.031 (.165)	.163 (.242)	.007
DA l FEF-DMN r HF	-.077 (.121)	-.02 (.133)	.015 (.18)	.012
DA r MT-DMN r lFG	-.032 (.164)	.054 (.17)	.068 (.12)	.002
DA l FEF-DMN vmPFC	-.094 (.143)	-.017 (.133)	-.014 (.155)	.019
DA r FEF-DMN vmPFC	-.104 (.137)	-.05 (.126)	-.034 (.159)	.043
DA l SPL-DMN pCC	-.075 (.167)	-.025 (.189)	.015 (.167)	.040
DA l MT-DMN vmPFC	-.06 (.159)	-.015 (.153)	.016 (.119)	.033
DA l MT-DMN dmPFC	-.072 (.143)	.001 (.19)	.001 (.151)	.040
DA r SOG-DMN vmPFC	-.126 (.157)	-.094 (.181)	.032 (.174)	.005
DA r MT-FP l aINS	0 (.123)	.013 (.147)	.085 (.109)	.034
DA r FEF-FP l MFG BA6	.04 (.181)	.075 (.14)	.158 (.163)	.045
DA r iPCS-FP l MFG BA6	-.026 (.187)	-.016 (.15)	.09 (.125)	.028
DMN r STS-DMN r TPJ	.058 (.145)	.099 (.173)	.159 (.166)	.018
DMN pCC-FP l dlPFC	-.073 (.174)	-.059 (.166)	.034 (.135)	.023
DMN l lFG-FP l MFG BA9	-.029 (.14)	.017 (.121)	.041 (.181)	.013
DMN r STS-FP r aIPL	-.01 (.163)	0 (.143)	.087 (.121)	.027
DMN l lFG-FP r SFG	-.071 (.156)	-.013 (.162)	.019 (.172)	.006

Supplementary Table 1. Interregional connections with significant ordered connectivity effects. Correlation values are presented in mean (standard deviation) according to group. *P* values refer to those obtained with the Jonckheere-Terpstra test (10000 permutations). Network region abbreviations refer to those presented in Table 1. HC: healthy controls; PD-MCI: Parkinson's disease patients with mild cognitive impairment; PD-NMCI: Parkinson's disease patients without mild cognitive impairment.

Intergroup contrast	Cortical region	Cluster size (mm^2)	Clusterwise *p*	MNI305 coordinates of maximum (x,y,z)
HC > PD-MCI	Left supramarginal gyrus, lateral occipital cortex calcarine cortex	3,724.8	.0001	-50.2,-53,41.8
	Left inferior occipital gyrus, temporo-occipital junction	2,897.0	.0003	-35.3,-84.9,-0.8
	Right precuneus, lateral occipital cortex	3,403.7	.0001	7.9,-57.4,44.7
	Right lateral occipital cortex, temporo-occipital junction	3,326.4	.0001	21.3,-98.5,7.5
HC > PD-NMCI	Left lateral occipital, superior parietal cortex	1,700.8	.0151	-19.8,-72.2,38
	Right middle, inferior temporal gyri	1,482.8	.0372	60.2,-16.3,-21.7
	Right lateral occipital cortex	1,522.2	.0325	35.3,-62.5,45

Supplementary Table 2. Significant intergroup differences in cortical thickness. HC: healthy controls; PD-MCI: Parkinson's disease patients with mild cognitive impairment; PD-NMCI: Parkinson's disease patients without mild cognitive impairment.

study 2

FUNCTIONAL BRAIN NETWORKS AND COGNITIVE DEFICITS IN PARKINSON'S DISEASE

Human Brain Mapping 2014

Hugo César Baggio, Roser Sala Llonch, Bàrbara Segura, Maria José Martí, Francesc Valldeoriola, Yaroslau Compta, Eduardo Tolosa, Carme Junqué

◆ Human Brain Mapping 35:4620–4634 (2014) ◆

Functional Brain Networks and Cognitive Deficits in Parkinson's Disease

Hugo-Cesar Baggio,[1] Roser Sala-Llonch,[1] Bàrbara Segura,[1] Maria-José Marti,[2,3,4] Francesc Valldeoriola,[2,3,4] Yaroslau Compta,[2,3] Eduardo Tolosa,[2,3,4] and Carme Junqué[1,3,4]*

[1]Departament de Psiquiatria i Psicobiologia Clinica, Universitat de Barcelona, Spain
[2]Parkinson's Disease and Movement Disorders Unit, Neurology Service, Institut Clínic de Neurociències (ICN), Hospital Clínic de Barcelona, Spain
[3]Centro de Investigación en Red de Enfermedades Neurodegenerativas (CIBERNED), Hospital Clínic de Barcelona, Spain
[4]Institut d'Investigacions Biomèdiques August Pi i Sunyer (IDIBAPS), Barcelona, Spain

Abstract: Graph-theoretical analyses of functional networks obtained with resting-state functional magnetic resonance imaging (fMRI) have recently proven to be a useful approach for the study of the substrates underlying cognitive deficits in different diseases. We used this technique to investigate whether cognitive deficits in Parkinson's disease (PD) are associated with changes in global and local network measures. Thirty-six healthy controls (HC) and 66 PD patients matched for age, sex, and education were classified as having mild cognitive impairment (MCI) or not based on performance in the three mainly affected cognitive domains in PD: attention/executive, visuospatial/visuoperceptual (VS/VP), and declarative memory. Resting-state fMRI and graph theory analyses were used to evaluate network measures. We have found that patients with MCI had connectivity reductions predominantly affecting long-range connections as well as increased local interconnectedness manifested as higher measures of clustering, small-worldness, and modularity. The latter measures also tended to correlate negatively with cognitive performance in VS/VP and memory functions. Hub structure was also reorganized: normal hubs displayed reduced centrality and degree in MCI PD patients. Our study indicates that the topological properties of brain networks are changed in PD patients with cognitive deficits. Our findings provide novel data regarding the functional substrate of cognitive impairment in PD, which may prove to have value as a prognostic marker. *Hum Brain Mapp 35:4620–4634, 2014.* © 2014 Wiley Periodicals, Inc.

Key words: Parkinson's disease; cognitive impairment; connectivity; graph theory; fMRI

Additional Supporting Information may be found in the online version of this article.

Contract grant sponsor: Spanish Ministry of Science and Innovation; Contract grant number: PSI2010–16174; Contract grant sponsor: Generalitat de Catalunya; Contract grant numbers: 2009SGR0836 and 2009SGR0941; Contract grant sponsor: FI-DGR; Contract grant number: 2011FI_B 00045; Contract grant sponsor: CIBERNED.

*Correspondence to: Prof. Carme Junqué, Department of Psychiatry and Clinical Psychobiology, University of Barcelona, Casanova 143 (08036) Barcelona, Spain. E-mail: cjunque@ub.edu

Received for publication 10 July 2013; Revised 10 January 2014; Accepted 14 February 2014.

DOI 10.1002/hbm.22499

Published online 17 March 2014 in Wiley Online Library (wileyonlinelibrary.com).

INTRODUCTION

Parkinson's disease (PD), beyond its hallmark motor symptoms, causes variable degrees of cognitive impairment in a high percentage of patients. The prevalence of cognitive deficits in untreated, newly diagnosed patients has been described to be between 19 and 24% [Aarsland et al., 2009; Muslimovic et al., 2005]. In non-demented patients, the most frequently affected cognitive functions are attention/executive (A/E, involving attention, working memory, set shifting, planning, or inhibition), episodic memory and visuospatial/visuoperceptual (VS/VP) [Aarsland et al., 2009; Elgh et al., 2009; Foltynie et al., 2004; Muslimovic et al., 2005]. Patients with cognitive impairment that does not significantly interfere with daily life activities, that is, with mild cognitive impairment (MCI), are at a higher risk of subsequently developing dementia [Janvin et al., 2006; Williams-Gray et al., 2007], which over time affects around 80% of patients [Aarsland et al., 2005]. The risk of future dementia appears to vary according to the type of deficit observed, being higher in patients with cognitive deficits with posterior cortical substrates and not related to dopamine imbalances [Williams-Gray et al., 2009].

The study of cognition is increasingly focusing on an integrated model of brain function rather than on the study of individual areas. In this framework, resting-state functional magnetic resonance imaging (fMRI) can be used to detect interregional correlations in blood oxygen level-dependent (BOLD) signal fluctuations [Biswal et al., 1995], considered to reflect baseline neuronal brain activity [Gusnard et al., 2001], which in turn allows the study of intrinsic large-scale brain network organization [Biswal et al., 1995; Fox and Raichle, 2007]. In recent years, graph-theory-based complex network analysis, which describes important properties of complex systems by quantifying topologies of their respective network representations [Rubinov and Sporns, 2010], has been increasingly used in the study of the functional and structural organization of the nervous system [Bullmore and Sporns, 2009]. For graph-theoretical analysis of neural networks through fMRI, anatomical brain regions are considered as nodes, linked by edges, which represent the connectivity measured by the temporal correlation of BOLD signal fluctuations between the nodes [Rubinov and Sporns, 2010]. Network integration and segregation are measured by the characteristic path length and the clustering coefficient, respectively. Networks which display a balance between these two measures are considered to be small-world networks [Sporns and Honey, 2006], characterized by high local specialization (high clustering) and some global "shortcuts" (low path length), allowing fast information transfer with reduced energy expenditure [Karbowski, 2001; Rubinov and Sporns, 2010]. Small-world topology has been described in human brain functional [Achard et al., 2006] and structural [Sporns et al., 2007] networks.

This approach has been used in the study of large-scale network properties both in healthy subjects [Achard et al., 2006] and in neurodegenerative diseases such as Alzheimer's disease [He et al., 2008; Lo et al., 2010; Sanz-Arigita et al., 2010; Stam et al., 2007; Supekar et al., 2008]. Despite ample evidence of changes in connectivity related to motor or cognitive circuits in PD [Hacker et al., 2012; Ibarretxe-Bilbao et al., 2011; Segura et al., 2013; Wu et al., 2011], little is known about whole-brain network topology changes associated with this disease. To our knowledge, no published studies addressed graph-theory parameters associated with cognitive deficits in PD.

The principal aim of this work was to explore global and local measures of connectivity and network integration and segregation through a graph-theoretical approach in a large sample of nondemented PD patients using resting-state fMRI. Specifically, we wanted to study how these measures of connectivity would relate to the presence of cognitive deficits in this disease to better understand the functional implications of these deficits on brain function from a network perspective, and as part of an effort to find neuroimaging markers of cognitive decline and dementia. We hypothesized that PD patients with MCI would have disrupted functional brain topological organization, and that specific types of deficit would be associated with distinct patterns of network disruption.

MATERIALS AND METHODS

Participants

Eighty-four non-demented PD patients and 38 healthy controls (HC) matched for age, sex and years of education were included. Patients were recruited from the Movement Disorders Unit, Hospital Clínic, in Barcelona. HC were recruited from individuals who volunteered to participate in scientific studies at the Institut de l'Envelliment, Universitat Autònoma de Barcelona. The inclusion criterion for patients was the fulfillment of the UK PD Society Brain Bank diagnostic criteria for PD [Daniel and Lees, 1993]. Exclusion criteria were: (i) Mini-Mental State Examination scores <25 or the presence of dementia according to the Movement Disorder Society criteria [Emre et al., 2007], (ii) Hoehn and Yahr (HY) score $>$ III, (ii) presence of other significant psychiatric, neurological, or systemic comorbidity, (iv) pathological MRI findings other than mild white matter hyperintensities or, in patients, findings not compatible with PD in the FLAIR sequence, (v) root mean square head motion >0.3 mm translation or $0.6°$ rotation.

All patients except one were taking antiparkinsonian drugs, consisting of different combinations of levodopa, cathecol-O-methyl transferase inhibitors, monoamine oxidase inhibitors, dopamine agonists, and amantadine. The medication was not changed for the study and all assessments (clinical, neuropsychological, and neuroimaging) were done while patients were in the on state. Levodopa equivalent daily dose (LEDD) was calculated as suggested

by Tomlinson et al. [2010]. Motor disease severity was evaluated using HY staging and the Unified PD Rating Scale motor section (UPDRS-III). The study was approved by the ethics committee of the University of Barcelona, and all subjects provided written informed consent to participate.

Neuropsychological Assessment

All subjects underwent a neuropsychological battery to assess VS/VP, memory and A/E functions. The tests administered were as follows (for a full description, see [Lezak et al., 2004]).

VS/VP functions

Benton's Visual Form Discrimination and Judgment of Line Orientation tests.

Memory

Learning and recall memory were assessed using Rey's Auditory Verbal Learning Test total learning and free recall (after 20 min) scores.

A/E functions

Difference between backward and forward digit spans from the Wechsler Adult Intelligence Scale-III Digits subtest; difference between Trail-Making Test part A and part B scores; phonemic fluency scores (number of words beginning with the letter "P" produced in 60 s), and Stroop Color-Word Test (SCWT) interference scores. The Beck Depression Inventory II (BDI) and the MMSE were also administered to all subjects.

MRI Acquisition

Images for all subjects were obtained with a 3T MRI scanner (MAGNETOM Trio, Siemens, Germany), using an 8-channel head coil. The scanning protocol included a resting-state, 5-min-long functional gradient-echo echo-planar imaging sequence (150 T2*-weighted volumes, TR = 2 s, TE = 19 ms, flip angle = 90°, slice thickness = 3 mm, FOV = 240 mm, in which subjects were instructed to keep their eyes closed, not to think of anything in particular and not to fall asleep), a high-resolution 3D structural T1-weighted MPRAGE sequence acquired sagittally (TR = 2.3 s, TE = 2.98 ms, 240 slices, FOV = 256 mm; 1 mm isotropic voxel) and a T2-weighted axial FLAIR sequence (TR = 9 s and TE = 96 ms).

Processing of Resting-State fMRI Data

The preprocessing was carried out using FSL-5.0 (http://www.fmrib.ox.ac.uk/fsl/) and AFNI (http://afni.nimh.nih.gov/afni). Briefly, it included removal of the first 5 volumes to allow for T1 saturation effects, skull stripping, grandmean scaling, and temporal filtering (bandpass filtering of 0.01–0.1 Hz). To control for the effects of subject head movement, physiological artifacts (e.g., breathing and vascular) and other non-neural sources of signal variation on the estimation of functional connectivity, motion correction (using FSL's MCFLIRT), and regression of nuisance signals (six motion parameters, cerebrospinal fluid, and white matter) were performed.

Head motion was calculated separately for translatory and rotatory movements according to the following formula:

$$\frac{1}{M-1}\sum_{i=2}^{M}\sqrt{|x_i-x_{i-1}\ |^2+|y_i-y_{i-1}\ |^2+|z_i-z_{i-1}\ |^2}$$

where x_i, y_i, and z_i are translations or rotations in three axes at timepoint i, and M is the total number of timepoints (145) [Liu et al., 2008].

Quality Control

From the initially recruited sample, four patients were excluded due to macroscopic movement artifacts and 14 due to head motion > 0.3 mm translation or > 0.6° rotation. Two controls were excluded due to microvascular white matter changes, leaving a final sample of 66 PD patients and 36 HC. Despite rigorous head motion exclusion criteria, rotational head motion was significantly higher ($t = 3.304$ and $P = 0.001$) in the patient [mean = 0.044° and standard deviation (SD) = 0.035] than in the control group (mean = 0.028° and SD = 0.011). Evaluating patient subgroups, rotational head motion was found to be significantly higher in non-MCI patients than in controls ($P = 0.028$, post-hoc Bonferroni test). No significant differences were found between controls and MCI patients or between patient subgroups. No significant intergroup differences were found in translational motion (see Table II).

Atlas-Based Definition of Nodes

We used the AAL atlas [Tzourio-Mazoyer et al., 2002], the parcellation scheme most frequently used in fMRI graph-theory studies [Tijms et al., 2013], to parcellate the cerebral gray matter into 45 regions of interest (ROI) per hemisphere (see Table I). Nonlinear registration using FNIRT (http://fsl.fmrib.ox.ac.uk/fsl/fslwiki/FNIRT) was used to transform the AAL ROIs to each subject's T1-weighted image space; subsequently, a linear registration [Jenkinson and Smith, 2001] was applied to bring the ROIs from each subject's T1-weighted to native functional space.

Network Computation and Parameters

BOLD signal temporal series were averaged throughout all voxels within each ROI [Biswal et al., 1995]. The

TABLE I. Regions used as nodes and corresponding labels

Region	Label	Region	Label
Prefrontal nodes		45,46 Amygdala	AMYG
1,2 Superior frontal gyrus (medial orbital)	ORBsupmed	47,48 Hippocampus	HIP
3,4 Inferior frontal gyrus (opercular part)	IFGoperc	49,50 Parahippocampal gyrus	PHG
5,6 Inferior frontal gyrus (orbital part)	ORBinf	51,52 Heschl gyrus	HES
7,8 Inferior frontal gyrus (triangular part)	IFGtriang	53,54 Superior temporal gyrus	STG
9,10 Superior frontal gyrus (dorsolateral)	SFGdor	55,56 Middle temporal gyrus	MTG
11,12 Middle frontal gyrus (orbital part)	ORBmid	57,58 Inferior temporal gyrus	ITG
13,14 Middle frontal gyrus	MFG	59,60 Fusiform gyrus	FFG
15,16 Superior frontal gyrus (orbital part)	ORBsup	Parietal nodes	
17,18 Superior frontal gyrus (medial)	SFGmed	61,62 Angular gyrus	ANG
19,20 Anterior cingulate and paracingulate gyrus	ACG	63,64 Supramarginal gyrus	SMG
21,22 Olfactory cortex	OLF	65,66 Postcentral gyrus	PoCG
23,24 Rectus gyrus	REC	67,68 Paracentral lobule	PCL
Other frontal nodes		69,70 Posterior cingulate gyrus	PCG
25,26 Precentral gyrus	PreCG	71,72 Precuneus	PCUN
27,28 Rolandic operculum	ROL	73,74 Superior parietal gyrus	SPG
29,30 Supplementary motor area	SMA	75,76 Inferior parietal lobule	IPL
31,32 Median cingulate and paracingulate gyrus	DCG	77,78 Thalamus	THA
33,34 Insula	INS	Occipital nodes	
Corpus striatum		79,80 Cuneus	CUN
35,36 Caudate nucleus	CAU	81,82 Calcarine fissure and surrounding cortex	CAL
37,38 Globus pallidum	PAL	83,84 Lingual gyrus	LING
39,40 Putamen	PUT	85,86 Superior occipital gyrus	SOG
Temporal nodes		87,88 Middle occipital gyrus	MOG
41,42 Temporal pole: middle temporal gyrus	TPOmid		
43,44 Temporal pole: superior temporal gyrus	TPOsup		

Numbers refer to left-hemispheric (odd) or right-hemispheric regions (even).

connectivity between two ROIs was estimated using Pearson's correlation between their timeseries. A 90 × 90 matrix for each subject was thus obtained, representing all the edges. Networks were constructed using only positive *r* values [Chen et al., 2013; Tian et al., 2007; Wang et al., 2011]. Because there is no agreement on the selection of a threshold to define biologically relevant connections, we used a sparsity (S – existing number of edges in a graph divided by the number of all possible edges) threshold to create a set of undirected graphs, using correlation strength as edge weights, for each subject [Bassett and Bullmore, 2006; Zhang et al., 2012], while minimizing the effects of overall connectivity differences [Achard and Bullmore, 2007]. Sparsity is a measure of network density; using it as a threshold to networks with equal numbers of nodes such as in this study ensures that all subjects' networks will also have the same number of edges, making them more suitable for comparisons [van Wijk et al., 2010]. We evaluated the consistency of the global measures over a range of sparsities ($5\% \leq S \leq 25\%$, at 2.5% steps) [Bullmore and Bassett, 2011; Fornito et al., 2010; Wang et al., 2009]. Since a similar trend for intergroup differences was observed over the range of thresholds for global measures, only results using an *S* of 15% are reported for regional measures analysis.

The obtained networks were analyzed in terms of their global (or whole-brain) characteristics, as well as regional/local (or nodal) measures (for a more detailed, see [Rubinov and Sporns, 2010]) using the Brain Connectivity Toolbox [Rubinov and Sporns, 2010]. The parameters evaluated were the following.

Local/Regional Measures (of a Node)

Clustering coefficient is the number of connections between a node's neighbors divided by the number of possible such connections, or the probability that a node's neighbors are also connected to each other, indicating how close they are to forming a clique.

The *local efficiency* of a node is calculated as the global efficiency of the subgraph formed by this node's neighbors. It is a measure of clustering and indicates the capacity of this subgraph to exchange information if that node is eliminated [Achard and Bullmore, 2007].

A node's *connectivity degree* is the number of edges linked to a node (i.e., number of input/output connections). This measure can be interpreted as a node's accessibility.

Betweenness centrality (BC) is the number of shortest paths between any two nodes that go through a given

TABLE II. Sociodemographic, clinical and head motion characteristics of participants with intergroup comparisons

	HC	PD		
		Non-MCI	MCI	
	$n = 36$	$n = 43$	$n = 23$	Test stats (P)
Age (yrs.)	63.4 (10.5)	64.0 (9.8)	66.7 (12.2)	0.724/0.487
Sex (female:male)	17:19	20:23	9:14	0.431/0.806[a]
Years of education	10.3 (4.0)	10.8 (5.1)	9.74 (4.0)	2.422/0.094
MMSE	**29.70 (.47)**	**29.35 (0.90)**	**28.52 (1.20)**	**13.270/<0.001**
Hand dominance (r:l)	34:2	42:1	23:0	1.616/0.446[a]
BDI	**5.81 (5.66)**	**8.9 (6.1)**	**11.9 (6.7)**	**7.234/0.001**
Age at onset (yrs.)	–	57.8 (10.2)	57.7 (13.8)	0.062/.951[b]
Disease duration	–	**6.1 (4.4)**	**9.0 (5.5)**	**2.327/0.023[b]**
LEDD (mg)	–	**646.7 (419.2)**	**939.7 (490.2)**	**2.549/0.013[b]**
HY stage (1:2:3)	–	**20:21:2**	**3:16:4**	**8.640/0.013[a]**
UPDRS-III	–	**14.1 (7.5)**	**18.6 (8.7)**	**2.156/0.035[b]**
Head rotation (degrees)	**0.03 (0.01)**	**0.05 (0.04)**	**0.04 (0.03)**	**3.566/0.032**
Head translation (mm)	0.08 (0.05)	0.07 (0.04)	0.08 (0.05)	0.332/0.719

Results are presented in means (SD). Statistically significant results ($P < 0.05$) are marked in bold. Disease duration: duration of motor symptoms, in years. Test stats: F-statistics, [a]Pearson's chi-square, or [b]Student's t. Post-hoc analyses for BDI scores showed significant differences between MCI patients and HC ($P = 0.001$, post-hoc Bonferroni test). MMSE scores in MCI patients were lower than in HC and non-MCI patients ($P < 0.001$ and $P = 0.001$, respectively, post-hoc Bonferroni test). Non-MCI patients' head rotation was significantly different from controls' ($P = 0.028$, post-hoc Bonferroni test).

node, and indicates the importance of that node to the network. Brain *hubs* are highly connected or central nodes [Sporns et al., 2007], which play an important role in global network communication [Achard et al., 2006]. These nodes tend to have numerous (high degree) and relevant (high BC) connections [Ottet et al., 2013]. For each subject group, nodes were scored according to the sum of their rank position in BC and node degree. The 20% highest-scoring nodes were classified as hubs.

Global Measures

The *clustering coefficient* of a network is defined as the average of the clustering coefficients of all nodes in the network. It quantifies the local interconnectivity of a network and reflects functional segregation, or the ability for specialized processing within densely interconnected groups of brain regions.

Characteristic path length, defined as the average of the shortest path length or distance between any pair of nodes in a network. The minimum path length between two nodes is the smallest number of edges that must be traversed to connect them. Lower values indicate higher routing efficiency, as information exchange involves fewer steps.

Small-world coefficient: this measure is defined as the ratio of the average clustering coefficient to the characteristic path length divided by the ratio of the same measures of equivalent random networks [Humphries and Gurney, 2008]. Small-world networks usually have small-world coefficients >1.

Global efficiency: measures the ability of a network to transmit parallel information at the global level. It inversely correlates with path length but is not susceptible to the presence of disconnected nodes.

Modularity: indicates the degree to which a network can be subdivided into well-delineated modules made up of densely interconnected nodes with few intermodular connections, and which may represent network functional subcomponents [Grossberg, 2000]. For the study of the distribution of network modules by group, mean group functional matrices were constructed with the ratio of mean to SD of all subjects' matrices as proposed by Chen et al. [2013] to minimize intersubject variation in edge connectivity strength (see formula in Supporting Information).

The mean network global connectivity was calculated as the mean of all positive interregional timeseries correlation r values. This measure was calculated for the unthresholded correlation matrices as well as for the networks constructed after applying each sparsity threshold (from 200 edges at 5% sparsity to 1001 at 25% sparsity). Cutoff r values were calculated as the r coefficient of the weakest edge included in each subject's thresholded correlation matrix for each S threshold. For intergroup comparisons in interregional connectivity strengths, r coefficients were converted to z coefficients using Fisher's r to z transformation.

Neuropsychological Data Analysis

Initially, z scores for each test and subject were calculated based on the HC group's means and SDs. Expected z scores adjusted for age, sex and education for each test and each subject were calculated based on a multiple

regression analysis performed in the HC group [Aarsland et al., 2009].

We classified subjects as having MCI if the actual z score for a given test was at least 1.5 lower than the expected score in at least two tests in one domain or in at least one test per domain in at least two domains. As was expected [Muslimovic et al., 2005], most such subjects had deficits in more than one function, precluding the creation of patient groups with single-domain impairments.

Statistical Analyses

All statistical analyses were performed using SPSS Statistics 20.0.0 (Chicago, IL, http://www-01.ibm.com/software/analytics/spss/). Statistical significance threshold was set at $P < 0.05$. Pearson's chi-squared test was used to compare categorical variables (hand dominance, sex, and HY stage). Student's t-test was used to compare head motion, clinical, and connectivity data means between patients and controls. Three-level one-way ANOVAs were used to compare head motion, clinical and sociodemographic data between HC and patient subgroups (non-MCI, MCI). Three-level one-way analyses of covariance were used to compare network measures (normally distributed) between HC and patient subgroups while controlling for variables that presented intergroup differences in the previous step. Significance P values were adjusted using post-hoc Bonferroni tests considering the number of intergroup comparisons. Test statistics and significance levels are given in Supporting Information Table SII. To study the effects of different types of deficits on the evaluated network parameters in the PD group, the entire patient sample was analyzed through linear regression models entering the difference between expected and actual z scores for each of the three cognitive domains assessed plus relevant normally distributed variables that significantly correlated with these scores as independent variables. Non-normally distributed variables were analyzed using Spearman rank correlations, Mann-Whitney U-tests, and Kruskal-Wallis tests.

RESULTS

Sociodemographic and Clinical Features

Twenty-three patients (34.8%) fulfilled criteria for MCI. Table II shows sociodemographic, clinical and head motion data and the corresponding group comparisons. Supporting Information Table SI shows the results of neuropsychological assessment and group comparisons.

Mean Connectivity Changes

No significant intergroup differences were observed for global mean connectivity values (Supporting Information Table SII). The exploratory analysis of correlation strengths over all edges, controlling for the effect of rotational head movement, revealed that the collapsed sample of PD patients had several widespread connectivity decrements, most often affecting interlobular edges, as well as some increments, mainly in interlobular prefrontal connections (see Supporting Information Figs. S1 and S2). The analysis of PD subgroups revealed that MCI patients had widespread reductions compared with HC; connectivity increases were also present, mostly involving shorter-range frontal and temporal links (see Fig. 1 and Supporting Information Fig. S2). Non-MCI patients were also seen to have some connectivity reductions compared with HC mainly involving connections between frontal, occipital and parietal areas. A more detailed description of the pattern of interregional connectivity changes in PD subgroups can be found in Supporting Information Figure S3. No significant group differences in cutoff r coefficients were observed for any of the sparsity thresholds applied (see Supporting Information Fig. S4).

Global Network Topological Parameters

The networks of HC and both PD subgroups displayed small-world and modular characteristics (see Fig. 2). No significant differences were found for any of the global measures when comparing HC and the collapsed PD-patient group at any of the sparsity thresholds applied, with or without controlling for differences in BDI scores and rotational head motion.

Global measures analysis revealed that MCI patients presented significantly higher small-world and modularity coefficients than HC and non-MCI patients (see Fig. 2 and Supporting Information Table SII). Clustering coefficients were higher in MCI than in non-MCI patients at stricter thresholding (see Fig. 2 and Supporting Information Table SII).

Community Structure and Hub Distribution

Figure 3 shows the nodes that ranked highest in clustering coefficient and BC in each group and were therefore classified as hubs, as well as the modular structure identified in each group. Mean brain networks in the three groups were decomposed into four basic modules: fronto-parietal, insulo-operculo-striatal, fronto-parieto-parahippocampal, and occipito-temporal (see Fig. 3). In HC, an additional module composed of the thalami was identified. A significant group effect was found for the number of modules (Kruskal-Wallis $H = 6.756$, $P = 0.034$); Bonferroni-corrected post-hoc Mann-Whitney tests showed a tendency for more modules in MCI patients than in HC ($P = 0.069$; see Fig. 3). The number of modules did not correlate significantly with motion parameters.

Local Network Topological Parameters

To assess the reorganization of local topological measures (node degree, BC, nodal clustering coefficient, and local

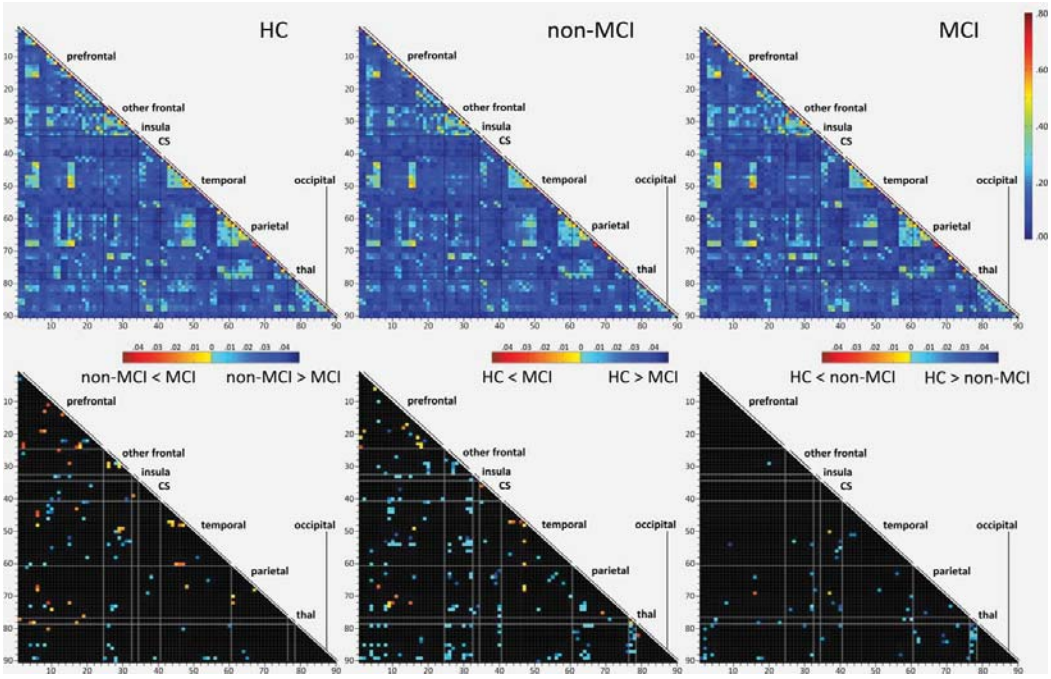

Figure 1.

Comparisons of interregional connectivity strength between HC and PD subgroups. Top row: mean connectivity matrices according to group (Pearson's *r* coefficients, indicated in the color bar) for all pairs of ROIs. Bottom row: edges with significant post-hoc group differences ($P < 0.05$) in z correlation values are marked in color. Bottom left: non-MCI versus MCI patients; bottom middle: HC vs. MCI patients; bottom right: HC vs. non-MCI patients. Color bars indicate post-hoc Bonferroni test *P* values according to direction of differences. Anatomical regions, ordered in roughly anterior-posterior sequence and grouped according to lobes or subcortical structures, are numbered in the vertical and horizontal axes according to Table I. CS: corpus striatum; thal: thalamus.

efficiency) in the subgroups of PD patients, we correlated the mean nodal values for the HC group and the differences between each individual subject's value and the mean value in HC [Achard et al., 2012]. This strategy allows the analysis of whether changes in nodal parameters in the patient groups are related to their respective values in HC, and also provides a visual representation of increases or decreases in these properties in individual nodes. Inter-group comparisons of z-transformed correlation coefficients revealed that, for BC, both PD subgroups had significantly more negative correlations than HC, indicating that hubs tend to lose centrality, and nodes which normally have low centrality undergo the most significant increases ($F = 11.090$, $P < 0.001$; post-hoc Bonferroni test: PD-MCI > HC $P < 0.001$, PD-non-MCI > HC $P = 0.001$) in PD patients. For node degree, a similar effect was found in PD-MCI compared with HC ($F = 4.429$, $P = 0.014$; post-hoc Bonferroni test: PD-MCI > HC $P = 0.011$; see Fig. 4). No significant differences in correlation coefficients were found for measures of nodal clustering coefficient and local efficiency.

Figures 4 and 5 show the distribution of mean changes in nodal parameters as a function of mean values in HC for both PD subgroups. Differences between MCI patients' values and HC's for clustering coefficient and local efficiency were more often positive, indicating a tendency for increased clustering, especially for nodes that in HC belong to the occipito-temporal or the fronto-parietal modules (see Fig. 5).

Effect of Types of Cognitive Deficits on Topological Measures

VS/VP scores did not correlate significantly with A/E or memory scores, with clinical/demographical variables

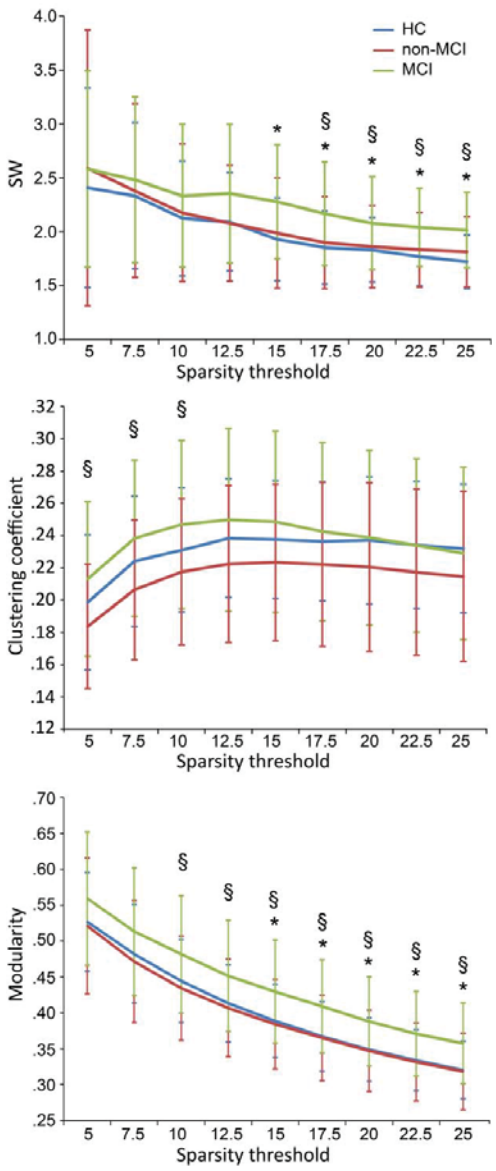

Figure 2.

Small-world, modularity, and clustering coefficients (vertical axis) as a function of sparsity thresholds (horizontal axis) for HC and PD subgroups. * Indicates significant differences between HC and MCI patients ($P < 0.05$, post-hoc Bonferroni test); § indicates significant differences between non-MCI and MCI patients ($P < 0.05$, post-hoc Bonferroni test). SW: small-world coefficient. [Color figure can be viewed in the online issue, which is available at wileyonlinelibrary.com.]

such as age, education, LEDD, disease duration, or UPDRS-III or BDI scores, or with head motion parameters; a simple regression model was therefore used to evaluate the corresponding cognitive function. A/E scores significantly correlated with memory scores ($r = 0.31$ and $P = 0.011$); the latter, in turn, also correlated significantly with age ($r = -0.34$, and $P = 0.006$) and LEDD ($r = -0.27$ and $P = 0.027$). These variables were entered as independent variables in the analysis of A/E and memory functions in a multiple regression model.

Regression analyses performed in the patient group revealed that composite z scores for VS/VP and memory correlated negatively with clustering, modularity and small-world coefficients over a range of thresholds (see Fig. 6). A/E scores, however, did not correlate significantly with global measures at any of the thresholds applied.

At the regional level, measures of clustering (clustering coefficient and local efficiency), degree and BC had mainly negative correlations with VS/VP scores, predominantly in temporal and parietal cortices, as well as with basal ganglia, thalamus, and medial temporal nodes (see Fig. 6 and Supporting Information Table SIII). Memory scores were likewise seen to correlate with local parameters predominantly in frontal and temporal areas. These scores correlated negatively with measures of clustering in prefrontal and medial temporal regions. Node degree correlated with these scores in frontal and occipital areas (see Fig. 6 and Supporting Information). Significant nodal correlates for A/E scores were found mainly in frontal regions. BC in several frontal areas correlated both positively and negatively with these scores (see Fig. 6 and Supporting Information Table SIII).

No significant correlations were found between HC scores in any of the three cognitive domains assessed and global network measures at any of the thresholds applied.

DISCUSSION

In this study, we evaluated brain network topologies associated with the presence of cognitive deficits in a large sample of nondemented, treated PD patients through resting-state fMRI. We thresholded subjects' correlation matrices to construct weighted, undirected networks composed of identical numbers of nodes and edges. Our findings suggest that graph-theoretical approaches can evidence cerebral functional network reorganization in PD patients in association with cognitive deficits and may prove useful as imaging biomarkers of cognitive decline in this disease. Our main findings were that MCI PD patients' functional connectomes had increased modularity and small-worldness. Although more advanced disease may partially account for these changes, regression analyses controlling for clinical confounds showed that global parameters of clustering, modularity, and small-worldness were negatively associated with performance in VS/VP and memory functions. These findings suggest that the

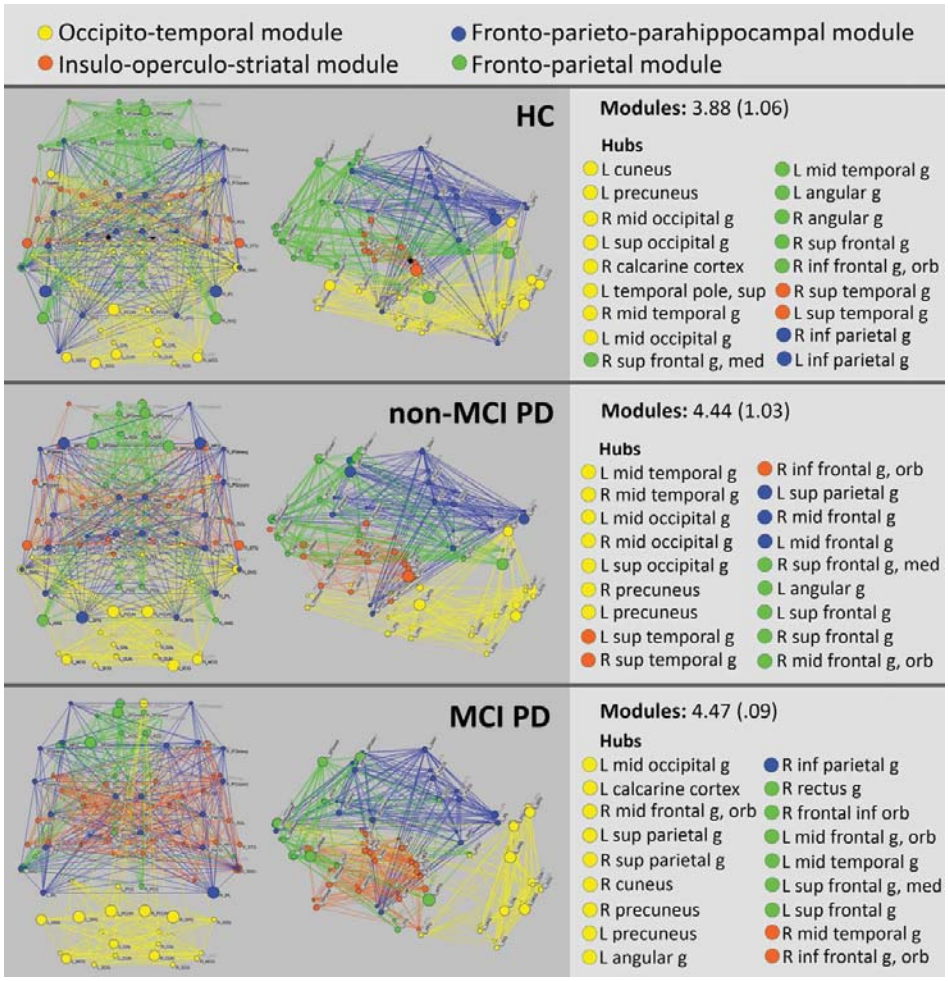

Figure 3.

Community structure and hub distribution according to group. Colors in nodes and links correspond to the modules indicated at the top of the figure. Black nodes in the HC group represent the thalami. Only intramodular edges are shown. Mean number of modules and SDs per group are shown at the right. Nodes classified as hubs in each group are listed, as well as the communities to which they belong in each group's mean network.

presence of cognitive impairments is per se associated with network topological reorganization in nondemented PD patients.

In this study, widespread long-range connectivity decreases were observed in the PD group, most notably in patients with MCI. In this group, these decrements were seen to affect connections between all major cortical and subcortical areas. Connectivity increases of a possible compensatory nature were also observed, mainly affecting shorter connections within the frontal and temporal lobes. The presence of both decreased and increased edge strength explains the absence of intergroup mean global connectivity differences. Previous resting-state functional connectivity fMRI studies in PD have found connectivity increases and decreases depending on the networks or circuits studied. Wu et al. [2009], in a study addressing

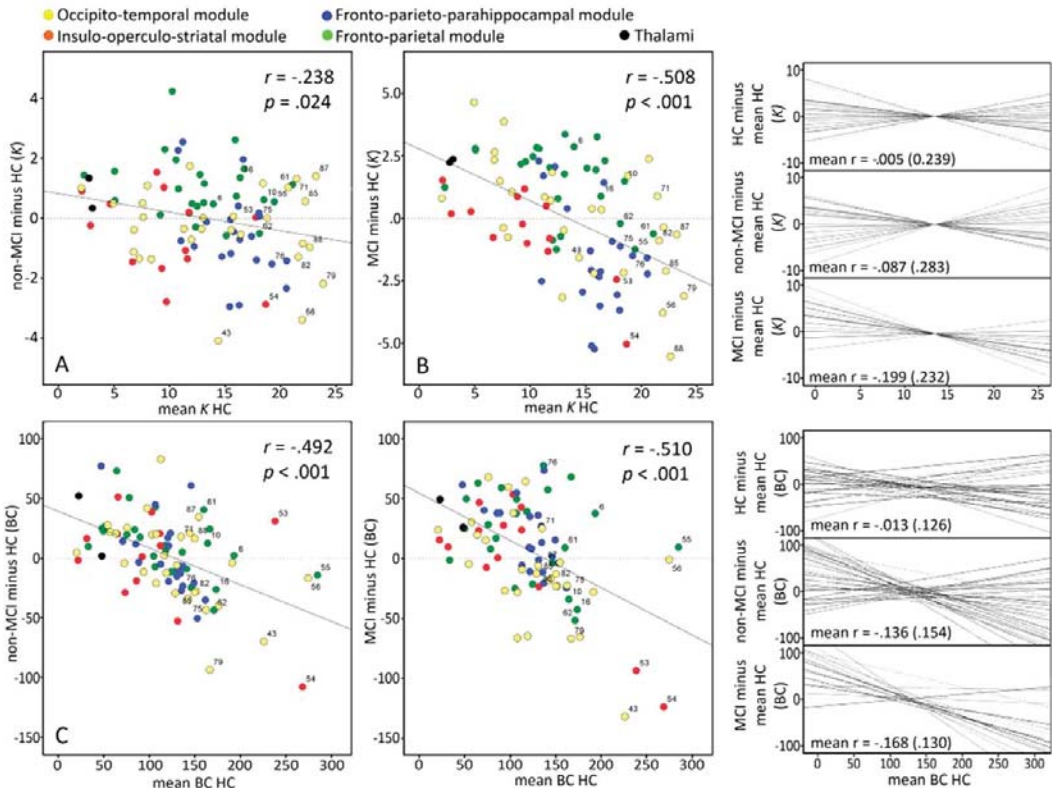

Figure 4.

Changes in measures of node degree and BC in non-MCI and MCI PD patients relative to HC as a function of HC's means. Left side: mean differences between PD-non-MCI and HC (**A**, **C**) and between PD-MCI and HC (**B**, **D**) for node degree, *K*, (A, B) and BC (B, D) are plotted against the mean values in the HC group (horizontal axes) for all nodes. Nodes classified as hubs in the control group are numbered (see Table I). Colors indicate the modules to which each node belongs in HC as indicated at the top of the figure. Right side: correlation between HC's mean values for K (above) and BC (below; horizontal axes) and the individual differences between subjects' values in the corresponding parameters and mean HC values (vertical axes). Mean *r* correlation values and SDs according to group are shown. [Color figure can be viewed in the online issue, which is available at wileyonlinelibrary.com.]

motor network connectivity, described increases in the off state, which were normalized after levodopa administration. In another study, the same group found both increments and decrements in the rostral supplementary motor area's connectivity compared with HC [Wu et al., 2011]. More recently, Tessitore et al. [2012] described functional connectivity decreases between regions of the default mode network (in parietal cortical and medial temporal areas) and the rest of the same network in cognitively preserved PD patients. Recent evidence indicates that white matter degeneration plays a role in PD-related cognitive impairment [Agosta et al., 2013; Baggio et al., 2012; Hattori et al., 2012]. Studies using genetic animal models suggest that primary axonopathy is part of the PD pathological process [Li et al., 2009; see also Burke and O'Malley, 2013]. We hypothesize that the observed connectivity decrements result from structural connectivity deficits due to neurite dysfunction, and that these changes contribute to cognitive impairment in PD. No group differences were found in the measures of integration (characteristic path length and global efficiency) assessed in this study, probably due to the strengthening of alternative pathways. Nonetheless, this hypothesis would merit testing through the combined analysis of connectivity patterns and white matter

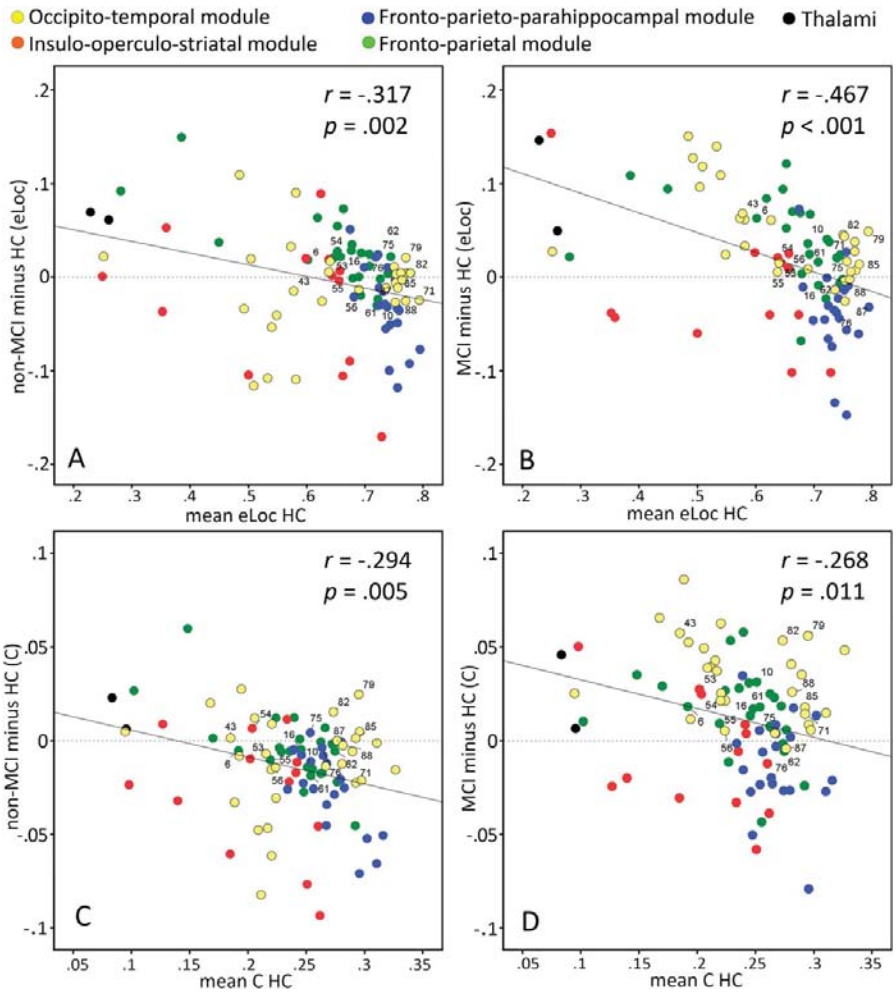

Figure 5.

Changes in nodal parameters of segregation in non-MCI and MCI PD patients relative to HC as a function of HC's means. Mean differences between PD-non-MCI and HC (**A**, **C**) and between PD-MCI and HC (**B**, **D**) for node nodal clustering coefficients, *C*, (A, B) and local efficiency, *eLoc*, (B, D) are plotted against the mean values in the HC group (horizontal axes) for all nodes. Nodes classified as hubs in HC are numbered (see Table I). Colors indicate the modules to which each node belongs in the HC group as indicated at the top of the figure. [Color figure can be viewed in the online issue, which is available at wileyonlinelibrary.com.]

integrity. Evidence from animal studies using genetic models also indicates that α-synuclein aggregates lead to impairments in neurotransmitter release and subsequent synaptic dysfunctions, further contributing to connectivity impairments [Scott et al., 2010].

The overall topographic distribution of the network modules was preserved in the PD group, although brain modularity was seen to be increased in patients with MCI. This finding is probably related to the increases in these patients' local interconnectedness (i.e., higher nodal clustering coefficients and local efficiency), which were found to preferentially involve nodes that normally belong to the occipito-temporal and fronto-parietal modules, and which also lead to increases in the calculated small-world

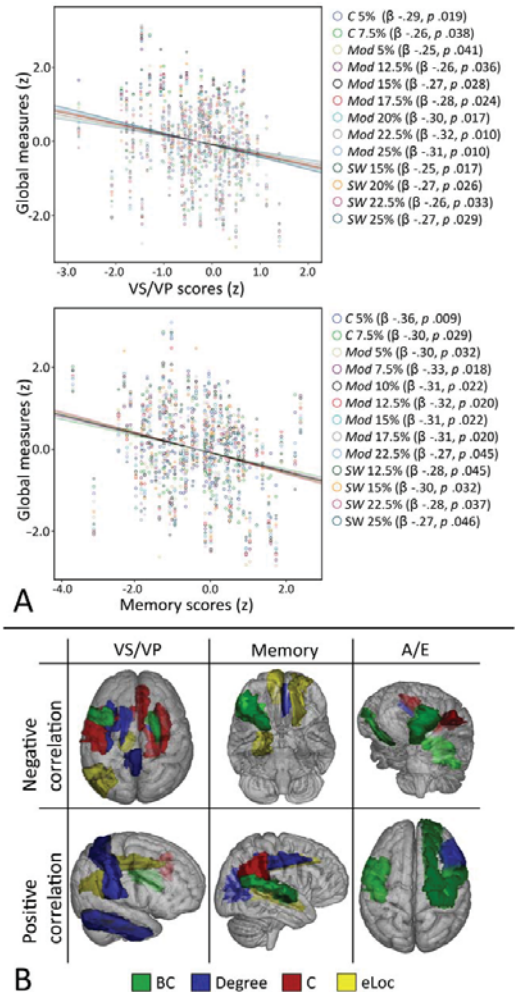

Figure 6.

Relationship between network parameters and composite scores for memory and VS/VP functions. **A**: Significant linear regression analysis results for global measures and VS/VP (top) and memory (bottom) z scores. β: standardized beta regression score. **B**: Regions where regional measures correlated significantly with A/E, memory, or VS/VP scores. Top row: negative correlations; bottom row: positive correlations. *C*: clustering coefficient; Mod: modularity; SW: small-world coefficient; eLoc: local efficiency. [Color figure can be viewed in the online issue, which is available at wileyonlinelibrary.com.]

coefficients. It could be speculated that the increments in local interconnectivity result from shorter-range, within-module compensatory plasticity mechanisms as a response to long-range connectivity loss or primary cortical pathology [Compta et al., 2011].

We also evaluated changes in parameters that identify the most relevant nodes to information traffic, that is, network hubs. We found that PD, especially in the presence of cognitive deficits, was associated with a reorganization of hub structure, characterized by reduced importance—as measured by BC and degree—of nodes that are normal hubs and increased importance of nodes that normally have low network relevance. The increase in hubness was most noticeable in prefrontal nodes, several of which were classified as hubs only in the PD subgroups. Our findings indicate that, in PD, hubs may be especially vulnerable to the degenerative pathogenic process that amounts to cognitive impairment, as has been described in Alzheimer's disease [Stam et al., 2009] and hypothesized to be derived from these region's higher metabolic activity [de Haan et al., 2012]. Considering the relevance of Alzheimer's type pathology in the genesis of cognitive deficits in PD [Compta et al., 2011], a common mechanism could underlie these changes in both diseases.

The analysis of topological patterns associated with specific types of deficits revealed that VS/VP and memory deficits, although not mutually correlated, were associated with the same global parameters that were altered in MCI patients. A/E deficits, however, did not correlate with global network measures. Dopaminergic antagonism has been seen to reduce both global and local efficiency in healthy subjects [Achard and Bullmore, 2007]. PD patients off medication (i.e., in a state of dopamine deficiency) have also been described to have reduced global and local efficiency [Skidmore et al., 2011]. The extrapolation of these data to treated PD subjects is not straightforward, however, as these patients are not in a consistent hypodopaminergic state. Midbrain dopaminergic neuron loss progresses heterogeneously [Damier et al., 1999]. Affected areas thus coexist with spared areas, which may ultimately suffer dopaminergic overstimulation or dopamine overdose as a result of antiparkinsonian treatments [Gotham et al., 1986]. Longitudinal population-based studies indicate that the presence of deficits related to dopamine imbalance in PD does not increase the risk of subsequent dementia, whereas deficits with posterior-cortical, non-dopaminergic bases are markers of worse cognitive prognosis [Williams-Gray et al., 2007, 2009]. The role played by primary cortical pathology in cognitive impairment and in the development of dementia in PD, which according to post-mortem studies can be related to synucleinopathy as well as to Alzheimer's-type pathology [Compta et al., 2011; Fields et al., 2011; see also Ferrer, 2009], is likely to explain these associations. VS/VP deficits in PD appear to be independent from dopamine imbalances [Lange et al., 1992] and are accompanied by temporo-parieto-occipital gray matter atrophy [Pereira et al., 2009]. And although striatofrontal circuit disruptions are considered to play a part in declarative memory deficits associated with PD [Dujardin et al., 2001], recent work has described structural hippocampal changes associated with

these impairments [Apostolova et al., 2012; Beyer et al., 2013; Carlesimo et al., 2012; Pereira et al., 2013]. The global changes observed in this study to be associated with MCI and with VS/VP and memory deficits may, therefore, reflect primary white-matter changes as well as the gray-matter pathological processes responsible for more severe cognitive decline and conversion to dementia. Future longitudinal studies are needed to establish if these changes have predictive value for worse cognitive outcomes. The regional network reorganization associated with A/E deficits, however, may be a reflection of the dopamine imbalances affecting frontal areas, a finding compatible with the known relationship between these impairments and frontostriatal dopaminergic imbalances [see, Cools and D'Esposito, 2011]. These data provide valuable evidence about the different pathological implications of distinct types of neuropsychological impairment in PD.

The results found in this study do not conform to the patterns described in Alzheimer's disease, currently the best-studied neurodegenerative process. Graph theory studies in this disease with different methodological approaches have yielded variable results [see Tijms et al., 2013], but studies using resting-state fMRI have described reduced [Supekar et al., 2008] or unchanged [Sanz-Arigita et al., 2010] clustering coefficients. Characteristic path lengths have been described to be reduced in patients with AD [Sanz-Arigita et al., 2010] and increased in patients at risk for this disease [Wang et al., 2013]. Our findings of increased segregation and modularity with no significant changes in integration may therefore be more specific of cognitive impairment in PD.

One possible limitation of the present work is that patients were evaluated in the on state, that is, under the influence of dopaminergic medication. As previous work has shown [Achard et al., 2006], dopaminergic manipulations impact measures of network efficiency. Besides the constraint of conceivably more severe motion artifacts in the off state, with subsequent effects on functional connectivity estimations [van Dijk et al., 2012], we wanted to study cognitive deficits and their substrate as they occur in patients' daily lives, that is, under the effect of their usual medication. In this way, we expect our findings can be extrapolated to the clinical setting and can be more useful in future efforts to establish neuropsychological and neuroimaging biomarkers for dementia. Additionally, despite the rigorous head motion exclusion criteria and preprocessing steps aimed at minimizing the effect of motion artifacts, we cannot guarantee that our results were not influenced to some degree by them. Nonetheless, the fact that connectivity changes were more significant in the MCI group—which displayed less pronounced head motion than the non-MCI group—indicates that the observed effect has actual biological origins.

In conclusion, our results indicate that complex network analysis through resting-state fMRI is a useful method for the investigation of functional changes related to cognitive decline in PD. This study suggests that MCI in PD is accompanied by increases in network modularity and small-world coefficients, as well as by changes in network hub regions. Additionally, cognitive deficits in PD are accompanied by network disruptions characterized by the weakening of long-range connections alongside increases in local connectedness. The observed pattern of these changes and their anatomical distribution indicates that they may be part of the distinct substrates underlying different types of PD-related cognitive impairment. Future longitudinal studies could provide relevant information about the potential use of specific changes in network parameters as predictors of subsequent cognitive decline.

REFERENCES

Aarsland D, Zaccai J, Brayne C (2005): A systematic review of prevalence studies of dementia in Parkinson's disease. Mov Disord 20:1255–1263.

Aarsland D, Bronnick K, Larsen JP, Tysnes OB, Alves G, Norwegian ParkWest Study Group (2009): Cognitive impairment in incident, untreated Parkinson disease: The Norwegian ParkWest study. Neurology 72:1121–1126.

Achard S, Bullmore E (2007): Efficiency and cost of economical brain functional networks. PLoS Comput Biol 3:e17.

Achard S, Salvador R, Whitcher B, Suckling J, Bullmore E (2006): A resilient, low-frequency, small-world human brain functional network with highly connected association cortical hubs. J Neurosci 26:63–72.

Achard S, Delon-Martin C, Vértes PE, Renard F, Schenck M, Schneider F, Heinrich C, Kremer S, Bullmore ET (2012): Hubs of brain functional networks are radically reorganized in comatose patients. Proc Natl Acad Sci USA 109:20608–20613.

Agosta F, Canu E, Stojkovic T, Pievani M, Tomic A, Sarro L, Dragasevic N, Copetti M, Comi G, Kostic VS, Filippi M (2013): The topography of brain damage at different stages of Parkinson's disease. Hum Brain Mapp 34:2798–2807.

Apostolova L, Alves G, Hwang KS, Babakchanian S, Bronnick KS, Larsen JP, Thompson PM, Chou YY, Tysnes OB, Vefring HK, Beyer MK (2012): Hippocampal and ventricular changes in Parkinson's disease mild cognitive impairment. Neurobiol Aging 33:2113–2124.

Baggio HC, Segura B, Ibarretxe-Bilbao N, Valldeoriola F, Marti MJ, Compta Y, Tolosa E, Junque C (2012): Structural correlates of facial emotion recognition deficits in Parkinson's disease patients. Neuropsychologia 50:2121–2128.

Bassett DS, Bullmore E (2006): Small-world brain networks. Neuroscientist 12:512–523.

Beyer MK, Bronnick KS, Hwang KS, Bergsland N, Tysnes OB, Larsen JP, Thompson PM, Somme JH, Apostolova LG (2013): Verbal memory is associated with structural hippocampal changes in newly diagnosed Parkinson's disease. J Neurol Neurosurg Psychiatry 84:23–28.

Biswal B, Yetkin FZ, Haughton VM, Hyde JS (1995): Functional connectivity in the motor cortex of resting human brain using echo-planar MRI. Magn Reson Med 34:537–541.

Bullmore E, Bassett D (2011): Brain graphs: Graphical models of the human brain connectome. Annu Rev Clin Psychol 7:113-140.

Bullmore E, Sporns O (2009): Complex brain networks: Graph theoretical analysis of structural and functional systems. Nat Rev Neurosci 10:186–198.

Burke RE, O'Malley K (2013): Axon degeneration in Parkinson's disease. Exp Neurol 246:72–83.

Carlesimo GA, Piras F, Assogna F, Pontieri FE, Caltagirone C, Spalletta G (2012): Hippocampal abnormalities and memory deficits in Parkinson disease: A multimodal imaging study. Neurology 78:1939–1945.

Chen G, Zhang HY, Xie C, Chen G, Zhang ZJ, Teng GJ, Li SJ (2013): Modular reorganization of brain resting state networks and its independent validation in Alzheimer's disease patients. Front Hum Neurosci 7:456.

Compta Y, Parkkinen L, O'Sullivan SS, Vandrovcova J, Holton JL, Collins C, Lashley T, Kallis C, Williams DR, de Silva R, Lees AJ, Revesz T (2011): Lewy- and Alzheimer-type pathologies in Parkinson;s disease dementia: Which is more important? Brain 134:1493–1505.

Cools R, D'Esposito M (2011): Inverted-U-shaped dopamine actions on human working memory and cognitive control. Biol Psychiatry 69:e113–e125.

Damier P, Hirsch EC, Agid Y, Graybiel AM (1999): The substantia nigra of the human brain. II. Patterns of loss of dopamine-containing neurons in Parkinson's disease. Brain 122 (Pt 8):1437–1448.

Daniel SE, Lees AJ (1993): Parkinson's Disease Society Brain Bank, London: Overview and research. J Neural Transm Suppl. 39:165–172.

de Haan W, Mott K, van Straaten EC, Scheltens P, Stam CJ (2012): Activity dependent degeneration explains hub vulnerability in Alzheimer's disease. PLoS Comput Biol 8:e1002582.

Dujardin K, Defebvre L, Grunberg C, Becquet E, Destee A (2001): Memory and executive function in sporadic and familial Parkinson's disease. Brain 124:389–398.

Elgh E, Domellof M, Linder J, Edstrom M, Stenlund H, Forsgren L (2009): Cognitive function in early Parkinson's disease: A population-based study. Eur J Neurol 16:1278–1284.

Emre M, Aarsland D, Brown R, Burn DJ, Duyckaerts C, Mizuno Y, Broe GA, Cummings J, Dickson DW, Gauthier S, Goldman J, Goetz C, Korczyn A, Lees A, Levy R, Litvan I, McKeith I, Olanow W, Poewe W, Quinn N, Sampaio C, Tolosa E, Dubois B (2007): Clinical diagnostic criteria for dementia associated with Parkinson's disease. Mov Disord 22:1689–1707.

Ferrer I (2009): Early involvement of the cerebral cortex in Parkinson's disease: Convergence of multiple metabolic defects. Prog Neurobiol 88:89–103.

Fields JA, Ferman TJ, Boeve BF, Smith GE (2011): Neuropsychological assessment of patients with dementing illness. Nat Rev Neurol 7:677–687.

Foltynie T, Goldberg TE, Lewis SG, Blackwell AD, Kolachana BS, Weinberger DR, Robbins TW, Barker RA (2004): Planning ability in Parkinson's disease is influenced by the COMT val158-met polymorphism. Mov Disord 19:885–891.

Fornito A, Zalesky A, Bullmore ET (2010): Network scaling effects in graph analytic studies of human resting-state FMRI data. Front Syst Neurosci 4:22.

Fox MD, Raichle ME (2007): Spontaneous fluctuations in brain activity observed with functional magnetic resonance imaging. Nat Rev Neurosci 8:700–711.

Gotham AM, Brown RG, Marsden CD (1986): Levodopa treatment may benefit or impair "frontal" function in Parkinson's disease. Lancet 2:970–971.

Grossberg S (2000): The complementary brain: Unifying brain dynamics and modularity. Trends Cogn Sci 4:233–246.

Gusnard DA, Raichle ME, Raichle ME (2001): Searching for a baseline: Functional imaging and the resting human brain. Nat Rev Neurosci 2:685–694.

Hacker CD, Perlmutter JS, Criswell SR, Ances BM, Snyder AZ (2012): Resting state functional connectivity of the striatum in Parkinson's disease. Brain 135:3699–3711.

Hattori T, Orimo S, Aoki S, Ito K, Abe O, Amano A, Sato R, Sakai K, Mizusawa H (2012): Cognitive status correlates with white matter alteration in Parkinson's disease. Hum Brain Mapp 33: 727–739.

He Y, Chen Z, Evans A (2008): Structural insights into aberrant topological patterns of large-scale cortical networks in Alzheimer's disease. J Neurosci 28:4756–4766.

Humphries MD, Gurney K (2008): Network 'small-world-ness': A quantitative method for determining canonical network equivalence. PLoS One 3:e0002051.

Ibarretxe-Bilbao N, Zarei M, Junque C, Marti MJ, Segura B, Vendrell P, Valldeoriola F, Bargallo N, Tolosa E (2011): Dysfunctions of cerebral networks precede recognition memory deficits in early Parkinson's disease. Neuroimage 57:589–597.

Janvin CC, Larsen JP, Aarsland D, Hugdahl K (2006): Subtypes of mild cognitive impairment in Parkinson's disease: Progression to dementia. Mov Disord 21:1343–1349.

Jenkinson M, Smith S (2001): A global optimisation method for robust affine registration of brain images. Med Image Anal 5: 143–156.

Karbowski J (2001): Optimal wiring principle and plateaus in the degree of separation for cortical neurons. Phys Rev Lett 86: 3674–3677.

Lange KW, Robbins TW, Marsden CD, James M, Owen AM, Paul GM (1992): L-dopa withdrawal in Parkinson's disease selectively impairs cognitive performance in tests sensitive to frontal lobe dysfunction. Psychopharmacology (Berl) 107:394–404.

Lezak MD, Howieson DB, Loring DW. 2004. Neuropsychological Assessment. New York: Oxford.

Li Y, Liu W, Oo TF, Wang L, Tang Y, Jackson-Lewis V, Zhou C, Geghman K, Bogdanov M, Przedborski S, Beal MF, Burke RE, Li C (2009): Mutant LRRK2(R1441G) BAC transgenic mice recapitulate cardinal features of Parkinson's disease. Nat Neurosci 12:826–828.

Liu Y, Liang M, Zhou Y, He Y, Hao Y, Song M, Yu C, Liu H, Liu Z, Jiang T (2008): Disrupted small-world networks in schizophrenia. Brain 131:945–961.

Lo CY, Wang PN, Chou KH, Wang J, He Y, Lin CP (2010): Diffusion tensor tractography reveals abnormal topological organization in structural cortical networks in Alzheimer's disease. J Neurosci 30:16876–16885.

Muslimovic D, Post B, Speelman JD, Schmand B (2005): Cognitive profile of patients with newly diagnosed Parkinson disease. Neurology 65:1239–1245.

Ottet MC, Schaer M, Debbané M, Cammoun L, Thiran JP, Eliez S (2013): Graph theory reveals dysconnected hubs in 22q11DS and altered nodal efficiency in patients with hallucinations. Front Hum Neurosci 7:402.

Pereira JB, Junque C, Marti MJ, Ramirez-Ruiz B, Bargallo N, Tolosa E (2009): Neuroanatomical substrate of visuospatial and visuoperceptual impairment in Parkinson's disease. Mov Disord 24:1193–1199.

Pereira JB, Junque C, Bartres-Faz D, Ramirez-Ruiz B, Marti MJ, Tolosa E (2013): Regional vulnerability of hippocampal subfields and memory deficits in Parkinson's disease. Hippocampus 23:720–728.

Rubinov M, Sporns O (2010): Complex network measures of brain connectivity: Uses and interpretations. Neuroimage 52:1059–1069.

Sanz-Arigita EJ, Schoonheim MM, Damoiseaux JS, Rombouts SA, Maris E, Barkhof F, Scheltens P, Stam CJ (2010): Loss of 'small-world' networks in Alzheimer's disease: Graph analysis of FMRI resting-state functional connectivity. PLoS One 5:e13788.

Scott DA, Tabarean I, Tang Y, Cartier A, Masliah E, Roy S (2010): A pathologic cascade leading to synaptic dysfunction in alpha-synuclein-induced neurodegeneration. J Neurosci 30:8083–8095.

Segura B, Ibarretxe-Bilbao N, Sala-Llonch R, Baggio HC, Marti MJ, Valldeoriola F, Vendrell P, Bargallo N, Tolosa E, Junque C (2013): Progressive changes in a recognition memory network in Parkinson's disease. J Neurol Neurosurg Psychiatry 84:370–378.

Skidmore F, Korenkevych D, Liu Y, He G, Bullmore E, Pardalos PM (2011): Connectivity brain networks based on wavelet correlation analysis in Parkinson fMRI data. Neurosci Lett 499:47–51.

Sporns O, Honey CJ (2006): Small worlds inside big brains. Proc Natl Acad Sci USA 103:19219–19220.

Sporns O, Honey CJ, Kotter R (2007): Identification and classification of hubs in brain networks. PLoS One 2:e1049.

Stam CJ, Jones BF, Nolte G, Breakspear M, Scheltens P (2007): Small-world networks and functional connectivity in Alzheimer's disease. Cereb Cortex 17:92–99.

Stam CJ, de Haan W, Daffertshofer A, Jones BF, Manshanden I, van Cappellen van Walsum AM, Montez T, Verbunt JP, de Munck JC, van Dijk BW, Berendse HW, Scheltens P (2009): Graph theoretical analysis of magnetoencephalographic functional connectivity in Alzheimer's disease. Brain 132:213–224.

Supekar K, Menon V, Rubin D, Musen M, Greicius MD (2008): Network analysis of intrinsic functional brain connectivity in Alzheimer's disease. PLoS Comput Biol 4:e1000100.

Tessitore A, Esposito F, Vitale C, Santangelo G, Amboni M, Russo A, Corbo D, Cirillo G, Barone P, Tedeschi G (2012): Default-mode network connectivity in cognitively unimpaired patients with Parkinson disease. Neurology 79:2226–2232.

Tian L, Jiang T, Liang M, Li X, He Y, Wang K, Cao B, Jiang T (2007): Stabilities of negative correlations between blood oxygen level-dependent signals associated with sensory and motor cortices. Hum Brain Mapp 28:681–690.

Tijms BM, Wink AM, de Haan W, van der Flier WM, Stam CJ, Scheltens P, Barkhof F (2013): Alzheimer's disease: Connecting findings from graph theoretical studies of brain networks. Neurobiol Aging 34:2023–2036.

Tomlinson CL, Stowe R, Patel S, Rick C, Gray R, Clarke CE (2010): Systematic review of levodopa dose equivalency reporting in Parkinson's disease. Mov Disord 25:2649–2653.

Tzourio-Mazoyer N, Landeau B, Papathanassiou D, Crivello F, Etard O, Delcroix N, Mazoyer B, Joliot M (2002): Automated anatomical labeling of activations in SPM using a macroscopic anatomical parcellation of the MNI MRI single-subject brain. Neuroimage 15:273–289.

Van Dijk KR, Sabuncu MR, Buckner RL (2012): The influence of head motion on intrinsic functional connectivity MRI. Neuroimage 59:431–438.

van Wijk BC, Stam CJ, Daffertshofer A (2010): Comparing brain networks of different size and connectivity density using graph theory. PLoS One 5:e13701.

Wang J, Zuo X, Dai Z, Xia M, Zhao Z, Zhao X, Jia J, Han Y, He Y (2013): Disrupted functional brain connectome in individuals at risk for Alzheimer's disease. Biol Psychiatry 73:472–481.

Wang JH, Zuo XN, Gohel S, Milham MP, Biswal BB, He Y (2011): Graph theoretical analysis of functional brain networks: Test-retest evaluation on short- and long-term resting-state functional MRI data. PLoS One 6:e21976.

Wang L, Zhu C, He Y, Zang Y, Cao Q, Zhang H, Zhong Q, Wang Y (2009): Altered small-world brain functional networks in children with attention-deficit/hyperactivity disorder. Hum Brain Mapp 30:638–649.

Williams-Gray CH, Foltynie T, Brayne CE, Robbins TW, Barker RA (2007): Evolution of cognitive dysfunction in an incident Parkinson's disease cohort. Brain 130:1787–1798.

Williams-Gray CH, Evans JR, Goris A, Foltynie T, Ban M, Robbins TW, Brayne C, Kolachana BS, Weinberger DR, Sawcer SJ, Barker RA (2009): The distinct cognitive syndromes of Parkinson's disease: 5 year follow-up of the CamPaIGN cohort. Brain 132:2958–2969.

Wu T, Wang L, Chen Y, Zhao C, Li K, Chan P (2009): Changes of functional connectivity of the motor network in the resting state in Parkinson's disease. Neurosci Lett 460:6–10.

Wu T, Long X, Wang L, Hallett M, Zang Y, Li K, Chan P (2011): Functional connectivity of cortical motor areas in the resting state in Parkinson's disease. Hum Brain Mapp 32:1443–1457.

Zhang Y, Lin L, Lin CP, Zhou Y, Chou KH, Lo CY, Su TP, Jiang T (2012): Abnormal topological organization of structural brain networks in schizophrenia. Schizophr Res 141:109–118.

SUPPLEMENTARY MATERIALS

Formula used to calculate mean group connectivity matrices for community structure analysis:

$$a_{i,j} = \frac{\frac{1}{n}\sum_{k=1}^{n} r_{k,i,j}}{\sqrt{\frac{1}{n}\sum_{k=1}^{n}\left(r_{k,i,j} - \mu_{i,j}\right)^2}}$$

Where *r* is the correlation value between nodes *i* and *j*, *k* is the subject number, *n* is the number of subjects in the respective group, and *a* is the value for each element of the mean correlation matrix. To determine each group's community module structure, we used Newman's spectral algorithm as implemented in the Brain Connectivity Toolbox (Chen *et al*., 2013).

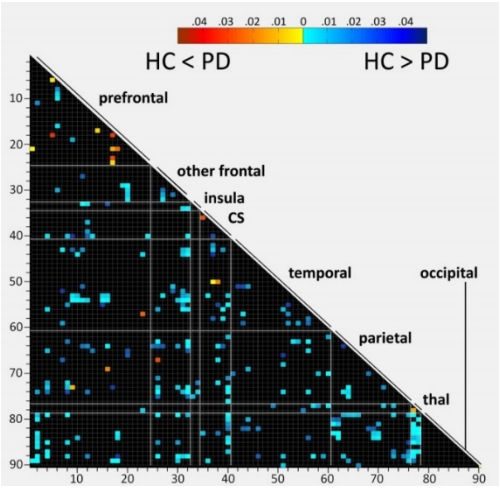

Supplementary Figure 1. Comparisons of interregional connectivity strength between HC and Parkinson's disease patients. Edges with significantly different (p<.05) z correlation values between HC and Parkinson's disease patients are marked in color. Color bar indicates p values according to direction of differences. Anatomical regions, ordered in roughly anterior-posterior sequence and grouped according to lobes or subcortical structures, are numbered in the vertical and horizontal axes according to Table I. *CS*: corpus striatum; *thal*: thalamus.

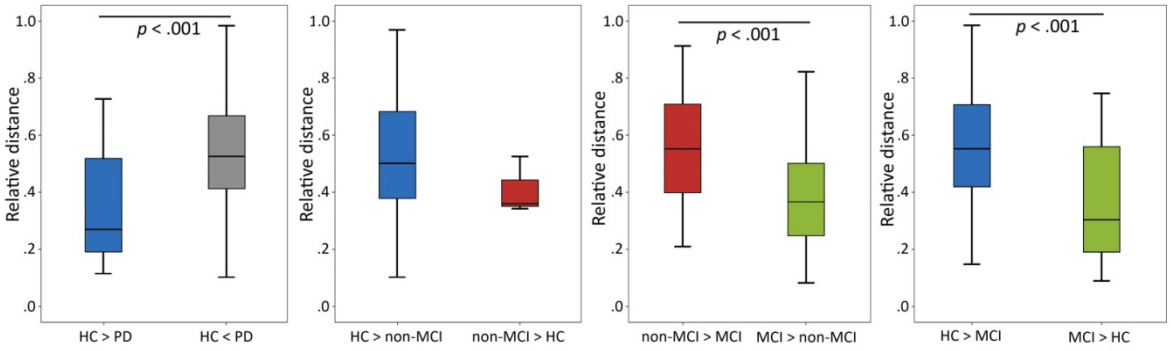

Supplementary figure 2. Changes in interregional connectivity according to anatomical edge length. Plots represent the distribution of connections for which a significant group effect was found according to their relative length, calculated as the relative distance between each region's central coordinates. Connections that were weakened in the PD group and in the MCI group were significantly longer than those that were strengthened (p<.001, *post-hoc* Bonferroni test).

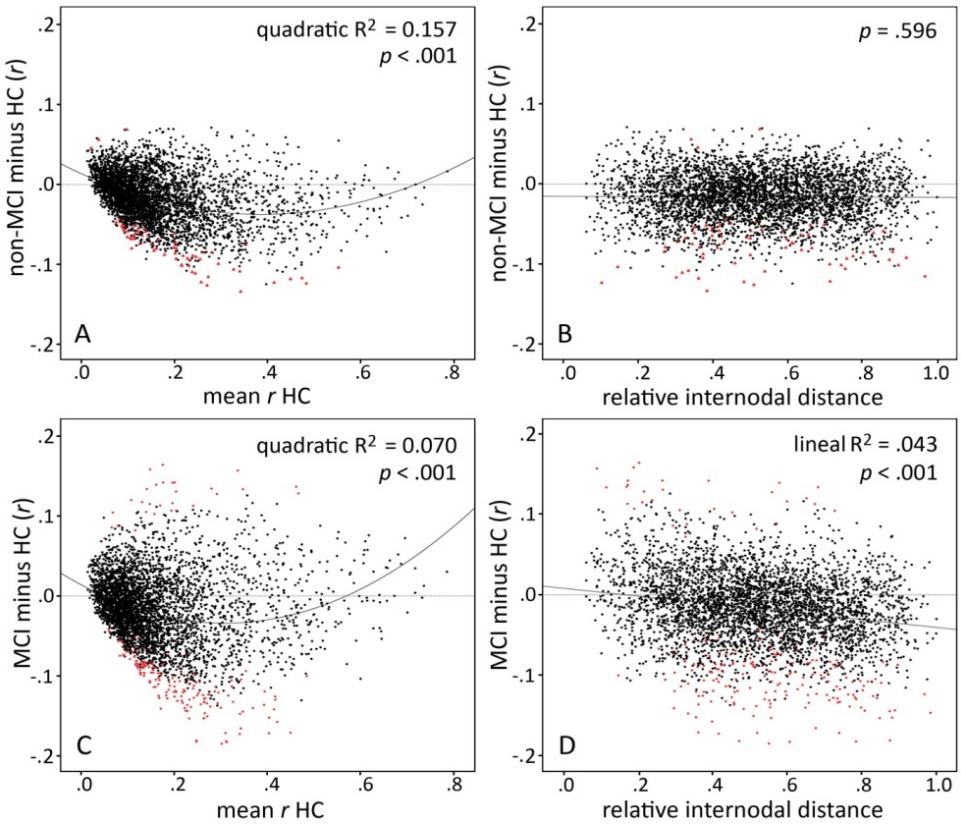

Supplementary Figure 3. Changes in interregional connectivity in non-MCI and MCI PD patients relative to controls as a function of connection strength and length. The differences between interregional connectivity in *r* values between non-MCI patients and controls (A, B) and between MCI patients and controls (C, D) are plotted against mean *r* values for controls (A, C) and mean relative internodal distance (B, D). Red dots indicate edges with *r* values that differed significantly between non-MCI or MCI PD patients and controls. As can be seen in A and C, a quadratic relation was observed between changes in interregional connectivity strength and the corresponding strength in the control group, indicating greater weakening in edges of intermediate strength in both non-MCI and MCI PD patients. B shows that edge weakening in non-MCI patients does not correlate significantly with edge length; on the other hand, connection length displayed a weak negative correlation with the difference between *r* values in MCI patients and controls, indicating that longer-range connections tend to undergo greater weakening than shorter edges in this patient group.

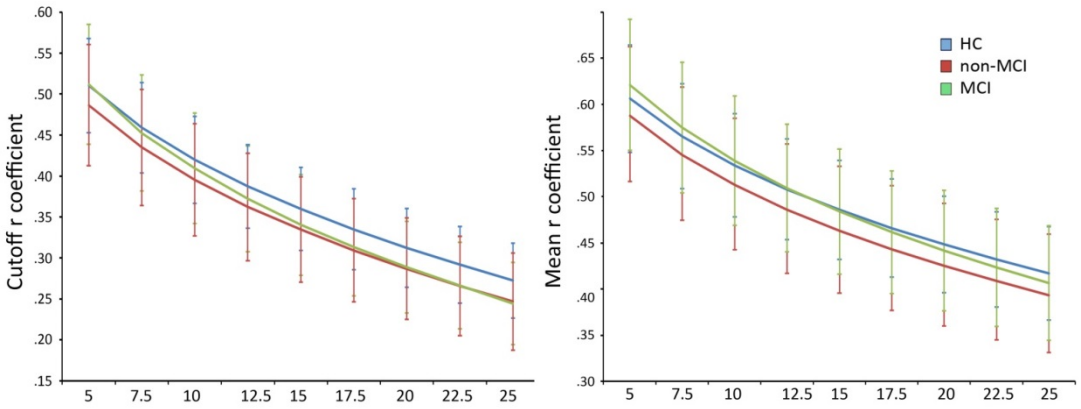

Supplementary figure 4. Cutoff and mean r coefficients according to group and sparsity threshold. Left: minimum r value (vertical axis) included in the weighted networks by group as a function of sparsity threshold (horizontal axis, in percentage). Right: mean r value of the edges included in the weighted networks (vertical axis) by group as a function of sparsity threshold (horizontal axis, in percentage). No significant group differences were found.

	HC	PD-NMCI	PD-MCI	**F/*p***
VFD	29.61 (2.70)	29.09 (2.34)	26.26 (.56)	**11.226/<.001**
JLO	23.94 (3.99)	23.12 (3.93)	19.43 (5.12)	**8.526/<.001**
RAVLT total	44.67 (6.05)	44.47 (9.08)	33.65 (7.76)	**17.281/<.001**
RAVLT retrieval	9.08 (2.10)	8.58 (2.64)	6.04 (2.87)	**11.134/<.001**
Digits backwards minus forwards	-1.69 (1.16)	-1.81 (1.03)	-1.17 (1.07)	2.695/.073
Stroop interference	-2.42 (8.96)	-.97 (9.92)	-3.00 (5.68)	.464/.630
TMT A-B	-50.17 (23.93)	-57.33 (29.58)	-142.38 (101.36)	**23.474/<.001**
Phonemic fluency	16.57 (5.03)	16.40 (4.962)	11.74 (5.33)	**7.758/.001**
VS/VP z score	-.012 (.572)	-.169 (.601)	-1.001 (.865)	**17.562/<.001**
Memory z score	-.010 (.818)	-.092 (1.028)	-1.350 (1.131)	**15.479/<.001**
A/E z score	.027 (.537)	-.022 (.519)	-.752 (.980)	**11.772/<.001**

Supplementary Table I. Neuropsychological performance results for healthy controls and Parkinson's disease patients according to MCI status. Results are presented in *means (SD)*. *PD-NMCI*: Parkinson's disease patients without MCI; *PD-MCI*: patients with MCI; *Digits backwards minus forwards*: difference between backward and forward digit spans; *TMT A-B*: difference between TMT parts A and B. Z scores for cognitive domains refer to the difference between actual z scores and expected age, sex and education-adjusted z scores. For all significant F-test comparisons, *post-hoc* analyses showed that MCI patients' scores were significantly worse than non-MCI patients' and healthy controls', with no significant differences between the latter (p<.05, *post-hoc* Bonferroni test).

	HC	PD-NMCI	PD-MCI	F/*p*	η²
Global mean *r*	.174 (.028)	.158 (.035)	.157 (.029)	NS	
C 5.0%	**.199 (.042)**	**.184 (.038)**	**.213 (.048)**	**3.840 (.025)**	**.072**
C 7.5%	**.224 (.040)**	**.206 (.043)**	**.238 (.048)**	**4.302 (.016)**	**.080**
C 10.0%	**.231 (.038)**	**.218 (.045)**	**.247 (.052)**	**3.273 (.042)**	**.062**
C 12.5%	.238 (.037)	.222 (.049)	.250 (.057)	NS	-
C 15.0%	.238 (.037)	.223 (.049)	.248 (.056)	NS	-
C 17.5%	.236 (.037)	.222 (.051)	.242 (.055)	NS	-
C 20.0%	.237 (.039)	.220 (.052)	.239 (.054)	NS	-
C 22.5%	.234 (.039)	.217 (.052)	.234 (.054)	NS	-
C 25.0%	.232 (.040)	.215 (.053)	.229 (.053)	NS	-
L 5.0%	2.943 (.791)	2.920 (1.097)	3.507 (1.406)	NS	-
L 7.5%	1.850 (.451)	1.762 (.557)	1.930 (.639)	NS	-
L 10.0%	1.366 (.301)	1.312 (.380)	1.370 (.358)	NS	-
L 12.5%	1.108 (.223)	1.047 (.278)	1.086 (.273)	NS	-
L 15.0%	.937 (.180)	.876 (.219)	.904 (.209)	NS	-
L 17.5%	.816 (.149)	.763 (.185)	.777 (.172)	NS	-
L 20.0%	.723 (.126)	.676 (.164)	.684 (.143)	NS	-
L 22.5%	.650 (.113)	.607 (.149)	.609 (.125)	NS	-
L 25.0%	.591 (.101)	.547 (.133)	.549 (.112)	NS	-
M 5.0%	.527 (.069)	.521 (.095)	.559 (.093)	NS	-
M 7.5%	.482 (.069)	.472 (.085)	.513 (.089)	NS	-
M 10.0%	**.445 (.058)**	**.435 (.073)**	**.482 (.082)**	**3.533 (.033)**	**.067**
M 12.5%	**.413 (.054)**	**.407 (.068)**	**.452 (.077)**	**3.748 (.027)**	**.070**
M 15.0%	**.389 (.051)**	**.384 (.062)**	**.430 (.072)**	**4.566 (.013)**	**.084**
M 17.5%	**.367 (.048)**	**.365 (.060)**	**.409 (.065)**	**4.989 (.009)**	**.092**
M 20.0%	**.349 (.044)**	**.347 (.056)**	**.388 (.062)**	**4.980 (.009)**	**.091**
M 22.5%	**.334 (.042)**	**.332 (.054)**	**.371 (.059)**	**4.923 (.009)**	**.090**
M 25.0%	**.320 (.040)**	**.318 (.053)**	**.358 (.056)**	**5.300 (.007)**	**.097**
SW 5.0%	2.411 (.926)	2.593 (1.283)	2.584 (.912)	NS	-
SW 7.5%	2.335 (.680)	2.381 (.806)	2.485 (.771)	NS	-
SW 10.0%	2.125 (.535)	2.176 (.638)	2.334 (.664)	NS	-
SW 12.5%	2.094 (.457)	2.081 (.540)	2.357 (.646)	NS	-
SW 15.0%	**1.930 (.385)**	**1.989 (.513)**	**2.280 (.528)**	**4.129 (.019)**	**.077**
SW 17.5%	**1.854 (.339)**	**1.900 (.430)**	**2.168 (.482)**	**4.493 (.014)**	**.083**
SW 20.0%	**1.833 (.300)**	**1.862 (.380)**	**2.079 (.432)**	**3.587 (.031)**	**.068**
SW 22.5%	**1.769 (.272)**	**1.833 (.347)**	**2.042 (.365)**	**5.112 (.008)**	**.094**
SW 25.0%	**1.722 (.248)**	**1.814 (.327)**	**2.015 (.351)**	**6.444 (.002)**	**.115**
Eglob 5.0%	**.203 (.032)**	**.205 (.045)**	**.180 (.036)**	**3.554 (.032)**	**.067**
Eglob 7.5%	.293 (.039)	.300 (.049)	.286 (.043)	NS	-
Eglob 10.0%	.365 (.038)	.367 (.050)	.363 (.040)	NS	-
Eglob 12.5%	.419 (.035)	.424 (.045)	.420 (.038)	NS	-
Eglob 15.0%	.464 (.033)	.471 (.039)	.467 (.032)	NS	-
Eglob 17.5%	.502 (.028)	.506 (.034)	.507 (.029)	NS	-
Eglob 20.0%	.535 (.024)	.537 (.030)	.538 (.022)	NS	-
Eglob 22.5%	.563 (.021)	.564 (.027)	.566 (.017)	NS	-
Eglob 25.0%	.588 (.017)	.590 (.022)	.591 (.014)	NS	-

Supplementary Table II. Mean global connectivity and global graph-theoretical measures results according to group and intergroup comparison results. Percentages indicate the sparsity thresholds. Data are presented in means (SD). η^2: partial eta-squared; *Global mean r*: mean of all positive interregional-correlation *r* values; *M*: modularity; *C*: clustering coefficient; *SW*: small-world coefficient; *L*: path length; *Eglob*: global efficiency. NS: statistically non-significant omnibus test results ($p>.05$, *post-hoc* Bonferroni test).

study 3

CORTICAL THINNING ASSOCIATED WITH MILD COGNITIVE IMPAIRMENT IN PARKINSON'S DISEASE

Movement Disorders 2014

Bàrbara Segura, Hugo César Baggio, Maria José Martí, Francesc Valldeoriola, Yaroslau Compta, Anna Isabel García Díaz, Pere Vendrell, Núria Bargalló, Eduardo Tolosa, Carme Junqué

RESEARCH ARTICLE

Cortical Thinning Associated With Mild Cognitive Impairment in Parkinson's Disease

Bàrbara Segura, PhD,[1,2] Hugo César Baggio, MD,[1,2] Maria Josep Marti, MD, PhD,[1,3,4] Francesc Valldeoriola, MD, PhD,[1,3,4] Yaroslau Compta, MD, PhD,[1,3,4] Anna Isabel Garcia-Diaz, PhD,[2] Pere Vendrell, PhD,[1,2,3] Núria Bargallo, MD, PhD,[5] Eduardo Tolosa, MD, PhD,[1,3,4,6] and Carme Junque, PhD[1,2,3]*

[1]*Institute of Biomedical Research August Pi i Sunyer (IDIBAPS), Catalonia, Spain*
[2]*Department of Psychiatry and Clinical Psychobiology, University of Barcelona, Catalonia, Spain*
[3]*Centro de Investigación en Red de Enfermedades Neurodegenerativas (CIBERNED), Hospital Clínic de Barcelona, Catalonia, Spain*
[4]*Neurology Service, Institut Clínic de Neurociències (ICN), Parkinson's Disease and Movement Disorders Unit, Hospital Clínic de Barcelona, Catalonia, Spain*
[5]*Centre de Diagnostic per la Imatge, Hospital Clinic, Barcelona, Catalonia, Spain*
[6]*University of Barcelona, Catalonia, Spain*

ABSTRACT: The aim of this study was to investigate patterns of cortical atrophy associated with mild cognitive impairment in a large sample of nondemented Parkinson's disease (PD) patients, and its relation with specific neuropsychological deficits. Magnetic resonance imaging (MRI) and neuropsychological assessment were performed in a sample of 90 nondemented PD patients and 32 healthy controls. All underwent a neuropsychological battery including tests that assess different cognitive domains: attention and working memory, executive functions, memory, language, and visuoperceptual-visuospatial functions. Patients were classified according to their cognitive status as PD patients without mild cognitive impairment (MCI; n = 43) and PD patients with MCI (n = 47). Freesurfer software was used to obtain maps of cortical thickness for group comparisons and correlation with neuropsychological performance. Patients with MCI showed regional cortical thinning in parietotemporal regions, increased global atrophy (global cortical thinning, total gray matter volume reduction, and ventricular enlargement), as well as significant cognitive impairment in memory, executive, and visuospatial and visuoperceptual domains. Correlation analyses showed that all neuropsychological tests were associated with cortical thinning in parietotemporal regions and to a lesser extent in frontal regions. These results provide neuroanatomic support to the concept of MCI classified according to Movement Disorders Society criteria. The posterior pattern of atrophy in temporoparietal regions could be a structural neuroimaging marker of cognitive impairment in nondemented PD patients. All of the neuropsychological tests reflected regional brain atrophy, but no specific patterns were seen corresponding to impairment in distinct cognitive domains. © 2014 International Parkinson and Movement Disorder Society

Key Words: Parkinson's disease; cortical thickness; cognition

*Correspondence to: Dr. Carme Junque, PhD, Department of Psychiatry and Clinical Psychobiology, University of Barcelona, Casanova 143 (08036) Barcelona, Catalonia, Spain, E-mail: cjunque@ub.edu

Funding agencies: This work was funded by the Spanish Ministry of Science and Innovation [PSI2013-41393 grant to C.J., H.C.B., P.V, A.I.G and B.S.], and by Generalitat de Catalunya [2009 SGR0836 to E.T., 2014SGR 98 to C.J.] and an FI-DGR grant [2011FI_B 00045] to H.C.B., and CIBERNED.

Relevant conflicts of interest/financial disclosures: Nothing to report. Full financial disclosures and author roles may be found in the online version of this article.

Received: 17 March 2014; **Revised:** 23 May 2014; **Accepted:** 2 July 2014

Published online 00 Month 2014 in Wiley Online Library (wileyonlinelibrary.com). DOI: 10.1002/mds.25982

Parkinson's disease (PD) is associated with cognitive decline[1-4] that may predict dementia at later stages.[5-7] Between 18.9% and 38.2% of patients meet mild cognitive impairment (MCI) criteria.[8] Indeed, the proportion of patients fulfilling MCI criteria increased from one third to approximately 50% of patients without dementia after 5 years from diagnosis.[9] A great variability was seen in the description and proportion of subtypes of MCI in PD,[3,6,10,11] perhaps because of the number and type of tests used and the classification of the tests by domains.

The recognition of PD patients with MCI (PD MCI) has led to studies searching for biological markers associated with this diagnosis. Several magnetic resonance imaging (MRI) studies have investigated the

relationship between brain atrophy and specific cognitive deficits in nondemented PD, such as deficits in memory,[12-19] verbal fluency,[20] visuospatial and visuoperceptual ability,[21] and decision-making and emotional processing.[22,23] Recently, Filoteo et al.,[24] using region-of-interest analyses, associated subtle changes in multiple cognitive domains with distinct patterns of regionally specific volume changes in nondemented PD patients. However, to the best of our knowledge, no published MRI studies have focused on whole brain neuroanatomical correlates of the different tests included in cognitive domains assessed by an extensive neuropsychological battery.

Few studies have investigated the neuroanatomical correlates of MCI. Initially, voxel-based morphometry (VBM) analyses showed that PD-MCI had reduced cortical gray matter (GM) density in the left middle frontal gyrus, precentral gyrus, left superior temporal lobe, and right inferior temporal lobe in comparison with cognitively intact PD patients.[25] In contrast, Song et al.[26] reported GM density decreases in frontal regions of PD-MCI patients in comparison with PD without MCI (PD non-MCI). Recently, VBM analyses with a large sample of 148 PD patients did not show any areas of significant GM loss in participants with PD-MCI compared with controls.[27]

To clarify these controversial results, certain methodological issues need to be addressed. Both VBM and volumetric analyses may be insufficient to detect early cortical changes in PD MCI patients. Recent studies using cortical thickness measures suggest that this method may be more sensitive than VBM to identify regional GM changes associated with PD.[28] Cortical changes associated specifically with MCI in PD have not been investigated in depth. In a small sample, Biundo et al.[29] showed significant regional thinning in right parietal-frontal areas and in left temporal-occipital areas in PD MCI in comparison with PD non-MCI. Studying a bigger sample, Pagonabarraga et al.,[30] using an uncorrected level of significance, showed both increases and decreases in cortical thickness of PD MCI patients in comparison with PD non-MCI, and Hanganu et al.[31] did not find significant cortical thinning in PD MCI subjects compared with PD non-MCI, but detected a small cluster with increased thickness in the left middle temporal gyrus. Recently, Pereira et al[32] studied a large multicentric cohort of drug-naïve PD patients with early PD; they found mainly temporal and parietal cortical thinning in the PD MCI group compared with PD non-MCI patients, using a cognitive-domain approach.

In light of these previous results, the aims of this study were (1) to investigate whether different anatomical patterns of cortical atrophy distinguish PD patients with MCI from patients without cognitive impairment in a large sample of nondemented PD patients and (2) whether different anatomical patterns of cortical atrophy are associated with neuropsychological deficits commonly related to specific cognitive domains. This is of crucial importance for validating MCI criteria, and may help to clarify the neural correlates of cognitive impairment in PD.

Methods

Subjects

The study included 121 consecutive PD patients recruited from an outpatient movement disorders clinic (Parkinson's Disease and Movement Disorders Unit, Department of Neurology, Hospital Clinic, Barcelona, Catalonia, Spain) and 49 healthy controls who volunteered to take part in studies addressing age-related processes at the *Institut de l'Envelliment* (Aging Institute). The inclusion criteria were: (1) fulfilling the UK PD Society Brain Bank diagnostic criteria for PD[33]; (2) no surgical treatment with deep brain stimulation. The exclusion criteria were: (1) presence of dementia according to the Movement Disorders Society criteria[33]; (2) Hoehn and Yahr (H&Y) scale score greater than 3; (3) juvenile-onset PD; (4) presence of psychiatric or neurological comorbidity; (5) low global intelligence quotient estimated by the Vocabulary subtest of the Wechsler Adult Intelligence Scale, 3rd edition (scaled score ≤ 7 points); (6) Mini-mental state examination score below 25; (7) presence of claustrophobia; (8) pathological MRI findings other than mild white matter hyperintensities in long-TR sequences; and (9) MRI artefacts.

Ninety PD patients and 32 healthy volunteers were finally selected. Twelve patients and eight controls were excluded because they fulfilled criteria for dementia or other neurological disease, six PD patients for psychiatric comorbidity, one PD patient who scored higher than 3 on the H&Y scale, one PD patient who presented young-onset PD, three PD patients and one control who presented low global intelligence quotient scores, two PD patients for claustrophobia, three healthy subjects who did not complete the neuropsychological assessment, and two controls and two PD patients because of MRI artefacts. We also excluded four patients and three controls aged younger than 50 years.

Motor symptoms were assessed by means of the UPDRS-III motor section. All PD patients were taking antiparkinsonian drugs, consisting of different combinations of levodopa (L-dopa), Catechol-O-methyltransferase (COMT) inhibitors, monoamine oxidase inhibitors, dopamine agonists, and amantadine.

This study was approved by the ethics committee of the University of Barcelona. Written informed consent was obtained from all study subjects after full explanation of the procedures involved.

Neuropsychological Assessment

We selected a neuropsychological battery to assess cognitive functions usually impaired in PD.[2,3] This battery is recommended by the Movement Disorder Society task force to evaluate cognitive functions in PD[8,34] and is able to detect MCI in PD (level I or level II criteria for PD-MCI, bar language, for which a single measure was used.[10] Attention and working memory were assessed with the Trail Making Test (TMT) (in seconds), part A (TMT A) and part B (TMT B), Digit Span Forward and Backward, and the Stroop Colour-word Test and Symbol Digits Modalities Tests (SDMT); executive functions were evaluated with phonemic (words beginning with the letter "p" in 1 minute) and semantic (animals in 1 minute) fluencies; language was assessed by the total number of correct responses in the short version of the Boston Naming Test, memory through total learning recall (sum of correct responses from trial I to trial V), and delayed recall (total recall after 20 min) through scores on Rey's Auditory Verbal Learning Test (RAVLT). Visuospatial and visuoperceptual functions were assessed with Benton's Judgement of Line Orientation (JLO) and Visual Form Discrimination (VFD) tests.

Initially, *z* scores for each test and for each subject were calculated based on the control group's means and standard deviations. Expected *z* scores adjusted for age, sex, and education for each test and each subject were calculated based on a multiple regression analysis performed in the healthy control group.[3]

We classified subjects as having MCI if the *z* score for a given test was at least 1.5 lower than the expected score in at least two tests in one domain, or in at least one test per domain in at least two domains. As expected,[2] most subjects with abnormalities had deficits in more than one function, precluding the creation of patient groups with single-domain impairments. Patients' cognitive complaints were recorded during the clinical interview.

Z composite scores were computed to obtain global cognitive measures (attention and working memory, executive, memory, and visuospatial/visuoperceptual functions).

Neuropsychological and Clinical Statistical Analysis

All statistical analyses were performed using SPSS Statistics 20, release version 20.0.0 (Armonk, NY, http://www-01.ibm.com/software/analytics/spss/). Statistical significance threshold was set at $P < 0.05$. Pearson's chi-square test was used to compare categorical variables (sex and H&Y stage). Separate-variance test (Welch t) was used to test between-group differences (HC, PD MCI, PD non-MCI) in quantitative clinical and demographic variables. Analyses of covariance including age and education as confounding variables were used to compare the performance on neuropsychological tests and composite scores for each domain. Bonferroni correction was used to control for the number of intergroup comparisons.

Image Acquisition

Magnetic resonance images were acquired with a 3T scanner (MAGNETOM Trio, Siemens, Germany). The scanning protocol included high-resolution three-dimensional T1-weighted images acquired in the sagittal plane (TR = 2,300 ms, TE = 2.98 ms, TI 900 ms, 240 slices, FOV = 256 mm; matrix size = 256 × 256; 1 mm isotropic voxel) and axial FLAIR sequence (TR = 9,000 ms, TE = 96 ms).

Cortical Thickness

Cortical thickness was estimated using the automated *FreeSurfer* stream (version 5.1; available at: http://surfer.nmr.harvard.edu). The procedures carried out by *FreeSurfer* software include removal of nonbrain data, intensity normalization,[35]), tessellation of the GM/white matter boundary, automated topology correction,[36,37] and accurate surface deformation to identify tissue borders).[38-40] Cortical thickness is then calculated as the distance between the white matter and GM surfaces at each vertex of the reconstructed cortical mantle.[40] In our study, results for each subject were visually inspected to ensure accuracy of registration, skull stripping, segmentation, and cortical surface reconstruction. Maps were smoothed using a circularly symmetric Gaussian kernel across the surface with a full width at half maximum (FWHM) of 15 mm.

Comparisons between groups were assessed using a vertex-by-vertex general linear model. The model included cortical thickness as a dependent factor and diagnosis (controls, PD non-MCI, PD MCI) as an independent factor, and also included age and education as nuisance variables (https://surfer.nmr.mgh.harvard.edu/fswiki/FsgdFormat). All results were corrected for multiple comparisons by using a precached cluster-wise Monte-Carlo Simulation. Significance level was set at $P < 0.05$.

In the PD patient group, the vertex-by-vertex general linear model was used to assess the relationship between cortical thickness and neuropsychological tests. Positive and negative associations between a specific neuropsychological test and cortical thickness were analyzed using Qdec. Initially, a simple model without covariates was tested for each neuropsychological measure. Complementarily, we performed a conservative analysis of covariance including age, education, and sex as confounding variables. An initial vertex-wise threshold was set to $P = 0.005$ (2.3) to find clusters. To avoid clusters appearing significant

TABLE 1. Sociodemographic and clinical data from study groups

	HC (n = 32)	PD non-MCI (n = 43)	PD MCI (n = 47)	Test stats/*P*
Age (yrs)	64.69 ± 8.63	60.77 ± 10.51	67.72 ± 9.71	5.243/**0.007**
Sex (female/male)	16/16	29/21	23/17	0.58 χ^2/0.747
Years of education	11.00 ± 4.15	12.02 ± 5.05	9.19 ± 5.24	3.47/**0.036**
MMSE	29.69 ± 0.47	29.47 ± 0.74	28.68 ± 1.29	11.998/**<0.001**
BDI	6.00 ± 5.65	8.71 ± 5.41	12.63 ± 6.41	11.174/**<0.001**
Disease duration		6.23 ± 4.05	9.73 ± 6.37	9.845/**0.002**
LEDD		692.81 ± 452.801	916.15 ± 507.944	4.863/**0.030**
HY (1/1.5/2/2.5/3)		14/5/19/3/2	8/0/25/6/8	11.900 χ^2/**0.018**
UPDRS-III		13.16 ± 7.67	17.79 ± 11.07	6.378/**0.023**

MMSE, mini-mental state examination; BDI, Beck's Depression Inventory-II scores; Disease duration, duration of motor symptoms, in years; LEDD, Levodopa equivalent daily dose, in mg; HY, Hoehn and Yahr scale; Pearson's chi-square (χ^2). Age showed significant differences between PD MCI and PD non-MCI patients ($P = 0.003$, Bonferroni correction). MMSE showed significant differences between PD MCI and both PD non-MCI and HC ($P < .001$, Bonferroni correction). BDI showed significant differences between PD MCI and both PD non-MCI ($P < .010$, Bonferroni correction) and HC ($P < .001$, Bonferroni correction).

purely by chance (i.e., false positives), Monte-Carlo simulation with 10,000 repeats was tested (absolute value). Results were reported at cluster-wise probability significance level set at $P < 0.05$.

Global Atrophy Measures

Global average thickness for both hemispheres was calculated ([lh thickness*lh surfarea] + [rh.thickness * rh.surface area]/[lh surface area + rh surface area]).

Total GM volume and total subcortical volumes, as well as mean lateral ventricular volume and estimated total intracranial volume (eTIV) were obtained automatically via whole brain segmentation.[41] An analysis of covariance including eTIV, age, and education was used to compare subcortical volumes between groups. Significant *P* values were adjusted using post hoc Bonferroni tests considering the number of intergroup comparisons.

Results

Forty-seven patients (52.2%) fulfilled the criteria for MCI. Table 1 shows sociodemographic and clinical data and the corresponding group comparisons.

Neuropsychological Differences Between Groups

Table 2 shows differences in neuropsychological performance between groups. MCI patient scores were significantly worse than those of non-MCI patients and healthy controls in all tests except Forward and Backward Digits. Forty-two patients (46.6%) showed impairments in attention and working memory, 31 (34.4%) in memory, 26 (28.8%) in executive and also visuoperceptual and visuospatial domains, and only four (0.4%) in language.

Global Atrophy Comparison Between Groups

Significant differences were found in global atrophy between healthy controls and PD patient groups according to MCI status. The PD MCI patients showed decreased total mean thickness and total GM volume, as well as increased mean lateral ventricle volume in comparison with healthy controls and PD non-MCI. No significant differences were found in total subcortical volume (Table 3). Finally, no significant results were seen after the inclusion of disease duration as a nuisance variable in the covaried model.

Cortical Thickness Comparison Between Groups

Surface-based cortical thickness analyses showed a group effect according to cognitive status (Fig. 1). PD MCI (PD MCI < HC) showed cortical thinning in widespread bilateral regions, including parietal (superior and inferior, supramarginal, and also precuneus regions), temporal (posterior middle temporal, inferior temporal, fusiform, and parahippocampal regions), and occipital cortices (bilateral posterior occipital), but also in left frontal superior and rostral middle areas. There were significant differences between controls and PD non-MCI (PD non-MCI < HC) specifically in bilateral superior parietal regions. PD MCI (PD MCI < PD non-MCI) showed significant thinning in right precuneus and supramarginal regions compared to PD with non-MCI. There were no significant results after including disease duration as a nuisance factor in the co-varied model.

Correlations Between Neuropsychological Tests and Cortical Thickness in PD Patients

Vertex-wise regression analyses showed correlations between regional cortical thickness and neuropsychological test performance (Supplemental Data). We found a common posterior atrophy pattern for all the neuropsychological tests evaluated, and there were no specific patterns of atrophy related to neuropsychological domains.

Stroop Test (Words, Colours, and Word-Colours), TMT A, semantic fluency, and RAVLT total learning performance correlated with GM thinning in bilateral

TABLE 2. Neuropsychological performance results for healthy controls and Parkinson's disease patients according to MCI status

	HC n=32 mean (SD)	PD non-MCI n=43 mean (SD)	PD MCI n=47 mean (SD)	F (*p*)
Neuropsychological tests				
VFD	29.44 (2.75)	29.47 (2.22)	26.17 (3.81)	**11.171 (<0.001)**
JLO	23.88 (3.46)	23.42 (3.93)	19.67 (4.99)	**7.90 (0.001)**
RAVLT total	44.75 (6.27)	46.19 (8.23)	32.81 (7.47)	**33.05 (<0.001)**
RAVLT retrieval	9.13 (2.12)	9.26 (2.60)	6.00 (2.30)	**18.92 (<0.001)**
SDMT	48.41 (9.59)	46.68 (10.59)	31.45 (15.13)	**23.76 (<0.001)**
Digits Forwards	5.87 (1.43)	6.12 (1.22)	5.21 (1.30)	2.429 (0.093)
Digits Backwards	4.19 (1.28)	4.51 (0.99)	3.83 (0.89)	1.982 (0.142)
Stroop Words	100.16 (14.31)	98.90 (21.28)	72.68 (17.12)	24.465 **(<0.001)**
Stroop Colours	62.47 (15.32)	66.31 (12.39)	47.30 (11.91)	18.50 **(<0.001)**
Stroop Words-Colours	35.81 (11.91)	38.81 (11.06)	26.30 (10.72)	8.66 **(<0.001)**
TMT A	38.94 (14.90)	37.09 (15.69)	80.83 (61.78)	**10.283 (<0.001)**
TMT B	90.41 (31.54)	90.21 (35.94)	187.78 (122.34)	**21.40 (<0.001)**
Phonemic fluency	16.71 (5.15)	18.02 (4.92)	12.02 (5.11)	**11.05 (<0.001)**
Semantic fluency	21.61 (5.94)	20.65 (5.259)	15.32 (7.390)	**7.42 (<0.001)**
BNT	13.66 (1.07)	13.67 (1.02)	12.83 (1.28)	3.119 (0.05)
Z composite score				
Attention/Working memory	0.07 (0.47)	0.09 (0.39)	−0.07 (0.47)	0.974 (0.381)
Executive	0.06 (0.88)	0.14 (0.86)	−0.97 (0.97)	**12.821 (<0.0001)**
Memory	0.05 (0.93)	0.19 (1.24)	−1.67 (1.01)	**32.511 (<0.0001)**
Visoperceptual/visuospatial	0.01 (0.71)	−0.05 (0.67)	−1.10 (1.08)	**16.78 (<0.0001)**
Language z score (BNT)	0.13 (0.87)	0.14 (0.83)	− 0.55 (1.21)	3.12 (0.048)
Impaired subjects per domain				
Attention/Working memory[a]	4	11	42	
Executive[a]	0	4	26	
Memory[a]	1	5	31	
Visoperceptual/visuospatial[a]	0	4	26	
Language[a]	1	3	4	

MCI patients' scores were significantly worse than non-MCI patients' and healthy controls' ($p<.05$, Bonferroni correction).
[a]Number of subjects impaired in one or more tests in this domain. In the healthy control group, no subjects showed impairments in more than one test, *i.e.*, none fulfilled criteria for MCI. Trail Making Test (TMT) part A (TMT A) and part B (TMT B), Symbol Digits Modalities Tests (SDMT); short version of the Boston Naming Test (BNT), Rey's Auditory Verbal Learning Test (RAVLT); Benton's Judgement of Line Orientation (JLO) and Visual Form Discrimination (VFD).

medial and lateral areas. Performance on VFD, JLO, and TMT B was associated only with medial temporal-parietal atrophy. Atrophy in anterior regions, mostly left superior frontal gyrus, also correlated with Stroop Test, TMT A, SDMT, phonemic fluency, and RAVLT total learning. In addition, negative correlations with SDMT and JLO were also found in rostral middle frontal gyrus (Supplemental Data Fig. 1 and Table 2). After controlling for the effects of age, education, and sex, only Stroop Words Test and Semantic fluency showed a significant positive correlation with cortical thickness. Stroop Words Test correlated with left medial orbitofrontal, right superior temporal, and right insula. Semantic fluency correlated with right precuneus and lingual gyrus thickness. (Fig. 2 and Supplemental Data Table 3). No significant results were seen after, including disease duration as a nuisance factor in the covaried model.

TABLE 3. Global atrophy results for healthy controls and Parkinson's disease patients according to MCI status, controlling for the effect of age and education

	HC (n = 32) Mean (SD)	PD non-MCI (n = 43) Mean (SD)	PD MCI (n = 47) Mean (SD)	*F* (*P*)
Global thickness (mm)	2.49 (0.09)	2.47 (0.10)	2.41 (0.10)	**6.412 (0.002)**
Total GM (cm^3)	610.36 (51.79)	605.06(59.68)	589.95 (57.85)	**3.652 (0.029)**[a]
Subcortical GM (cm^3)	168.97(20.07)	173.14(20.98)	171.02 (18.44)	1.533 (0.220)[a]
Lateral ventricles (cm^3)	9.60 (4.05)	10.65 (5.57)	13.64 (7.85)	**3.058 (0.051)**[a]

[a]ANCOVA analyses with age, education, and eTIV as confounding variables. Global cortical thickness showed significant differences between HC and PD MCI patients ($P < 0.006$, Bonferroni correction). Total GM showed significant differences between HC and PD non-MCI patients ($P = 0.031$, Bonferroni correction). Mean lateral ventricular volumes showed significant differences between HC and PD MCI patients ($P = 0.046$, Bonferroni correction).
MCI, mild cognitive impairment; HC, healthy controls; PD, Parkinson's disease; GM, gray matter; SD, standard deviation; ANCOVA, analysis of covariance; eTIV, estimated total intracranial volume.

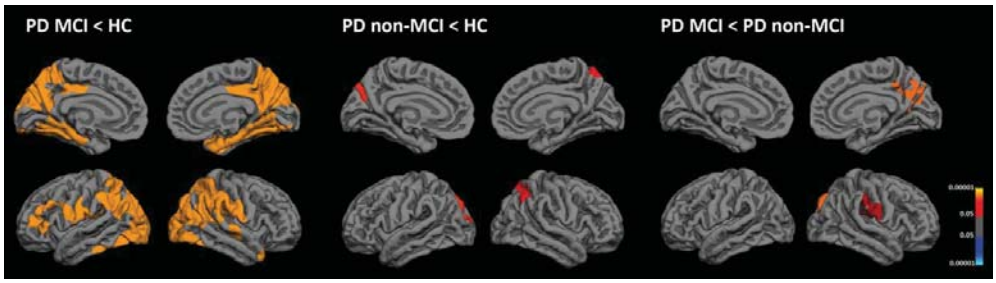

FIG. 1. Vertex-wise comparison of cortical thickness between healthy controls (HC), Parkinson's disease patients without mild cognitive impairment (PD non-MCI), and Parkinson's disease patients with mild cognitive impairment (PD MCI), after controlling for the effects of age and education. The scale bar shows *P* values.

Discussion

Patients with MCI showed a posterior pattern of atrophy, characterized by cortical thinning in the bilateral superior parietal and supramarginal regions and in the inferior temporal area, parahippocampal gyrus, fusiform gyrus, and precuneus. Cortical thinning was also observed in the left rostral frontal region. Moreover, PD MCI and PD non-MCI patients differed in right lateral parietal regions and precuneus.

Our results of cortical thickness reductions in the parietal, temporal and frontal regions could be related to previous positron emission tomography data[42] showing that PD-MCI patients exhibited reduced fluorodeoxyglucose (FDG) uptake in the parietal and occipital lobes and in localized areas of the frontal and temporal lobes compared with controls. In addition, longitudinal neuropsychological studies suggest that the dementia process is heralded by posterior-cortically-based cognitive deficits.[43,44] In sum, parieto-occipital changes seem to correspond to the deterioration that may eventually lead to dementia, possibly reflecting gradual loss of synaptic terminals, dendritic arborization, and size of neuronal cell bodies.

In our study, PD groups differed by degree of atrophy in right lateral parietal regions and the precuneus. This finding, together with the right asymmetry of atrophy detected in the PD non-MCI group compared with controls, suggested an asymmetric pattern of deterioration, initially involving parietal and temporal regions, and progressively widespread to bilateral atrophy. Asymmetric atrophy has been found in previous studies when PD patients were compared with controls.[28]

Recently, PD MCI patients have been studied using cortical thickness measures. However, no consensus has been reached in relation to cortical thickness differences between PD MCI and PD non-MCI; both increases and decreases have been reported in PD MCI, probably because of small sample sizes.[29-31] As

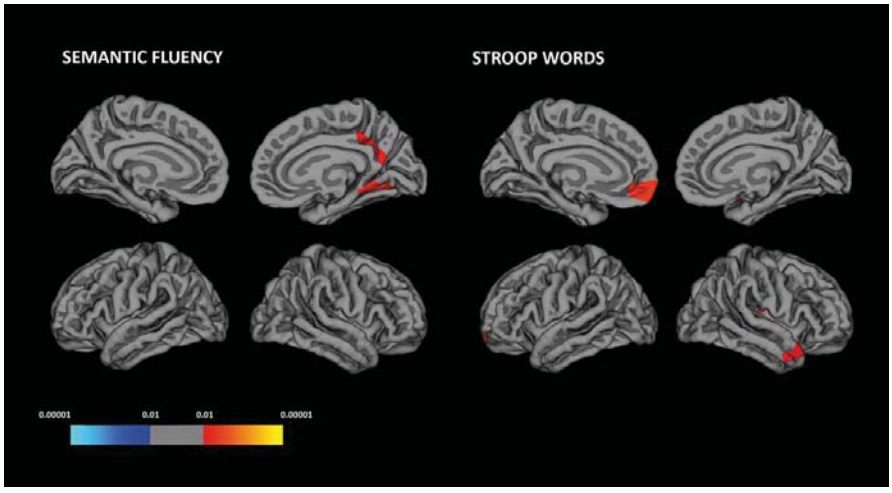

FIG. 2. Significant correlation between cortical thickness and neuropsychological tests, after controlling age, education, and sex effects. The scale bar shows *P* values.

expected, we observed thinning in PD MCI involving the supramarginal gyrus and the precuneus.

In addition to differences in regional cortical thickness, PD MCI patients had a reduction of global GM volume together with increased ventricular volume in comparison with PD non-MCI and healthy controls. These results, similar to those of previous studies,[46-48] confirm that cognitive deficits seen in PD MCI are related to structural brain changes, probably in combination with neurochemical changes.

The current study also aimed to establish whether specific neuropsychological tests used in clinical practice reflect the degree of regional atrophy in PD patients. Cognitive domains are defined under the assumption that they represent specific functions mediated by specific brain regions. The 'anterior' (frontal) pattern is putatively associated with executive functions, the 'posterior' (temporo-parietal) pattern with visuospatial and visuoperceptual functions, and hippocampal degeneration with the amnestic pattern.[49] Grouping different tests into a single function without knowing the specific correlates of each test may generate confusion. The study of neuroanatomical correlates of specific tests is the first step in the discussion of domains and in determining whether subtypes of mild cognitive impairment exist in PD, and consequently whether they are useful in predicting the evolution to dementia. In line with this statement, our results showed a common posterior atrophy pattern for all of the neuropsychological tests evaluated. Only the Stroop Test, SDMT, and phonemic fluency, classified by recent guidelines[10] as measures of attention and executive function, respectively, had an extended pattern including medial anterior regions. We did not observe any specific dorsolateral prefrontal or limbic pattern of correlations. Analyzing the global patterns of correlations, a group of tests including Stroop Test (Words, Colours, and Word-Colours), TMT A, semantic fluency, and RAVLT total learning correlated with extensive GM loss involving bilateral medial and lateral cortical regions, whereas VFD, JLO, and TMT B only correlated with medial temporal-parietal regions. Analyses of covariance only showed a positive correlation between semantic fluency and temporal-parietal regions and a positive correlation between Stroop words and left medial orbitofrontal, right superior temporal, and right insular regions. In sum, we did not find specific patterns of atrophy related to the neuropsychological domains, either with or without the use of covariates in the analyses.

Interestingly, semantic fluency performance remained significantly correlated with the precuneus after controlling for the effects of age, education, and sex. These results agree in part with current pathophysiological models that dissociate the substrates and prognostic values of different types of cognitive impairment in PD and show that tests with posterior cortical bases (semantic fluency and ability to draw an interlocking pentagon) reflecting probable nondopaminergic cortical Lewy body or Alzheimer's type pathology were associated with dementia, whereas frontostriatal executive deficits were not.[44] Our results indicate that semantic fluency is an easily administered test that should be included in the neuropsychological assessment of PD patients.

The consecutive recruitment of PD patients from an outpatient movement disorders clinic involves certain differences in clinical and demographical variables between PD groups. In this regard, disease duration was longer in PD MCI than in PD non-MCI patients. In our study, additional analyses including disease duration as a nuisance variable in the co-varied models did not show significant results. A previous study has shown that neurodegeneration is likely to occur faster in PD patients with MCI.[31] Cortical degeneration was more advanced in patients who have PD MCI than in those without at the same stage of disease. In accordance with previous longitudinal studies,[43-45] disease duration is correlated with PD patients' deterioration, including cognitive impairment and brain atrophy. In this sense, controlling for the effects of disease duration could represent an overcorrection, masking actual intergroup effects.

One possible limitation of our study is that, despite the inclusion of a variety of tests in the main cognitive domains defined in recent guidelines (attention and working memory, executive functions, memory, and visuospatial and visuoperceptive functions),[8] we did not include the same number of tests in each cognitive domain, and language was assessed only with the Boston Naming Test. This limitation may have raised the possibility of false-negative cases in the PD non-MCI group but would not have affected the classification of subjects currently included in PD MCI group.

In sum, degeneration was characterized by a posterior pattern of atrophy mostly involving posterior parietal-temporal areas, which extended to frontal regions in the PD MCI group compared with healthy controls. All of the neuroanatomical correlates associated with neuropsychological tests involve this posterior pattern of atrophy, semantic fluency being the neuropsychological test with the most significant association. Our findings therefore suggest the presence of posterior structural degenerative brain changes in PD MCI patients, evidencing a structural neuroimaging marker of this pathological condition and its possible evolution to dementia. ■

Acknowledgment: Without the support of the patients, their families, and control subjects, this work would have not been possible.

References

1. Foltynie T, Brayne CEG, Robbins TW, Barker RA. The cognitive ability of an incident cohort of Parkinson's patients in the UK: the CamPaIGN study. Brain 2004;127:550-560.
2. Muslimovic D, Post B, Speelman JD, Schmand B. Cognitive profile of patients with newly diagnosed Parkinson disease. Neurology 2005;65:1239-1245.
3. Aarsland D, Brønnick K, Larsen JP, Tysnes OB, Alves G. Cognitive impairment in incident, untreated Parkinson disease: the Norwegian ParkWest study. Neurology 2009;72:1121-1126.
4. Elgh E, Domellöf M, Linder J, Edström M, Stenlund H, Forsgren L. Cognitive function in early Parkinson's disease: a population-based study. Eur J Neurol 2009;16:1278-1284.
5. Aarsland D, Andersen K, Larsen JP, Lolk A, Nielsen H, Kragh-Sørensen P. Risk of dementia in Parkinson's disease: a community-based, prospective study. Neurology 2001;56:730-736.
6. Janvin CC, Larsen JP, Aarsland D, Hugdahl K. Subtypes of mild cognitive impairment in Parkinson's disease: progression to dementia. Mov Disord 2006;21:1343-1349.
7. Pedersen KF, Larsen JP, Tysnes O-B, Alves G. Prognosis of mild cognitive impairment in early Parkinson disease: the Norwegian ParkWest study. JAMA Neurol 2013;70:580-586.
8. Litvan I, Aarsland D, Adler CH, et al. MDS Task Force on mild cognitive impairment in Parkinson's disease: critical review of PD-MCI. Mov Disord 2011;26:1814-1824.
9. Broeders M, Velseboer DC, de Bie R, et al. Cognitive change in newly-diagnosed patients with Parkinson's disease: a 5-year follow-up study. J Int Neuropsychol Soc 2013;19:695-708.
10. Caviness JN, Driver-Dunckley E, Connor DJ, et al. Defining mild cognitive impairment in Parkinson's disease. Mov Disord 2007;22:1272-1277.
11. Litvan I, Goldman JG, Tröster AI, et al. Diagnostic criteria for mild cognitive impairment in Parkinson's disease: Movement Disorder Society Task Force guidelines. Mov Disord 2012;27:349-356.
12. Riekkinen P, Kejonen K, Laakso MP, Soininen H, Partanen K, Riekkinen M. Hippocampal atrophy is related to impaired memory, but not frontal functions in non-demented Parkinson's disease patients. Neuroreport 1998;9:1507-1511.
13. Brück A, Kurki T, Kaasinen V, Vahlberg T, Rinne JO. Hippocampal and prefrontal atrophy in patients with early non-demented Parkinson's disease is related to cognitive impairment. J Neurol Neurosurg Psychiatry 2004;75:1467-1469.
14. Tam CWC, Burton EJ, McKeith IG, Burn DJ, O'Brien JT. Temporal lobe atrophy on MRI in Parkinson disease with dementia: a comparison with Alzheimer disease and dementia with Lewy bodies. Neurology 2005;64:861-865.
15. Camicioli R, Moore MM, Kinney A, Corbridge E, Glassberg K, Kaye JA. Parkinson's disease is associated with hippocampal atrophy. Mov Disord 2003;18:784-790.
16. Ibarretxe-Bilbao N, Ramírez-Ruiz B, Tolosa E, et al. Hippocampal head atrophy predominance in Parkinson's disease with hallucinations and with dementia. J Neurol 2008;255:1324-1331.
17. Junqué C, Ramírez-Ruiz B, Tolosa E, et al. Amygdalar and hippocampal MRI volumetric reductions in Parkinson's disease with dementia. Mov Disord 2005;20:540-544.
18. Pereira JB, Junqué C, Bartrés-Faz D, Ramírez-Ruiz B, Marti M-J, Tolosa E. Regional vulnerability of hippocampal subfields and memory deficits in Parkinson's disease. Hippocampus 2013;23:720-728.
19. Pereira JB, Junqué C, Martí MJ, Ramirez-Ruiz B, Bartrés-Faz D, Tolosa E. Structural brain correlates of verbal fluency in Parkinson's disease. Neuroreport 2009;20:741-744.
20. Pereira JB, Junqué C, Martí M-J, Ramirez-Ruiz B, Bargalló N, Tolosa E. Neuroanatomical substrate of visuospatial and visuoperceptual impairment in Parkinson's disease. Mov Disord 2009;24:1193-1199.
21. Ibarretxe-Bilbao N, Junque C, Tolosa E, et al. Neuroanatomical correlates of impaired decision-making and facial emotion recognition in early Parkinson's disease. Eur J Neurosci 2009;30:1162-1171.
22. Baggio HC, Segura B, Ibarretxe-Bilbao N, et al. Structural correlates of facial emotion recognition deficits in Parkinson's disease patients. Neuropsychologia 2012;50:2121-2128.
23. Filoteo JV, Reed JD, Litvan I, Harrington DL. Volumetric correlates of cognitive functioning in nondemented patients with Parkinson's disease. Mov Disord 2013; doi: 10.1002/mds.25633.
24. Beyer MK, Janvin CC, Larsen JP, Aarsland D. A magnetic resonance imaging study of patients with Parkinson's disease with mild cognitive impairment and dementia using voxel-based morphometry. J Neurol Neurosurg Psychiatry 2007;78:254-259.
25. Song SK, Lee JE, Park H-J, Sohn YH, Lee JD, Lee PH. The pattern of cortical atrophy in patients with Parkinson's disease according to cognitive status. Mov Disord 2011;26:289-296.
26. Yarnall AJ, Breen DP, Duncan GW et al. Characterizing mild cognitive impairment in incident Parkinson disease: The ICICLE-PD Study. Neurology 2014;82:308-316.
27. Pereira JB, Ibarretxe-Bilbao N, Marti M-J, et al. Assessment of cortical degeneration in patients with Parkinson's disease by voxel-based morphometry, cortical folding, and cortical thickness. Hum Brain Mapp 2012;33:2521-2534.
28. Biundo R, Calabrese M, Weis L et al. Anatomical correlates of cognitive functions in early Parkinson's disease patients. PLoS One 2013;8:e64222.
29. Pagonabarraga J, Corcuera-Solano I, Vives-Gilabert Y et al. Pattern of regional cortical thinning associated with cognitive deterioration in Parkinson's disease. PLoS One 2013;8:e54980.
30. Hanganu A, Bedetti C, Jubault T, et al. Mild cognitive impairment in patients with Parkinson's disease is associated with increased cortical degeneration. Mov Disord 2013;28:1360-1369.
31. Pereira JB, Svenningsson P, Weintraub D, Brønnick K, Lebedev A, Westman E, Aarsland D. Initial cognitive decline is associated with cortical thinning in early Parkinson disease. Neurology 2014;82:2017-2025.
32. Dubois B, Burn D, Goetz C, et al. Diagnostic procedures for Parkinson's disease dementia: recommendations from the movement disorder society task force. Mov Disord 2007;22:2314-2324.
33. Daniel SE, Lees AJ. Parkinson's Disease Society Brain Bank, London: overview and research. J Neural Transm Suppl 1993;39:165-172.
34. Sled JG, Zijdenbos AP, Evans AC. A nonparametric method for automatic correction of intensity nonuniformity in MRI data. IEEE Trans Med Imaging 1998;17:87-97.
35. Fischl B, Liu A, Dale AM. Automated manifold surgery: constructing geometrically accurate and topologically correct models of the human cerebral cortex. IEEE Trans Med Imaging 2001;J20:70-80.
36. Ségonne F, Pacheco J, Fischl B. Geometrically accurate topology-correction of cortical surfaces using nonseparating loops. IEEE Trans Med Imaging 2007;26:518-529.
37. Dale AM, Fischl B, Sereno MI. Cortical surface-based analysis. I. Segmentation and surface reconstruction. Neuroimage 1999;9:179-194.
38. Dale AM, Sereno MI. Improved localizadon of cortical activity by combining EEG and MEG with MRI cortical surface reconstruction: a linear approach. J Cogn Neurosci 1993;5:162-176.
39. Fischl B, Dale AM. Measuring the thickness of the human cerebral cortex from magnetic resonance images. Proc Natl Acad Sci U S A 2000;97:11050-11055.
40. Fischl B, Salat DH, Busa E, et al. Whole brain segmentation: automated labeling of neuroanatomical structures in the human brain. Neuron 2002;33:341-355.
41. Garcia-Garcia D, Clavero P, Gasca Salas C, et al. Posterior parietooccipital hypometabolism may differentiate mild cognitive impairment from dementia in Parkinson's disease. Eur J Nucl Med Mol Imaging 2012;39:1767-1777.
42. Williams-Gray CH, Foltynie T, Brayne CEG, Robbins TW, Barker RA. Evolution of cognitive dysfunction in an incident Parkinson's disease cohort. Brain 2007;130:1787-1798.
43. Williams-Gray CH, Evans JR, Goris A, et al. The distinct cognitive syndromes of Parkinson's disease: 5 year follow-up of the CamPaIGN cohort. Brain 2009;132:2958-2969.
44. Ibarretxe-Bilbao N, Junque C, Segura B, Baggio HC, Marti MJ, Valldeoriola F, Bargallo N, Tolosa E. Progression of cortical thinning in early Parkinson's disease. Mov Disord 2012;27:1746-1753.

45. Dalaker TO, Zivadinov R, Ramasamy DP, et al. Ventricular enlargement and mild cognitive impairment in early Parkinson's disease. Mov Disord 2011;26:297-301.

46. Apostolova L, Alves G, Hwang KS, et al. Hippocampal and ventricular changes in Parkinson's disease mild cognitive impairment. Neurobiol Aging 2012;33:2113-2124.

47. Weintraub D, Doshi J, Koka D, et al. Neurodegeneration across stages of cognitive decline in Parkinson disease. Arch Neurol 2011; 68:1562-1568.

48. Lezak MD. *Neuropsychological Assessment*. Oxford: Oxford University Press; 2012.

Supporting Data

Additional Supporting Information may be found in the online version of this article at the publisher's web-site.

SUPPLEMENTARY MATERIALS

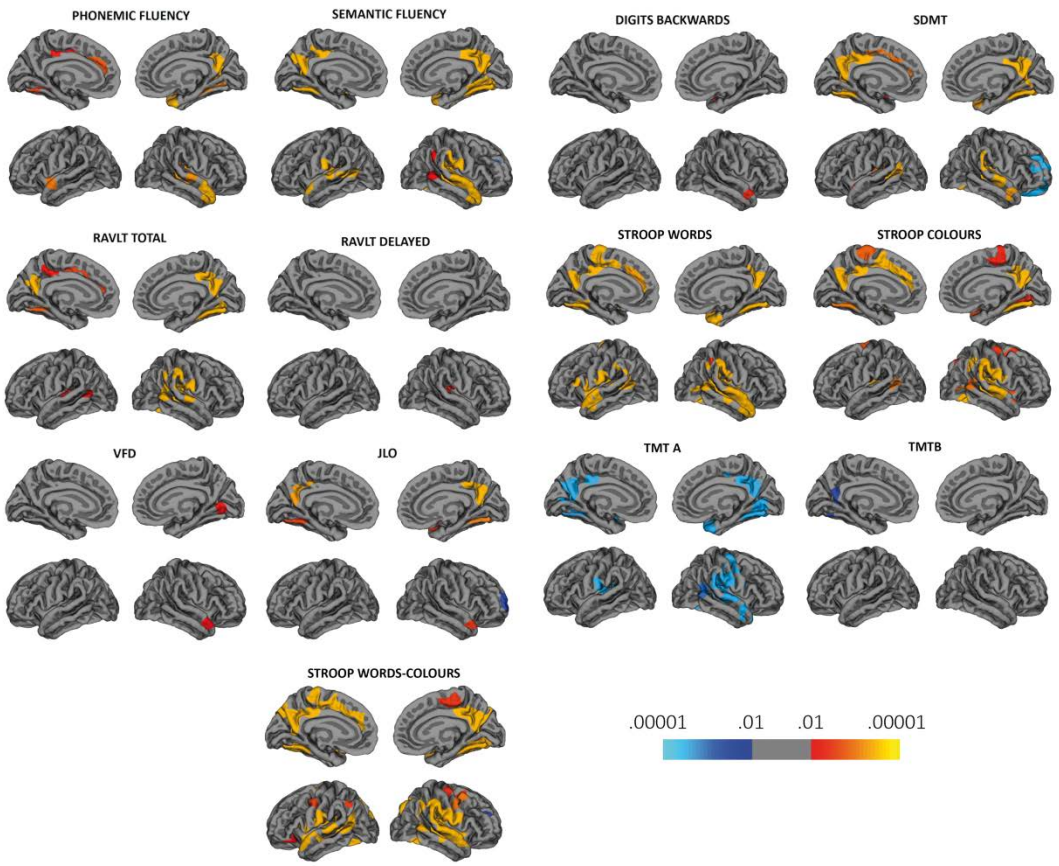

Supplementary figure 1. Significant correlation between cortical thickness and neuropsychological tests. The color bar shows *p* values.

Cortical region	Size (mm2)	MNI coordinates (x y z)*	z-Max	Corrected cluster *p*-value
HC > PD-NMCI				
RH Superior Parietal	2219.34	27.1 -60.5 45.0	4.001	.0020
LH Superior Parietal	2398.29	-19.8 -72.2 38.0	2.972	.0013
HC > PD-MCI				
RH Superior Parietal	27428.22	27.4 -60.0 45.8	5.660	.0010
LH Lateral Occipital	24385.79	-24.9 -94.8 14.1	5.740	.0001
PD-NMCI > PD-MCI				
RH Supramarginal	1580.07	53.1 -26.5 37.9	3.291	.0260
Precuneus	2764.79	8.0 -66.8 29.8	2.764	.0003

Supplementary Material Table 1. Cortical thickness for healthy controls and Parkinson's disease patients according to MCI status, after controlling for the effect of age and education. * MNI305 space. Results were obtained using Monte Carlo simulation with 10000 iterations applied to cortical thickness maps to provide clusterwise correction for multiple comparisons. Significant clusters were reported at $p<0.05$. z-Max indicates the maximum $-\log_{10}(p\text{-value})$ in the cluster.

	Cortical region	Coordinates (x y z)*	Size (mm^2)	z-Max	Corrected cluster *p*-value
Stroop Words	R Superior frontal	-13.9 41.4 13.5	1016.84	5.728	0.0002
	R Fusiform	-30.5 -63.9 -5.9	1430.51	5.327	0.0001
	R Insula	-34.4 -15.3 17.9	5406.54	4.868	0.0001
	R Banksts	-55.3 -48.9 4.2	1556.88	4.708	0.0001
	R Posterior cingulate	-5.7 -26.9 36.9	2820.44	3.966	0.0001
	L Insula	35.9 -10.4 18.6	7124.40	6.664	0.0001
	L Fusiform	32.0 -75.0 -4.1	1783.32	5.145	0.0001
	L Supramarginal	57.2 -23.8 37.7	2178.13	5.142	0.0001
	L Precuneus	5.7 -63.8 32.0	1200.89	4.216	0.0001
	L Superiorparietal	33.6 -35.3 36.2	688.49	3.258	0.0078
Stroop Colors	L Insula	-31.2 -23.8 15.3	1810.45	6.218	0.0001
	L Posterior cingulate	-5.5 -31.0 34.9	1741.69	5.662	0.0001
	L Superior frontal	-9.7 4.1 45.0	2140.27	5.101	0.0001
	L Fusiform	-30.5 -65.8 -4.3	974.31	4.982	0.0005
	L Inferior parietal	-48.3 -61.2 12.5	964.95	4.812	0.0006
	L Precentral	-13.8 -10.8 60.1	819.32	3.933	0.0017
	R Insula	32.6 -20.3 16.5	5343.71	7.405	0.0001
	R fusiform	32.1 -72.9 -5.6	1797.47	6.397	0.0001
	R Precuneus	5.7 -63.0 30.0	1820.89	4.630	0.0001
	R middle temporal	53.4 -56.3 8.0	868.00	4.431	0.0008
	R superior temporal	42.5 4.9 -21.6	806.48	4.252	0.0025
	R superior frontal	20.6 12.5 51.3	691.36	4.126	0.0075
	R supramarginal	34.0 -35.0 36.2	1343.18	3.864	0.0001
	R Paracentral	6.3 -22.9 51.0	603.83	3.774	0.0165
	R lingual	22.2 -50.2 -3.5	689.39	3.417	0.0077
	R superior parietal	26.3 -67.9 26.2	491.82	3.107	0.0406
Stroop Words and Colors	L fusiform	-34.3 -44.1 -8.9	2038.27	7.546	0.0001
	L insula	-34.6 -13.7 17.8	6865.11	7.153	0.0001
	L precuneus	-12.2 -54.2 12.3	3555.51	5.765	0.0001
	L superiorfrontal	-9.8 4.7 43.4	2574.41	5.309	0.0001
	L precentral	-50.8 -0.5 37.7	705.52	4.235	0.0049
	L supramarginal	-46.3 -37.1 40.7	678.20	3.663	0.0074
	R superiortemporal	44.2 1.1 -19.2	9480.53	7.191	0.0001
	R fusiform	28.1 -44.5 -11.4	3165.48	6.054	0.0001
	R precuneus	4.7 -55.0 18.6	3700.90	5.696	0.0001
	R paracentral	6.1 -21.9 50.2	682.05	5.126	0.0082
	R precentral	54.3 1.2 36.3	870.57	4.095	0.0008
	R superiorfrontal	22.7 1.8 43.4	643.42	3.817	0.0116
TMT A	L superiortemporal	-45.9 -37.3 12.4	2596.58	-5.034	0.0001
	L posteriorcingulate	-5.2 -30.0 34.7	2812.62	-4.652	0.0001
	L inferiorparietal	-47.6 -61.2 12.3	501.20	-4.567	0.0330
	L fusiform	-34.3 -44.1 -8.9	1030.37	-4.067	0.0002
	R superiortemporal	39.8 5.2 -23.1	5966.78	-6.499	0.0001
	R lingual	7.2 -66.7 5.0	2678.34	-5.452	0.0001
	R middletemporal	54.1 -54.4 10.3	894.92	-4.879	0.0006
	R precuneus	8.0 -51.5 20.9	1454.84	-3.957	0.0001
	R precentral	39.0 -11.0 55.1	1442.20	-3.345	0.0001
TMT B	R precuneus	-5.3 -55.8 20.0	635.93	-3.845	0.0099
	R fusiform	-30.4 -66.1 -6.1	591.22	-3.541	0.0145
SDMT	L precuneus	-5.3 -58.2 17.3	2789.11	6.323	0.0001
	L fusiform	-35.4 -42.4 -8.7	1382.66	5.407	0.0001
	L superiortemporal	-45.1 -37.6 12.8	944.63	5.318	0.0006
	L inferiorparietal	-48.2 -61.5 11.7	1515.09	3.858	0.0001
	L superiortemporal	-47.7 -17.5 -0.5	580.28	3.378	0.0164
	L superiorfrontal	-13.4 19.3 30.2	938.31	3.207	0.0006
	R rostralmiddlefrontal	23.8 41.2 17.8	3095.34	-5.933	0.0001

	R precuneus	8.1 -50.1 20.3	2054.89	5.896	0.0001
	R supramarginal	50.0 -34.7 17.7	2941.42	5.577	0.0001
	R fusiform	29.1 -52.5 -8.5	1631.70	5.347	0.0001
	R superiortemporal	42.6 7.0 -22.2	1025.13	4.787	0.0002
Digits Backwards	R superiortemporal	51.5 7.4 -16.4	679.70	3.256	0.0117
Semantic Fluency	L posteriorcingulate	-5.6 -27.9 37.5	2460.93	5.147	0.0001
	L fusiform	-34.3 -43.0 -10.0	1153.99	5.021	0.0001
	L insula	-31.7 -28.4 13.2	3103.69	4.589	0.0001
	L bankssts	-53.0 -39.4 7.2	1246.19	4.373	0.0001
	R lingual	22.3 -46.4 -4.6	2858.65	6.853	0.0001
	R precuneus	4.6 -55.2 19.8	2581.56	6.552	0.0001
	R superiortemporal	59.6 -6.2 0.1	6365.59	5.248	0.0001
	R rostralmiddlefrontal	25.4 39.8 16.7	862.24	-4.000	0.0011
Phonemic Fluency	L superiorfrontal	-13.1 42.5 14.2	817.27	5.176	0.0019
	L superiortemporal	-51.4 -2.9 -6.6	911.90	4.527	0.0007
	L fusiform	-30.6 -65.2 -5.0	729.44	4.023	0.0041
	R superiortemporal	44.0 1.1 -19.4	2135.47	6.585	0.0001
	R precuneus	23.0 -55.9 19.9	1612.36	5.257	0.0001
	R postcentral	37.7 -6.1 16.7	1074.58	5.004	0.0003
	R superiortemporal	60.2 -18.3 -0.0	1108.06	4.228	0.0003
	R lingual	25.3 -59.4 -1.6	972.18	3.573	0.0004
RAVLT TOTAL	L fusiform	-29.9 -64.5 -2.1	823.29	5.415	0.0015
	L inferiorparietal	-48.0 -61.4 10.4	566.60	4.858	0.0188
	L precuneus	-5.9 -56.8 23.9	1469.20	3.738	0.0001
	L precuneus	-8.9 -41.5 45.7	522.68	3.434	0.02830
	L caudalanteriorcingulate	-11.3 31.8 16.4	718.86	3.376	0.00470
	L fusiform	-29.9 -64.5 -2.1	823.29	5.415	0.00150
	R middletemporal	53.5 -57.2 7.4	5191.17	5.423	0.00010
	R fusiform	31.4 -39.6 -13.5	2238.94	5.073	0.00010
	R precuneus	5.5 -53.5 18.9	1680.13	5.014	0.00010
RAVLT delayed	L insula	32.3 -26.5 13.8	651.27	4.228	0.01450
JLO	L precuneu	-4.4 -58.6 19.5	1019.66	4.380	0.00020
	L fusiform	-28.9 -71.7 -4.2	714.35	3.710	0.00480
	R precuneus	6.6 -56.7 36.4	1486.99	5.447	0.00010
	R fusiform	28.4 -69.9 -3.4	944.91	5.112	0.00050
	R superiortemporal	41.2 1.9 -20.7	743.64	5.054	0.00680
	R rostralmiddlefrontal	18.9 58.6 8.5	764.63	-3.801	0.00590
VFD	R superiortemporal	51.1 8.9 -16.1	523.83	5.831	0.03930
	R lingual	7.4 -67.1 4.4	571.40	4.951	0.02570

Supplementary Material Table 2. Cortical areas showing significant correlation between cortical thickness and neuropsychological tests, within PD patients group. JLO: Judgment Line Orientation; RAVLT: Rey Auditory Verbal Learning Test; TMT: Trail Making Test; VFD: Visual Form Discrimination; L= Left hemisphere; R= Right hemisphere. Results were obtained using Monte Carlo simulation with 10,000 iterations applied to CTh maps to provide clusterwise correction for multiple comparisons 2.3. Significant clusters were reported at $p<0.05$. * MNI305 space. z-Max indicates the maximum $-\log_{10}$(pvalue) in the cluster.

Cortical region	Coordinates (x y z)*	Size (mm²)	z-Max	Corrected cluster *p*-value
Semantic Fluency				
R Lingual	20.3 -45.9 -5.4	657.55	6.051	0.0098
R Precuneus	13.3 -42.5 37.2	494.59	2.753	0.0398
Stroop P				
L medialorbitofrontal	-6.4 55.6 -12.1	651.88	3.686	0.0088
L superiortemporal	44.2 4.5 -20.4	533.79	3.092	0.0266
L insula	33.0 10.1 11.1	634.09	4.132	0.0121

Supplementary Material Table 3. Cortical areas showing significant correlation between cortical thickness and neuropsychological tests after controlling for the effects of age, education and gender, within PD patients group. Results were obtained using Monte Carlo simulation with 10,000 iterations applied to CTh maps to provide clusterwise correction for multiple comparisons 2.3. Significant clusters were reported at p<0.05. * MNI305 space. z-Max indicates the maximum -$\log_{10}$(p value) in the cluster.

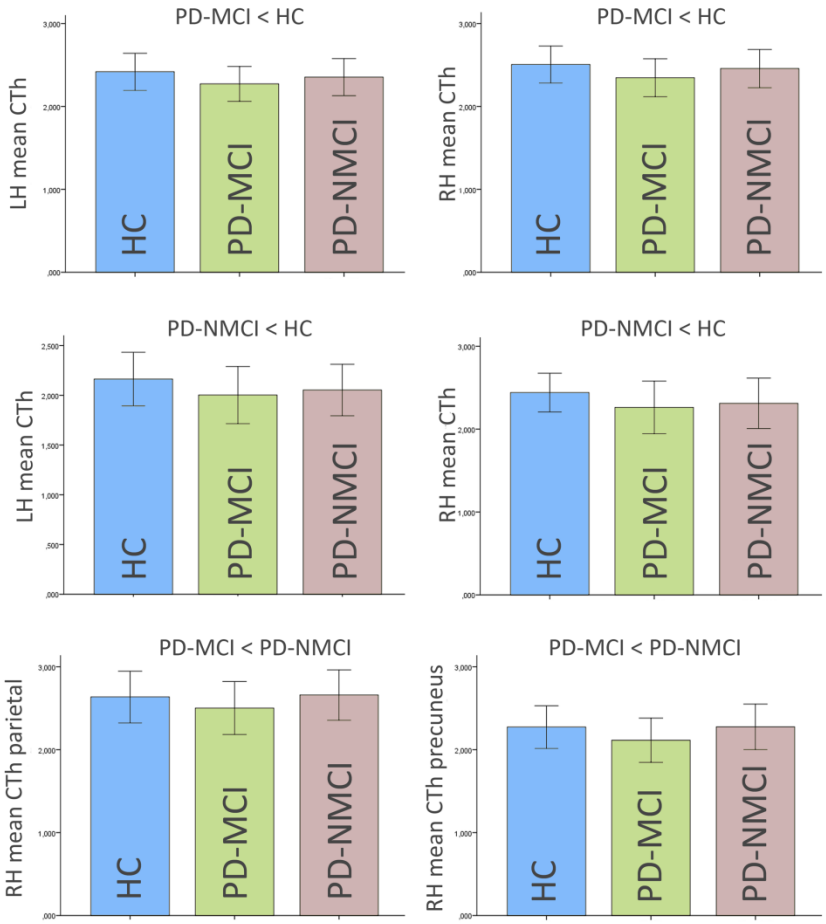

Supplementary figure 2. Mean cortical thickness of significant clusters from vertex-wise comparison between healthy controls (HC), Parkinson's disease patients without mild cognitive impairment (PD-NMCI) and Parkinson's disease patient with mild cognitive impairment (PD-MCI), after controlling for the effect of age and education.

study 4

STRUCTURAL CORRELATES OF FACIAL EMOTION RECOGNITION DEFICITS IN PARKINSON'S DISEASE PATIENTS

Neuropsychologia 2012

Hugo César Baggio, Bàrbara Segura, Naroa Ibarretxe Bilbao, Francesc Valldeoriola, Maria José Martí, Yaroslau Compta, Eduardo Tolosa, Carme Junqué

Neuropsychologia 50 (2012) 2121–2128

Contents lists available at SciVerse ScienceDirect

Neuropsychologia

journal homepage: www.elsevier.com/locate/neuropsychologia

Structural correlates of facial emotion recognition deficits in Parkinson's disease patients

H.C. Baggio [a], B. Segura [a], N. Ibarretxe-Bilbao [a,e], F. Valldeoriola [b,c,d], M.J. Marti [b,c,d], Y. Compta [b,c,d], E. Tolosa [b,c,d], C. Junqué [a,b,c,*]

[a] Department of Psychiatry and Clinical Psychobiology, University of Barcelona, Spain
[b] Servicio de Neurología, Centro de Investigación en Red de Enfermedades Neurodegenerativas (CIBERNED), Hospital Clínic, Universidad de Barcelona, Spain
[c] Institute of Biomedical Research August Pi i Sunyer (IDIBAPS), Barcelona, Spain
[d] Movement Disorders Unit, Neurology Service, Institut Clínic de Neurociències (ICN), Hospital Clínic de Barcelona, Spain
[e] Department of Methods and Experimental Psychology, Faculty of Psychology and Education, University of Deusto

ARTICLE INFO

Article history:
Received 19 October 2011
Received in revised form
16 May 2012
Accepted 20 May 2012
Available online 26 May 2012

Keywords:
Emotion recognition
Parkinson's disease
Magnetic resonance imaging
Voxel-based morphometry
Diffusion tensor imaging

ABSTRACT

The ability to recognize facial emotion expressions, especially negative ones, is described to be impaired in Parkinson's disease (PD) patients. Previous neuroimaging work evaluating the neural substrate of facial emotion recognition (FER) in healthy and pathological subjects has mostly focused on functional changes. This study was designed to evaluate gray matter (GM) and white matter (WM) correlates of FER in a large sample of PD. Thirty-nine PD patients and 23 healthy controls (HC) were tested with the Ekman 60 test for FER and with magnetic resonance imaging. Effects of associated depressive symptoms were taken into account. In accordance with previous studies, PD patients performed significantly worse in recognizing sadness, anger and disgust. In PD patients, voxel-based morphometry analysis revealed areas of positive correlation between individual emotion recognition and GM volume: in the right orbitofrontal cortex, amygdala and postcentral gyrus and sadness identification; in the right occipital fusiform gyrus, ventral striatum and subgenual cortex and anger identification, and in the anterior cingulate cortex (ACC) and disgust identification. WM analysis through diffusion tensor imaging revealed significant positive correlations between fractional anisotropy levels in the frontal portion of the right inferior fronto-occipital fasciculus and the performance in the identification of sadness. These findings shed light on the structural neural bases of the deficits presented by PD patients in this skill.

1. Introduction

Parkinson's disease (PD) is more typically characterized by its motor features. In recent years, however, the interest in its non-motor manifestations has increased significantly. Among these manifestations, cognitive deficits are commonly found even in recently diagnosed PD patients. Memory and executive function are the most prominently, but not the only, affected domains (Muslimovic, Post, Speelman & Schmand, 2005). The capacity to accurately identify emotions in others' facial expressions, a skill of great importance for normal social interaction, has been described in several studies to be impaired in PD (Yip, Lee, Ho, Tsang & Li, 2003; Dujardin et al., 2004; Kan, Kawamura, Hasegawa, Mochizuki & Nakamura, 2002; Ariatti, Benuzzi & Nichelli, 2008; Sprengelmeyer et al., 2003; Lawrence, Goerendt & Brooks, 2007; Suzuki, Hoshino, Shigemasu & Kawamura, 2006), though somewhat inconsistently. While most of these studies suggest a selective deficit in identifying negative emotions, results vary as to which specific emotions have their identification selectively or predominantly affected. Still other studies failed to identify any facial emotion recognition impairments in PD patients (Pell & Leonard, 2005; Dujardin et al., 2004; Biseul et al., 2005). These different results might be due to different evaluation methods, as well as to different patient samples with respect to relevant variables such as age, education, medication status, cognitive impairment and disease severity or duration. Furthermore, not all studies have taken into account the presence of associated depressive disorders, present in up to 50% of PD patients (Reijnders, Ehrt, Weber, Aarsland & Leentjens, 2008; Slaughter, Slaughter, Nichols, Holmes & Martens, 2001), which also lead to facial emotion recognition (FER) deficits (Leppanen, 2006).

The finding that pathological processes such as PD, depression or Huntington's disease (Calder et al., 2010) may cause deficits in

* Corresponding author. Departament de Psiquiatria i Psicobiologia Clínica. Universitat de Barcelona, Casanova 143, Barcelona (08036), Spain. Tel.: +34 93 402 45 70; fax: +34 93 403 52 94.
E-mail address: cjunque@ub.edu (C. Junqué).

0028-3932/$ - see front matter © 2012 Elsevier Ltd. All rights reserved.
http://dx.doi.org/10.1016/j.neuropsychologia.2012.05.020

the identification of specific emotions, as well as data obtained from functional neuroimaging and electrophysiological studies and studies with patients with focal lesions indicate that the recognition of different emotions relies on different (Adolphs, Tranel & Damasio, 2003; Fusar-Poli et al., 2009; Calder, Keane, Manes, Antoun & Young, 2000; Krolak-Salmon et al., 2003; Adolphs, 2002; Adolphs, Tranel, Damasio & Damasio, 1994; Calder et al., 1996; Phillips et al., 1997) though overlapping neural substrates (Heberlein, Padon, Gillihan, Farah & Fellows, 2008; Hornak et al., 2003; Adolphs, Damasio, Tranel, Cooper & Damasio, 2000).

Most published neuroimaging studies concerning the neural substrate of emotional processing used functional techniques. Knowledge about the ability of MRI to identify structural correlates for individual emotion recognition is very limited, both in pathological and in healthy subjects samples. In the specific case of PD patients, only one published work addressed structural correlates of FER deficits. In this study, done by our group, gray matter (GM) volumes in the amygdalae and orbitofrontal cortex (OFC) were found to correlate positively with overall emotion recognition (Ibarretxe-Bilbao et al., 2009). The neural substrate of the recognition of individual emotions, however, was not studied.

Besides the better-studied GM changes in PD, there is increasing evidence that white matter (WM) microstructural changes detectable by magnetic resonance diffusion tensor imaging techniques occur early in the course of the disease (Gattellaro et al., 2009; Karagulle Kendi, Lehericy, Luciana, Ugurbil & Tuite, 2008) and that WM changes may contribute to cognitive deficits by means of impaired connectivity (Vernooij et al., 2009). There is little knowledge, however, about how such changes may relate to facial emotion recognition deficits.

Our aim in the present work was to study the relationship between the capacity to recognize specific emotions in facial expressions and gray and white matter structural parameters evaluated through state-of-the-art MRI techniques in a large sample of non-demented PD patients.

2. Methods

2.1. Subjects

Thirty-nine PD patients and 23 age-matched healthy controls (HC) were included. Patients were recruited from the Movement Disorders Unit, Neurology Department, Hospital Clínic, in Barcelona. The inclusion criterion was the fulfillment of the UK PD Society Brain Bank (PDSBB) diagnostic criteria for PD (Daniel & Lees, 1993). The exclusion criteria were: (i) presence of dementia according to the Movement Disorders Society criteria (Emre et al., 2007), (ii) presence of Beck Depression Inventory-II scores higher than 16, suggested as a specific cut-off point for diagnosing depression in PD patients by Leentjens, Verhey, Luijckx and Troost (2000), (iii) presence of other significant psychiatric or neurological comorbidity, (iv) pathological magnetic resonance imaging findings other than mild WM hyperintensities in long-TR sequences or those that could be related to PD.

All PD patients were taking antiparkinsonian drugs, consisting of different combinations of L-dopa ($n=11$), L-dopa with COMT inhibitors ($n=12$), MAO inhibitors ($n=10$), dopamine agonists ($n=17$) and amantadine ($n=4$). The medication was not changed for the study and all assessments were done while patients were in the on state. To evaluate possible medication effects, levodopa equivalent daily doses were calculated as suggested by Tomlinson et al. (2010).

The study was approved by the ethics committee of the University of Barcelona, and all subjects provided written informed consent to participate.

2.2. Neuropsychological assessment

All subjects underwent a thorough neuropsychological battery to assess the cognitive functions more frequently impaired in non-demented PD patients: memory, visuospatial, visuoperceptive and executive functions (Muslimovic et al., 2005; Foltynie, Brayne, Robbins & Barker, 2004; Aarsland et al., 2009). In addition to the Mini-Mental State Examination (MMSE), we administered the following tests: Rey Auditory Verbal Learning Test, Digits subset of the Wechsler Adults Intelligence Scale (WAIS-III), Stroop Color–Word Test, phonemic and semantic fluencies, Trail Making Tests A and B, Benton's Visual Form Discrimination Test and Judgment of Line Orientation Test, and Visual Object and Space Perception Battery (Lezak, Howieson, & Loring, 2004). We also administered the Cumming's Neuropsychiatric Inventory (Cummings et al., 1994) and the Beck Depression Inventory-II (Beck, Steer & Brown, 1996) to identify neuropsychiatric symptoms associated with PD.

2.3. Facial emotion recognition assessment

All subjects were tested with the Ekman 60 test for recognition of emotions in facial expressions. In this test, 60 pictures of faces from the Ekman and Friesen series of Pictures of Facial Affect (Ekman & Friesen, 1976) are presented consecutively. The subject is required to the label each picture as to the emotion predominantly expressed in it from a list of six possible choices (anger, fear, sadness, disgust, happiness and surprise, translated to Spanish as enfado, miedo, tristeza, asco, alegría y sorpresa, respectively). Each photograph is shown on a computer screen for 5 s, but there is no time limit to make the choice.

Each of the six individual emotions is represented in ten out of the total sixty pictures. Results are presented in number of correct answers out of 10 for each emotion and in total correct answers out of 60 for total Ekman scores.

2.4. Statistical analysis

Analyses were carried out using the PASW Version 17.0.2 (SPSS, Inc., Chicago, IL, USA). Group differences in demographic, clinical and neuropsychological characteristics were analyzed with independent two-tailed Student's t-tests for normally-distributed variables, the Mann–Whitney U test for non-normally distributed ones, and the chi-squared test for categorical variables. To control for possible effects of associated depressive symptoms and cognitive decline when measuring differences between Ekman test results between groups, BDI and MMSE scores were entered as covariates in two-level analyses of covariance (ANCOVAs). Associations between demographic, clinical and cognitive variables and FER scores were analyzed using Pearson's correlation for normally distributed variables and Spearman's rank correlations for those that did not present a normal distribution. Statistical significance threshold was set at $p<0.05$.

2.5. Image acquisition and analysis

Magnetic resonance images were acquired with a 3T scanner (TIM Trio, Siemens, Germany). High-resolution 3-dimensional T1-weighted images were acquired in the sagittal plane (TR 2300 ms, TE 2.98 ms, TI 900 ms; 256×256 matrix, 1 mm isotropic voxel). Sagittal diffusion tensor images were obtained using a single-shot EPI sequence (TR 5533 ms, TE 88 ms), with diffusion encoding in 30 directions at $b=0$ and 1000 s/mm^2.

Structural data was analyzed with FSL-VBM (Douaud et al., 2007), a voxel-based morphometry-style analysis carried out with FSL tools. First, nonbrain tissue from structural images was extracted. After segmentation, GM images were aligned to MNI152 standard space using affine registration. The resulting images were averaged to create a study-specific template, to which the native GM images were then non-linearly re-registered. The registered partial volume images were then modulated (to correct for local expansion or contraction) by dividing by the Jacobian of the warp field. The modulated segmented images were then smoothed with an isotropic Gaussian kernel with a sigma of 3 mm. Finally, voxelwise general linear model was applied using permutation-based non-parametric testing, correcting for multiple comparisons across space.

Voxelwise statistical analysis of the fractional anisotropy (FA) data was carried out using TBSS (Tract-Based Spatial Statistics, [Smith et al. (2006)]), part of FSL (Smith et al., 2004). First, FA images were created by fitting a tensor model to the raw diffusion data using FDT, and then brain-extracted using BET (Smith et al., 2002). All subjects' FA data were then aligned into a common space using the nonlinear registration tool FNIRT (Andersson, Jenkinson & Smith, 2007a, 2007b), which uses a b-spline representation of the registration warp field (Rueckert et al., 1999). Next, the mean FA image was created and thinned to create a mean FA skeleton which represents the centers of all tracts common to the group. Each subject's aligned FA data was then projected onto this skeleton and the resulting data fed into voxelwise cross-subject statistics.

Structures used as regions of interest (ROIs) for GM analysis were chosen based on literature about the neural substrate of emotion processing, which includes data from lesion studies and functional MRI studies (Adolphs, 2002; Fusar-Poli et al., 2009; Adolphs et al., 2000; Calder, Keane, Lawrence & Manes, 2004). All GM structures were evaluated bilaterally. The masks for the GM ROI analyses were created based on the Harvard–Oxford probabilistic cortical and subcortical atlases (Smith et al., 2004). For WM masks, some tracts used as ROIs were chosen based on previous studies indicating their relevance in emotional processing, such as the inferior fronto-occipital fasciculus and the inferior longitudinal fasciculus (Philippi, Mehta, Grabowski, Adolphs & Rudrauf, 2009; Rudrauf et al., 2008). We also included associative tracts that are anatomically connected to the cortical or subcortical structures we included as ROIs for the GM analysis, to

investigate possible structural connectivity abnormalities between areas critical for emotion processing. The Johns Hopkins University white-matter tractography atlas was used to create the WM tract masks, which were evaluated bilaterally. Both atlases are available in FSL (http://www.fmrib.ox.ac.uk/fsl/data/atlas-descriptions.html). For GM analyses, the ROIs used were:

OFC
Anterior cingulate cortex (ACC)
Striatum
Postcentral gyrus (PCG)
Hippocampus
Fusiform gyrus
Insula
Parahippocampal gyrus (PHG)
Ventromedial prefrontal cortex
Amygdala
Inferior and middle frontal gyri

For WM analysis, the tracts used as ROIs were:

Inferior fronto-occipital fasciculus (IFOF)
Superior longitudinal fasciculus (SLF)
Inferior longitudinal fasciculus (ILF)
Uncinate fasciculus
Cingulum
Forceps minor

Statistical significance threshold was set at $p < 0.05$, corrected for multiple comparisons through familywise error (FWE) correction (Worsley et al., 1996).

For all correlation analyses, BDI scores were entered as covariates of no interest. Analyses of correlation between FER scores and structural parameters were repeated adding age as another covariate of no interest. Correlation coefficients (r) were calculated using mean GM volume or FA levels from the whole clusters rather than from the maxima to avoid the non-independence error.

3. Results

3.1. Subjects

There were no significant differences in age, gender or years of education between groups. Demographical and clinical results with group comparisons can be seen in Table 1. No subjects fulfilled the Movement Disorders Society criteria for dementia (Emre et al., 2007).

Table 2 shows neuropsychological assessment results with group comparisons. For the evaluation of visuospatial/visuoperceptive function, part of the sample (11 HC, 22 PD patients) was administered Benton's Visual Form Discrimination and Judgment of Line Orientation tests, whereas another part (12 HC, 17 PD patients) was administered Visual Object and Space Perception Battery Silhouettes test. No significant differences were observed between HC and PD patients' scores in these subsamples ($p > 0.05$).

3.2. Facial emotion recognition

As can be seen in Table 3, PD patients' total Ekman test scores and subscores in the identification of fear, sadness, anger and disgust were significantly lower than controls'. *Happiness* scores were similar in the two groups, and a ceiling effect was observed for this emotion. Scores for the identification of surprise were lower in PD patients, approaching statistical significance. There were significant effects of group in the two-level ANCOVAs, using BDI and MMSE scores as covariates, for the identification of facial expressions of anger, sadness and disgust, as well as for total Ekman scores.

No significant correlations were found between individual emotion recognition subscores or total Ekman scores and clinical variables such as disease duration, motor severity scales (Hoehn and Yahr [HY] and UDPRS) or levodopa equivalent daily dose (LEDD) (see Table 4).

3.3. Gray matter analysis

3.3.1. Correlation analyses between GM volume and emotional Ekman 60 test subscores

Whole-brain voxelwise analysis: this analysis showed no significant correlations between Ekman test scores and GM volume.

ROI analysis, *sadness* scores: significant positive correlations were found between patients' *sadness* scores and GM volume in the right OFC – a small cluster in its lateral portion, corresponding to Brodmann areas 11/47, and a medial cluster in the transition of Brodmann areas 11 and 14, – in the medial part of the right amygdala, and in the dorsal part of the right postcentral gyrus ($p < 0.05$, FWE-corrected) (Fig. 1A–C).

ROI analysis, *anger* scores: *anger* scores correlated positively with GM volume in the ventral striatum bilaterally (nuclei

Table 1
Demographic and clinical characteristics of HC and PD groups expressed in mean ± standard deviation.

	HC (n=23)	PD (n=39)	p	Test stats
Age	61.0 ± 9.7	63.5 ± 11.4	.37	−.90
Gender (male/female)	12/11	27/12	.28	1.80χ
Education yrs.	11.4 ± 3.6	11.4 ± 5.6	.95	−.05
Dis Dur	-	5.6 ± 3.8		
UPDRS-III	-	16.5 ± 8.3	-	
H&Y	-	1.8 ± 0.5	-	
LEDD	-	560.3 ± 410.4	-	
MMSE	29.3 ± .6	28.7 ± 1.4	.153	358.50†
BDI	3.4 ± 3.6	7.5 ± 5.3	.002*	238.00†

Dis Dur: Duration of motor symptoms, in years. UPDRS-III: Unified Parkinson's Disease Rating Scale-III, motor section. LEDD: Levodopa equivalent daily dose. Test stats: Student's t, chi-square (χ) or Mann–Whitney U test statistics. "*" indicates significance level $p < 0.05$.

Table 2
Neuropsychological assessment results of HC and PD groups expressed in mean ± standard deviation.

	HC	PD	p	Test stats
Total digit	14.1 ± 4.4	13.4 ± 3.6	.493	.690
Stroop interference	−4.3 ± 10.6	−6.6 ± 10.2	.760	.316
RAVLT total	46.5 ± 9.0	40.9 ± 12.6	**.045***	2.048
RAVLT delayed	9.4 ± 2.7	8.7 ± 3.4	.385	.874
RAVLT recognition	13.9 ± 1.4	13.8 ± 1.6	.797	432.0†
TMTA	37.6 ± 13.8	63.9 ± 49.1	**.003***	−3.151
TMTB	80.6 ± 26.0	144.1 ± 112.5	**.046***	260.0†
Phonemic fluency	16.8 ± 4.3	15.4 ± 6.0	.368	.907
Semantic fluency	20.8 ± 6.5	17.1 ± 6.4	**.029***	2.233
NPI	2.4 ± 3.4	4.6 ± 5.4	.170	305.5†

Test stats: Student's t-test or Mann–Whitney U test (†) statistics. RAVLT: Rey Auditory Visual Learning Test. TMTA: Trail-making test A. TMTB: Trail-making test B. NPI: Cumming's Neuropsychiatric Inventory. "*" indicates significance level $p < 0.05$.

Table 3
Ekman test results expressed in total scores and subscores according to emotion and according to group.

	HC (n=23)	PD (n=43)	p	p covariate	Test stats	F
Total ET score	50.8 ± 3.7	44.9 ± 5.9	.0001*	.007*	4.32	7.95
Fear	7.2 ± 2.1	5.6 ± 2.8	.001*	.221	2.55	1.53
Sadness	8.3 ± 1.4	6.9 ± 1.9	.001*	.010*	3.34	7.12
Anger	8.7 ± 1.2	7.0 ± 2.0	.001*†	.013*	214.5†	6.51
Disgust	8.3 ± 2.0	7.3 ± 2.0	.027*†	.035*	299.5†	4.66
Surprise	9.0 ± 1.1	8.5 ± 1.4	.073†	.844	330.5†	.039
Happiness	9.8 ± 0.4	9.7 ± 0.7	.544†	.972	419.0†	.001

'p' indicates significance levels from Student's t or Mann–Whitney U (†) tests comparing HC and PD scores. 'p covariate' indicates significance levels from two-level ANCOVAs comparing HC and PD scores using BDI and MMSE scores as covariates. "*" indicates significance level $p < 0.05$. Test stats: Student's t or Mann–Whitney U (†) test statistics. F: Two-level ANCOVA F statistic. ET: Ekman 60 test.

Table 4
Correlation coefficients/significance levels (p) between Ekman total scores and subscores and clinical variables in the PD group.

	Age	LEDD	Dis Dur	MMSE†	UPDRS	HY	BDI
Total ET score	−.35/.028*	.01/.974	.04/.837	.36/.024*	−.18/.274	−.08/.651	−.34/.036*
Fear	−.26/.111	−.01/.977	.05/.764	.36/.024*	−.21/.210	−.04/.827	−.33/.041*
Sadness	−.24/.134	.11/.512	.12/.491	.09/.596	−.21/.211	−.06/.737	−.09/.589
Anger†	−.28/.083	−.09/.608	.086/.614	.08/.637	−.07/.683	−.03/.855	−.07/.669
Disgust†	−.07/.658	−.10/.555	−.25/.139	.05/.776	−.10/.539	−.15/.359	.03/.838
Surprise†	−.10/.531	.12/.465	.09/.608	.10/.550	−.19/.244	−.11/.520	−.15/.374
Happiness†	.25/.129	−.04/.808	−.18/.300	.22/.178	−.11/.510	.07/.665	−.13/.421

Correlation coefficients refer to Pearson's correlation except for the variables marked with "†", for which Spearman's rank correlation was used. "*" indicates statistically significant correlations ($p < 0.05$). ET: Ekman 60 test scores. LEDD: Levodopa equivalent daily dose. Dis Dur: duration of motor symptoms. MMSE: Mini-Mental State Examination scores. BDI: Beck Depression Inventory-II scores.

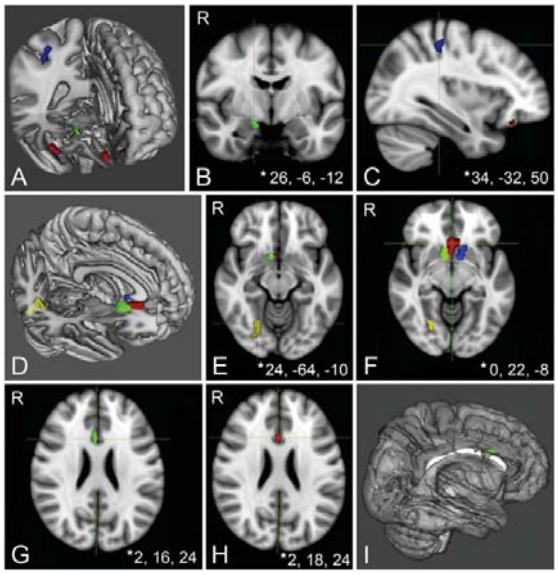

Fig. 1. Clusters of significant positive correlation between Ekman test scores and GM volume in PD patients ($p < 0.05$ FWE-corrected). ROI analysis. (A)–(C): Positive correlation between GM volume and *sadness* scores in PD patients (green: right amygdala; blue: right postcentral gyrus; red: right orbitofrontal cortex). (D)–(F): Positive correlation between *anger* scores and GM volume in the right occipital fusiform gyrus (red), subgenual cortex (red) and ventral striata (blue and green). (G)–(I): Positive correlation between GM volume in the anterior cingulate cortex and *disgust* scores (green) and total Ekman scores (red). "*" indicates MNI coordinates (x, y, z) at the crosshair. (For interpretation of the references to color in this figure legend, the reader is referred to the web version of this article.)

accumbens), in the right occipital fusiform gyrus and in the subgenual cortex (Brodmann areas 25 and 32) (Fig. 1D–F).

ROI analysis, *disgust* scores: a positive correlation was found between *disgust* scores and GM volume in the dorsal ACC (Brodmann area 24) ($p < 0.05$, FWE-corrected) (Fig. 1G–I).

ROI analysis, total Ekman scores: total emotion recognition scores correlated positively with GM volume in the dorsal ACC, in an area that partially overlaps the cluster of significant correlation between GM volume and *disgust* scores ($p < 0.05$, FWE-corrected) (Fig. 1H and I). Correlations between GM volume and Ekman scores in this area remained significant even after subtracting *disgust* scores from total Ekman scores ($r = 0.35$, $p = 0.03$).

Intergroup analyses revealed that PD patients had significantly reduced GM volumes compared with controls in all of the clusters described above, except in the right nucleus accumbens (Table 5, Supplementary Fig. 1). The location of the maxima of the clusters of significant correlation as well as their volumes and correlation coefficients are presented in Table 5.

When adding age as a covariate of no interest, all correlations remained significant ($p < 0.05$, FWE-corrected) with the exception of those between right amygdala GM volume and sadness scores ($p = 0.12$, FWE-corrected), between right lateral OFC GM volume and sadness scores ($p = 0.09$, FWE-corrected), and between total Ekman scores and ACC GM volume ($p = 0.06$, FWE-corrected).

3.4. White matter analysis

3.4.1. Correlation analysis between FA and Ekman 60 test subscores in PD patients

Whole-FA skeleton voxelwise analysis revealed a strong positive correlation between *sadness* scores and FA levels in a cluster in the right frontal lobe WM, with its maximum located in the topography of the inferior fronto-occipital fasciculus but also involving the forceps minor and body of the corpus callosum (Fig. 2A–C). Intergroup analysis revealed that PD patients had significantly lower FA levels in this cluster than HC (Table 6, Supplementary Fig. 1).

A smaller cluster was observed at the body of the corpus callosum extending to the left centrum semiovale ($p < 0.05$, FWE-corrected). In this region, FA levels in PD patients were not significantly different from those of the control group (Table 6 and Fig. 2B).

ROI analysis revealed additional areas of correlation between FA levels and *sadness* scores in the left temporal lobe white matter, comprising the topographies of the inferior fronto-occipital fasciculus and the inferior longitudinal fasciculus (Table 6 and Fig. 2) ($p < 0.05$, FWE-corrected). There were, however, no significant differences in FA levels between groups in these topographies.

All the correlations described above remained statistically significant after correcting for patient age ($p < 0.05$, FWE-corrected). No correlations were found between FA and other Ekman subscores or total Ekman scores either in whole-FA skeleton or in ROI analyses.

4. Discussion

In the present study, we found an overall impairment in FER in PD patients as this group's total Ekman test scores were significantly lower than those of the control group. Analyzing the performance for each emotion separately, PD patients presented an impaired recognition of all the negative emotions assessed, whereas no differences were observed for the recognition of surprise and happiness. Controlling for the potential confounding effects of associated mood changes and cognitive decline, however, performance in the recognition of all the negative emotions

Table 5
Clusters of significant positive correlation between GM volume and *sadness*, *disgust*, *anger* and total Ekman scores (ROI analysis, $p < 0.05$ FWE-corrected).

	Structure	MNI coordinates of maxima (*x,y,z*)	Volume (mm^3)	*r*/*p*	Group comparison (*t*/*p* values)
Sadness	Right OFC (lateral)	40, 30, −20	280	.45/.025	2.182/.033*
	Right OFC (medial)	4, 42, −28	1008	.53/.013	2.246/.028*
	Right PCG	34, −32, 50	264	.49/.030	3.656/.001*
	Right amygdala	16, −6, −12	184	.49/.036	4.380/ <.001*
Anger	Right occipital fusiform gyrus	24, −64, −10	1480	.54/.017	3.664/.001*
	Subgenual cortex	6, 10, −10	1720	.64/.016	2.419/.019*
	Right NAcc	6, 4, −8	1192	.49/.001	.703/.485
	Left NAcc	−6, 4, −6	1328	.45/.010	3.094/.003*
Disgust	ACC	2, 16, 22	296	.51/.035	2.895/.005*
Total Ekman	ACC	2, 18, 24	160	.46/.038	2.594/.012*

OFC: orbitofrontal cortex. PCG: postcentral gyrus. NAcc: Nucleus accumbens. ACC: anterior cingulate cortex. "*r*": Pearson's correlation coefficients. *p*: significance levels. "*" indicates significant ($p < 0.05$) group differences in GM volume.

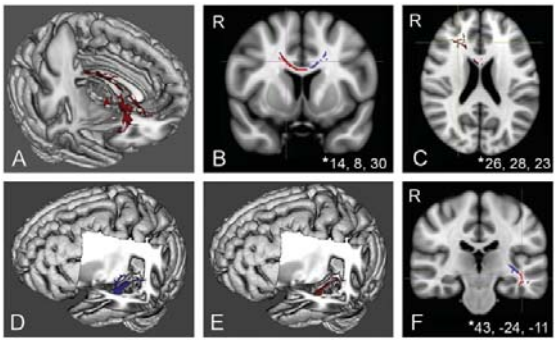

Fig. 2. Clusters of significant positive correlation between FA levels and *sadness* scores in PD patients ($p < 0.05$ FWE-corrected). (A)–(C): Whole-FA skeleton analysis. Red areas depict a cluster of positive correlation between *sadness* scores and FA levels involving the topography of the right IFOF and forceps minor (red). Blue areas represent a cluster that extends from the body of the corpus callosum to the left centrum semiovale. (D)–(F): Colored areas depict clusters of positive correlation between *sadness* scores and FA levels in the left IFOF (blue) and left ILF (red) topographies. "*" indicates MNI coordinates (*x*, *y*, *z*) at the crosshair. (For interpretation of the references to color in this figure legend, the reader is reffered to the web version of this article.)

with the exception of fear (anger, sadness and disgust) remained significantly worse in PD patients than in HC.

As has also been observed in other studies (Suzuki et al., 2006; Ibarretxe-Bilbao et al., 2009; Kan et al., 2002), a ceiling effect was observed for happiness, and fear was the least accurately identified emotion, both by HC and PD patients.

Given the multiple roles played by dopamine in distinct neural systems and the fact that the affectation of dopamine pathways in PD is heterogeneous and variable from one patient to another, dopaminergic medication can either have a corrective or an overdosing effect, depending on the structure or function evaluated (Gotham, Brown & Marsen, 1987; Delaveau et al., 2009). Previous work has evidenced that dopamine manipulations can alter FER (Lawrence, Calder, McGowan & Grasby, 2002; Lawrence et al., 2007) or modulate the activity of structures involved in it (Tessitore et al., 2002; Delaveau, Salgado-Pineda, Wicker, Micallef-Roll & Blin, 2005; Cools, Lewis, Clark, Barker & Robbins, 2007). In our sample, however, there was no relationship between levodopa equivalent daily dose and performance in the recognition of any individual emotion or overall emotion recognition.

We found several brain regions where GM volume correlated positively with the ability to identify individual emotions – specifically, the same emotions PD patients did worse at recognizing than healthy controls, – and where patients presented GM loss compared with controls. Though depressive symptoms are known to be a cause of FER impairments (Leppanen, 2006), these were taken into account in our analyses. *A posteriori* analyses showed no correlation between severity of depressive symptoms and GM parameters in the regions where the latter correlated with FER.

The impaired recognition of sadness was associated with GM loss in two areas of the right OFC – a medial area and a smaller, more lateral one, – in the dorsal part of the right postcentral gyrus and in the medial right amygdala. All of these areas have been implicated in the recognition of emotions, especially negative ones (Adolphs, 2002; Fusar-Poli et al., 2009). The orbitofrontal cortex plays a role in FER through different potential mechanisms, such as top-down perceptual processing modulation or through motor or somatosensory simulation of the observed state (Adolphs, 2002). Also, the critical role played by the right somatosensory cortex in facial emotion recognition, evaluated in lesion (Adolphs et al., 2000) as well as transcranial magnetic stimulation studies (Pitcher, Garrido, Walsh & Duchaine, 2008), supports the hypothesis that representation in this cortical area is critical for FER. These findings lend support to simulationist theories of emotion recognition, according to which the identification of a given emotion relies on the reactivation of sensorimotor networks involved in experiencing it (Niedenthal, 2007; Goldman & Sripada, 2005).

Performance in the recognition of anger correlated with GM volume in the right occipital fusiform gyrus, in the subgenual cortex and in the ventral striatum (nuclei accumbens). These findings are consistent with a study by Calder et al. (2004), in which patients with damage to the ventral striatal area were shown to have a disproportionate impairment in the recognition of this emotion.

The fusiform gyrus is classically implicated in the processing of static features of faces and in the recognition of identity (Kanwisher, McDermott & Chun, 1997; Adolphs, 2002). It also appears to play a role in the processing of emotional faces, although its activation has not usually been described to be associated specifically with the presentation of angry ones in functional studies (Fusar-Poli et al., 2009). The subgenual cortex is part of the so-called emotional subdivision of the ACC, and is involved in the evaluation of emotional salience of stimuli and in the regulation of emotional responses (Bush, Luu & Posner, 2000).

Previous work has evidenced that patients with lesions in ventromedial prefrontal cortical areas (including those we found to correlate with the identification of sadness and anger in PD patients) may have an impaired ability to process the affective attributes of emotional stimuli or to experience the emotion associated with these stimuli (Bechara, Damasio & Damasio, 2000), both of which might lead to the incorrect identification of emotions in others. Our results indicate that distinct parts of the ventromedial prefrontal cortex may play different roles in the processing of specific emotions.

Table 6
Clusters of significant positive correlation between FA and *sadness* scores ($p < 0.05$, FWE – corrected).

Topography	MNI coordinates of maxima (*x*, *y*, *z*)	Cluster volumen (mm^3)	*r*/*p*	Group comparison (t/ *p* values)
Right IFOF, right forceps minor[a]	34, 37, 4	1312	.53/.033	1.856/.032*
Body of corpus callosum, left centrum semiovale	−9, 5, 17	228	.47/.046	2.195/.069
Left ILF[b]	−43, −24, −11	342	.59/.004	.029/.977
Left IFOF[b]	−40, −25, −5	454	.56/.004	.057/.955

IFOF: inferior fronto-occipital fasciculus. SLF: superior longitudinal fasciculus. ILF: inferior longitudinal fasciculus. "*r*": Pearson's correlation coefficients. "∗" indicates significant ($p < 0.05$) group differences in FA levels.

[a] Whole-FA skeleton analysis.

[b] ROI analysis.

GM volume in the dorsal ACC correlated positively with the identification of disgust. Though this area has classically been considered as part of the "cognitive" subdivision of the ACC, this dichotomic view restricting emotional processing to the ventral anterior cingulate has been called into question (Etkin, Egner & Kalisch, 2011). In fact, a similar part of the dorsal ACC was seen to be activated while healthy subjects watched facial expressions of disgust and also when they experienced this emotion themselves in the study by Wicker et al. (2003).

Some of the pictures used in the Ekman 60 test are somewhat ambiguous, and the subject must weigh the conflicting information and determine which emotion predominates. The dorsal ACC is also involved in emotional conflict resolution (Etkin et al., 2011; Egner, Etkin, Gale & Hirsch, 2008), and might therefore be engaged in this kind of task. Indeed, we found that the dorsal ACC GM volume correlates with overall Ekman performance.

When entering age as a covariate, statistical significance was lost for the correlations between sadness identification and both right amygdala and right lateral orbitofrontal cortex GM, and between total Ekman scores and ACC GM, though a trend remained for the last two. This could at first glance suggest that the observed effects are a result of aging rather than of PD; in our sample, however, patient's age did not correlate with the performance in identifying sadness. In fact, this is in line with the proposed biologic interaction between age and the pathological effects of PD on GM neuronal loss in non-dopaminergic structures (Levy, 2007). According to this model, brain structures more affected by PD (including the medial temporal lobe, the ACC and the OFC) would present age-related changes earlier than other structures, so that correcting for the effects of aging might also obscure PD-related effects. More studies are necessary to evaluate this effect in neuroimaging analyses.

It is noteworthy that group comparisons in the areas described above revealed GM loss in structures such as the occipital fusiform gyrus and the precentral gyrus in PD patients compared to HC. According to the progression model proposed by Braak, Ghebremedhin, Rüb, Bratzke and Del Tredici (2004), these structures should be affected by α-synucleinopathy late in the disease course – later than structures such as the right ventral striatum, where GM volume loss was not present, – and our sample was not composed of patients with advanced disease. It might however be misleading to expect GM loss patterns to correspond rigidly to the six-stage model proposed by Braak et al. (2004) of ascending Lewy body pathology. Not only because up to 43% of PD cases may fail to conform to this model (Jellinger, 2008), but also because PD-related factors other than synucleinopathy could lead to neuronal death. Long-term loss of cholinergic input secondary to nucleus basalis magnocellularis lesion in rats is associated with frontoparietal cortical, hippocampal and amygdalar atrophy (Arendash, Millard, Dunn & Meyer, 1987). The equivalent nucleus in humans is affected relatively early in the course of PD (Braak et al., 2004). To our knowledge, however, the relationship between loss of cholinergic innervation and regional atrophy in PD has not been adequately studied, so this remains speculative. Another important contributor to cognitive dysfunction in PD is the coexistence of Alzheimer-type pathology (Jellinger, Seppi, Wenning & Poewe, 2002). The association of Lewy and Alzheimer-type pathologies has recently been found to be strongly associated with dementia in PD (Compta et al., 2011), and could conceivably be associated with specific patterns of neuronal loss.

Recent neuroimaging studies point to the existence of early WM degeneration in PD (Gattellaro et al., 2009; Karagulle Kendi et al., 2008), and basic research studies support this. While it might be tempting to think that axonal changes would be a result of α-synucleinopathy-induced neuronal death and therefore a late finding in the disease course, recent evidence suggests that axonal degeneration may precede neuronal cell body death, and may contribute importantly to the manifestations of neurodegenerative diseases, including PD (Raff, Whitmore & Finn, 2002; Conforti, Adalbert & Coleman, 2007; Hilliard, 2009). Additionally, axons may present inflammatory changes even before degenerating, as suggested by an animal study with mutant α-synuclein transgenic mice which revealed early widespread axonal swelling (Martin et al., 2006). A similar process could feasibly take place in PD patients, in whom extensive axonal α-synuclein inclusions have been described (Braak, Sandmann-Keil, Gai, Braak, 1999). Taken together, these findings suggest that WM changes might occur independently from GM changes in PD, and at its early stages. FA decrements are a sensitive marker of WM degeneration, and may be related to axonal loss, demyelination or edema (Lu et al., 2004); as such, they could represent a useful marker for detecting these changes at an early stage.

We have found an area in the right frontal lobe where FA levels correlated with the performance in identifying facial expressions of sadness and were reduced compared to controls'. The fasciculus mostly affected was the IFOF, which runs from the frontal lobes to the parietal, temporal and occipital lobes and is usually considered to be implicated in semantic processing (Martino, Brogna, Robles, Vergani & Duffau, 2010; Duffau et al., 2005). Recently, however, Philippi et al. (2009), studying patients with focal brain lesions, described overall impairments in FER associated with damage to the right IFOF, more specifically in the recognition of fear, anger and sadness. These results indicate that the IFOF has an important role in emotional processing, as might be reasonably surmised since it connects areas such as the OFC, the medial temporal lobe and the insula to the visual cortex. Our findings provide neuroimaging evidence that the integrity of the IFOF is critical for the processing of facial emotions.

Besides the structures discussed above, we also found significant correlations between anger recognition and GM volume in the right ventral striatum, and between sadness recognition and FA levels in the temporal part of the left IFOF and ILF, but no group differences in these structural parameters could be found in these regions. Though we cannot exclude that disease-related degenerative processes in these structures might be contributing to FER impairments in some patients, these findings could also

represent a physiological correlate of the recognition of these emotions.

Structural techniques may have limitations when studying anatomic correlates for functional deficits such as the ones addressed in this study. It has been demonstrated that cognitive deficits in PD do not correlate with Lewy body and Lewy neurite pathology (Jellinger, 2008), and that neurons affected by α-synucleinopathy probably cease to function long before dying (Braak et al., 2004). The same could be the case for Alzheimer-type pathology. Changes in cortical and subcortical innervation (not only dopaminergic) from brainstem or basal forebrain nuclei (Bohnen et al., 2006; Shimada et al., 2009) are another factor that seems to contribute to functional deficits. Structural techniques may not have sufficient sensitivity to detect such changes until these factors amount to cell death. We have, nonetheless, been able to detect structural changes in a sample of patients that on average did not have advanced PD from either a motor or a cognitive perspective.

In conclusion, we have found evidence that strongly supports previously described impairments in the identification of negative facial emotions in PD patients. The results of our structural analyses are novel insofar as they reveal that the deficits in the recognition of specific facial emotions in PD, rather than being solely accompanied by functional changes, have specific structural correlates, especially in GM structures but also related to WM microstructural integrity. And, to our knowledge, this is the first study to show that the neural substrate of the processing of individual emotions can be evaluated through structural gray and white matter MRI techniques.

Acknowledgments

This study was supported by Generalitat de Catalunya [2009SGR0836 to E.T., 2009SGR0941 to C. J.), PSI2010-16174 to C.J., H.C.B and B.S, and an FI-DGR grant (2011FI_B 00045) to H.C.B.

Appendix A. Supplementary information

Supplementary data associated with this article can be found in the online version at http://dx.doi.org/10.1016/j.neuropsychologia.2012.05.020.

References

Aarsland, D., Bronnick, K., Larsen, J. P., Tysnes, O. B., Alves, G., & Norwegian ParkWest Study Group (2009). Cognitive impairment in incident, untreated Parkinson disease: the Norwegian ParkWest study. *Neurology*, *72*, 1121–1126.
Adolphs, R., Tranel, D., Damasio, H., & Damasio, A. (1994). Impaired recognition of emotion in facial expressions following bilateral damage to the human amygdala. *Nature*, *372*, 669–672.
Adolphs, R. (2002). Neural systems for recognizing emotion. *Current Opinion in Neurobiology*, *12*, 169–177.
Adolphs, R., Damasio, H., Tranel, D., Cooper, G., & Damasio, A. R. (2000). A role for somatosensory cortices in the visual recognition of emotion as revealed by 3-D lesion mapping. *The Journal of Neuroscience*, *20*, 2683–2690.
Adolphs, R., Tranel, D., & Damasio, A. R. (2003). Dissociable neural systems for recognizing emotions. *Brain and Cognition*, *52*, 61–69.
Andersson, J.L.R., Jenkinson, M., & Smith, S. (2007). Non-linear optimisation. FMRIB technical report TR07JA1 from 〈www.fmrib.ox.ac.uk/analysis/techrep〉.
Andersson, J.L.R., Jenkinson, M., & Smith, S. (2007). Non-linear registration, aka Spatial normalization. FMRIB technical report TR07JA2 from 〈www.fmrib.ox.ac.uk/analysis/techrep〉.
Arendash, G. W., Millard, W. J., Dunn, A. J., & Meyer, E. M. (1987). Long-term neuropathological and neurochemical effects of nucleus basalis lesions in the rat. *Science*, *238*, 952–956.
Ariatti, A., Benuzzi, F., & Nichelli, P. (2008). Recognition of emotions from visual and prosodic cues in Parkinson's disease. *Neurological Sciences*, *29*, 219–227.
Bechara, A., Damasio, H., & Damasio, A. (2000). Emotion, decision making and the orbitofrontal cortex. *Cerebral Cortex*, *10*, 295–307.
Beck, A. T., Steer, R. A., & Brown, G. K. (1996). *Manual for the Beck Depression Inventory-II*. San Antonio, TX: Psychological Corporation.
Biseul, I., Sauleau, P., Haegelen, C., Trebon, P., Drapier, D., Raoul, S., Drapier, S., Lallement, F., Rivier, I., Lajat, Y., & Verin, M. (2005). Fear recognition is impaired by subthalamic nucleus stimulation in Parkinson's disease. *Neuropsychologia*, *43*, 1054–1059.
Bohnen, N. I., Kaufer, D. I., Hendrickson, R., Ivanco, L. S., Lopresti, B. J., Constantine, G. M., Mathis, C. A., Davis, J. G., Moore, R. Y., & Dekosky, S. T. (2006). Cognitive correlates of cortical cholinergic denervation in Parkinson's disease and parkinsonian dementia. *Journal of Neurology*, *253*, 242–247.
Braak, H., Ghebremedhin, E., Rüb, U., Bratzke, H., & Del Tredici, K. (2004). Stages in the development of Parkinson's disease-related pathology. *Cell and Tissue Research*, *318*, 121–134.
Braak, H., Sandmann-Keil, D., Gai, W., & Braak, E. (1999). Extensive axonal Lewy neurites in Parkinson's disease: a novel pathological feature revealed by alpha-synuclein immunocytochemistry. *Neuroscience Letters*, *265*, 67–69.
Bush, G., Luu, P., & Posner, M. I. (2000). Cognitive and emotional influences in anterior cingulate cortex. *Trends in Cognitive Sciences*, *4*, 215–222.
Calder, A., Young, A. W., Rowland, D., Perrett, D. I., Hodges, J. R., & Etcoff, N. L. (1996). Facial emotion recognition after bilateral amygdala damage: differentially severe impairment of fear. *Cognitive Neuropsychology*, *13*, 699–745.
Calder, A. J., Keane, J., Manes, F., Antoun, N., & Young, A. W. (2000). Impaired recognition and experience of disgust following brain injury. *Nature Neuroscience*, *3*, 1077–1078.
Calder, A. J., Keane, J., Young, A. W., Lawrence, A. D., Mason, S., & Barker, R. A. (2010). The relation between anger and different forms of disgust: implications for emotion recognition impairments in Huntington's disease. *Neuropsychologia*, *48*, 2719–2729.
Calder, A. J., Keane, J., Lawrence, A. D., & Manes, F. (2004). Impaired recognition of anger following damage to the ventral striatum. *Brain*, *127*, 1958–1969.
Compta, Y., Parkkinen, L., O'Sullivan, S. O., Vandrovcova, J., Holton, J. L., Collins, C., Lashley, T., Kallis, C., Williams, D. R., de Silva, R., Lees, A. J., & Revesz, T. (2011). Lewy- and Alzheimer-type pathologies in Parkinson's disease dementia: which is more important?. *Brain*, *134*, 1493–1505.
Conforti, L., Adalbert, R., & Coleman, M. P. (2007). Neuronal death: where does the end begin?. *Trends in Neurosciences*, *30*, 159–166.
Cummings, J. L., Mega, M., Gray, K., Rosenberg-Thompson, S., Carusi, D. A., & Gornbein, J. (1994). The Neuropsychiatric Inventory: Comprehensive assessment of psychopathology in dementia. *Neurology*, *44*, 2308–2314.
Cools, R., Lewis, S. J., Clark, L., Barker, R. A., & Robbins, T. W. (2007). L-DOPA disrupts activity in the nucleus accumbens during reversal learning in Parkinson's disease. *Neuropsychopharmacology*, *32*, 180–189.
Daniel, S. E., & Lees, A. J. (1993). Parkinson's Disease Society Brain Bank, London: overview and research. *Journal of Neural Transmission Supplementum*, *39*, 154–172.
Delaveau, P., Salgado-Pineda, P., Wicker, B., Micallef-Roll, J., & Blin, O. (2005). Effect of levodopa on healthy volunteers' facial emotion perception: an FMRI study. *Clinical Neuropharmacology*, *28*, 255–261.
Delaveau, P., Salgado-Pineda, P., Witjas, T., Micallef-Roll, J., Fakra, E., Azulay, J. P., & Blin, O. (2009). Dopaminergic modulation of amygdala activity during emotion recognition in patients with Parkinson disease. *Journal of Clinical Psychopharmacology*, *29*, 548–554.
Douaud, G., Smith, S., Jenkinson, M., Behrens, T., Johansen-Berg, H., Vickers, J., James, S., Voets, N., Watkins, K., Matthews, P. M., & James, A. (2007). Anatomically related grey and white matter abnormalities in adolescent-onset schizophrenia. *Brain*, *130*, 2375–2386.
Duffau, H., Gatignol, P., Mandonnet, E., Peruzzi, P., Tzourio-Mazoyer, N., & Capelle, L. (2005). New insights into the anatomo-functional connectivity of the semantic system: a study using cortico-subcortical electrostimulations. *Brain*, *128*, 797–810.
Dujardin, K., Blairy, S., Defebvre, L., Duhem, S., Noël, Y., Hess, U., & Destée, A. (2004). Deficits in decoding emotional facial expressions in Parkinson's disease. *Neuropsychologia*, *42*, 239–250.
Egner, T., Etkin, A., Gale, S., & Hirsch, J. (2008). Dissociable neural systems resolve conflict from emotional versus nonemotional distracters. *Cerebral Cortex*, *18*, 1475–1484.
Ekman, P., & Friesen, W. V. (1976). *Pictures of Facial Affect*. Palo-alto: Consulting Psychologists Press.
Emre, M., Aarsland, D., Brown, R., Burn, D. J., Duyckaerts, C., Mizuno, Y., Broe, G. A., Cummings, J., Dickson, D. W., Gauthier, S., Goldman, J., Goetz, C., Korczyn, A., Lees, A., Levy, R., Litvan, I., McKeith, I., Olanow, W., Poewe, W., Quinn, N., Sampaio, C., Tolosa, E., & Dubois, B. (2007). Clinical diagnostic criteria for dementia associated with Parkinson's disease. *Movement Disorders*, *22*, 1689–1707.
Etkin, A., Egner, T., & Kalisch, R. (2011). Emotional processing in anterior cingulate and medial prefrontal cortex. *Trends in Cognitive Sciences*, *15*, 85–93.
Foltynie, T., Brayne, C. E., Robbins, T. W., & Barker, R. A. (2004). The cognitive ability of an incident cohort of Parkinson's patients in the UK. The CamPaIGN study. *Brain*, *127*, 550–560.
Fusar-Poli, P., Placentino, A., Carletti, F., Landi, P., Allen, P., Surguladze, S., Benedetti, F., Abbamonte, M., Gasparotti, R., Barale, F., Perez, J., McGuire, P., & Politi, P. (2009). Functional atlas of emotional faces processing: a voxel-based meta-analysis of 105 functional magnetic resonance imaging studies. *Journal of Psychiatry and Neuroscience*, *34*, 418–432.
Gattellaro, G., Minati, L., Grisoli, M., Mariani, C., Carella, F., Osio, M., Ciceri, E., Albanese, A., & Bruzzone, M. G. (2009). White matter involvement in

idiopathic Parkinson disease: a diffusion tensor imaging study. *American Journal Neuroradiology*, *30*, 1222–1226.
Goldman, A. I., & Sripada, C. S. (2005). Simulationist models of face-based emotion recognition. *Cognition*, *94*, 193–213.
Gotham, A. M., Brown, R. G., & Marsen, C. D. (1987). "Frontal" cognitive function in patients with Parkinson's disease "on" and "off" levodopa. *Brain*, *111*, 299–321.
Heberlein, A. S., Padon, A. A., Gillihan, S. J., Farah, M. J., & Fellows, L. K. (2008). Ventromedial frontal lobe plays a critical role in facial emotion recognition. *Journal of Cognitive Neuroscience*, *20*, 721–733.
Hilliard, M. A. (2009). Axonal degeneration and regeneration: a mechanistic tug-of-war. *Journal of Neurochemistry*, *108*, 23–32.
Hornak, J., Bramham, J., Rolls, E. T., Morris, R. G., O'Doherty, J., Bullock, P. R., & Polkey, C. E. (2003). Changes in emotion after circumscribed surgical lesions of the orbitofrontal and cingulate cortices. *Brain*, *126*, 1691–1712.
Ibarretxe-Bilbao, N., Junque, C., Tolosa, E., Marti, M. J., Valldeoriola, F., Bargallo, N., & Zarei, M. (2009). Neuroanatomical correlates of impaired decision-making and facial emotion recognition in early Parkinson's disease. *The European Journal of Neuroscience*, *30*, 1162–1171.
Jellinger, K. A., Seppi, K., Wenning, G. K., & Poewe, W. (2002). Impact of coexistent Alzheimer pathology on the natural history of Parkinson's disease. *Journal of Neural Transmission*, *109*, 329–339.
Jellinger, K. A. (2008). A critical reappraisal of current staging of Lewy-related pathology in human brain. *Acta Neuropathologica*, *116*, 1–16.
Kan, Y., Kawamura, M., Hasegawa, Y., Mochizuki, S., & Nakamura, K. (2002). Recognition of emotion from facial, prosodic and written verbal stimuli in Parkinson's disease. *Cortex*, *38*, 623–630.
Kanwisher, N., McDermott, J., & Chun, M. M. (1997). The fusiform face area: a module in human extrastriate cortex specialized for face perception. *The Journal of Neuroscience*, *17*, 4302–4311.
Karagulle Kendi, A. T., Lehericy, S., Luciana, M., Ugurbil, K., & Tuite, P. (2008). Altered diffusion in the frontal lobe in Parkinson disease. *American Journal Neuroradiology*, *29*, 501–505.
Krolak-Salmon, P., Hénaff, M. A., Isnard, J., Tallon-Baudry, C., Guénot, M., Vighetto, A., Bertrand, O., & Mauguière, F. (2003). An attention modulated response to disgust in human ventral anterior insula. *Annals of Neurology*, *53*, 446–453.
Lawrence, A. D., Calder, A. J., McGowan, S. W., & Grasby, P. M. (2002). Selective disruption of the recognition of facial expressions of anger. *Neuroreport*, *13*, 881–884.
Lawrence, A. D., Goerendt, I. K., & Brooks, D. J. (2007). Impaired recognition of facial expressions of anger in Parkinson's disease patients acutely withdrawn from dopamine replacement therapy. *Neuropsychologia*, *45*, 65–74.
Leentjens, A. F., Verhey, F. R., Luijckx, G. J., & Troost, J. (2000). The validity of the Beck Depression Inventory as a screening and diagnostic instrument for depression in patients with Parkinson's disease. *Movement Disorders*, *15*, 1221–1224.
Leppanen, J. M. (2006). Emotional information processing in mood disorders: a review of behavioral and neuroimaging findings. *Current Opinion in Psychiatry*, *19*, 34–39.
Levy, G. (2007). The relationship of Parkinson disease with aging. *Archives of Neurology*, *64*, 1242–1246.
Lezak, M. D., Howieson, D. B., & Loring, D. W. (2004). *Neuropsychological Assessment*. New York, NY: Oxford.
Lu, S., Ahn, D., Johnson, G., Law, M., Zagzag, D., & Grossman, R. I. (2004). Diffusion-tensor MR imaging of intracranial neoplasia and associated peritumoral edema: introduction of the tumor infiltration index. *Radiology*, *232*, 221–228.
Martin, L. J., Pan, Y., Price, A. C., Sterling, W., Copeland, N. G., Jenkins, N. A., Price, D. L., & Lee, M. K. (2006). Parkinson's disease alpha-synuclein transgenic mice develop neuronal mitochondrial degeneration and cell death. *The Journal of Neuroscience*, *26*, 41–50.
Martino, J., Brogna, C., Robles, S. G., Vergani, F., & Duffau, H. (2010). Anatomic dissection of the inferior fronto-occipital fasciculus revisited in the lights of brain stimulation data. *Cortex*, *46*, 691–699.
Muslimovic, D., Post, B., Speelman, J. D., & Schmand, B. (2005). Cognitive profile of patients with newly diagnosed Parkinson disease. *Neurology*, *65*, 1239–1245.
Niedenthal, P. M. (2007). Embodying emotion. *Science*, *316*, 1002–1005.
Pell, M. D., & Leonard, C. L. (2005). Facial expression decoding in early Parkinson's disease. *Brain Research Cognitive Brain Research*, *23*, 327–340.
Philippi, C. L., Mehta, S., Grabowski, T., Adolphs, R., & Rudrauff, D. (2009). Damage to association fiber tracts impairs recognition of the facial expression of emotion. *The Journal of Neuroscience*, *29*, 15089–15099.
Phillips, M. L., Young, A. W., Senior, C., Brammer, M., Andrew, C., Calder, A. J., Bullmore, E. T., Perrett, D. I., Rowland, D., Williams, S. C., Gray, J. A., & David, A. S. (1997). A specific neural substrate for perceiving facial expressions of disgust. *Nature*, *389*, 495–498.
Pitcher, D., Garrido, L., Walsh, V., & Duchai, B. C. (2008). Transcranial magnetic stimulation disrupts the perception and embodiment of facial expressions. *Journal of Neuroscience*, *28*, 8929–8933.
Raff, M. C., Whitmore, A. V., & Finn, J. T. (2002). Axonal self-destruction and neurodegeneration. *Science*, *296*, 868–871.
Reijnders, J. S., Ehrt, U., Weber, W. E., Aarsland, D., & Leentjens, A. F. (2008). A systematic review of prevalence studies of depression in Parkinson's disease. *Movement Disorders*, *23*, 183–189.
Rudrauf, D., David, O., Lachaux, J. P., Kovach, C. K., Martinerie, J., Renault, B., & Damasio, A. (2008). Rapid interactions between the ventral visual stream and emotion-related structures rely on a two-pathway architecture. *The Journal of Neuroscience*, *28*, 2793–2803.
Rueckert, D., Sonoda, L. I., Hayes, C., Hill, D. L. G., Leach, M. O., & Hawkes, D. J. (1999). Non-rigid registration using free-form deformations: application to breast MR images. *IEEE Transactions on Medical Imaging*, *18*, 712–721.
Shimada, H., Hirano, S., Shinotoh, H., Aotsuka, A., Sato, K., Tanaka, N., Ota, T., Asahina, M., Fukushi, K., Kuwabara, S., Hattori, T., Suhara, T., & Irie, T. (2009). Mapping of brain acetylcholinesterase alterations in Lewy body disease by PET. *Neurology*, *73*, 273–278.
Slaughter, J. R., Slaughter, K. A., Nichols, D., Holmes, S. E., & Martens, M. P. (2001). Prevalence, clinical manifestations, etiology, and treatment of depression in Parkinson's disease. *The Journal of Neuropsychiatry and Clinical Neurosciences*, *13*, 187–196.
Smith, S. M (2002). Fast robust automated brain extraction. *Human Brain Mapping*, *17*, 143–155.
Smith, S. M., Jenkinson, M., Johansen-Berg, H., Rueckert, D., Nichols, T. E., Mackay, C. E., Watkins, K. E., Ciccarelli, O., Cader, M. Z., Matthews, P. M., & Behrens, T. E. (2006). Tract-based spatial statistics: voxelwise analysis of multi-subject diffusion data. *Neuroimage*, *31*, 1487–1505.
Smith, S. M., Jenkinson, M., Woolrich, M. W., Beckmann, C. F., Behrens, T. E., Johansen-Berg, H., Bannister, P. R., De Luca, M., Drobnjak, I., Flitney, D. E., Niazy, R. K., Saunders, J., Vickers, J., Zhang, Y., De Stefano, N., Brady, J. M., & Matthews, P. M. (2004). Advances in functional and structural MR image analysis and implementation as FSL. *Neuroimage*, *23*(Suppl. 1), S208–S219.
Sprengelmeyer, R., Young, A. W., Mahn, K., Schroeder, U., Woitalla, D., Büttner, T., Kuhn, W., & Przuntek, H. (2003). Facial expression recognition in people with medicated and unmedicated Parkinson's disease. *Neuropsychologia*, *41*, 1047–1057.
Suzuki, A., Hoshino, T., Shigemasu, K., & Kawamura, M. (2006). Disgust-specific impairment of facial expression recognition in Parkinson's disease. *Brain*, *129*, 707–717.
Tessitore, A., Hariri, A. R., Fera, F., Smith, W. G., Chase, T. N., Hyde, T. M., Weinberger, D. R., & Mattay, V. S. (2002). Dopamine modulates the response of the human amygdala: a study in Parkinson's disease. *The Journal of Neuroscience*, *22*, 9099–9103.
Tomlinson, C. L., Stowe, R., Patel, S., Rick, C., Gray, R., & Clarke, C. E. (2010). Systematic review of levodopa equivalency reporting in Parkinson's disease. *Movement Disorders*, *25*, 2649–2653.
Vernooij, M. W., Ikram, M. A., Vrooman, H. A., Wielopolski, P. A., Krestin, G. P., Hofman, A., Niessen, W. J., Van der Lugt, A., & Breteler, M. M. (2009). White matter microstructural integrity and cognitive function in a general elderly population. *Archives of General Psychiatry*, *66*, 545–553.
Wicker, B., Keysers, C., Plailly, J., Royet, J. P., Gallese, V., & Rizzolatti, G. (2003). Both of us disgusted in my insula: the common neural basis of seeing and feeling disgust. *Neuron*, *40*, 655–664.
Worsley, K. J., Marrett, S., Neelin, P., Vandal, A. C., Friston, K. J., & Evans, A. C. (1996). A unified statistical approach for determining significant signals in images of cerebral activation. *Human Brain Mapping*, *4*, 58–73.
Yip, J. T., Lee, T. M., Ho, S. L., Tsang, K. L., & Li, L. S. (2003). Emotion recognition in patients with idiopathic Parkinson's disease. *Movement Disorders*, *18*, 1115–1122.

SUPPLEMENTARY MATERIALS

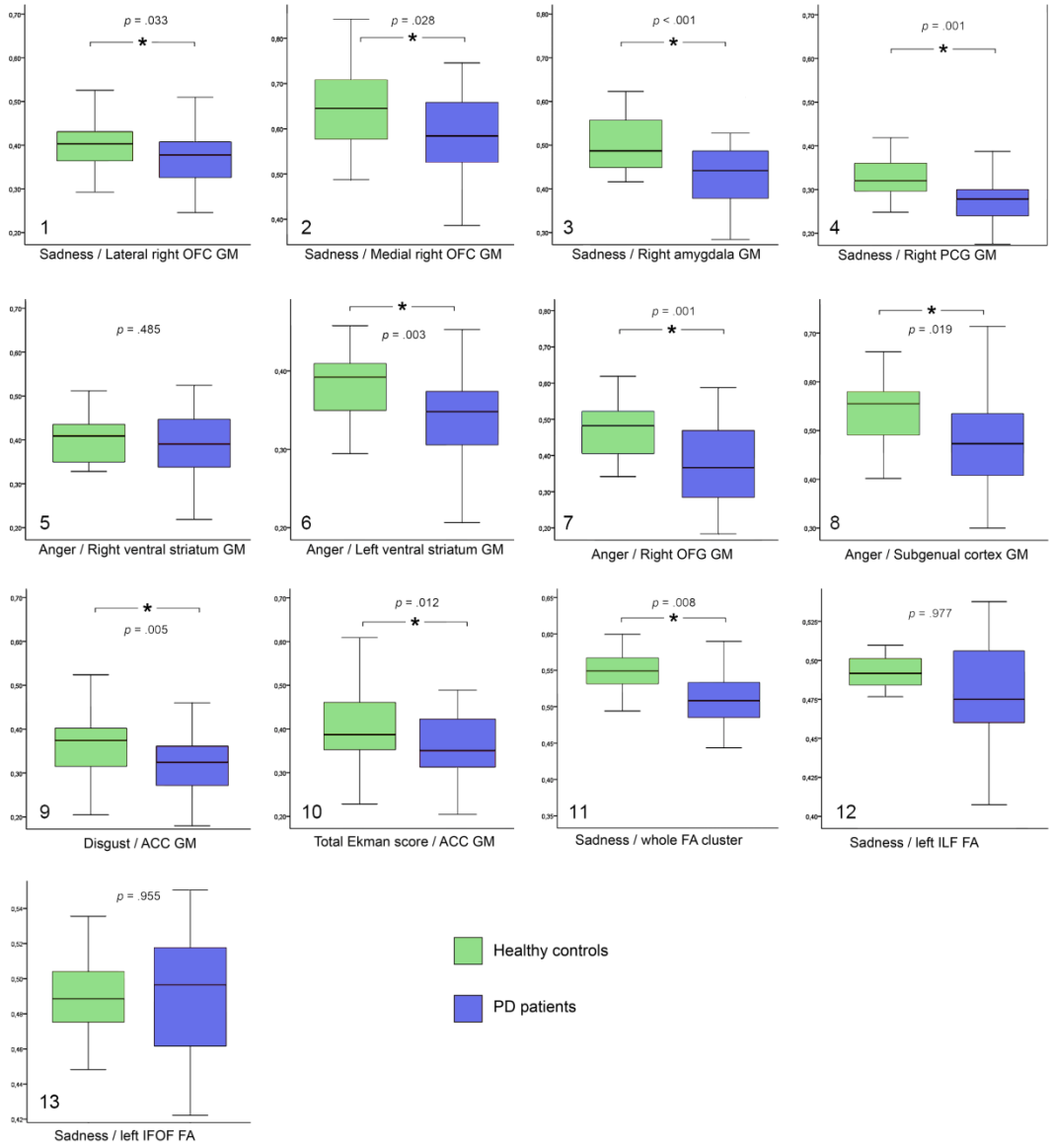

Supplementary Figure 1. Plots showing the distribution of mean gray matter (GM) volume (1-10) or FA levels (11-12), in arbitrary units, in the clusters of significant correlation between these parameters and Ekman test scores, in the HC and PD patient groups. "*" indicates significant group differences (p<0.05). OFC: orbitofrontal cortex. PCG: precentral gyrus. OFG: occipital fusiform gyrus. ILF: inferior longitudinal fasciculus. IFOF: inferior fronto-occipital fasciculus

study 5

RESTING-STATE FRONTOSTRIATAL FUNCTIONAL CONNECTIVITY IN PARKINSON'S DISEASE-RELATED APATHY

Hugo César Baggio, Bàrbara Segura, José Garrido Millán, Maria José Marti, Yaroslau Compta, Francesc Valldeoriola, Eduardo Tolosa, Carme Junqué

ABSTRACT

Background: One of the most common neuropsychiatric symptoms in PD is apathy, affecting between 23 and 70% of patients and thought to be related to frontostriatal dopamine deficits. In the present study, we assessed functional resting-state frontostriatal connectivity and structural changes associated with the presence of apathy in a large sample of PD subjects and healthy controls, while controlling for the presence of comorbid depression and cognitive decline.

Methods: Thirty-one healthy controls (HC) and 62 age, sex and education-matched PD patients underwent resting-state functional MRI. Apathy symptoms were evaluated with the Apathy Scale (AS). The 11 Beck Depression Inventory-II items that measure dysphoric mood symptoms as well as relevant neuropsychological scores were used as nuisance factors in connectivity analyses. Voxel-wise analyses of connectivity between frontal lobes (limbic, executive, rostral motor and caudal motor regions), striata (limbic, executive, sensorimotor regions) and thalami were performed. Subcortical volumetry/shape analysis and fronto-subcortical voxel-based morphometry were performed to assess structural changes.

Results: Twenty-five PD patients were classified as apathetic (PD-A) (AS>13). PD-A patients showed connectivity reductions compared with HC and with non-apathetic patients (PD-NA), mainly in left-sided circuits, and predominantly involving limbic striatal and frontal territories. Similarly, severity of apathy negatively correlated with connectivity in these circuits. No significant effects were found in structural analyses.

Conclusions: Our results indicate that the presence of apathy in PD is associated with connectivity reductions in frontostriatal circuits, predominating in the left hemisphere and mainly involving its limbic components.

INTRODUCTION

Parkinson's disease (PD) can be associated with several non-motor symptoms. Among them, one of the most common neuropsychiatric manifestations is apathy. Described to affect between 23 and 70% of PD patients [Cubo et al., 2012; Kirsch-Darrow et al., 2006; Pedersen et al., 2010], apathy is characterized by behavioral (reduced goal-directed behavior), cognitive (lack of interest) and affective (flattened affect) symptoms [Kirsch-Darrow et al., 2006].

Although the pathophysiologic bases of apathy in PD are not clear, dopamine deficits affecting frontostriatal loops are thought to play an important role. Apathy is known to occur as a result of lesions affecting the medial and orbital parts of the prefrontal cortex and the portions of the basal ganglia connected to them, namely the ventral striatum [Levy and Dubois, 2006]. In PD, severity of apathy has been found to correlate with frontal gray matter (GM) [Reijnders et al., 2010] and with ventral striatal volume reductions [Carriere et al., 2014]. Apathy following subthalamic nucleus stimulation surgery has been shown to be associated with mesolimbic dopaminergic denervation [Thobois et al., 2010], and is amenable to dopaminergic therapy [Czernecki et al., 2008; Thobois et al., 2013]. These findings give further support to the relevance of frontostriatal circuits in PD-related apathy; to our knowledge, nonetheless, no published studies evaluated the presence of associated functional connectivity changes.

Resting-state fMRI, which analyzes spontaneous blood-oxygen-level dependent signal fluctuations, is a frequently-used tool in the assessment of connectivity changes in neurological and psychiatric diseases. Considering that apathetic patients have an impaired ability to spontaneously switch from the resting state to goal directed behavior, the analysis of the resting state may be especially informative in the study of apathy, as suggested by Skidmore *et al.* [Skidmore et al., 2013].

The presence of apathy in PD is described to be associated with cognitive deficits [Butterfield et al., 2010; Dujardin et al., 2007; Pluck and Brown, 2002] and with a higher risk of subsequent dementia [Dujardin et al., 2009]. Moreover, in PD, it often coexists with depression, and the symptomology of both syndromes overlaps [Kirsch-Darrow et al., 2006] – specifically, symptoms of apathy often occur as part of the depressive syndrome [Marin, 1990]. Although there's evidence to support that apathy exists as a distinct entity in PD [Aarsland et al., 1999; Dujardin et al., 2007; Isella et al., 2002; Kirsch-Darrow et al., 2006; Starkstein et al., 1992], the study of its neural substrates, as well as its clinical detection, are complicated by such overlap. The identification of specific symptoms of depression, such as dysphoria or feelings of guilt, punishment and self-criticalness, may be useful in the differential diagnosis [Kirsch-Darrow et al., 2006].

Our aim in the present study was to evaluate resting-state functional connectivity and structural changes affecting the frontostriatal pathways in a large sample of PD patients and matched controls, while controlling for the associated effects of cognitive decline and depressive symptoms. We hypothesized that the presence of apathy in PD patients would be associated with disrupted connectivity in circuits, especially affecting the ventral striatum and the ventromedial prefrontal cortex. Considering that dopamine modulates frontostriatal connectivity, and that dopamine deficiency due to nigral degeneration precedes forebrain GM pathology in PD [Braak et al., 2003], we also expected that connectivity changes would be more marked than structural degeneration.

METHODS

Eighty-four non-demented PD patients and 38 healthy controls (HC) matched for age, sex and years of education were included. Patients were recruited from the Parkinson's Disease and Movement Disorders Unit, Hospital Clínic de Barcelona. HC were recruited from individuals who volunteered to participate in scientific studies at the Institut de l'Envelliment, Universitat Autònoma de Barcelona. The inclusion criterion for patients was the fulfillment of the UK PD Society Brain Bank diagnostic criteria for PD [Daniel and Lees, 1993]. Exclusion criteria were: (i) Mini-Mental State Examination scores < 25 or presence of dementia according to the Movement Disorder Society criteria [Emre et al., 2007], (ii) Hoehn and Yahr (HY) score > III, (ii) presence of other significant neurological, systemic or psychiatric (except depressive symptoms) comorbidity, (iv) pathological MRI findings other than mild white matter hyperintensities, (v) root mean square head motion > 0.3 mm translation or 0.6 degrees rotation.

Four patients were excluded due to macroscopic movement, 14 due to head motion > 0.3 mm translation or > 0.6^0 rotation, and one for being an outlier in connectivity analyses. Eight HC (2 due to microvascular white matter changes, 5 due to incomplete filling of the AS) were excluded, leaving a final sample of 31 HC and 65 PD patients.

All patients except one were taking antiparkinsonian drugs, consisting of different combinations of levodopa, cathecol-O-methyl transferase inhibitors, monoamine oxidase inhibitors, dopamine agonists and amantadine. The medication was not changed for the study and all assessments were done while patients were in the *on* state. Levodopa equivalent daily dose (LEDD) was calculated as suggested by Tomlinson *et al.* [Tomlinson et al., 2010]. Motor disease severity was evaluated using HY staging and the Unified Parkinson's Disease Rating Scale motor section (UPDRS-III).

The study was approved by the ethics committee of the University of Barcelona, and all subjects provided written informed consent to participate.

Neuropsychiatric evaluation

Apathy symptoms were evaluated with the self-administered Apathy Scale (AS), recommended for patients with PD [Leentjens et al., 2008]. Subjects were classified as apathetic if they scored >13 in the AS [Starkstein et al., 1992].

We also administered the Beck Depression Inventory-II (BDI) to all subjects. Kirsch-Darrow *et al.* evaluated the BDI and dissociated its items into 4 factors (apathy, dysphoric mood, loss of interest/pleasure, somatic factor) [Kirsch-Darrow et al., 2011]; the *loss of interest/pleasure* factor was shown to be sensitive to symptoms of both depression and apathy, whereas the *somatic* factor can be influenced by other PD-related symptoms. The 11 items comprising the *dysphoric mood* factor loaded on negativity/sadness – symptoms not related to apathy –, and showed the lowest correlation with apathetic symptoms. We therefore used the score in these 11 items (henceforth referred to as *dysphoric mood score*) as covariates of no interest in connectivity analyses to control for the presence of associated depression.

Neuropsychological assessment

Subjects were administered a thorough neuropsychological battery assessing cognitive functions frequently impaired in PD, using the following tests:

Attention/executive functions: backward minus forward digit spans; Trail-Making Test part A minus part B scores; phonemic fluency scores (words beginning with "P" produced in 60 seconds), and Stroop Color-Word Test interference scores). *Visuospatial/visuoperceptual functions:* Benton's Visual Form Discrimination and Judgment of Line Orientation tests. *Memory:* Rey's Auditory Verbal Learning Test total learning and 20-minute free recall scores. Composite z-scores for each cognitive

function (referred to as *A/E scores*, *memory scores* and *VS/VP scores*) were calculated as the mean of the z-scores of all tests within that function.

MRI acquisition

Images for all subjects were obtained with a 3T MRI scanner (MAGNETOM Trio, Siemens, Germany), using an 8-channel head coil. The scanning protocol included a resting-state, 5-minute-long functional gradient-echo echo-planar imaging sequence (150 T2*-weighted volumes, TR=2 s, TE=19 ms, flip angle=90^0, slice thickness=3 mm, FOV=240 mm, in which subjects were instructed to keep their eyes closed, not to think of anything in particular and not to fall asleep), a high-resolution 3D structural T1-weighted MPRAGE sequence acquired sagittally (TR=2.3 s, TE=2.98 ms, 240 slices, FOV=256 mm; 1 mm isotropic voxel) and a T2-weighted axial FLAIR sequence (TR=9 s, TE=96 ms).

Processing of fMRI

The preprocessing of resting-state images was performed with FSL (http://www.fmrib.ox.ac.uk/fsl/) and AFNI (http://afni.nimh.nih.gov/afni). Briefly, it included removal of the first 5 volumes to allow for T1 saturation effects, skull stripping, grandmean scaling and temporal filtering (bandpass filtering of 0.01-0.1 Hz). To control for the effect of subject head movement, physiological artifacts (e.g., breathing and vascular) and other non-neural sources of signal variation on the estimation of connectivity, motion correction and regression of nuisance signals (six motion parameters, cerebrospinal fluid and white matter) were performed. To remove the effects of images corrupted by motion, a scrubbing procedure, as suggested elsewhere [Power et al., 2012] was applied. Images were then smoothed with a 6-mm full-width at half maximum Gaussian kernel.

Additionally, individual subject head motion was calculated for translatory and rotatory movements according to the following formula:

$$\frac{1}{M-1}\sum_{i=2}^{M}\sqrt{|x_i - x_{i-1}|^2 + |y_i - y_{i-1}|^2 + |z_i - z_{i-1}|^2},$$

where x_i, y_i and z_i are translations or rotations in the three axes at timepoint i, and M is the total number of timepoints (145) [Liu et al., 2008].

Definition of regions of interest

The frontal cortices were parcellated into *limbic* (anterior orbital gyrus, posterior orbital gyrus, medial orbital gyrus, gyrus rectus, and subcallosal gyrus/ventral anterior cingulate), *executive* (rostral superior and middle frontal gyri and dorsal prefrontal cortex), *rostral motor* (caudal portions of lateral and medial superior frontal gyrus, caudal middle and inferior frontal gyrus) and *caudal motor* (precentral gyrus and caudal premotor area), as described by Tziortzi *et al*. [Tziortzi et al., 2014]. In this study, these frontal divisions were used as seeds for probabilistic tractography analyses that defined the functional striatal subregions included in the Oxford-GSK-Imanova Striatal Connectivity Atlas, which we used to parcellate the striata into limbic, executive and sensorimotor regions. We also included the thalami, defined using the Harvard-Oxford subcortical structural atlas. The Supplementary Figure displays the frontal and striatal segmentation scheme used.

To obtain each seed region's resting-state fMRI time series, the mask for each structure was non-linearly registered to each subject's T1-weighted image using FSL FNIRT, and subsequently registered to native functional space through linear transformation with FSL FLIRT.

Connectivity analysis

Interregional connectivity analyses were performed with FSL (release 5.0.4, http://fsl.fmrib.ox.ac.uk/fsl/fslwiki/FSL) and AFNI tools. Initially, a mean time series was obtained from each seed region (4 frontal, 3 striatal, 1 thalamic per hemisphere) by averaging the time series of every voxel contained in it prior to the smoothing step, in native functional space. Subsequently, these time series were correlated with the time series of every voxel inside the regions of interest, thus

producing a correlation map for each ROI in which each voxel's value is given by the resulting Pearson's r coefficient. These maps were then converted to z maps using Fisher's r to z transformation.

Cortical and subcortical gray matter volume analysis – voxel-based morphometry

Structural data was analyzed with FSL-VBM [Douaud et al., 2007], a voxel-based morphometry (VBM)-style analysis carried out with FSL. First, nonbrain tissue from structural images was extracted. After segmentation, GM images were aligned to MNI152 standard space using affine registration. The resulting images were averaged to create a study-specific template, to which the native GM images were then non-linearly re-registered. The registered partial volume images were then modulated (to correct for local expansion or contraction) by dividing by the Jacobian of the warp field. The modulated segmented images were then smoothed with an isotropic Gaussian kernel with a sigma of 3 mm.

Subcortical volumetry and shape analysis

Subcortical structures of interest (nucleus accumbens, pallidum, caudate nucleus, putamen and thalamus) were segmented using FIRST as implemented in FSL. Since subcortical structural volumes scale with head size, we used FSL SIENAX to calculate intracranial volumes (adding total GM, total WM and cerebrospinal volumes), to be entered as nuisance factors in volume analyses. For shape analysis, surface meshes were fitted for each region of interest as a vertex distribution model, modelling its shape. Multivariate testing was then performed on the 3-dimensional coordinates of each vertex, followed by multiple-comparison correction, thus allowing the detection of localized structural changes [Patenaude et al., 2011].

White-matter hyperintensity load analysis

To detect and quantify global (periventricular + deep) WM hyperintensity load, we used an automated segmentation procedure [Ithapu et al., 2014] using FLAIR and T1-weighted images. Results are given in normalized volumes taking brain volume into account.

Statistical analysis

A voxelwise general linear model was applied using permutation-based non-parametric testing (5000 permutations, using FSL) for connectivity and VBM, testing all voxels inside the regions of interest (frontal lobes, striata, thalami), as well as for shape analyses. To evaluate the association between the presence of apathy and changes in functional connectivity, GM volume or shape, we performed both intergroup comparisons (HC, PD-NA, PD-A) and correlations (AS scores). Sex and dysphoric mood scores were entered as covariates of no interest in all analyses. Since group differences were found for A/E and memory scores, these variables were entered in intergroup analyses; for correlation analyses memory scores were entered as a nuisance factor as they correlated with AS scores. Significance level was set at $p<.05$, corrected for multiple comparisons using the false-discovery rate (FDR).

Statistical analyses for sociodemographic/clinical data as well as subcortical volume were performed using SPSS Statistics 20.0.0 (Chicago, IL, http://www-01.ibm.com/software/analytics/spss/). Pearson's chi-square test was used to compare categorical variables (hand dominance, sex, HY stage). Student's t-test was used to compare clinical and connectivity data means between patient subgroups (PD-NA, PD-A). Three-level one-way ANOVAs were used to compare clinical and sociodemographic data between HC and patient subgroups. Three-level one-way analyses of covariance were used to compare subcortical volumes between HC and patient subgroups while controlling for variables that presented intergroup differences in the previous step. Pearson's correlation was used to evaluate the relationship between demographic, clinical and neuropsychological measures. Partial correlations were performed in the HC group and in the collapsed PD group to assess the relationship between subcortical volumes and AS scores, while controlling for the variables that correlated significantly with them. Statistical significance threshold was set at $p<.05$.

RESULTS

Neuropsychiatric assessment

Twenty-six PD patients (41.3%) were classified as apathetic (AS>13). Table 1 shows sociodemographic, clinical and head motion characteristics of the subject groups. There were no intergroup differences in age or years of education, although there were significant sex differences (men tended to be overrepresented in the apathetic PD (PD-A) group). As expected, BDI dysphoric mood scores were significantly higher in apathetic patients (PD-A) than in non-apathetic patients (PD-NA). LEDD and measures of disease severity (HY, UPDRS scores) or duration were not significantly different between PD-A and PD-NA, and did not correlate significantly with AS, BDI or dysphoric mood scores.

The proportion of PD patients taking antidepressant medication was similar in both groups (6 PD-NA, 5 PD-A, p=0.702, Pearson's chi-square=0.146); AS and neuropsychological scores were not significantly different between medicated and unmedicated patients.

AS scores significantly correlated with memory scores (r=-0.36, p=.004), whereas no significant effects were found for A/E (p=0.503) or MMSE (p=0.694) scores. Dysphoric mood scores did not correlate significantly with cognitive scores.

	HC n=31	**PD-NA n=37**	**PD-A n=25**	**Test stats/*p***	**Significant post-hoc Bonferroni test (*p*)**
Age	64.55 (9.21)	63.43 (8.45)	65.60 (12.89)	.352/.704	
Education (yrs.)	11.00 (4.28)	11.16 (5.39)	8.88 (3.57)	2.118/.126	
Sex (male/female)	15/16	17/20	20/5	**8.088/.018** χ	
MMSE	29.68 (0.48)	29.14 (1.06)	28.96 (1.17)	**4.621/.012**	PD-A<HC (.017), PD-NA<HC (.061)
AS	7.31 (4.44)	7.49 (3.60)	19.36 (4.13)	**79.742/<.001**	PD-A>HC (<.001), PD-A>PD-NA (<.001)
BDI	6.37 (5.90)	7.22 (4.44)	14.8 (5.39)	**21.497/<.001**	
Dysphoric mood score	2.16 (2.49)	2.32 (2.33)	5.60 (2.90)	**15.834/<.001**	
Hand dominance (r/l)	30/1	36/1	25/0	.773/.679 χ	
Disease duration	-	7.54 (5.52)	7.24 (4.13)	.245/.807 †	
UPDRS	-	15.37 (8.48)	15.56 (7.94)	.087/.931 †	
HY (I/II/III)	-	13/22/2	8/13/4	1.921/.383 χ	
LEDD (mg)	-	687.8 (459.9)	845.2 (471.3)	1.309/.196 †	
A/E scores	.09 (.61)	-.24 (0.89)	-.51 (1.11)	**3.257/.043**	PD-A<HC (.040)
Memory scores	.06 (.90)	-.17 (1.42)	-1.16 (1.07)	**8.142/.001**	PD-A<HC (.001), PD-A<PD-NA (.005)
VS/VP scores	.00 (.80)	-.41 (.82)	-.48 (1.12)	2.503/.098	
Rotatory head movement (mm)	.03 (.01)	.05 (.04)	.04 (.02)	**4.952/.009**	PD-NA>HC (.028)
Translatory head movement (degrees)	.08 (.05)	.07 (.04)	.07 (.04)	.428/.653	
Normalized WM hyperintensity volume	799.2 (1017)	792.9 (1354.4)	1000.9 (992.7)	.287/.751	

Table 1. Sociodemographic, clinical, head motion and white-matter hyperintensity characteristics of participants with intergroup comparisons. Results are presented in means (SD). Statistically significant results (p<.05) are marked in bold. *AS*: apathy scale; *BDI*: Beck depression inventory-II; *Disease duration*: duration of motor symptoms, in years; *UPDRS*: unified Parkinson's disease rating scale, motor section; *HY*: Hoehn and Yahr scale; *LEDD*: levodopa equivalent daily dose; *A/E*: attention/executive; *VS/VP*: visuospatial/visuoperceptual; *WM*: white matter. *HC*: healthy controls; *PD-NA*: Parkinson's disease patients without apathy; *PD-A*: Parkinson's disease patients with apathy. *Test stats*: F-statistics, Pearson's chi-square (χ) or Student's t (†).

Fronto-striatal-thalamic connectivity analysis

PD-A patients showed significant connectivity reductions (p<.05, FDR-corrected) compared with HC and with PD-NA, mainly in left sided circuits and involving limbic regions (see Table 2 and Figure 1). Compared with HC, PD-A displayed reduced connectivity between the limbic striatal division and the rest of the left striatum. Moreover, the connectivity between the limbic division of the left striatum and the left frontal lobe was significantly reduced in PD-A compared with PD-NA; in PD-A compared to HC, there was suggestive evidence (p=.06, FDR-corrected) of reduced connectivity in the left orbitofrontal cortex and inferior frontal gyrus.

Correlation analyses in the collapsed PD sample showed that AS scores correlated negatively with the functional connectivity between both limbic and executive divisions of the left striatum and the left frontal lobe, and between the limbic region of the left frontal lobe and the left striatum. Additionally, AS scores correlated negatively with the functional connectivity between the different subdivisions of the left frontal lobe (see Figure 2 and Supplementary Table).

No significant connectivity changes were observed between PD-NA and HC, and no significant correlations were found in the HC group.

Significant intergroup and correlation analysis results are summarized schematically in Figure 3.

Connectivity results were maintained after adding head movement parameters as nuisance factors.

Seed	Contrast	Volume (mm^3)	maximum		Topography
			MNI coordinates (x,y,z)	p value	
Left limbic frontal lobe	HC>PD-A	1359	-15,6,-6	.032	Left limbic/executive/SM striatum
	PD-NA>PD-A	693	-27,-6,3	.016	Left executive/SM striatum
		666	-15,-18,21	.033	Left executive/limbic striatum
		99	-18,12,-12	.044	Left limbic striatum
Right limbic frontal lobe	HC>PD-NA	279	27,-3,-6	.005	Right executive/limbic striatum
	HC>PD-A	468	27,0,-9	.005	
Left limbic striatum	HC>PD-A	936	-21,-6,-6	.018	Left posterior limbic/executive/SM striatum
	PD-NA>PD-A	2142	-36,-24,51	.045	Left precentral gyrus
		1224	-27,27,21	.045	Left frontal pole
		477	-18,54,9	.045	Left paracingulate, frontal pole
		477	-36,27,-18	.045	Left OFC
		234	-60,-6,39	.045	Left PCG
		216	-9,-18,78	.045	
		216	-60,3,15	.045	
		99	-39,54,12	.048	Left frontal pole

Table 2. Significant intergroup connectivity differences. Description of clusters of significant intergroup connectivity differences, controlling for dysphoric mood, memory and attentional/executive scores, as well as sex. *HC*: healthy controls; *PD-A*: Parkinson's disease patients with apathy; *PD-NA*: Parkinson's disease patients without apathy. *SM*: sensorimotor; *OFC*: orbitofrontal cortex; *PCG*: precentral gyrus.

VBM, subcortical volume and shape analysis

No significant group differences or correlations with AS scores were observed for GM volume or subcortical volume/shape.

White-matter hyperintensity load

There were no significant intergroup differences or correlations between connectivity values in the clusters of significant intergroup differences and WM hyperintensity load.

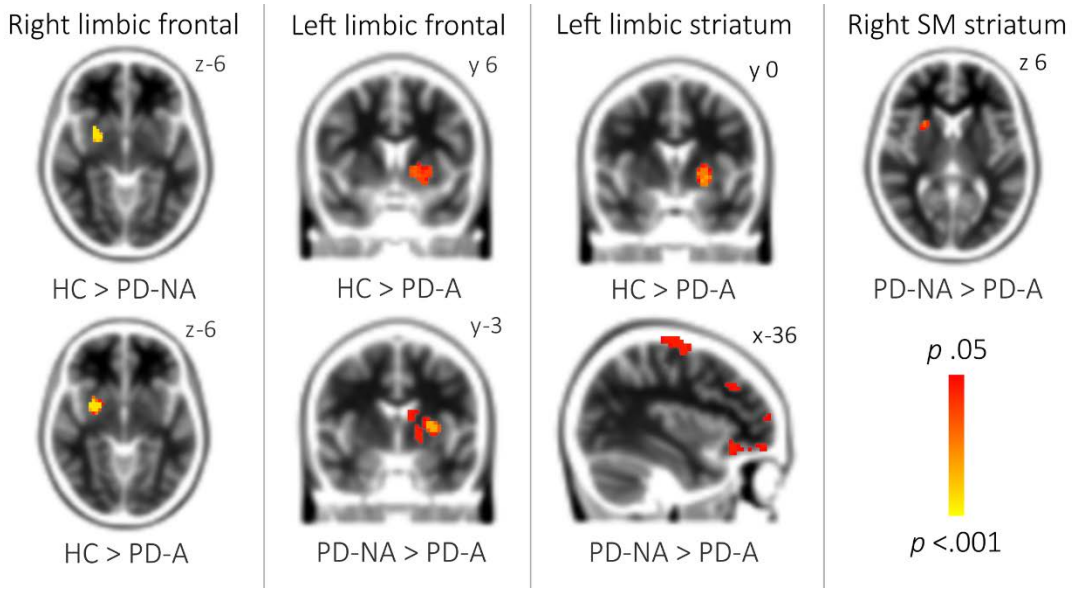

Figure 1. Significant intergroup connectivity differences. Color clusters indicate areas of significant (p<.05, false-discovery rate correction) intergroup differences in connectivity with the seed regions indicated at the top, controlling for sex, dysphoric mood scores, memory scores and attention/executive scores. Corrected p-values are indicated in the color bar. MNI coordinates of the slices shown are indicated. Right hemisphere is shown on the left in axial and coronal views. *SM*: sensorimotor; *HC*: healthy controls; *PD-A*: Parkinson's disease patients with apathy; *PD-NA*: Parkinson's disease patients without apathy.

DISCUSSION

The main finding of our study is that the presence of apathy in PD is associated with resting-state connectivity reductions affecting frontostriatal circuits, predominantly in the left hemisphere. These changes were observed while controlling for the presence of associated depressive symptoms and cognitive impairment, and were not accompanied by significant structural changes, suggesting that frontostriatal connectivity disruption plays a relevant role in PD-related apathy.

Our results indicate that the occurrence of apathy in PD is accompanied by a reduction in resting-state functional connectivity mainly affecting the limbic divisions of the striatum and of the prefrontal cortex. These structures are central components of the brain's reward and motivation systems [Haber, 2011], recently shown to be involved in PD-related apathy [Martínez-Horta et al., 2014]. Moreover, the limbic division of the left striatum showed reduced connectivity with the ipsilateral frontal cortex and with the rest of the left striatum. The limbic striatum is hypothesized to influence motor activity as the *limbic-motor interface* [Mogenson et al., 1980]; Haber *et al.* found evidence that the mechanism through which this region influences other striatal regions – and, consequently, prefrontal and motor cortices – involves a "striatonigrostriatal spiral" through connections with mesencephalic dopaminergic nuclei [Haber et al., 2000]. Dopamine deficits have been shown to result in reduced frontostriatal functional connectivity [Nagano-Saito et al., 2008]. The loss of mesencephalic dopaminergic neurons might thereby lead to the intrastriatal, frontostriatal and, ultimately, frontofrontal connectivity disruptions found in our study. Finally, the worsening of apathetic symptoms during the *off* state [Czernecki et al., 2002] and after dopaminergic treatment reduction following deep brain stimulation surgery [Czernecki et al., 2008], as well as its improvement with dopaminergic treatment [Devos et al., 2014; Thobois et al., 2010], suggest that dopamine deficiency is involved in PD-related apathy.

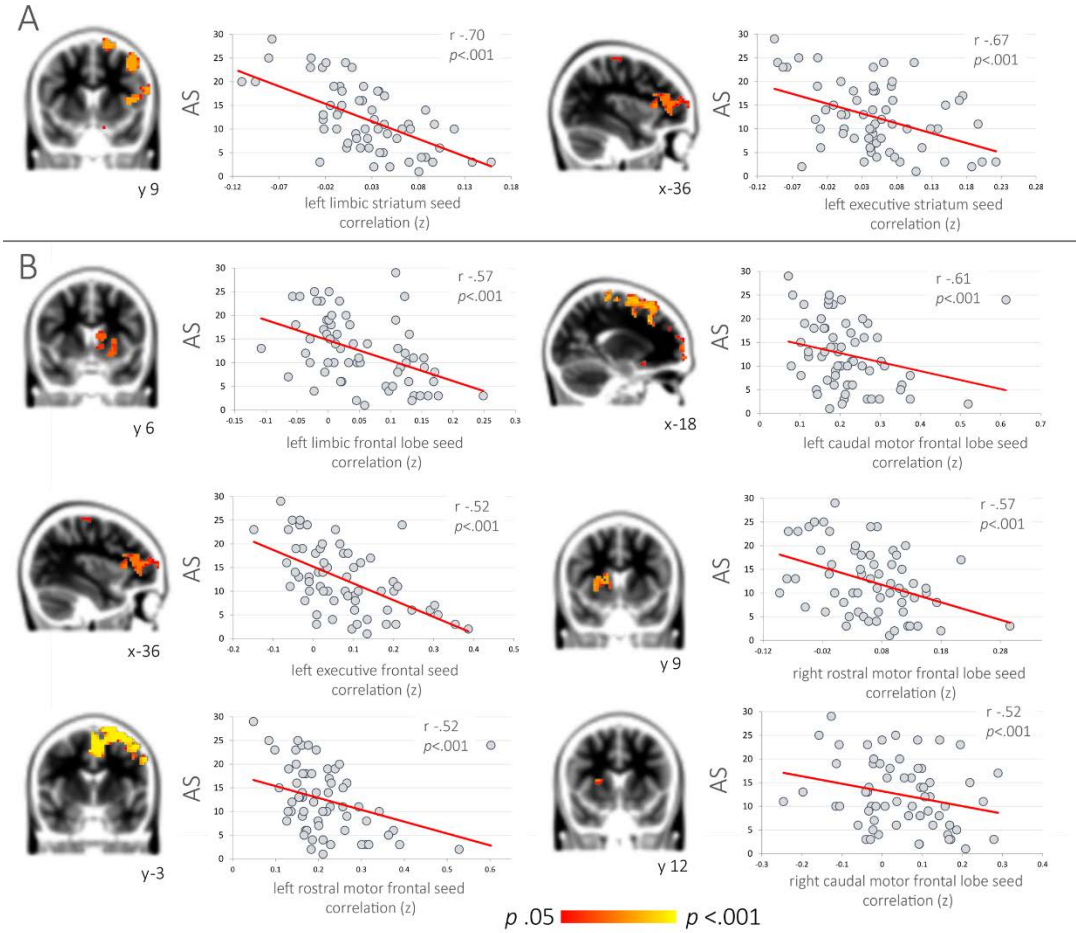

Figure 2. Significant correlation between connectivity and apathy scale scores in the Parkinson's disease patient group. Color clusters indicate areas of significant (p<.05, false-discovery rate correction) negative correlation between apathy scores and connectivity with the seed regions indicated in the adjacent scatterplots (*A*: striatal seeds; *B*: frontal seeds), controlling for sex, dysphoric mood scores and memory scores. Corrected p-values are indicated in the color bar. Scatterplots show the relationship between mean z connectivity values in the main significant clusters and apathy scale (AS) scores. Right hemisphere is shown on the left in axial and coronal views.

Taken together with our results, the findings described above provide evidence that reduced striato-frontal resting-state functional connectivity is associated with the occurrence of apathy in PD, and is probably mediated by dopamine deficits. Furthermore, the "striatonigrostriatal spiral" model links the connections between the limbic striatum and other striatal/frontal regions not only to ventral tegmental area (VTA) but also to substantia nigra pars compacta dopaminergic neurons [Haber et al., 2000].

The connectivity correlates found in our study had a clear left-sided predominance. This finding, alongside recently published studies, indicates that laterality of neuropathological changes influences the risk of developing apathy. Cubo *et al.* (2012), in a large sample of PD patients assessed up to 2 years from diagnosis, found that subjects with left-predominant motor symptoms (*i.e.*, with lesser left-sided dopamine deficits) were less likely to be apathetic [Cubo et al., 2012]. In line with these observations, the striatal volume correlates for apathy described by Carriere *et al.* were more

pronounced in left-hemisphere structures [Carriere et al., 2014]. Furthermore, in a recent study, Porat *et al.* (2014) found that off-medication PD patients with greater left-sided dopamine deficits had impaired approach motivation – a symptom of apathy –, whereas right-sided predominance was associated with impaired loss avoidance (possibly related to impulse control disorders) [Porat et al., 2014]. No such relationship was found in our sample, which may be related to the fact that most patients had bilateral disease at assessment.

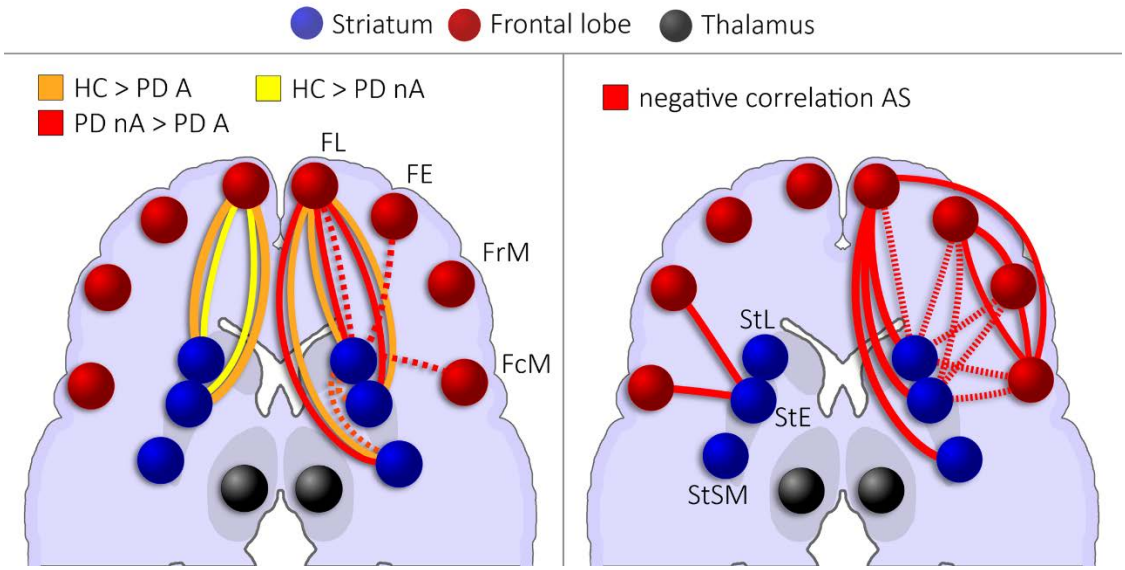

Figure 3. Schematic summary of significant findings. *Left:* significant intergroup connectivity differences (intergroup contrasts indicated by line color). *Right:* significant negative correlations between apathy scale scores and connectivity in the Parkinson's disease patient group. Continuous lines: results from frontal seed analyses; dashed lines: results from striatal seed analyses. Right hemisphere is depicted on the left. *HC*: healthy control group; *PD-A*: Parkinson's disease patients with apathy; *PD-NA*: Parkinson's disease patients without apathy; *FL*: frontal lobe, limbic division; *FE*: frontal lobe, executive division; *FrM*: frontal lobe, rostral motor division; *FcM*: frontal lobe, caudal motor division; *StL*: striatum, limbic division; *StE*: striatum, executive division; *StSM*: striatum, sensorimotor division.

GM atrophy, which was not found in our study, has been inconsistently reported in association with apathy in PD. Reijnders *et al.* described that the degree of apathy correlated with frontal, insular and parietal reductions in GM volume [Reijnders et al., 2010], whereas Isella *et al.* failed to find structural correlates [Isella et al., 2002]. Carriere *et al.*, on the other hand, evaluating patients with dopamine-resistant apathy through shape analysis, found striatal volume reductions, mainly in the nucleus accumbens, but no cortical thinning [Carriere et al., 2014]. These variable results may be a consequence of the distinct techniques used, different sample characteristics and different control over potential confounds such as cognitive deficits and motor disability [Kostić and Filippi, 2011]. Taking into consideration the known patterns of PD evolution, it is conceivable that apathy in early PD is mediated by disrupted frontostriatal connectivity secondary to mesencephalic dopaminergic neuron degeneration; and, as the degenerative process progresses to forebrain structures, frontal and striatal atrophy acquire a more important role in its pathophysiology. Longitudinal and radionuclide imaging studies are necessary to confirm this hypothesis and help disentangle the neurochemical and anatomical substrates of apathy in PD.

Finally, apathy in our study was seen to be associated with worse cognitive performance, namely in attention/executive and memory functions, giving support to the association between apathy and

cognitive deficits in PD [Butterfield et al., 2010; Dujardin et al., 2007; Pluck and Brown, 2002]. Apathy was also more common in male patients, a finding that has been inconsistently reported [Dujardin et al., 2007; Pedersen et al., 2010; Pluck and Brown, 2002].

Some limitations must be considered when interpreting our results. Groups were not matched for depressive symptoms or cognitive status. Although we did correct all connectivity analyses for these variables, we cannot exclude that they influenced the results obtained. Nonetheless, considering the high coexistence of apathy and depression or cognitive decline, our study sample is probably representative of the general population of apathetic PD patients. Additionally, despite rigorous exclusion criteria, our study groups were not matched for head movement, which can have significant effects on connectivity parameters [Van Dijk et al., 2012]. We have nonetheless applied several preprocessing steps to minimize these effects. The fact that results were maintained after adding movement parameters as covariates, and that the main group differences were found between HC and PD-A (which did not differ in head movement measures) suggests that the observed effects are not artifactual. Finally, although we did not find GM structural correlates for apathy, we cannot exclude that white matter degeneration is related to the connectivity changes observed.

In conclusion, our findings suggest that apathy in PD is associated with reduced resting-state connectivity in frontostriatal circuits, mainly affecting its left-hemisphere limbic/ventromedial regions but also extending to premotor and primary motor regions, even in the absence of significant structural degeneration and while controlling for associated depression and cognitive decline. These findings are compatible with the purported involvement of dopamine deficits in frontostriatal pathways in the genesis of apathy symptoms in PD.

SUPPLEMENTARY MATERIALS

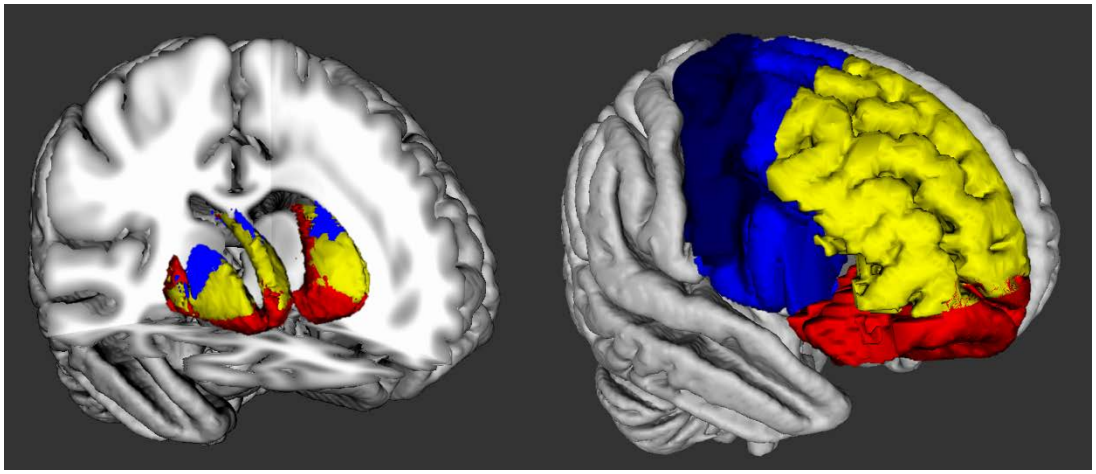

Supplementary Figure. Frontal and striatal divisions used as seeds in connectivity analyses. Top figure shows the striatal segmentation into limbic (red), executive (yellow) and sensorimotor (blue) divisions. Bottom figure displays the frontal cortical segmentation into limbic (red), executive (yellow), rostral motor (light blue) and caudal motor (dark blue).

Seed	Volume (mm^3)	MNI coordinates of maximum (x,y,z)	r/p	Topography
Left limbic striatum	12825	-57,15,0	-.70/<.001	Left IFG, frontal operculum, PCG, MFG, FP
	306	-27,30,-6	-.41/.001	Left OFC
	225	-12,48,21	-.51/<.001	Left anterior paracingulate
	153	-12,-24,78	-.32/.015	Left PCG
Left executive striatum	2466	-36,39,0	-.67/<.001	Left IFG, frontal pole, frontal operculum
	765	-18,-9,69	-.50/<.001	Left PCG, SFG
Left limbic frontal lobe	2205	-21,3,-12	-.57/<.001	Left limbic/executive/SM striatum
Left executive frontal lobe	2034	-39,-18,60	-.52/<.001	Left PCG, MFG
	1332	-21,54,-3	-.57/<.001	Left frontal pole
	963	-6,-9,45	-.46/<.001	Left PCG, SMA
	135	-18,-24,63	-.42/.001	
Left RMF lobe	15264	-60,-6,39	-.64/<.001	Left PCG, SMA, SFG, FP
Left CMF lobe	14373	-54,0,33	-.61/<.001	Left PCG, MFG, SFG, SMA
	1233	-12,69,-9	-.44/.001	Left frontal pole
	585	-21,39,24	-.59/<.001	
Right RMF lobe	945	30,12,-3	-.57/<.001	Right executive striatum
Right CMF lobe	108	27,12,9	-.52/<.001	Right executive striatum

Supplementary Table. Significant correlation between connectivity and apathy scale scores in the PD group. Description of clusters of significant negative correlation between apathy scale scores and connectivity levels, controlling for dysphoric mood and memory scores, as well as sex. *r*: partial correlation coefficient, obtained from the average value of all voxels inside the respective cluster. *RMF*: rostral motor frontal; *CMF*: caudal motor frontal; *FP*: frontal pole. *IFG*: inferior frontal gyrus; *MFG*: middle frontal gyrus; *OFC*: orbitofrontal cortex; *PCG*: precentral gyrus; *SM*: sensorimotor; *SMA*: supplementary motor area.

REFERENCES

1. Aarsland D, Larsen JP, Lim NG, Janvin C, Karlsen K, Tandberg E, Cummings JL (1999): Range of neuropsychiatric disturbances in patients with Parkinson's disease. J Neurol Neurosurg Psychiatry 67:492–6.
2. Braak H, Tredici K Del, Rüb U, de Vos R a. ., Jansen Steur EN., Braak E (2003): Staging of brain pathology related to sporadic Parkinson's disease. Neurobiol Aging 24:197–211.
3. Butterfield LC, Cimino CR, Oelke LE, Hauser R a, Sanchez-Ramos J (2010): The independent influence of apathy and depression on cognitive functioning in Parkinson's disease. Neuropsychology 24:721–30.
4. Carriere N, Besson P, Dujardin K, Duhamel A, Defebvre L, Delmaire C, Devos D (2014): Apathy in Parkinson's disease is associated with nucleus accumbens atrophy: A magnetic resonance imaging shape analysis. Mov Disord 00:1–7.
5. Cubo E, Benito-León J, Coronell C, Armesto D (2012): Clinical correlates of apathy in patients recently diagnosed with Parkinson's disease: the ANIMO study. Neuroepidemiology 38:48–55.
6. Czernecki V, Pillon B, Houeto JL, Pochon JB, Levy R, Dubois B (2002): Motivation, reward, and Parkinson's disease: influence of dopatherapy. Neuropsychologia 40:2257–67.
7. Czernecki V, Schüpbach M, Yaici S, Lévy R, Bardinet E, Yelnik J, Dubois B, Agid Y (2008): Apathy following subthalamic stimulation in Parkinson disease: a dopamine responsive symptom. Mov Disord 23:964–9.
8. Daniel SE, Lees AJ (1993): Parkinson's Disease Society Brain Bank, London: overview and research. J Neural Transm Suppl 39:165–72.
9. Devos D, Moreau C, Maltête D, Lefaucheur R, Kreisler A, Eusebio A, Defer G, Ouk T, Azulay J-P, Krystkowiak P, Witjas T, Delliaux M, Destée A, Duhamel A, Bordet R, Defebvre L, Dujardin K (2014): Rivastigmine in apathetic but dementia and depression-free patients with Parkinson's disease: a double-blind, placebo-controlled, randomised clinical trial. J Neurol Neurosurg Psychiatry 85:668–74.
10. Van Dijk KR a, Sabuncu MR, Buckner RL (2012): The influence of head motion on intrinsic functional connectivity MRI. Neuroimage 59:431–8.
11. Douaud G, Smith S, Jenkinson M, Behrens T, Johansen-Berg H, Vickers J, James S, Voets N, Watkins K, Matthews PM, James A (2007): Anatomically related grey and white matter abnormalities in adolescent-onset schizophrenia. Brain 130:2375–86.
12. Dujardin K, Sockeel P, Delliaux M, Destée A, Defebvre L (2009): Apathy may herald cognitive decline and dementia in Parkinson's disease. Mov Disord 24:2391–7.
13. Dujardin K, Sockeel P, Devos D, Delliaux M, Krystkowiak P, Destée A, Defebvre L (2007): Characteristics of apathy in Parkinson's disease. Mov Disord 22:778–84.
14. Emre M, Aarsland D, Brown R, Burn DJ, Duyckaerts C, Mizuno Y, Broe GA, Cummings J, Dickson DW, Gauthier S, Goldman J, Goetz C, Korczyn A, Lees A, Levy R, Litvan I, McKeith I, Olanow W, Poewe W, Quinn N, Sampaio C, Tolosa E, Dubois B (2007): Clinical diagnostic criteria for dementia associated with Parkinson's disease. Mov Disord 22:1689–707; quiz 1837.
15. Haber SN (2011): Neuroanatomy of Reward: A View from the Ventral Striatum. In: Gottfried, J, editor. Neurobiology of Sensation and Reward. Boca Raton (FL): CRC Press.
16. Haber SN, Fudge JL, McFarland NR (2000): Striatonigrostriatal pathways in primates form an ascending spiral from the shell to the dorsolateral striatum. J Neurosci 20:2369–82.
17. Isella V, Melzi P, Grimaldi M, Iurlaro S, Piolti R, Ferrarese C, Frattola L, Appollonio I (2002): Clinical, neuropsychological, and morphometric correlates of apathy in Parkinson's disease. Mov Disord 17:366–71.
18. Ithapu V, Singh V, Lindner C, Austin BP, Hinrichs C, Carlsson CM, Bendlin BB, Johnson SC (2014): Extracting and summarizing white matter hyperintensities using supervised segmentation methods in Alzheimer's disease risk and aging studies. Hum Brain Mapp 4235:4219–4235.
19. Kirsch-Darrow L, Fernandez HH, Fernandez HF, Marsiske M, Okun MS, Bowers D (2006): Dissociating apathy and depression in Parkinson disease. Neurology 67:33–8.
20. Kirsch-Darrow L, Marsiske M, Okun MS, Bauer R, Bowers D (2011): Apathy and depression: separate factors in Parkinson's disease. J Int Neuropsychol Soc 17:1058–66.
21. Kostić VS, Filippi M (2011): Neuroanatomical correlates of depression and apathy in Parkinson's disease: magnetic resonance imaging studies. J Neurol Sci 310:61–3.
22. Leentjens AFG, Dujardin K, Marsh L, Martinez-Martin P, Richard IH, Starkstein SE, Weintraub D, Sampaio C, Poewe W, Rascol O, Stebbins GT, Goetz CG (2008): Apathy and anhedonia rating scales in Parkinson's disease: critique and recommendations. Mov Disord 23:2004–14.
23. Levy R, Dubois B (2006): Apathy and the functional anatomy of the prefrontal cortex-basal ganglia circuits. Cereb Cortex 16:916–28.
24. Liu Y, Liang M, Zhou Y, He Y, Hao Y, Song M, Yu C, Liu H, Liu Z, Jiang T (2008): Disrupted small-world networks in schizophrenia. Brain 131:945–61.
25. Marin RS (1990): Differential diagnosis and classification of apathy. Am J Psychiatry 147:22–30.

26. Martínez-Horta S, Riba J, de Bobadilla RF, Pagonabarraga J, Pascual-Sedano B, Antonijoan RM, Romero S, Mañanas MÀ, García-Sanchez C, Kulisevsky J (2014): Apathy in Parkinson's disease: neurophysiological evidence of impaired incentive processing. J Neurosci 34:5918–26.
27. Mogenson GJ, Jones DL, Yim CHIYIU (1980): From motivation to action: functional interface between the limbic system and the motor system. Prog Neurobiol 14:69–97.
28. Nagano-Saito A, Leyton M, Monchi O, Goldberg YK, He Y, Dagher A (2008): Dopamine depletion impairs frontostriatal functional connectivity during a set-shifting task. J Neurosci 28:3697–706.
29. Patenaude B, Smith SM, Kennedy DN, Jenkinson M (2011): A Bayesian model of shape and appearance for subcortical brain segmentation. Neuroimage 56:907–22.
30. Pedersen KF, Alves G, Brønnick K, Aarsland D, Tysnes O-B, Larsen JP (2010): Apathy in drug-naïve patients with incident Parkinson's disease: the Norwegian ParkWest study. J Neurol 257:217–23.
31. Pluck GC, Brown RG (2002): Apathy in Parkinson ' s disease. J Neurol Neurosurg Psychiatry 73:636–643.
32. Porat O, Hassin-Baer S, Cohen OS, Markus A, Tomer R (2014): Asymmetric dopamine loss differentially affects effort to maximize gain or minimize loss. Cortex 51:82–91.
33. Power JD, Barnes KA, Snyder AZ, Schlaggar BL, Petersen SE (2012): Spurious but systematic correlations in functional connectivity MRI networks arise from subject motion. Neuroimage 59:2142–54.
34. Reijnders JSAM, Scholtissen B, Weber WEJ, Aalten P, Verhey FRJ, Leentjens AFG (2010): Neuroanatomical correlates of apathy in Parkinson's disease: A magnetic resonance imaging study using voxel-based morphometry. Mov Disord 25:2318–25.
35. Skidmore FM, Yang M, Baxter L, von Deneen K, Collingwood J, He G, Tandon R, Korenkevych D, Savenkov a, Heilman KM, Gold M, Liu Y (2013): Apathy, depression, and motor symptoms have distinct and separable resting activity patterns in idiopathic Parkinson disease. Neuroimage 81:484–95.
36. Starkstein SE, Mayberg HS, Preziosi TJ, Andrezejewski P, Leiguarda R, Robinson RG (1992): Reliability, validity, and clinical correlates of apathy in Parkinson's disease. J Neuropsychiatry Clin Neurosci 4:134–9.
37. Thobois S, Ardouin C, Lhommée E, Klinger H, Lagrange C, Xie J, Fraix V, Coelho Braga MC, Hassani R, Kistner A, Juphard A, Seigneuret E, Chabardes S, Mertens P, Polo G, Reilhac A, Costes N, LeBars D, Savasta M, Tremblay L, Quesada J-L, Bosson J-L, Benabid A-L, Broussolle E, Pollak P, Krack P (2010): Non-motor dopamine withdrawal syndrome after surgery for Parkinson's disease: predictors and underlying mesolimbic denervation. Brain 133:1111–27.
38. Thobois S, Lhommée E, Klinger H, Ardouin C, Schmitt E, Bichon A, Kistner A, Castrioto A, Xie J, Fraix V, Pelissier P, Chabardes S, Mertens P, Quesada J-L, Bosson J-L, Pollak P, Broussolle E, Krack P (2013): Parkinsonian apathy responds to dopaminergic stimulation of D2/D3 receptors with piribedil. Brain 136:1568–77.
39. Tomlinson CL, Stowe R, Patel S, Rick C, Gray R, Clarke CE (2010): Systematic review of levodopa dose equivalency reporting in Parkinson's disease. Mov Disord 25:2649–2653.
40. Tziortzi AC, Haber SN, Searle GE, Tsoumpas C, Long CJ, Shotbolt P, Douaud G, Jbabdi S, Behrens TEJ, Rabiner E a, Jenkinson M, Gunn RN (2014): Connectivity-based functional analysis of dopamine release in the striatum using diffusion-weighted MRI and positron emission tomography. Cereb Cortex 24:1165–77.

study 6

PROGRESSIVE CHANGES IN A RECOGNITION MEMORY NETWORK IN PARKINSON'S DISEASE

Journal of Neurology, Neurosurgery and Psychiatry 2013

Bàrbara Segura, Naroa Ibarretxe Bilbao, Roser Sala Llonch, Hugo César Baggio, Maria José Martí, Francesc Valldeoriola, Pere Vendrell, Núria Bargalló, Eduardo Tolosa, Carme Junqué

RESEARCH PAPER

Progressive changes in a recognition memory network in Parkinson's disease

Bàrbara Segura,[1] Naroa Ibarretxe-Bilbao,[1,2,3] Roser Sala-Llonch,[1] Hugo Cesar Baggio,[1] María Jose Martí,[2,4,5] Francesc Valldeoriola,[2,4,5] Pere Vendrell,[1,2,4] Nuria Bargalló,[4,6] Eduard Tolosa,[2,4,5] Carme Junqué[1,2,4]

► Additional supplementary material is published online only. To view these files please visit the journal online (http://dx.doi.org/10.1136/jnnp-2012-302822).

[1]Department of Psychiatry and Clinical Psychobiology, University of Barcelona, Barcelona, Spain
[2]Centro de Investigación en Red de Enfermedades Neurodegenerativas (CIBERNED), Hospital Clínic de Barcelona, Barcelona, Spain
[3]Department of Methods and Experimental Psychology, Faculty of Psychology and Education, University of Deusto, Bilbao, Spain
[4]Institute of Biomedical Research August Pi i Sunyer (IDIBAPS), Barcelona, Spain
[5]Parkinson's Disease and Movement Disorders Unit, Neurology Service, Institut Clínic de Neurociències (ICN), Hospital Clínic de Barcelona, Barcelona, Spain
[6]Centre de Diagnòstic per la Imatge Hospital Clinic de Barcelona (CDIC), Hospital Clínic de Barcelona, Barcelona, Spain

Correspondence to
Professor C Junque, Department of Psychiatry and Clinical Psychobiology, University of Barcelona, Casanova 143, Barcelona 08036, Spain; cjunque@ub.edu

Received 21 March 2012
Revised 31 August 2012
Accepted 20 September 2012
Published Online First 31 October 2012

ABSTRACT

Background In a previous functional MRI (fMRI) study, we found that patients with Parkinson's disease (PD) presented with dysfunctions in the recruitment of recognition memory networks. We aimed to investigate the changes in these networks over time.

Methods We studied 17 PD patients and 13 age and sex matched healthy subjects. In both groups fMRI (recognition memory paradigm) and neuropsychological assessments were obtained at baseline and at follow-up. To analyse changes over time in functional networks, model free (independent component analysis) analyses of the fMRI data were carried out. Then, a cross correlation approach was used to assess the changes in the strength of functional connectivity.

Results At follow-up, patients showed reduced recruitment of one network, including decreased activation in the orbitofrontal cortices, middle frontal gyri, frontal poles, anterior paracingulate cortex, superior parietal lobes and left middle temporal gyrus, as well as decreased deactivation in the anterior paracingulate gyrus and precuneus. Cross correlation analyses over time showed a decrease in the strength of functional connectivity between the middle frontal gyrus and the superior parietal lobe in PD patients.

Conclusions Model free fMRI and cross correlation connectivity analyses were able to detect progressive changes in functional networks involved in recognition memory in PD patients at early disease stages and without overt clinical deterioration. Functional connectivity analyses could be useful to monitor changes in brain networks underlying neuropsychological deficits in PD.

INTRODUCTION

Cognitive dysfunction occurs at the early stages of Parkinson's disease (PD) and most frequently involves impairment of memory, executive and visuoperceptual functions.[1 2] Regarding memory dysfunction, learning and delayed recall are known to be impaired in early disease stages. Recognition memory is not usually impaired at these stages, although it is in patients who fulfil the diagnostic criteria for dementia. In addition, recognition memory dysfunction has been related to the level of difficulty of the task.[3 4]

Functional connectivity refers to temporal correlations (concurrent activity) of spatially remote neurophysiological events. Functional MRI (fMRI) data can be analysed using model free fMRI approaches in order to obtain whole brain patterns of functional connectivity, as well as with cross correlation methods to quantify connectivity strength between two predefined brain regions, called *seeds*. While the first approach can be used as an exploratory method without a priori knowledge of the functional pattern, the second needs prior hypotheses regarding the brain regions that are considered to be connected.[5]

Tensorial probabilistic independent component analysis is a model free approach to analyse fMRI data. This method identifies patterns of coherent blood oxygen level dependent signal fluctuations across all voxels in the brain and groups such patterns into *components* in the spatial, temporal and subject domains.[6] Distinct functional networks made up of different brain areas can be characterised as distinct components using this technique. Studies using model free analyses have helped detect subtle progressive changes in brain function in other degenerative diseases, such as Alzheimer's disease.[7]

In a previous study, we used tensorial probabilistic independent component analysis to detect alterations in the functional cerebral network involved in recognition memory.[8] Compared with controls, PD patients showed a decreased task related activation in areas involved in this network. We also observed decreased task related deactivations in the default mode network (DMN), a group of spatially segregated brain structures which are more active during tasks that direct attention away from external stimuli or during the resting state, with functions related either to internal mentation or to the exploratory monitoring of the external environment when focused attention is reduced.[9] These results indicated that functional brain changes related to memory processes can occur prior to overt recognition memory deficits in PD patients.

In PD, different connectivity analysis methods have demonstrated abnormal patterns of interaction within brain networks involved in motor performance,[10–13] cognitive tasks such as attention to action[14] and card sorting tasks,[15] or in the resting state,[16 17] but deterioration over time of these connectivity patterns has not been investigated.

A longitudinal (^{18}F)-fluorodeoxyglucose–positron emission tomography (FDG-PET) study reported a progressive decline in metabolic activity in the medial prefrontal and parietal associative regions,[18]

which sustain cognitive functions that are impaired in PD.[19] However, to the best of our knowledge, specific recognition memory network deterioration and loss of functional connectivity strength between its specific areas has not been studied.

The two main aims of this study were: (1) to investigate how deterioration in recognition memory network activation patterns progresses using a model free approach and (2) to study the possible loss of functional connectivity strength between the main regions of this network over time.

METHODS

Participants

Patients were recruited from an outpatient Movement Disorders Clinical Neurology Service, Hospital Clinic i Provincial de Barcelona, in collaboration with the Department of Psychiatry and Clinical Psychobiology (University of Barcelona). Healthy controls were volunteers matched by age, gender and years of education with the patients. All subjects were right handed. The study subjects were part of a previously studied sample,[20] and were subsequently invited by telephone to participate in a follow-up evaluation (average period of 35.50 months, SD=1.85, range=31–40 months). At baseline, 24 early PD patients and 24 healthy controls participated in the study. In the follow-up assessment, 17 PD patients and 13 healthy controls agreed to participate (table 1).

Fourteen PD patients at baseline and all 17 patients at follow-up were taking antiparkinsonian drugs, consisting of different combinations of levodopa, levodopa with catechol-O-methyl transferase inhibitors, monoamine oxidase inhibitors, dopamine agonists and amantadine. All assessments were made while patients were in the on state. Levodopa equivalent daily doses (LEDD) were calculated as proposed by Tomlinson *et al*.[21] Six PD patients at baseline and four patients at follow-up were taking antidepressant drugs (see supplementary materials 1, available online only).

From the initial sample, two patients died, two moved to another province and three patients declined to participate. In the healthy control group, two subjects died, five subjects declined to participate and two could not be contacted. Two control subjects were excluded from the final analysis because of movement artefacts in the fMRI acquisition.

No significant differences were observed in baseline clinical or sociodemographic characteristics between the total initial sample and the final sample included in the longitudinal assessment, either for controls (age, sex and education, and Mini-Mental State Examination (MMSE), Beck Depression Inventory-II (BDI) or Neuropsychiatric Inventory (NPI) scores) or for PD patients (age, sex, education, disease duration, age at onset and LEDD, and MMSE, BDI, NPI, Unified Parkinson's Disease Rating Scale or Hoehn and Yahr scores) (see supplementary materials 1, available online only).

Table 1 Sociodemographic and clinical data for the participants at baseline

	PD (n=17)	Controls (n=13)	Test stats	p Value
Age (years)	59.59±8.29	57.15±10.57	0.17*	0.87
Sex (M/F)	13/4	10/3	0.001†	0.98
Education (years)	10.82±4.76	12.31±3.35	0.96*	0.35
Age at onset (years)	53.68±8.50	–	–	–
Disease duration (years)‡	2.91±1.04	–	–	–

Values are mean±SD.
Test stats: *Student's t test or †χ^2 test statistics.
‡Duration of motor symptoms.
PD, Parkinson's disease.

The inclusion criteria for participating in the study at baseline were: (i) fulfilment of the UK PD Society Brain Bank diagnostic criteria for PD[22]; (ii) Hoehn and Yahr stage ≤II; and (iii) disease duration ≤5 years. Exclusion criteria for all subjects were: (i) presence of dementia, as diagnosed by a neurologist according to the Movement Disorder Society diagnostic criteria for PD dementia[23]; (ii) presence of other neurological or psychiatric disorders, such as depression, which was evaluated by means of BDI[24]; and (iii) presence of visual hallucinations, assessed by the NPI questionnaire.[25]

The study was approved by the institutional ethics committee and all enrolled subjects gave written informed consent prior to taking part in the study.

Neuropsychological assessment

All participants underwent a comprehensive neuropsychological examination performed by a trained neuropsychologist (NI-B). The neuropsychologist in charge of the assessment was the same at the baseline and follow-up examinations. Verbal memory assessment was made using Rey's Auditory Verbal Learning Test (RAVLT).[26] The RAVLT variables computed were total learning, delayed memory recall after 20 min and recognition.

Additionally, other neuropsychological domains known to be impaired early in the course of PD were assessed using the forward digit span and backward digit span from the Wechsler Adults Intelligence Scale-III to measure working memory, and verbal fluency tests, including assessment of phonemic (total number of words starting with 'p' in 1 min) and semantic fluencies (number of animals in 1 min). Details of the neuropsychological battery used are described elsewhere.[8]

Statistical analyses of the neuropsychological and clinical variables were performed using the statistical package PASW-18 (SPSS, Inc, 2009, Chicago, Illinois, USA, http://www.spss.com). A general linear mixed model (GLM) for repeated measures was used to test whether variables changed in each group across time.

fMRI acquisition

Data were acquired with a 3 T Magnetom Tim Trio scanner (Siemens, Germany), using a multislice gradient echo, echo planar imaging functional sequence with the following parameters: repetition time (TR)=2000 ms; echo time (TE)=30 ms; 36×3 mm axial slices providing whole brain coverage. A T1 weighted structural image was also acquired for each subject with an MPRAGE 3D protocol (TR=2300 ms; TE=2.98 ms; inversion time=900 ms; FOV: 256×256 mm; 1 mm isotropic voxel).

Recognition memory fMRI paradigm

We used a recognition memory fMRI paradigm; the experimental design has been described in detail previously.[8]

In brief, before image acquisition, participants viewed a list of 35 words that they asked to remember. Afterwards, during scanning, subjects were asked to recognise the previously learned words from a list of 70 words. The experiment consisted of a 20 block design, with two conditions: recognition memory or control. In the recognition memory condition, participants had to recognise the previously learned words whereas in the control condition they had to detect the concatenation of letters 'AAAAAAA' from other possible combinations.

fMRI data analysis

Preprocessing of fMRI data

The following data preprocessing algorithm was carried out on the fMRI data set using FSL tools (FMRIB Software Library, http://www.fmrib.ox.ac.uk/fsl): motion correction using MCFLIRT,[27] removal of non-brain structures from the echo planar imaging volumes using BET,[28] spatial smoothing using a Gaussian kernel of 5 mm full width at half maximum (FWHM), mean based intensity normalisation of all volumes by the same factor (4D grand demean), high pass temporal filtering (FWHM=100 s) and Gaussian low pass temporal filtering (FWHM=11.2 s). The functional scans were registered to the MNI152 standard space through affine registration with FLIRT.[29]

Model based analysis

After preprocessing the data, model based fMRI data analysis was carried out using FEAT (FMRI Expert Analysis Tool) V.5.98, part of FSL. At the individual level, we obtained an activation map for each subject (recognition task>control task). Higher level analysis was then carried out using FLAME (FMRIB Local Analysis of Mixed Effects)[30 31] in order to explore between group differences and to obtain global average (one sample t test) activation maps (patients and controls). Z (gaussianised T/F) statistic images were thresholded using $Z>2.3$ and a corrected cluster significance threshold of $p\leq0.05$ using Gaussian random field theory to define each cluster's estimated significance level.

Independent component analysis

The preprocessing streamline was the same as that used in the model based analysis. Then, analysis of the task related fMRI images was carried out using tensorial independent component analysis, as implemented in the Multivariate Exploratory Linear Decomposition into Independent Components tool (MELODIC V.3.05),[6] part of FSL. MELODIC allows fMRI data to be decomposed into three-dimensional sets of vectors, also named independent components (IC), which describe signal variations across the temporal domain (time courses), the spatial domain (spatial maps) and the subject domain (subject modes). Spatial maps reflect brain regions of synchronous activations and deactivations, and subject modes reveal the strength of both of these activations and deactivations; higher subject mode values indicate higher activations and higher deactivations of the positive and negative parts of an IC, respectively. The number of IC dimensions was estimated by MELODIC using the Laplace approximation to the Bayesian evidence of the model order.[32] Spatial maps were thresholded modelling the probability of the noise class to 50% (using gamma densities).

The fMRI data set was decomposed into 18 IC. Afterwards, a selection of biologically relevant components was made, excluding the components that, according to the subject mode analysis, appeared to be driven by outliers, as well as artefactual components produced by motion, high frequency noise or vascular pulsations.[6] Five IC were finally selected, two associated with the task>control and three to the control>task contrast. Subsequently, we identified the main task related components by computing spatial correlations between the average activation maps obtained with FEAT and the selected IC. Z (gaussianised T/F) statistic images were thresholded using clusters determined by $Z\geq3$. IC1 was the task related component that showed the greatest spatial correlation with the task pattern identified in the model based analysis ($r=0.56$). Specific information about the other selected components is included in the supplementary materials (supplementary materials 2, available online only).

Cross correlation connectivity analysis

To investigate connectivity between the main activated regions of the recognition memory component, we created eight spherical 8 mm regions of interest (ROI) centred on the peak voxels of the most relevant clusters from the main task component obtained from the model free analysis (recognition memory network IC1).

From preprocessed fMRI data sets, the mean time course was extracted from each of these ROIs. Pearson's correlation coefficients were then computed between the time courses from each pair of ROIs and normalised using Fisher's r to Z transformation for each subject. A repeated measures GLM was used to test whether variables changed in each group across time. PASW-18 software was used to perform the statistical analyses.

The fMRI analysis pipeline is summarised in figure 1.

RESULTS

Clinical variables and neuropsychological performance

In the patient group, there were no statistically significant differences between baseline and follow-up LEDD or Hoehn and Yahr and Unified Parkinson's Disease Rating Scale motor section scores. Moreover, GLM analysis showed a significant time effect on MMSE and group effect on BDI. No significant group by time interaction was found for these variables. NPI did not show significant between group differences or over time changes (table 2).

Verbal memory performance, assessed by RAVLT, did not show any statistically significant effects for any of the variables analysed (table 2).

Supplementary materials 3 (available online only) show the results of the other neuropsychological tests used. Significant group differences were observed for semantic fluency and backward digit span. A significant group by time interaction was observed for forward digit span, resulting from a slight worsening in controls and a slight improvement in PD patients in performances over time.

Performance in the fMRI recognition memory task

In the fMRI recognition memory task performance, we found several significant time effects. Both patients and controls performed worse in the correct–reject responses at follow-up, but worsening was similar in both groups (group effect and group by time interaction were not significant). The main differences between groups were observed for false positive responses. For this variable, a significant group effect was seen—the performance of patients was worse than controls, and both groups presented a significant over time decline. In addition, the group by time interaction showed a trend to significance, indicating that the decline in this ability was more marked in patients (table 3).

fMRI data results

Model based analyses

Figure 2 depicts the areas involved in the recognition memory task for both groups. In both patients and controls, the regions that achieved significant activation during the task were located mainly in cortical areas, including the occipital lobes, bilateral orbitofrontal cortices and anterior paracingulate region (see also supplementary materials 4, available online only), but also included subcortical structures such as the left thalamus and the basal ganglia. This pattern was used to identify the main task related component in the model free analysis by

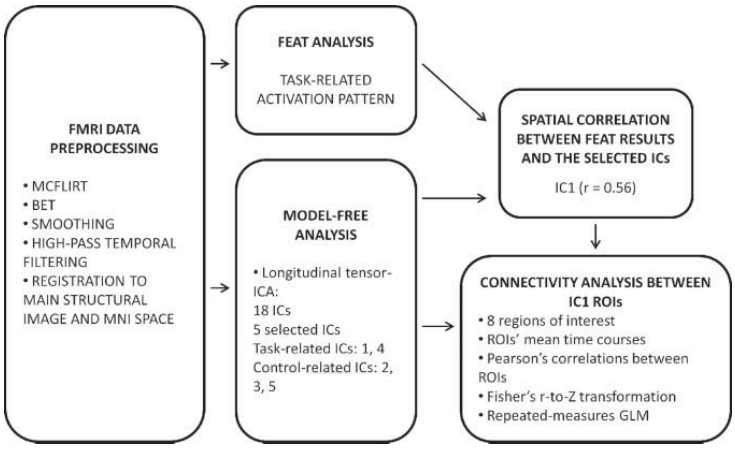

Figure 1 Functional MRI data preprocessing and analysis. GLM, general linear model; IC, independent components; ROIs, regions of interest.

calculating spatial correlations. Intergroup comparisons revealed no significant results.

Model free analysis

From the five task related components identified (see supplementary materials 1, available online only), IC1 was the only one to show decreased activity over time in PD patients ($p<0.04$). This independent component had a left hemisphere predominance and was characterised by activation in the bilateral orbitofrontal regions, bilateral middle frontal gyri, bilateral frontal poles, anterior paracingulate regions, bilateral superior parietal lobes and the posterior region of the left middle temporal gyrus. In the left frontal lobe, a single cluster of activation, with a peak in the left orbitofrontal area, included all of the above mentioned frontal regions. IC1 also involved deactivation in DMN areas, including the anterior part of the paracingulate gyrus and the precuneus (figure 3; see also supplementary materials 5, available online only).

Correlation analyses between IC1 activation and performance in the recognition task

A correlation analysis was performed between IC1 and individual activations–deactivations (subject modes) and recognition task results. In PD patients, there was a significant correlation between false positive errors and IC1 subject modes ($r=-0.403$, $p=0.027$), as well as with its complementary measure, the correct rejects ($r=0.403$, $p=0.027$). In the control group we did not observe any significant correlation.

Cross correlation connectivity analysis

The main spherical ROIs of 8 mm radius included the right middle frontal gyrus (RMFG), right superior parietal lobe, right frontal pole (RFP), right orbitofrontal cortex, anterior paracingulate cortex, left superior parietal lobe, left orbitofrontal cortex (LOFC) and left middle temporal gyrus. Longitudinal analyses of correlation coefficients between ROIs showed some significant effects, indicating deterioration of functional connectivity between specific regions of IC1 in PD patients. In this group, there was a decrease in functional connectivity (weaker positive correlation) between RMFG and bilateral superior parietal lobes, whereas the opposite effect was found in controls. Moreover, whereas in controls connectivity between RMFG and RFP decreased at follow-up, in PD patients it remained stable (table 4 and figure 4).

Correlation strength between the RFP and the left orbitofrontal cortex was significantly lower in PD patients than in

Table 2 Clinical data and memory performance at baseline and at follow-up, and time effect, group effect and group by time interaction

	PD (n=17)		Controls (n=13)				
	Baseline	Follow-up	Baseline	Follow-up	F (G×T)	F (G)	F (T)
MMSE	29.53 (0.51)	27.88 (2.55)	29.92 (0.28)	28.85 (0.69)	0.72	2.79	16.49*
BDI	7.53 (5.31)	5.65 (4.81)	3.31 (2.39)	2.62 (2.63)	0.59	7.50*	2.75
NPI	3.12 (5.38)	2.00 (1.90)	1.08 (1.44)	1.46 (1.66)	1.36	1.68	0.32
UPDRS	15.24 (3.68)	15.06 (4.41)	–	–	–	–	0.25
Hoehn and Yahr	1.77 (0.36)	1.85 (0.42)	–	–	–	–	0.68
LEDD	277.65 (308.51)	430.59 (350.78)	–	–	–	–	3.10
RAVLT learning	44.29 (12.20)	43.12 (10.69)	50.62 (9.09)	48.92 (10.10)	0.03	2.79	0.85
RAVLT delayed recall	8.59 (3.50)	9.41 (3.30)	10.39 (2.29)	9.92 (2.75)	2.03	1.25	0.16
RAVLT recognition	27.59 (2.24)	28.29 (2.34)	28.39 (1.9)	28.46 (1.94)	0.88	0.45	1.37

Values are mean (SD).
*Significant at $p \leq 0.05$.
The F values refer to those obtained with the repeated measures general linear model. F (G×T), group by time interaction; F (G), group effect; F (T), time effect.
BDI, Beck Depression Inventory-II; LEDD, levodopa equivalent daily dose; MMSE, Mini-Mental State Examination; NPI, Neuropsychiatric Inventory; PD, Parkinson's disease; RAVLT, Rey's Auditory Verbal Learning Test; UPDRS, Unified Parkinson's Disease Rating Scale, motor section.

Table 3 Functional MRI performance at baseline and at follow-up, time effect, group effect and group by time interaction

	PD (n=17)		Controls (n=13)				
	Baseline	Follow-up	Baseline	Follow-up	F (G×T)	F (G)	F (T)
Hits	54.69 (5.70)	54.94 (7.17)	54.85 (5.69)	56.62 (6.60)	0.16	0.29	0.24
Correct rejects	59.57 (9.98)	49.71 (20.04)	63.23 (9.09)	60.15 (6.69)	1.56	3.01	5.68*
False positives	11.31 (10.20)	27.19 (26.53)	6.77 (9.09)	9.85 (6.69)	3.44**	7.55*	5.13*
Missing	15.31 (7.17)	16.06 (8.37)	15.15 (5.70)	14.39 (6.50)	0.16	0.24	0.01
Reaction time	687.54 (152.83)	636.37 (134.28)	640.05 (83.75)	644.01 (70.12)	1.70	0.24	2.32

Values are mean (SD).
*p≤0.05, **p=0.07.
The F values refer to those obtained with the repeated measures general linear model. F (G×T), group by time interaction; F (G), group effect; F (T), time effect.
PD, Parkinson's disease.

controls. A significant over time decline in correlation strength between these structures was observed in both groups, with no significant group by time interaction. The strength of correlation between the right and left orbitofrontal cortices also decreased over time in both groups, with no significant group effect or group by time interaction (table 4). No other significant effects in the analyses of correlations between the selected ROIs were detected.

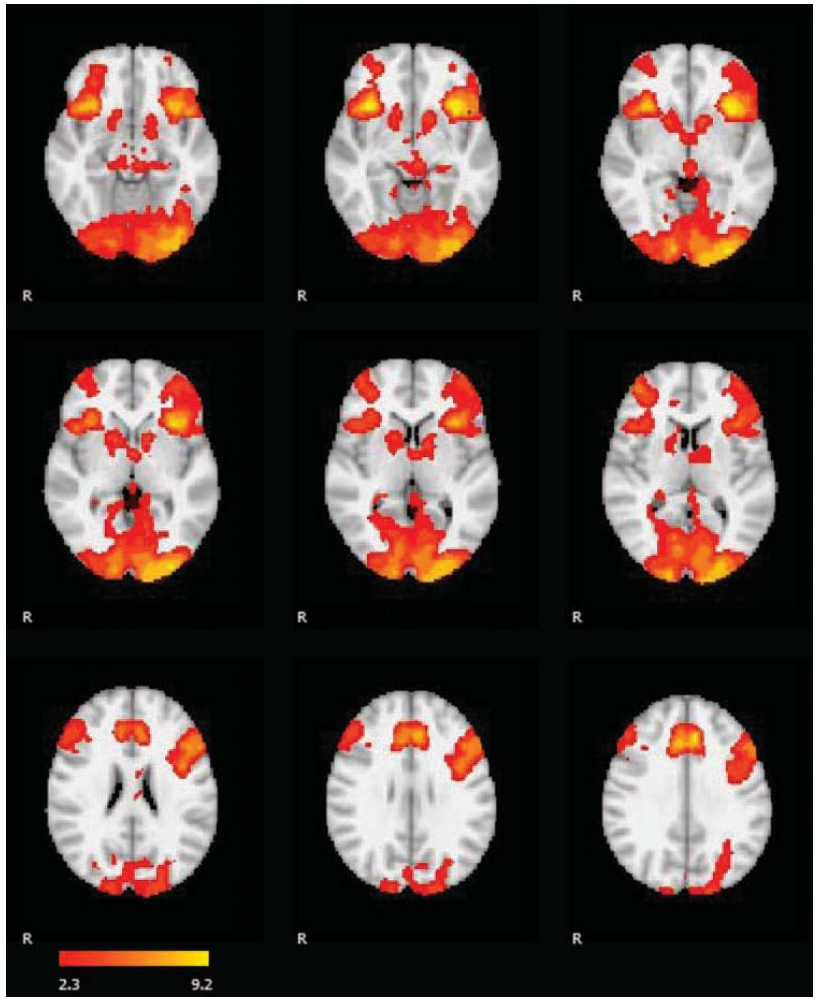

Figure 2 Functional MRI model based results. Average activation map (recognition task>control condition) was obtained from all subjects (Parkinson's disease patients and control group). Results are corrected at p<0.05 for multiple comparisons.

 J Neurol Neurosurg Psychiatry 2013;**84**:370–378. doi:10.1136/jnnp-2012-302822

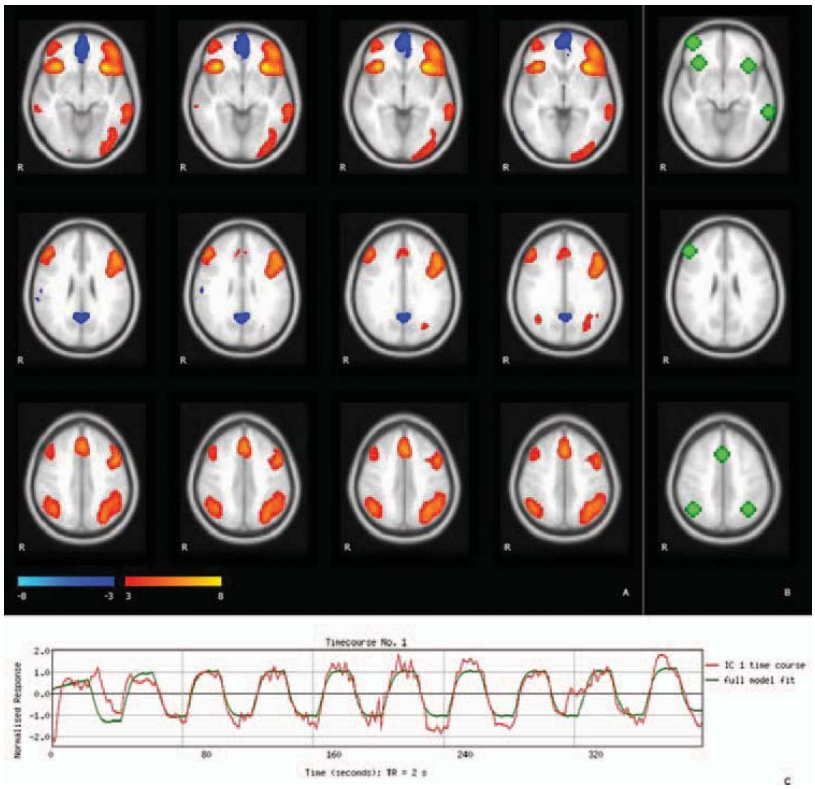

Figure 3 (A) Spatial pattern of independent component (IC)1 (recognition task>control), including activation areas (warm colours) and deactivation areas (cold colours). Parkinson's disease patients showed a decrease in activity in IC1 group over time ($p<0.04$). (B) Regions of interest (green) from peak voxels of task related activation areas in IC1, selected to perform cross correlation study (seed to seed connectivity). (C) Time courses represented the temporal profile of IC1 across group (red line) overlaid on the task paradigm (block design) (green line).

Finally, correlation strength between the right and left orbitofrontal cortices decreased over time in both groups (table 4). No other significant effects between the selected ROIs were detected.

DISCUSSION

In this study, we observed that PD patients presented with a progressive loss in the recognition memory network's pattern of activation and deactivation; moreover, the results revealed deterioration in the strength of connectivity between the main areas involved in this network.

In this study, with an average follow-up of 35.5 months, PD patients remained stable in terms of learning and memory, as assessed by clinical neuropsychological tests. However, we observed a decline in fMRI recognition task performance. The increase in false positive responses at follow-up was

Table 4 Correlation between verbal recognition network regions of interest at baseline and at follow-up, time effect, group effect and group by time interaction

	PD (n=17)		Controls (n=13)				
	Baseline	Follow-up	Baseline	Follow-up	F (G×T)	F (G)	F (T)
RMFG-RSPL	0.50 (0.26)	0.33 (0.20)	0.30 (0.22)	0.42 (0.29)	8.38*	0.52	0.31
RMFG-RFP	0.26 (0.33)	0.29 (0.25)	0.47 (0.14)	0.29 (0.17)	4.98*	1.92	2.38
RMFG-LSPL	0.45 (0.24)	0.25 (0.16)	0.31 (0.18)	0.42 (0.30)	8.09*	0.62	0.62
RFP-LOFC	0.24 (0.20)	0.10 (0.22)	0.32 (0.15)	0.25 (0.14)	1.13	4.34*	6.77*
ROFC-LOFC	0.37 (0.17)	0.24 (0.25)	0.51 (0.22)	0.37 (0.16)	0.04	3.87	13.67*

Values are mean (SD).
*$p \leq 0.05$.
Mean values are Pearson's correlation coefficients normalised using Fisher's r to Z transformation. The F values refer to those obtained with a repeated measures general linear model. F (G×T), group by time interaction; F (G), group effect; F (T), time effect.
LOFC, left orbitofrontal cortex; LSPL, left superior parietal lobe; PD, Parkinson's disease; RFP, right frontal pole; RMFG, right middle frontal gyrus; ROFC, right orbitofrontal cortex; RSPL, right superior parietal lobe.

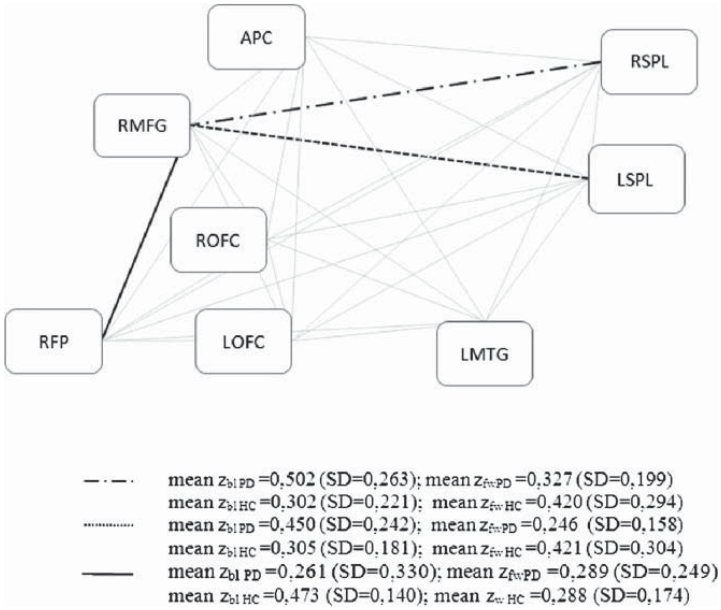

Figure 4 Results of cross correlation functional connectivity analysis (seed to seed connectivity). Functional connectivity between frontoparietal regions of interest was decreased; fronto-frontal connectivity was maintained in Parkinson's disease (PD). z: Fisher r to Z conversion. APC, anterior paracingulate cortex; bl, baseline; fw, follow-up; HC, healthy controls; LMTG, left middle temporal gyrus; LOFC, left orbitofrontal cortex; LSPL, left superior parietal lobe; RFP, right frontal pole; RMFG, right middle frontal gyrus; ROFC, right orbitofrontal cortex; RSPL, right superior parietal lobe.

significantly more marked in PD patients than in controls. This finding is in agreement with Whittington *et al*[4] who demonstrated that the recognition impairment in non-demented PD is seen in tasks of high demand (increased number of items). While in the RAVLT recognition part the number of stimuli is only 30, in the fMRI task there were 70 stimuli; this may have allowed the detection of subtle neuropsychological deficits not identified through standard clinical testing.

The regions that we found to be activated during the recognition memory task, involving both patients and controls, included several cortical areas (occipital lobes, bilateral orbitofrontal cortices and anterior paracingulate) and also subcortical structures involving bilaterally the basal ganglia and the left thalamus. However, the longitudinal data analyses showed that PD patients had decreased task related activity over time in cortical regions (IC1), but not in subcortical ones; specifically, the middle frontal gyrus, frontal pole, orbitofrontal cortex, anterior paracingulate gyrus, superior parietal lobe and the posterior portion of the middle temporal gyrus. All of these areas have been previously related to the recognition memory network.[8 33] Indeed, the cortical activation pattern observed in the current study is similar to those reported by Spaniol *et al*[34] after an fMRI meta-analysis. In all of the studies included in this meta-analysis, the activated regions were prefrontal and parietal bilaterally, with left hemispheric predominance.

Regarding the pattern of deactivation detected in the recognition memory network, we found decreased task related deactivation over time in PD patients, specifically in the anterior part of the paracingulate gyrus and the precuneus. Both of these areas are part of the DMN.[35 36] In our previous study, we detected that PD patients, compared with controls, failed to deactivate the precuneus during the recognition memory task.[8] Impaired deactivation of the precuneus in PD was also reported during the performance of a card sorting task.[15] There are no previous longitudinal studies of DMN dysfunction in PD, but abnormal patterns of deactivation in DMN have previously been reported as an indicator of progression in other neurodegenerative diseases.[37]

PD patients in our study committed more false positive errors in the fMRI task, and with significantly more marked over time worsening, compared with controls. These false positive errors correlated with the pattern of activation and deactivation in the recognition memory network, suggesting that appropriate recruitment of the recognition memory network entails a better performance. In line with these results, Van Eimeren *et al*[15] found a positive correlation between errors in an executive task and blood oxygen level dependent signal change in specific regions of the DMN, such as the precuneus and posterior cingulate cortex, meaning that the more deactivated those areas were, the better the performance.

The cross correlation analysis approach allowed us to evaluate variations in connectivity within the recognition memory network between baseline and follow-up. Previous PD cross sectional studies showed abnormal connectivity patterns during cognitive tasks.[14 15] Van Eimeren *et al*[15] studied cortical deactivation during an executive functions task as well as functional connectivity among the main areas of interest. Their results suggest functional frontostriatal disconnection in PD patients.

In the present study, connectivity analysis between the main regions of interest revealed that PD patients showed a progressive decrease in frontoparietal connectivity whereas connectivity between the frontal areas remained stable. Functional disconnection in PD may result from the primary synucleinopathy and the synaptic dysfunction associated with it[38] or it may be due to white matter microstructural damage, described in PD patients using diffusion tensor imaging techniques.[39–41] Decreased frontoparietal connectivity could be mediated by degeneration of tracts that connect these regions, such as the superior longitudinal fasciculus or the inferior fronto-occipital fasciculus, which have been described as being affected in non-demented PD patients.[40 42]

The fact that in PD patients connectivity between the right frontal regions remained stable, whereas in controls it declined, could be linked to loss of connectivity between the frontal and parietal regions observed in the former. We can speculate that affectation of long range connections could result in an increase in more local circuits as a functional compensation mechanism. Further studies are necessary to evaluate this hypothesis.

Frontoparietal connectivity may play an important role in PD related cognitive deficits, as previous work has found a cognitively relevant network in PD involving these areas. In a cross sectional study, Huang *et al*[19] identified a cognition related metabolic pattern in the network analysis of FDG-PET scans from 15 non-demented PD patients with mild to moderate motor symptoms. This pattern was characterised by relative hypometabolism of the dorsolateral prefrontal cortex, rostral supplementary motor area and superior parietal regions, associated with relative cerebellar/dentate nucleus metabolic increases. This network expression correlated significantly with indices of memory and executive functioning. The same authors performed a longitudinal FDG-PET study of PD patients without evident cognitive impairment. In accordance with our results, they found that disease progression was associated with declining metabolism in the prefrontal and parietal regions. Similarly, Carbon *et al*[43] found longitudinal changes in sequence learning performance and associated task related cerebral blood flow (H2 15O PET) in non-demented PD patients. After a 2 year follow-up period, significant declines in learning related activation were detected in parietal and temporo-occipital association areas and in the right dorsolateral prefrontal cortex.

In spite of previous evidence, progression of functional brain changes in PD patients remains controversial. In fact, after a longer follow-up period (4 years), Huang *et al*[18] found an inverse result—that is, an increase in cognition related metabolic pattern similar to motor related metabolic pattern progression. The authors related this result to incipient cognitive impairment. In contrast, Bohnen *et al*[44] found a decrease in metabolic activity (FDG-PET) in a small sample of patients who converted to PD with dementia after 2 years of follow-up. The metabolic reduction pattern included the thalamus and posterior cingulate, occipital, parietal and frontal areas, with mild reduction in the temporal lobe. The most prominent metabolic reduction in PD with dementia was seen in the cuneus and precuneus and in the mesiofrontal areas. In the future, progression of connectivity patterns between frontoparietal regions should be studied after longer follow-up periods.

Subjects in our study did not present with clinically significant cognitive impairments; however PD patients frequently present with cognitive deficits, specifically, visuospatial/visuoperceptual deficits, which, in severe cases, could interfere with the performance of tasks such as the recognition memory paradigm used in this study. Hence, this issue should ideally be controlled for in future studies. We also have to point out that all PD patients included in the sample were assessed under their usual antiparkinsonian medication. In order to consider potentially confounding effects of dopaminergic medications, future studies should address the same question in drug abstinent or naïve patients to elucidate the influence of dopaminergic medications on activation of the cerebral areas related to recognition memory. Although the PD patients in our sample presented with normal average BDI scores, these were higher than in controls; future studies should try to pair groups by severity of depressive symptoms, taking into account the effect of antidepressant medication. Finally, we also have to consider dropout of subjects from the initial sample to follow-up, a common limitation in longitudinal studies. However, comparisons between the initial sample and the one included in the longitudinal assessment, for controls and PD patients, showed no significant differences in demographic or clinical characteristics. Despite that in the future, our study should be replicated with a larger sample.

In conclusion, our results showed a decrease in the recognition memory network activation pattern over time and an abnormal connectivity pattern between the main regions involved in this memory network in PD patients. To the best of our knowledge, this is the first longitudinal study to reveal a progressive decrease in functional connectivity between areas involved in a cognitive network in PD patients.

Acknowledgements Without the support of the patients, their families and control subjects, this work would have not been possible. We also acknowledge the invaluable help of Silvia Juanes (University of Barcelona) for the support on the statistical analyses.

Contributors BS, RS-L and HCB: analysis and interpretation of the data, drafting the article, revising it critically for important intellectual content and final approval of the version to be published. NI-B: acquisition of the data, revising it critically for important intellectual content and final approval of the version to be published. MJM and FV: acquisition of the data, analysis and interpretation of the data, revising it critically for important intellectual content and final approval of the version to be published. PV and NB: analysis and interpretation of the data, revising it critically for important intellectual content and final approval of the version to be published. ET and CJ: conception and design, analysis and interpretation of the data, drafting the article, revising it critically for important intellectual content and final approval of the version to be published.

Funding This study was supported by the PSI2010-16174 from the Spanish government to CJ, HCB and BS, and by Generalitat de Catalunya (2009 SGR0836 to ET, 2009SGR0941 to CJ and an FI-DGR grant (2011FI_B 00045) to HCB, and CIBERNED.

Competing interests None.

Ethics approval The study was approved by the ethics committee of the Hospital Clinic de Barcelona.

Provenance and peer review Not commissioned; externally peer reviewed.

REFERENCES

1. **Aarsland D,** Bronnick K, Larsen JP, *et al*. Cognitive impairment in incident, untreated Parkinson disease: the Norwegian ParkWest study. *Neurology* 2009;**72**:1121–6.
2. **Elgh E,** Domellof M, Linder J, *et al*. Cognitive function in early Parkinson's disease: a population-based study. *Eur J Neurol* 2009;**16**:1278–84.
3. **Higginson CI,** Wheelock VL, Carroll KE, *et al*. Recognition memory in Parkinson's disease with and without dementia: evidence inconsistent with the retrieval deficit hypothesis. *J Clin Exp Neuropsychol* 2005;**27**:516–28.
4. **Whittington CJ,** Podd J, Stewart-Williams S. Memory deficits in Parkinson's disease. *J Clin Exp Neuropsychol* 2006;**28**:738–54.
5. **Li K,** Guo L, Nie J, *et al*. Review of methods for functional brain connectivity detection using fMRI. *Comput Med Imaging Graph* 2009;**33**:131–9.
6. **Beckmann CF,** Smith SM. Tensorial extensions of independent component analysis for multisubject FMRI analysis. *Neuroimage* 2005;**25**:294–311.
7. **Bai F,** Shi Y, Yuan Y, *et al*. Altered self-referential network in resting-state amnestic type mild cognitive impairment. *Cortex* 2012;**48**:604–13.
8. **Ibarretxe-Bilbao N,** Zarei M, Junque C, *et al*. Dysfunctions of cerebral networks precede recognition memory deficits in early Parkinson's disease. *Neuroimage* 2011;**57**:589–97.
9. **Buckner RL,** Andrews-Hanna JR, Schacter DL. The brain's default network: anatomy, function, and relevance to disease. *Ann N Y Acad Sci* 2008;**1124**:1–38.
10. **Jahanshahi M,** Jones CR, Zijlmans J, *et al*. Dopaminergic modulation of striato-frontal connectivity during motor timing in Parkinson's disease. *Brain* 2010;**133**:727–45.
11. **Palmer SJ,** Li J, Wang ZJ, *et al*. Joint amplitude and connectivity compensatory mechanisms in Parkinson's disease. *Neuroscience* 2010;**166**:1110–18.
12. **Wu T,** Chan P, Hallett M. Effective connectivity of neural networks in automatic movements in Parkinson's disease. *Neuroimage* 2010;**49**:2581–7.
13. **Wu T,** Wang L, Hallett M, *et al*. Effective connectivity of brain networks during self-initiated movement in Parkinson's disease. *Neuroimage* 2011;**55**:204–15.

14. **Rowe J,** Stephan KE, Friston K, *et al*. Attention to action in Parkinson's disease: impaired effective connectivity among frontal cortical regions. *Brain* 2002;**125**:276–89.
15. **van Eimeren T,** Monchi O, Ballanger B, *et al*. Dysfunction of the default mode network in Parkinson disease: a functional magnetic resonance imaging study. *Arch Neurol* 2009;**66**:877–83.
16. **Wu T,** Wang L, Chen Y, *et al*. Changes of functional connectivity of the motor network in the resting state in Parkinson's disease. *Neurosci Lett* 2009;**460**:6–10.
17. **Helmich RC,** Derikx LC, Bakker M, *et al*. Spatial remapping of cortico-striatal connectivity in Parkinson's disease. *Cereb Cortex* 2010;**20**:1175–86.
18. **Huang C,** Tang C, Feigin A, *et al*. Changes in network activity with the progression of Parkinson's disease. *Brain* 2007;**130**:1834–46.
19. **Huang C,** Mattis P, Tang C, *et al*. Metabolic brain networks associated with cognitive function in Parkinson's disease. *Neuroimage* 2007;**34**:714–23.
20. **Ibarretxe-Bilbao N,** Junque C, Marti MJ, *et al*. Olfactory impairment in Parkinson's disease and white matter abnormalities in central olfactory areas: A voxel-based diffusion tensor imaging study. *Mov Disord* 2010;**25**:1888–94.
21. **Tomlinson CL,** Stowe R, Patel S, *et al*. Systematic review of levodopa equivalency reporting in Parkinson's disease. *Mov Disord* 2010;**25**:2649–53.
22. **Daniel SE,** Lees AJ. Parkinson's Disease Society Brain Bank, London: overview and research. *J Neural Transm Suppl* 1993;**39**:165–72.
23. **Dubois B,** Burn D, Goetz C, *et al*. Diagnostic procedures for Parkinson's disease dementia: recommendations from the movement disorder society task force. *Mov Disord* 2007;**22**:2314–24.
24. **Beck AT,** Steer RA, Brown GK. *Manual for the beck depression inventory-II*. San Antonio, TX: Psychological Corporation, 1996.
25. **Cummings JL,** Mega M, Gray K, *et al*. The Neuropsychiatric Inventory: comprehensive assessment of psychopathology in dementia. *Neurology* 1994;**44**:2308–14.
26. **Rey A.** *El Examen Clínico en Psicología. Editorial Kapelusz*. Buenos Aires, Argentina: Editorial Kapelusz, 1962.
27. **Jenkinson M,** Bannister P, Brady M, *et al*. Improved optimization for the robust and accurate linear registration and motion correction of brain images. *Neuroimage* 2002;**17**:825–41.
28. **Smith SM.** Fast robust automated brain extraction. *Hum Brain Mapp* 2002;**17**:143–55.
29. **Jenkinson M,** Smith S. A global optimisation method for robust affine registration of brain images. *Med Image Anal* 2001;**5**:143–56.
30. **Beckmann CF,** Jenkinson M, Smith SM. General multilevel linear modeling for group analysis in FMRI. *Neuroimage* 2003;**20**:1052–63.
31. **Woolrich MW,** Behrens TE, Beckmann CF, *et al*. Multilevel linear modelling for FMRI group analysis using Bayesian inference. *Neuroimage* 2004;**21**:1732–47.
32. **Beckmann CF,** Smith SM. Probabilistic independent component analysis for functional magnetic resonance imaging. *IEEE Trans Med Imaging* 2004; **23**:137–52.
33. **Cabeza R,** Nyberg L. Imaging cognition II: An empirical review of 275 PET and fMRI studies. *J Cogn Neurosci* 2000;**12**:1–47.
34. **Spaniol J,** Davidson PS, Kim AS, *et al*. Event-related fMRI studies of episodic encoding and retrieval: meta-analyses using activation likelihood estimation. *Neuropsychologia* 2009;**47**:1765–79.
35. **Greicius MD,** Krasnow B, Reiss AL, *et al*. Functional connectivity in the resting brain: a network analysis of the default mode hypothesis. *Proc Natl Acad Sci USA* 2003;**100**:253–8.
36. **Raichle ME,** MacLeod AM, Snyder AZ, *et al*. A default mode of brain function. *Proc Natl Acad Sci USA* 2001;**98**:676–82.
37. **Petrella JR,** Sheldon FC, Prince SE, *et al*. Default mode network connectivity in stable vs progressive mild cognitive impairment. *Neurology* 2011;**76**:511–17.
38. **Schulz-Schaeffer WJ**. The synaptic pathology of alpha-synuclein aggregation in dementia with Lewy bodies, Parkinson's disease and Parkinson's disease dementia. *Acta Neuropathol* 2010;**120**:131–43.
39. **Karagulle-Kendi AT,** Lehericy S, Luciana M, *et al*. Altered diffusion in the frontal lobe in Parkinson disease. *AJNR Am J Neuroradiol* 2008;**29**:501–5.
40. **Gattellaro G,** Minati L, Grisoli M, *et al*. White matter involvement in idiopathic Parkinson disease: a diffusion tensor imaging study. *AJNR Am J Neuroradiol* 2009;**30**:1222–6.
41. **Rae CL,** Correia MM, Altena E, *et al*. White matter pathology in Parkinson's disease: The effect of imaging protocol differences and relevance to executive function. *Neuroimage* 2012;**62**:1675–84.
42. **Baggio HC,** Segura B, Ibarretxe-Bilbao N, *et al*. Structural correlates of facial emotion recognition deficits in Parkinson's disease patients. *Neuropsychologia* 2012;**50**:2121–8.
43. **Carbon M,** Reetz K, Ghilardi MF, *et al*. Early Parkinson's disease: longitudinal changes in brain activity during sequence learning. *Neurobiol Dis* 2010;**37**:455–60.
44. **Bohnen NI,** Koeppe RA, Minoshima S, *et al*. Cerebral glucose metabolic features of Parkinson disease and incident dementia: longitudinal study. *J Nucl Med* 2011;**52**:848–55.

SUPPLEMENTARY MATERIALS

	PD patients			HC		
	Initial sample (n=24)	**Final sample (n=17)**	**t / *p***	**Initial sample (n=24)**	**Final sample (n=13)**	**t/*p***
Age	56.13 (8.5)	56.56 (8.6)	-0.17/0.86	57.6 (8.9)	57.2 (10.1)	0.13/0.89
Education (yrs.)	11.0 (5.5)	10.8 (4.8)	0.82/0.94	13.00 (3.8)	12.3 (3.4)	0.55/0.59
MMSE	29.6 (0.5)	29.5 (0.5)	0.60/0.55	29.8 (0.4)	29.9 (0.3)	-0.75/0.46
BDI	6.8 (4.8)	7.5 (5.3)	-0.4/0.63	4.5 (5.1)	3.3 (2.4)	0.77/0.48
NPI	3.9 (7.3)	3.1 (5.4)	0.38/0.71	1.4 (1.7)	1.1 (1.4)	0.54/0.59
LEDD	299.6 (321.1)	277.7 (308.5)	0.22/0.83	-	-	-
Disease duration	3.1 (1.6)	2.9 (1.4)	0.31/0.76	-	-	-
Age at onset	53.1 (8.6)	53.7 (8.5)	-0.23/0.82	-	-	-

Supplementary material 1. Clinical and sociodemographic characteristics of initially recruited sample and of longitudinally followed subjects. Student's t-test statistics and significance value for sample comparisons according to group are shown. PD: Parkinson's disease; HC: healthy controls. MMSE: mini-mental state examination; BDI: Beck depression inventory-II; NPI: neuropsychiatric inventory; LEDD: levodopa equivalent daily dose. Disease duration refers to duration of motor symptoms, in years.

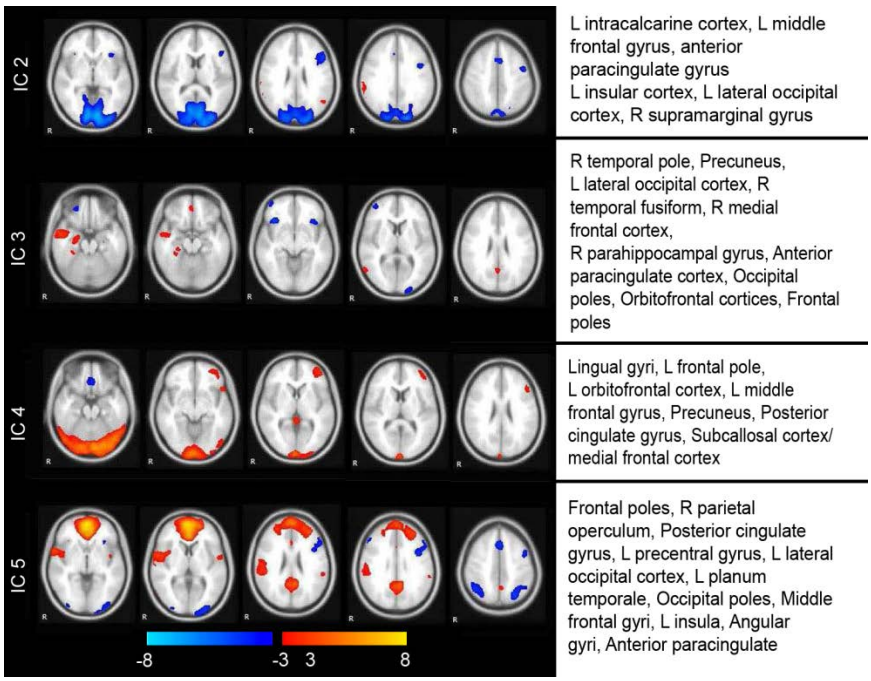

Supplementary material 2. Relevant components selected from model-free analysis results. Control-condition related components included IC2, IC3 and IC5 (recognition task<control condition). Recognition memory task related component is IC4 (recognition task>control condition). These ICs did not show time or group effect. (Left) Spatial patterns of IC2, IC3, IC4 and IC5, including activation areas (warm colors) and deactivation areas (cold colors). (Right) Peak voxels activation/ deactivations regions involved in each component. L: Left, R: Right.

	PD (n=17)		HC (n=13)		F(GxT)	F(G)	F(T)
	Baseline	**Follow-up**	**Baseline**	**Follow-up**			
Phonemic fluency	13.76 (5.04)	15.77 (6.53)	16.00 (5.23)	17.00 (5.16)	0.329	0.872	2.965
Semantic fluency	17.82 (4.80)	17.00 (5.58)	21.54 (4.56)	20.08 (4.82)	0.091	5.106*	1.163
Forward digit span	7.82 (1.63)	8.29 (1.99)	9.00 (1.35)	8.00 (2.04)	4.734*	0.613	0.613

Supplementary material 3. Neuropsychological performance at baseline and at follow-up and time effect, group effect and group-by-time interaction. Results are given in *means(standard deviations)*. The F values refer to those obtained with the repeated-measures general linear model. F(GxT): group-by-time interaction; F(G): group effect; F(T): time effect.

Anatomical region	Voxel	*p*	z-max	MNI coordinates x y z
LOP	22594	$3.4x10^{-39}$	8.11	-32 -94 -2
LOFC	6787	$5.86x10^{-17}$	9.16	-34 22 -8
ROFC	6230	$5.9x10^{-16}$	9.21	36 20 -8
APC	3680	$6.72x10^{-11}$	8.28	-6 30 32

Supplementary material 4. Local maxima of significant cluster list obtained from model-based FEAT analysis. LOP: Left Occipital Pole LOFC: left orbitofrontal cortex; ROFC: right orbitofrontal cortex; APC: anterior paracingulate cortex.

Anatomical region	Voxels	z-max	MNI coordinates x y z
LOFC	560	8.04	-34 22 -8
LSPL	183	5.9	-34 -58 44
LMTG	144	5.32	-62 -42 -12
APC	91	6.25	2 22 48
ROFC	89	7.43	34 26 -8
RSPL	72	5.77	42 -58 44
RMFG	61	5.98	50 34 28
RFP	25	4.76	42 54 -8

Supplementary material 5. Local maxima of significant cluster list obtained from activation areas that showed decreased activity in IC1 for the PD group over time (p<0.04). RMFG: right middle frontal gyrus; RSPL: right superior parietal lobe; RFP: right frontal pole; ROFC: right orbitofrontal cortex; APC: anterior paracingulate cortex; LSPL: left superior parietal lobe; LOFC: left orbitofrontal cortex; LMTG: left middle temporal gyrus.

study 7

PROGRESSION OF CORTICAL THINNING IN EARLY PARKINSON'S DISEASE

Movement Disorders 2012

Naroa Ibarretxe Bilbao, Carme Junqué, Bàrbara Segura, Hugo César Baggio, Maria José Martí, Francesc Valldeoriola, Núria Bargalló, Eduardo Tolosa

FEATURED ARTICLE

Progression of Cortical Thinning in Early Parkinson's Disease

Naroa Ibarretxe-Bilbao, PhD,[1,2,3,6] Carme Junque, PhD,[1,2,3]* Barbara Segura, PhD,[1,2,3] Hugo C. Baggio, MD,[1,2,3] Maria J. Marti, MD, PhD,[1,2,4] Francesc Valldeoriola, MD, PhD,[1,2,4] Nuria Bargallo, MD, PhD,[2,5] and Eduardo Tolosa, MD, PhD[1,2,4]

[1]*Centro de Investigación en Red de Enfermedades Neurodegenerativas (CIBERNED), Hospital Clínic de Barcelona, Catalonia, Spain*
[2]*Institute of Biomedical Research August Pi i Sunyer, Catalonia, Spain*
[3]*Department of Psychiatry and Clinical Psychobiology, University of Barcelona, Catalonia, Spain*
[4]*Parkinson's Disease and Movement Disorders Unit, Neurology Service, Institut Clínic de Neurociències, Hospital Clínic de Barcelona, Catalonia, Spain*
[5]*Centre de Diagnòstic per la Imatge Hospital Clínic de Barcelona, Hospital Clínic de Barcelona, Catalonia, Spain*
[6]*Department of Methods and Experimental Psychology, Faculty of Psychology and Education, University of Deusto, Basque Country, Bilbao, Spain*

ABSTRACT: The aim of this study was to investigate the progression of cortical thinning and gray-matter (GM) volume loss in early Parkinson's disease (PD). MRI and neuropsychological assessment were obtained at baseline and follow-up (mean ± standard deviation = 35.50 ± 1.88 months) in a group of 16 early-PD patients (H & Y stage ≤II and disease duration ≤5 years) and 15 healthy controls matched for age, gender, and years of education. *FreeSurfer* software was used for the analysis of cortical thickness as well as for cortical and subcortical volumetric analyses. Voxel-based morphometry analysis was performed using *SPM8*. Compared to controls, PD patients showed greater regional cortical thinning in bilateral frontotemporal regions as well as greater over-time total GM loss and amygdalar volume reduction. PD patients and controls presented similar over-time changes in cognitive functioning. In early-PD patients, global GM loss, amygdalar atrophy, and cortical thinning in frontotemporal regions are specifically associated with the PD-degenerative process. ©2012 *Movement* Disorder Society

Key Words: Parkinson's disease; cognition; longitudinal; cortical thickness

Cognitive dysfunctions appear early in the course of Parkinson's disease (PD). Cross-sectional, community-based studies have reported on impairments in executive functions,[1,2] attention and psychomotor speed,[3,4] memory,[1–4] visuospatial functions,[3] and verbal fluency[1,2] in newly diagnosed PD patients. Furthermore, longitudinal assessment of cognition in these early-PD patients shows a faster rate of cognitive decline than in control subjects.[5,6]

According to the neuropathological Braak stages,[7] alpha-synuclein pathology ascends from the brainstem and olfactory bulb, in the early stages, to the midbrain and diencephalic nuclei, and, later, to the neocortex. However, MRI findings do not fully conform to this neuropathological staging. Cross-sectional imaging studies in early PD, using different methodological approaches, have found highly variable, and usually not extensive, patterns of structural degeneration. Specifically, voxel-based morphometry (VBM) and volumetric techniques comparing early-PD patients and matched controls have shown white-matter (WM) loss in the brainstem[8] and gray-matter (GM) loss in the striatum,[9] amygdala,[10] and orbitofrontal cortex (OFC).[10] On the other hand, cortical thickness (CTh) studies have described focal cortical thinning in the OFC, ventrolateral prefrontal cortex, occipitoparietal

Additional Supporting Information may be found in the online version of this article.

***Correspondence to:** Dr. Carme Junque, Department of Psychiatry and Clinical Psychobiology, University of Barcelona, Casanova 143, 08036 Barcelona, Spain; cjunque@ub.edu

Funding agencies: This study was supported by Generalitat de Catalunya (2009SGR0836 [to E.T.] and 2009SGR0941 [to C. J.]), PSI2010-16174 (to C.J.), and CIBERNED (to N.I.-B.).

Relevant conflicts of interest/financial disclosures: Nothing to report. Full financial disclosures and author roles may be found in the online version of this article.

Received: 16 January 2012; **Revised:** 3 August 2012; **Accepted:** 16 September 2012
Published online 2 November 2012 in Wiley Online Library (wileyonlinelibrary.com). DOI: 10.1002/mds.25240

cortex,[9] and in the supplementary motor area.[11] These discrepant findings highlight the need for longitudinal studies using comprehensive techniques to help clarify the typical patterns of evolution of structural changes that take place early in PD.

The relationship between structural MRI changes and neuropsychological deficits in PD has not been extensively investigated, and the only available results come from cross-sectional studies.[12] PD patients with mild cognitive impairment have been found to have frontotemporal neocortical reductions, compared with PD patients with normal cognition,[13] and memory deficits have been observed to correlate with the degree of hippocampal atrophy.[14–16] Similarly, correlations have been found between visuospatial and -perceptual deficits and parietotemporal GM reductions[17] and between verbal fluency and frontal and temporal cortical atrophy.[18] Specifically for early PD, Ibarretxe-Bilbao et al. (2009) showed amygdalar and bilateral OFC degeneration associated with impaired recognition of emotions as well as GM volume loss in the left lateral OFC related to decision-making impairment.[10]

VBM and cortical-thickness analyses are sensitive to different, though overlapping, GM parameters that are altered in neurodegenerative processes: VBM provides a mixed measure of cortical GM, including cortical surface area and/or cortical folding as well as cortical thickness,[19] whereas cortical-thickness analysis has the advantage of providing a quantitative value that represents a physical property of the cortical mantle. These MRI techniques are considered to provide complementary information in different research settings.[20–22]

To our knowledge, no published MRI studies have focused on the progression of brain changes using cortical thickness and VBM analyses in early PD. Indeed, longitudinal MRI studies have only been carried out at more-advanced disease stages, showing progressive ventricular dilation[23,24] and progressive cerebral GM loss in nondemented PD,[25,26] PD patients at risk for dementia (patients with visual hallucinations),[27] and in patients with PD dementia (PDD).[26,28]

In the present study, we have performed a prospective assessment of a group of early-PD patients and a matched control group of healthy subjects. Subjects underwent MRI and neuropsychological assessment both at study entry and after a mean follow-up interval of 35.5 months. In a previous study, we reported on MRI findings at baseline showing GM volume loss in the amygdala and the OFC in early-PD patients[10] using a region-of-interest VBM approach. In the current study, we aimed to make a global assessment of the brain changes that take place over time in the early stages of PD using cortical-thickness analysis, whole-brain VBM, and volumetric analysis of the ventricular system and subcortical GM structures. We also aimed to investigate cognitive changes over time to establish whether these brain MRI measures correspond to possible neuropsychological changes.

TABLE 1. Demographical data at baseline

Demographics	PD (n = 16)	Controls (n = 15)	t^a, χ^b	*P* Value
Age	55.94 (8.10)	57.73 (9.53)	0.567[a]	0.575
Gender, male/female	12/4	12/3	0.111[b]	0.539
Education, years	11.00 (4.86)	12.60 (3.33)	1.075[a]	0.298
Age onset	52.97 (8.24)	—	—	—
Disease duration, years	2.97 (1.45)	—	—	—

Values are mean (SD).
[a]Student *t* test.
[b]Chi-squared test statistics.

Patients and Methods

Participants

Patients were recruited from an outpatient movement disorders clinic (Parkinson's Disease and Movement Disorders Unit, Department of Neurology, Hospital Clinic, Barcelona, Spain). Healthy subjects were recruited from friends and spouses of patients and matched for age, gender, and years of education. At baseline, 24 early-PD patients and 24 healthy subjects matched for age, gender, and years of education participated in the study (the same sample used in the study by Ibarretxe-Bilbao et al., 2009[10]). After a mean interval of 35.50 months (standard deviation [SD] = 1.85; range, 31–40), 16 PD patients and 15 healthy controls from this initial sample participated in the follow-up assessment. There were no significant differences between groups in terms of age, gender, and education. Demographical data of the participants at baseline examination are summarized in Table 1.

At the time of initial evaluation (baseline evaluation), the inclusion criteria for participating in the study were (1) fulfillment of the UK PD Society Brain Bank (PDSBB) diagnostic criteria for PD,[29] (2) H & Y stage $\leq$II, and (3) disease duration $\leq$5 years. Motor symptoms were assessed by means of the UPDRS-III motor section. Exclusion criteria were (1) presence of dementia diagnosed by a neurologist according to the *Movement* Disorder Society diagnostic criteria for PDD,[30] (2) presence of other neurological or psychiatric disorders, such as depression, defined by a Beck's Depression Inventory (BDI-II) score higher than 14,[31] and (3) the presence of visual hallucinations, as assessed by the Neuropsychiatric Inventory Questionnaire (NPI-Q).[32]

This study was approved by the institutional ethics committee. Written informed consent was obtained from all study subjects after full explanation of the procedures involved.

Neuropsychological Assessment

The neuropsychological assessment included the cognitive functions usually impaired in PD. The tests used were as follows: (1) forward and backward digit span from the Wechsler Adults Intelligence Scale (WAIS-III) as measures of immediate and working memory, respectively; (2) verbal memory with Rey's Auditory Verbal Learning Test (RAVLT) as a measure of declarative memory; (3) phonemic and semantic fluencies; (4) psychomotor speed and inhibition control with the Stroop test; and (5) visuomotor tracking and cognitive flexibility with the Trail Making test (TMT) (parts A and B). The neuropsychological battery was administered by a trained neuropsychologist (N.I.-B.), and completed in a single session lasting between 1 and 2 hours. The neuropsychologist in charge of the assessment was the same at baseline and follow-up examinations.

Neuropsychological and Clinical Statistical Analysis

Statistical analyses of neuropsychological and clinical variables were carried out using the statistical package, *PASW-18* (2009; SPSS, Inc., Chicago, IL). Changes in clinical and neuropsychological variables between baseline and follow-up were analyzed using the general linear mixed model (GLM) for repeated measures to test whether these variables differed across time between groups. A two-factor repeated-measures analysis of variance (2 × 2) (RMANOVA) was performed for each of the variables. Factors were group (PD patients and controls) and time (baseline and follow-up). Because groups were matched (there were no significant intergroup differences for age, gender, and education), these variable were not included in the model. On the other hand, the interval between neuropsychological assessments in months was entered as a covariate in the RMANOVA.

MRI Acquisition

Structural images at baseline and follow-up were acquired using a MAGNETOM Tim Trio 3T scanner (Siemens AG, Munich, Germany). High-resolution, three-dimensional (3D) T1-weighted images were acquired in the sagittal plane with an MPRAGE sequence (TR/TE 2,300/2.98 ms; TI 900 ms; 256 × 256 matrix, 1 mm isotropic voxel).

Cortical Thickness Analysis

Cross-sectional evaluation (to determine whether PD patients and controls regionally differ in cortical thickness at baseline) and longitudinal analysis (to compare CTh between the two time points [baseline and follow-up]) were performed using *FreeSurfer* software (version 5.1; available at: http://surfer.nmr.harvard.edu). In this procedure, a cortical surface 3D model of CTh is created using intensity and continuity information, as previously described in detail.[33] The initial processing of T1 high-resolution images includes several steps, which are performed independently for each subject and each time point: removal of nonbrain tissue,[34] automated Talairach transformation, intensity normalization,[35] tessellation of the GM/WM boundary, automated topology correction,[36,37] and surface deformation to optimally place the GM/WM and GM/cerebrospinal fluid (CSF) boundaries.[33] The resulting representation of cortical thickness is calculated as the distance between tissue boundaries (GM/WM and GM/CSF).[33] All surface models in our study were visually inspected for accuracy.

Subsequently, for the longitudinal processing, an unbiased within-subject template space and average image[38] are created using robust, inverse consistent registration.[39] Several processing steps, such as skull stripping, Talairach transformations, atlas registration, as well as spherical surface maps and parcellations are then initialized with common information from the within-subject template, significantly increasing reliability and statistical power.[40] Finally, both time points and the template are used to create the complete subjects directories, named *long run*. Regional differences between groups (patients and controls) in cortical measures were assessed using a vertex-by-vertex general linear model (one factor with two levels without covariates, corresponding to a Student *t* test statistical model). Maps were smoothed using a circularly symmetric Gaussian kernel across the surface with a full width at half maximum (FWHM) of 15 mm. Z Monte Carlo simulations with 10,000 iterations were applied to CTh maps to provide clusterwise correction for multiple comparisons,[41] and results were thresholded at a corrected *P* value of 0.05 ($Z = 1.3$). To perform main longitudinal analyses, we automatically obtained a measure of change from longitudinal data called *rate of thinning* (mm/year).

Mean rates of thinning for significant clusters were then extracted for each subject to perform correlational analyses with cognitive measures.

We used the same methodology to perform complementary analyses with other longitudinal measures: the *temporal average* (the average thickness between baseline and follow-up); the *percent change* (the rate of thinning divided by the baseline thickness); and the *symmetrized percent change* (the rate of thinning divided by the average thickness).

Volumetric Analysis of Subcortical Structures

The automated procedure for volumetric measures of brain structures implemented in *FreeSurfer* (version 5.1; available at: http://surfer.nmr.harvard.edu)[42] was used to obtain the volumes of subcortical structures.

TABLE 2. Clinical data at baseline and at follow-up and time effect, group effect, and interactions between time and group

	PD (n = 16)		Controls (n = 15)				
	Baseline	Follow-up	Baseline	Follow-up	F(T)	F(G)	F(G×T)
MMSE	29.56 (0.51)	27.94 (2.62)	29.87 (0.35)	28.80 (0.68)	17.358*	1.185	0.172
BDI-II	7.69 (5.44)	5.81 (4.92)	4.93 (5.80)	2.53 (2.47)	4.440*	3.281	0.035
NPI	3.31 (5.50)	2.00 (1.97)	1.53 (1.88)	2.33 (3.58)	0.168	1.099	0.960
UPDRS-III	15.44 (3.71)	15.38 (4.35)			0.069		
H & Y	1.81 (0.31)	1.91 (0.38)			0.285		
LEDD	282.50 (317.98)	444.38 (357.50)			0.721		

F values refer to those obtained through a repeated-measures GLM. F(T): time effect; F(G): group effect; F(G×T): interaction between time and group.
*Significant at $P < 0.05$.

Volumetric measures were automatically obtained from 7 GM structures (thalamus, caudate, putamen, pallidum, nucleus accumbens, hippocampus, and amygdala), as well as from the lateral, third, and fourth ventricles and the brainstem. For simplicity, we refer to these collectively as "subcortical structures," although, strictly speaking, the hippocampus and amygdala are not subcortical. Total cortical volume, total subcortical volume, and global GM volume were also obtained.

All the volumes obtained were compared using *PASW-18*. RMANOVA was used to longitudinally examine changes in deep GM structures, brainstem, ventricles, and total GM volumes. Scan number was specified as a within-subject factor "time" with two levels (baseline and follow-up MRI acquisitions) as well as a between-subject factor "group" with two levels (PD patients and healthy controls). All the volumetric analyses controlled for intracranial volume (ICV). No other covariables were included in the model. Partial correlation analyses were performed between change in brain volumes and cognition, also controlling for ICV.

Voxel-Based Morphometry Analysis

Image preprocessing for voxel-based morphometry analyses was done using *SPM8* (http://www.fil.ion.ucl.ac.uk/spm/software/spm8/). After realignment, baseline images were rigidly coregistered to the respective subject's follow-up image. All images were then segmented into GM, WM, and CSF probability maps with the New Segment tool of *SPM8*, an extended version of the "unified segmentation" model.[43]

In an attempt to obtain an accurate subject registration and, consequently, an adequate detection of within-subject longitudinal changes, subject-specific templates were created using the Diffeomorphic Anatomical Registration Through Exponentiated Lie algebra (DARTEL)[44] tool to nonlinearly register each subject's GM and WM baseline and follow-up images. Baseline and follow-up scans were subsequently normalized to their respective template, using the Jacobian determinants for modulation. A group template was then created using the baseline GM and WM images (normalized to the individual template) of the entire sample, also through DARTEL. Baseline and follow-up scans then underwent a second normalization, this time to the group template, again applying the Jacobian determinants for modulation. A third normalization was performed to bring each subject's baseline and follow-up GM images to the MNI space using an affine transformation, then smoothed with a Gaussian kernel of 12 mm FWHM. The final voxel dimension was 1.5 mm isotropic. A similar preprocessing approach was recently proposed by Asami et al.[45]

The final GM maps generated as described above were analyzed in a whole-brain voxelwise fashion. For cross-sectional baseline intergroup comparisons, images were entered into a two-sample *t* test model. For longitudinal analysis, subjects' images were entered into a full-factorial model with two factors (the two levels in the *group* factor were entered as independent, and the two levels in the *time* factor as nonindependent variables, with assumed unequal variance) to evaluate possible *group* × *time* interactions in GM volume.

Total intracranial volume (obtained through the sum of the native GM, WM, and CSF maps) was entered as a covariate of no interest in all these analyses. Subjects' interscan interval (in months) was also entered as a covariate of no interest in the interaction analyses.

Results were corrected for multiple comparisons using familywise-error correction,[46] with a significance threshold set at $P < 0.05$.

Results

Neuropsychological Tests and Clinical Variables

In PD patients, levodopa equivalent daily dose (LEDD), H & Y, and UPDRS-III motor section scores did not differ significantly between baseline and follow-up assessments (see Table 2).

RMANOVA revealed a significant time effect on Mini–Mental State Examination (MMSE) and depression scores, but no significant interactions between

TABLE 3. Neuropsychological data at baseline and at follow-up: time effect, group effect, and interaction between time and group

	PD (n = 16)		Controls (n = 15)				
	Baseline	Follow-up	Baseline	Follow-up	F(T)	F(G)	F(G×T)
Attention, immediate recall, and working memory							
Digit span (forward)	7.94 (1.61)	8.25 (2.05)	9.00 (1.31)	8.33 (2.29)	0.310	0.617	3.285
Digit span (backward)	5.38 (1.78)	5.69 (1.92)	7.07 (1.28)	7.27 (2.28)	0.890	5.275*	0.029
Digits total	13.31 (3.01)	13.93 (3.47)	16.07 (2.40)	15.60 (4.35)	0.021	2.769	1.239
WM (direct minus inverse)	2.56 (1.56)	2.69 (2.15)	1.93 (0.96)	1.00 (1.31)	1.327	6.280*	4.452*
Verbal memory							
RAVLT learning	45.38 (11.73)	44.06 (10.29)	50.60 (8.41)	48.53 (9.44)	0.268	2.072	0.248
RAVLT Delayed recall	8.88 (3.40)	9.67 (3.20)	10.33 (2.26)	9.87 (2.72)	0.143	1.444	2.462
RAVLT Recognition	27.69 (2.27)	28.56 (2.13)	28.40 (1.88)	28.40 (1.80)	1.851	0.008	3.342
RAVLT True recognition	13.68 (1.70)	14.00 (1.67)	14.20 (0.86)	14.07 (1.22)	0.179	0.019	1.257
RAVLT False recognition	1.00 (1.21)	0.44 (0.73)	0.73 (1.62)	0.67 (0.90)	1.310	0.234	1.974
Verbal fluencies							
Phonemic fluency	13.88 (5.19)	15.93 (6.71)	15.73 (4.95)	16.93 (4.79)	52.659*	0.602	0.001
Semantic fluency	18.19 (4.71)	17.19 (5.71)	20.47 (5.25)	19.80 (4.90)	1.031	1.661	2.192
Psychomotor speed and inhibition control							
SCWT Word (W)	100.19 (18.74)	92.19 (19.30)	109.80 (12.19)	102.40 (20.09)	9.927*	0.551	0.074
SCWT Color (C)	59.25 (12.83)	55.50 (16.67)	71.27 (11.34)	71.20 (6.66)	1.139	6.222*	1.123
SCWT Word-Color (PC)	34.31 (12.46)	33.13 (15.11)	43.13 (7.36)	42.87 (8.17)	0.485	1.662	0.266
Visuomotor tracking and cognitive flexibility							
TMTA	48.81 (28.25)	55.50 (39.43)	37.93 (12.30)	41.2 (16.97)	1.387	2.130	0.164
TMTB	146.13 (104.29)	158.88 (124.63)	87.87 (29.25)	80.47 (25.40)	0.133	5.335*	1.887

F values refer to those obtained through a repeated-measures GLM. F(T): time effect; F(G): group effect; F(G×T): interaction between time and group.
Abbreviations: WM, working memory; RAVLT, Rey's auditory verbal learning test; SCWT, Stroop color-word test; TMTA, Trail-making test, part A; TMTB, Trail-making test, part B. *Significant at $p < 0.05$.

groups and time. That is, both patients and controls showed lower scores over time, but the decline did not differ between groups. NPI-Q scores remained stable over time in both groups.

At baseline, PD patients showed worse cognitive performance than controls. There were significant differences in neuropsychological variables measuring working memory (backward digits: t = 3.015, P = 0.005), psychomotor speed (*Stroop colors*: t = 2.755, P = 0.010; words-colors: t = 2.417, P = 0.023), and cognitive flexibility (TMTB: t = −2.146, P = 0.046). Longitudinal analyses also showed a significant group effect in working memory (digit span backward), psychomotor speed (*Stroop colors*), and cognitive flexibility (TMTB). A significant time effect was observed for psychomotor speed assessed by the Stroop test (*Stroop words*). The only other cognitive variable for which a time effect was observed was phonemic fluency, as a result of both groups improving their performance at follow-up, suggesting a practice effect. There was no significant interaction between time and group for any of the variables analyzed (see Table 3).

Cortical Thickness

At baseline, there were no significant differences in cortical thickness between PD patients and the healthy control group (data not shown). However, rate-of-thinning (mm/year) analyses showed that PD patients had significantly greater progressive cortical thinning in the following areas than healthy controls at the corrected level ($P < 0.05$) (Fig. 1; Table 4): right superior frontal gyrus, extending to caudal middle frontal gyrus, precentral sulcus, and precentral gyrus; right frontal *pars opercularis* and precentral gyrus; right superior temporal gyrus extending to the adjacent temporal sulcus; left caudal middle frontal gyrus extending to rostral middle frontal gyrus and precentral region; and left middle temporal gyrus extending to parietal cortex.

At a more-conservative correction level ($P < 0.01$), clusters in the right hemisphere remained significant: in the caudal middle frontal gyrus (621.2 mm^2; x, y, and z Talairach coordinates of the maximum: 29.5, 7.5, and 47.3) and in the superior temporal gyrus (two clusters, one with 549.2 mm^2; x, y, and z Talairach coordinates of the maximum: 43.9, −4.2, and −16.2; and the other with 494.4 mm^2; x, y, and z Talairach coordinates of the maximum: 63.1, −31.1, and 5.6). The complementary longitudinal measures analyzed showed no significant group differences in the measure *temporal average*. However, the measures *percent change* and *symmetrized percent change* showed patterns of thinning in frontal and temporal regions similar to those obtained by means of the *rate of thinning* (see Supporting Fig. 1 for the results of the *symmetrized percent change*).

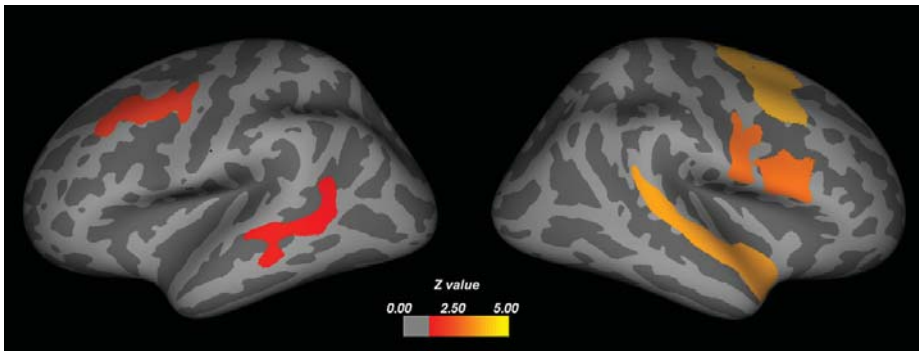

FIG. 1. Cortical areas showing significantly higher rate of thinning (mm/year) in PD patients, compared to controls. Color bar indicates the significance levels in the clusters of significantly higher thinning rate in PD patients than in healthy controls (in Z values). Results were obtained using Z Monte Carlo simulation with 10,000 iterations applied to CTh maps to provide clusterwise correction for multiple comparisons. Results were thresholded at a corrected *P* value of 0.05 (Z = 1.3).

There were no significant correlations between cognitive measures and mean rate of thinning (or between cognitive measures and the complementary longitudinal measures analyzed) in the clusters described above.

No areas of significantly higher rates of thinning in controls than in PD patients were observed.

Volumetric Analyses

Table 5 shows total GM, total cortical, and subcortical GM volumes (total and by structure) as well as ventricular volumes at baseline and follow-up. At baseline, there were no significant group differences in volumetric measures (data not shown). The loss from baseline to follow-up in subcortical deep GM structures besides the amygdalae was similar in both groups. We also observed a similar volume increase in the ventricular system in both groups.

Total GM volume reduction over time was greater in PD patients than in healthy controls; the time-group interaction was significant. Finally, PD patients also showed specific and significant loss in amygdalar and total cortical volumes (see Table 5). Total GM volume changes correlated with *Stroop words* performance decline in PD patients ($r = 0.541$; $P = 0.037$). Neither amygdalar volume changes nor total cortical volume reduction correlated with cognitive changes.

Voxel-Based Morphometry

No significant group differences in GM volume were found between healthy controls and PD patients at baseline in whole-brain analyses. Interaction analysis did not reveal any areas of differential GM loss across groups at the corrected level.

TABLE 4. Cortical areas showing significantly higher rates of thinning (mm/year) in PD patients, compared to controls, over time

Cortical Area	Cluster Size (mm^2)	Talairach Coordinates of the Maxima (x, y, and z)	Z Values	Clusterwise Probability (*P*)
Right hemisphere				
Superior frontal gyrus, caudal middle frontal region, precentral sulcus, and paracentral region	2,603.88	12.2, −4.5, 62.7	3.868	<0.001
Frontal pars opercularis and precentral gyrus	1,737.77	47.4, 12.3, 15.3	3.074	0.001
Superior temporal gyrus, superior temporal sulcus, and supramarginal region	1,197.26	43.9, −4.2, −16.2	5.115	<0.001
Left hemisphere				
Caudal middle frontal, precentral, and rostral middle frontal gyrus	1,373.34	−34.6, 23.0, 43.5	3.100	<0.005
Middle temporal gyrus, superior temporal gyrus, superior temporal sulcus, and inferior parietal lobe	1,062.84	−59.4, −49.6, 4.1	2.511	0.026

Results were corrected using familywise error correction with Z Monte Carlo simulation (10,000 iterations) and thresholded at a corrected *P* value of 0.05 (Z = 1.3).

TABLE 5. Volumetric data of subcortical GM structures, brainstem, and ventricles

	PD (n = 16)		Controls (n = 15)				
	Baseline	Follow-up	Baseline	Follow-up	F (T)	F(G)	F(G×T)
Thalamus	14.53 (1.80)	14.12 (1.90)	14.40 (1.51)	14.02 (1.41)	0.014	0.004	0.022
Caudate	7.05 (0.95)	6.77 (0.91)	7.46 (1.27)	7.22 (1.18)	0.883	2.583	0.184
Putamen	10.70 (1.56)	10.20 (1.63)	11.06 (1.16)	10.68 (1.12)	1.640	1.277	0.855
Pallidum	3.35 (0.46)	3.37 (0.42)	3.34 (0.40)	3.36 (0.41)	0.723	0.017	0.292
Hippocampus	8.76 (1.02)	8.51 (1.09)	8.58 (1.13)	8.44 (1.04)	0.046	0.048	1.421
Amygdala	3.23 (0.49)	3.07 (0.50)	3.19 (0.35)	3.18 (0.36)	0.098	0.132	5.661*
Accumbens	1.05 (0.25)	1.03 (0.23)	1.03 (0.16)	1.03 (0.15)	2.559	0.004	0.458
Lateral ventricles	22.28 (12.8)	24.45 (14.13)	20.73 (14.51)	22.72 (15.6)	1.542	0.037	0.020
Inferior lateral ventricles	0.75 (0.34)	0.81 (0.41)	0.83 (0.54)	0.85 (0.57)	0.243	0.218	1.492
3rd ventricle	1.32 (0.32)	1.40 (0.39)	1.31 (0.52)	1.38 (0.54)	0.698	0.002	0.001
4th ventricle	1.84 (0.62)	1.81 (0.59)	2.00 (0.48)	2.04 (0.51)	0.109	1.829	2.964
Brainstem	21.97 (1.86)	21.83 (1.80	22.59 (2.56)	22.47 (2.58)	3.858	1.055	0.003
Cortex volume	455.65 (53.3)	444.14 (47.46)	450.88 (42.09)	449.30 (38.41)	4.518*	0.104	7.049*
Subcortical GM volume	186.21 (16.6)	183.07 (18.04)	182.23 (16.66)	179.27 (16.40)	0.477	0.307	0.007
Total GM volume	641.86 (64.1)	627.21 (60.30)	633.11 (55.56)	628.57 (51.72)	4.100	0.002	5.400*

F values refer to those obtained through a repeated-measures GLM (2×2 MANOVA): group factor (PD and controls) and time factor (baseline and follow-up). F(T): time effect; F(G): group effect; F (G×T): interaction between time and group. All analyses were controlled by intracranial volume.
*Significant at $P < 0.05$.

For exploratory purposes, we report on the results without correction for multiple comparisons—at the uncorrected level, two clusters of greater GM volume loss in PD patients than in controls were observed: in the left inferior lateral occipital cortex (3.08 cm^3; x, y, and z MNI coordinates of the maximum: −22, −90, and −2; $P < 0.001$, uncorrected) and in the left angular gyrus (0.37 cm^3; x, y, and z MNI coordinates of the maximum: −34, −56, and 26; $P < 0.001$, uncorrected). We did not find any areas of significantly greater GM volume loss in healthy controls than in PD patients.

Discussion

In this longitudinal study, we have found that, compared to controls, our sample of early-PD patients presented a faster rate of cortical thinning with a bilateral frontotemporal pattern, total GM and total cortical volume loss, and amygdalar atrophy after an average interval of 35 months.

The first longitudinal studies in PD only evaluated global brain measures[25] or a limited number of GM areas.[28] Since then, longitudinal progression of PD has been evaluated in samples formed by older patients as well as with patients who had longer disease duration. In a previous work done by our group, after a follow-up of 25 months, GM loss was observed in limbic and paralimbic structures.[26] In another study, including patients with visual hallucinations, we also found limbic and paralimbic plus neocortical GM loss.[27] In this work, we also observed that the longitudinal GM loss correlated with several measures of cognitive decline.

To our knowledge, this is the first study to evaluate structural progressive changes in a cohort of early-PD patients. Our findings indicate that the degeneration of certain areas observed in other studies may not yet be detectable in nondemented, early-PD patients. The fact that our cohort was formed by younger patients could also be contributing to the absence of detectable atrophy in areas affected both by the disease and by the aging processes, such as the hippocampus,[47] because these two factors are considered to interact biologically in the process of neuronal cell loss in nondopaminergic structures.[48]

In the present study, PD patients presented lower scores in some cognitive functions, compared to controls, at baseline, but both groups progressed at the same rate of cognitive decline over time. Previous studies reported that longitudinal changes in neuropsychological test results in early PD are much more significant in older patients.[5] This observed interaction, both between age and cognitive decline, in PD could be the functional manifestation of the interaction between age-related and disease-related GM atrophy observed, though this remains speculative.

In Lewy body (LB) diseases, cognitive changes are expected to precede detectable structural changes,[49] and we have found greater structural, but no greater cognitive, over-time deterioration in PD patients, compared to controls. However, a growing body of evidence suggests that cognitive deficits in PD have two general pathophysiological bases: (1) frontostriatal deficits, common in the early stages of disease, related to dopaminergic activity and not associated with a higher risk of evolution to dementia and (2) deficits with a more-posterior cortical basis, which herald

further cognitive decline,[5,50] and which are possibly related to primary cortical LB or Alzheimer's disease (AD)-type pathology.[51] Indeed, at baseline, our sample of PD patients presented deficits in neuropsychological functions related to dopamine-modulated circuits, such as working memory,[52,53] cognitive flexibility,[53,54] and psychomotor speed.[55] It is not surprising that deficits with a more functional basis might not be accompanied by detectable structural deterioration. On the other hand, the structural changes detected longitudinally could be related to the second mechanism of cognitive decline described above, and compensatory processes in this sample of young, early-PD patients might be preventing detectable functional repercussions.

Cross-sectional structural MRI studies with early-PD patients, as pointed out in the introduction of the current article, show highly variable results, sometimes with limited or no significant GM changes, in comparison to controls.[8] Nonetheless, one study did find cortical changes in early-stage patients through CTh analysis.[9] In the analyses, thickness reductions were observed in frontal areas similar to the ones we have found to degenerate more rapidly in PD patients than in controls.

Overall, these results suggest that the different parameters evaluated provide complementary and related information on changes occurring in PD.

A common drawback in longitudinal studies is the loss of some of the initial subjects at follow-up. In this study, the final sample of 16 PD patients, though appropriate for longitudinal analyses, does not allow dividing them into subgroups to study relevant variables, such as the presence of dyskinesias, previously related to changes in the right inferior frontal gyrus,[56] or behavioral abnormalities. Also, we cannot exclude that subtle cognitive decline associated with the longitudinal structural changes described could be detected with a larger sample.

One caveat in both VBM and CTh analysis is that, as a result of the characteristics of the underlying neuroanatomy, GM and cortical thickness maps are nonstationary.[57] This, in turn, may lead to an overestimation of cluster sizes in areas of the images that display higher smoothing, and an underestimation in rougher areas,[58] affecting both the false-positive and false-negative rates of analyses that include cluster-size corrections.[59] Though cluster-size inference methods to correct for these effects are sometimes used in VBM analyses,[60,61] the permutation cluster-level correction implemented in cortical thickness analyses assumes images to be stationary and may thus be susceptible to such artifacts.

Conclusion

In conclusion, as in other neurodegenerative diseases such as AD, our findings suggest that the pathophysiological process of PD exerts specific deleterious effects in the brain, even preceding clinical manifestations of progressive decline in cognitive function.

References

1. Foltynie T, Brayne CE, Robbins TW, Barker RA. The cognitive ability of an incident cohort of Parkinson's patients in the UK. The CamPaIGN study. Brain 2004;127:550–560.
2. Muslimovic D, Post B, Speelman JD, Schmand B. Cognitive profile of patients with newly diagnosed Parkinson disease. Neurology 2005;65:1239–1245.
3. Aarsland D, Bronnick K, Larsen JP, Tysnes OB, Alves G, Norwegian ParkWest Study Group. Cognitive impairment in incident, untreated Parkinson disease: the Norwegian ParkWest study. Neurology 2009;72:1121–1126.
4. Elgh E, Domellof M, Linder J, Edstrom M, Stenlund H, Forsgren L. Cognitive function in early Parkinson's disease: a population-based study. Eur J Neurol 2009;16:1278–1284.
5. Williams-Gray CH, Foltynie T, Brayne CE, Robbins TW, Barker RA. Evolution of cognitive dysfunction in an incident Parkinson's disease cohort. Brain 2007;130:1787–1798.
6. Muslimovic D, Post B, Speelman JD, De Haan RJ, Schmand B. Cognitive decline in Parkinson's disease: a prospective longitudinal study. J Int Neuropsychol Soc 2009;15:426–437.
7. Braak H, Del Tredici K, Rub U, de Vos RA, Jansen Steur EN, Braak E. Staging of brain pathology related to sporadic Parkinson's disease. Neurobiol Aging 2003;24:197–211.
8. Jubault T, Brambati SM, Degroot C, et al. Regional brain stem atrophy in idiopathic Parkinson's disease detected by anatomical MRI. PLoS One 2009;4:e8247.
9. Tinaz S, Courtney MG, Stern CE. Focal cortical and subcortical atrophy in early Parkinson's disease. Mov Disord 2011;26:436–441.
10. Ibarretxe-Bilbao N, Junqué C, Tolosa E, et al. Neuroanatomical correlates of impaired decision-making and facial emotion recognition in early Parkinson's disease. Eur J Neurosci 2009;30: 1162–1171.
11. Jubault T, Gagnon JF, Karama S, et al. Patterns of cortical thickness and surface area in early Parkinson's disease. Neuroimage 2011;55:462–467.
12. Ibarretxe-Bilbao N, Junqué C, Marti MJ, Tolosa E. Brain structural MRI correlates of cognitive dysfunctions in Parkinson's disease. J Neurol Sci 2011;310:70–74.
13. Beyer MK, Janvin CC, Larsen JP, Aarsland D. A magnetic resonance imaging study of patients with Parkinson's disease with mild cognitive impairment and dementia using voxel-based morphometry. J Neurol Neurosurg Psychiatry 2007;78:254–259.
14. Camicioli R, Moore MM, Kinney A, Corbridge E, Glassberg K, Kaye JA. Parkinson's disease is associated with hippocampal atrophy. Mov Disord 2003;18:784–790.
15. Junqué C, Ramírez-Ruiz B, Tolosa E, et al. Amygdalar and hippocampal MRI volumetric reductions in Parkinson's disease with dementia. Mov Disord 2005;20:540–544.
16. Weintraub D, Doshi J, Koka D, et al. Neurodegeneration across stages of cognitive decline in Parkinson disease. Arch Neurol 201; 68:1562–1568.
17. Pereira JB, Junqué C, Martí MJ, Ramírez-Ruiz B, Bargalló N, Tolosa E. Neuroanatomical substrate of visuospatial and visuoperceptual impairment in Parkinson's disease. Mov Disord 2009;24: 1193–1199.
18. Pereira JB, Junqué C, Martí MJ, Ramírez-Ruiz B, Bartrés-Faz D, Tolosa E. Structural brain correlates of verbal fluency in Parkinson's disease. Neuroreport 2009;20:741–744.
19. Hutton C, Draganski B, Ashburner J, Weiskopf N. A comparison between voxel-based cortical thickness and voxel-based morphometry in normal aging. Neuroimage 2009;48:371–380.
20. Winkler AM, Kochunov P, Blangero J, et al. Cortical thickness or grey matter volume? The importance of selecting the phenotype for imaging genetics studies. Neuroimage 2010;53:1135–1146.
21. Labate A, Cerasa A, Mula M, et al. Neuroanatomic correlates of psychogenic nonepileptic seizures: a cortical thickness and VBM study. Epilepsia 2012;53:377–385.

22. Palaniyappan L, Liddle PF. Dissociable morphometric differences of the inferior parietal lobule in schizophrenia. Eur Arch Psychiatry Clin Neurosci 2012 [published online ahead of print March 28 2012].
23. Camicioli R, Sabino J, Gee M, et al. Ventricular dilatation and brain atrophy in patients with Parkinson's disease with incipient dementia. Mov Disord 2011;26:1443–1450.
24. Lewis MM, Smith AB, Styner M, et al. Asymmetrical lateral ventricular enlargement in Parkinson's disease. Eur J Neurol 2009;16: 475–481.
25. Hu MT, White SJ, Chaudhuri KR, Morris RG, Bydder GM, Brooks DJ. Correlating rates of cerebral atrophy in Parkinson's disease with measures of cognitive decline. J Neural Transm 2001; 108:571–580.
26. Ramírez-Ruiz B, Martí MJ, Tolosa E, et al. Longitudinal evaluation of cerebral morphological changes in Parkinson's disease with and without dementia. J Neurol 2005;252:1345–1352.
27. Ibarretxe-Bilbao N, Ramírez-Ruiz B, Junqué C, et al. Differential progression of brain atrophy in Parkinson's disease with and without visual hallucinations. J Neurol Neurosurg Psychiatry 2010;81: 650–657.
28. Paviour DC, Price SL, Jahanshahi M, Lees AJ, Fox NC. Longitudinal MRI in progressive supranuclear palsy and multiple system atrophy: rates and regions of atrophy. Brain 2006;129:1040–1049.
29. Daniel SE, Lees AJ. Parkinson's Disease Society Brain Bank, London: overview and research. J Neural Transm Suppl 1993;39: 165–172.
30. Dubois B, Burn D, Goetz C, et al. Diagnostic procedures for Parkinson's disease dementia: recommendations from the movement disorder society task force. Mov Disord 2007;22:2314–2324.
31. Beck AT, Steer RA, Brown GK. Manual for the Beck Depression Inventory-II. San Antonio, TX: Psychological Corporation, 1996.
32. Cummings JL, Mega M, Gray K, Rosenberg-Thompson S, Carusi DA, Gornbein J. The Neuropsychiatric Inventory: comprehensive assessment of psychopathology in dementia. Neurology 1994;44: 2308–2314.
33. Fischl B, Dale AM. Measuring the thickness of the human cerebral cortex from magnetic resonance images. Proc Natl Acad Sci U S A 2000;97:11050–11055.
34. Segonne F, Dale AM, Busa E, et al. A hybrid approach to the skull stripping problem in MRI. Neuroimage 2004;22:1060–1075.
35. Sled JG, Zijdenbos AP, Evans AC. A nonparametric method for automatic correction of intensity nonuniformity in MRI data. IEEE Trans Med Imaging 1998;17:87–97.
36. Fischl B, Liu A, Dale AM. Automated manifold surgery: constructing geometrically accurate and topologically correct models of the human cerebral cortex. IEEE Trans Med Imaging 2001;20:70–80.
37. Ségonne F, Pacheco J, Fischl B. Geometrically accurate topology-correction of cortical surfaces using nonseparating loops. IEEE Trans Med Imaging 2007;26:518–529.
38. Reuter M, Fischl B. Avoiding asymmetry-induced bias in longitudinal image processing. Neuroimage 2011;57:19–21.
39. Reuter M, Rosas HD, Fischl B. Highly accurate inverse consistent registration: a robust approach. Neuroimage 2010;53:1181–1196.
40. Reuter M, Schmansky NJ, Rosas HD, Fischl B. Within-subject template estimation for unbiased longitudinal image analysis. Neuroimage 2012;61:1402–1418.
41. Forman SD, Cohen JD, Fitzgerald M, Eddy WF, Mintun MA, Noll DC. Improved assessment of significant activation in functional magnetic resonance imaging (fMRI): use of a cluster-size threshold. Magn Reson Med 1995;33:636–647.
42. Fischl B, Salat DH, Busa E, et al. Whole brain segmentation: automated labeling of neuroanatomical structures in the human brain. Neuron 2002;33:341–355.
43. Ashburner J, Friston KJ. Unified segmentation. Neuroimage 2005; 26:839–851.
44. Ashburner J. A fast diffeomorphic image registration algorithm. Neuroimage 2007;38:95–113.
45. Asami T, Bouix S, Whitford TJ, Shenton ME, Salisbury DF, McCarley RW. Longitudinal loss of gray matter volume in patients with first-episode schizophrenia: DARTEL automated analysis and ROI validation. Neuroimage 2012;59:986–996.
46. Worsley KJ, Marrett S, Neelin P, Vandal AC, Friston KJ, Evans AC. A unified statistical approach for determining significant signals in images of cerebral activation. Human Brain Mapping 1996; 4:58–73.
47. Ibarretxe-Bilbao N, Ramírez-Ruiz B, Tolosa E, et al. Hippocampal head atrophy predominance in Parkinson's disease with hallucinations and with dementia. J Neurol 2008;255:1324–1331.
48. Levy G. The relationship of Parkinson disease with aging. Archives of Neurology 2007;64:1242–1246.
49. Fields JA, Ferman TJ, Boeve BF, Smith GE. Neuropsychological assessment of patients with dementing illness. Nat Rev Neurol 2011;7:677–687.
50. Williams-Gray CH, Evans JR, Goris A, et al. The distinct cognitive syndromes of Parkinson's disease: 5 year follow-up of the CamPaIGN cohort. Brain 2009;132:2958–2969.
51. Compta Y, Parkkinen L, O'Sullivan SS, et al. Lewy- and Alzheimer-type pathologies in Parkinson's disease dementia: which is more important? Brain 2011;134:1493–1505.
52. Castner SA, Williams GV, Goldman-Rakic PS. Reversal of antipsychotic-induced working memory deficits by short-term dopamine D1 receptor stimulation. Science 2000;287:2020–2022.
53. Cools R. Dopaminergic modulation of cognitive function-implications for L-DOPA treatment in Parkinson's disease. Neurosci Biobehav Rev 2006;30:1–23.
54. Fallon SJ, Williams-Gray CH, Barker RA, Owen AM, Hampshire A. Prefrontal dopamine levels determine the balance between cognitive stability and flexibility. Cereb Cortex 2012 [published online ahead of print February 20 2012].
55. Rihet P, Possamaï CA, Micallef-Roll J, Blin O, Hasbroucq T. Dopamine and human information processing: a reaction-time analysis of the effect of levodopa in healthy subjects. Psychopharmacology (Berl) 2002;163:62–67.
56. Cerasa A, Messina D, Pugliese P, et al. Increased prefrontal volume in PD with levodopa-induced dyskinesias: a voxel-based morphometry study. Mov Disord 2011;26:807–812.
57. Ashburner J, Friston KJ. Voxel-based morphometry--the methods. Neuroimage 2000;11:805–821.
58. Worsley KJ, Andermann M, Koulis T, MacDonald D, Evans AC. Detecting changes in nonisotropic images. Hum Brain Mapp 1999; 8:98–101.
59. Salimi-Khorshidi G, Smith SM, Nichols TE. Adjusting the effect of nonstationarity in cluster-based and TFCE inference. Neuroimage 2011;54:2006–2019.
60. Hayasaka S, Nichols TE. Validating cluster size inference: random field and permutation methods. Neuroimage 2003;20: 2343–2356.
61. Hayasaka S, Phan KL, Liberzon I, Worsley KJ, Nichols TE. Nonstationary cluster-size inference with random field and permutation methods. Neuroimage 2004;22:676–687.

SUPPLEMENTARY MATERIALS

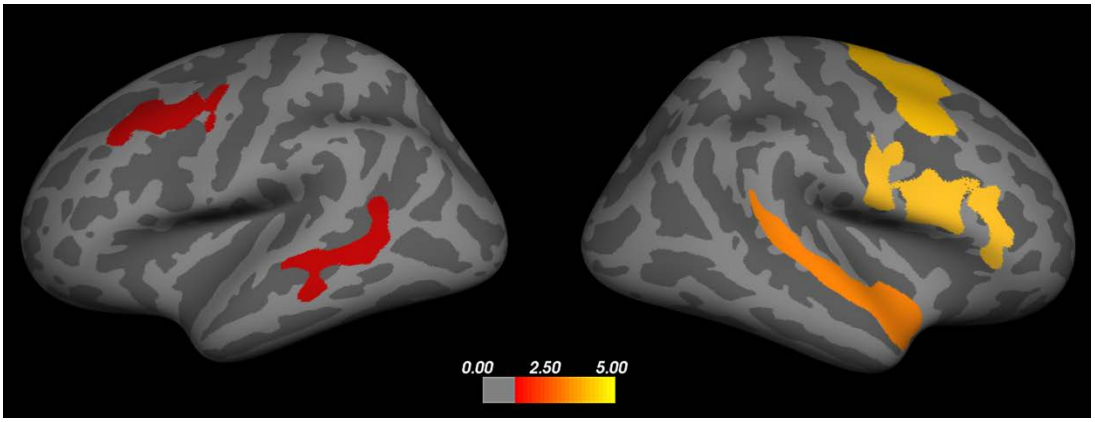

Supplementary Figure 1. Cortical areas showing significantly higher symmetrized percent change (in % per year) in PD patients compared with controls. The color bar shows the logarithmic scale of p values ($-\log_{10}$). Results were obtained using Z Monte Carlo simulation with 10,000 iterations applied to CTh maps to provide clusterwise correction for multiple comparisons. Results were thresholded at a corrected *p* value of 0.05.

chapter 5
DISCUSSION

The main objective of the present thesis was to investigate the contribution of changes in connectivity between distributed brain regions, as well as the contribution of regional brain atrophy, to the occurrence of different types of cognitive and neuropsychiatric impairments in non-demented PD patients. To this end, seven studies were performed to address specific questions, using different analytical perspectives.

MILD COGNITIVE IMPAIRMENT

In the first three studies presented in this thesis, large and overlapping samples of HC and PD patients were neuropsychologically assessed to determine the presence of deficits in different cognitive domains. This assessment, in turn, served as the basis for the classification of MCI. As expected [Aarsland et al., 2010; Goldman and Litvan, 2011; Litvan et al., 2011a], a high proportion of PD patients in our sample were classified as having MCI – from around 35% in the subsample included in the functional connectivity studies to 52.2% in the larger group of patients included in the CTh study. Most patients with MCI, however, had deficits in more than one cognitive domain, precluding the creation of subgroups according to type of deficit.

We used two different systems to determine the presence of MCI in these studies – a reflection of the evolving and, as yet, not firmly established consensus in the diagnosis of MCI in PD. In the functional connectivity studies (*studies 1* and *2*), we applied criteria similar to those used in several relevant epidemiological and neuroimaging articles [Aarsland et al., 2009a; Aarsland et al., 2010; Dalaker et al., 2010; Dalaker et al., 2011; Janvin et al., 2006], which considers 3 cognitive domains: attention/executive functions, memory and visuospatial. In *study 3*, we adopted a classification system in accordance with the recently-proposed MDS criteria [Litvan et al., 2012], considering 5 domains: attention/working memory, executive functions, memory, language and visuospatial. The main disparity between the two systems used is the inclusion of language in the 5-domain scheme. In line with previous findings [Emre, 2003], however, a small proportion (4.4%) of PD patients had language deficits. Differences in individual-subject classification are therefore limited, and diagnostic agreement was above 90% in our PD sample. Of note, Pereira *et al.* recently found that two diagnostic systems comparable to the ones we used yielded similar results in a CTh study [Pereira et al., 2014].

RESTING-STATE INTRINSIC CONNECTIVITY NETWORKS, STRUCTURAL DEGENERATION AND COGNITIVE IMPAIRMENT

In the first study, we evaluated the relationship between cognitive decline – and the presence of MCI – and the functional organization of a set of relevant large-scale ICNs. PD-MCI patients displayed abnormalities in the pattern of connectivity both within and between

networks. Recent evidence from multiple studies indicates that the dynamic interaction between brain regions organized into large-scale ICNs such as the DAN, the FPN, the DMN and the salience network is relevant for several cognitive processes, especially attentional and executive ones [Corbetta et al., 2008; Spreng et al., 2013]. Importantly, the anterior insula appears to be a critical structure in this network-switching mechanism [Menon and Uddin, 2010; Seeley et al., 2007]. The anterior insula is a key region in the monitoring of external and internal signals through *tonic alertness* [Sadaghiani and D'Esposito, 2014], promoting the *bottom-up* switching between large-scale networks when salient stimuli are detected [Menon and Uddin, 2010].

In accordance with Spreng *et al.* [Spreng et al., 2013], data-driven analysis (*study 1*) revealed that the anterior insula was part of the FPN, a network involved with the *top-down* allocation of attentional resources on a *phasic*, event-by-event basis, possibly also by effecting a network-switching mechanism [Menon and Uddin, 2010; Sadaghiani et al., 2012; Spreng et al., 2010; Spreng et al., 2013]. The anterior insula thus appears to be a critical region where bottom-up and top-down inputs compete to drive attentional processes. A connectivity disruption between this region and the DAN, as we observed, may conceivably lead to a deficient recruitment of this network during attention/executive tasks, resulting in the cognitive impairments observed in PD-MCI patients. Our work thus adds relevant information to recent evidence from studies using different modalities regarding the importance of insular changes in the genesis of non-motor symptoms in PD [Christopher et al., 2014a].

Changes in the anterior insula's dopamine-related gatekeeping role in large-scale network switch as a culprit in attention/executive impairment in PD

1. Attention/executive deficits in PD are related to dopamine [Williams-Gray et al., 2009];
2. Coupling of attention networks is related to dopamine [Dang et al., 2012];
3. The anterior insula is related to the coupling of attention networks [Menon and Uddin, 2010];
4. Insular dopamine loss is related to attention/executive deficits in PD [Christopher et al., 2014b];
5. *Reduced coupling between the anterior insula and the DAN is related to attention/executive deficits in PD* [Baggio et al., 2014b].

Future studies using alternative approaches such as task-based fMRI or tractography could shed light on the relationship between the connectivity patterns of the anterior insula with attention-related ICNs and the occurrence of attention/executive deficits in PD.

In line with the proposed role of the networks assessed in *study 1*, the connectivity reductions described above correlated with performance in attention/executive functions. Such deficits in non-demented PD are considered to be related to dopaminergic imbalances rather than to primary cortical pathology [Williams-Gray et al., 2009], and therefore can be expected to have stronger functional than structural correlates. Accordingly, the insular connectivity reductions observed in *study 1* were not accompanied by detectable GM atrophy, and correlated with LEDD; furthermore, attention/executive deficits did not correlate with the cortical thinning found in PD-MCI.

PD-MCI patients were also seen in *study 1* to have connectivity increases between parieto-occipital cortical areas and the DMN; these increases, in turn, correlated with visuospatial/visuoperceptual deficits and with posterior cortical thinning. Further analysis revealed that these posterior cortical areas, mainly belonging to the DAN, had reduced connectivity with anterior DAN and FPN regions; and that the apparent connectivity increments corresponded to the loss of their expected negative correlation with the DMN. Additionally, in *study 2* we performed a global analysis of network correlation that does not consider reduced anticorrelations as connectivity increments (see below); no significant increases in temporo-occipito-parietal connectivity was observed that could correspond to posterior cortical connectivity *increases* with the DMN. This observation gives further support to the notion that, rather than actual connectivity gains, the observed effect corresponded to the loss of the normal pattern of anticorrelation with the DMN. The association observed between these changes and visuospatial/visuoperceptual deficits may be causal – *i.e.*, directly related to connectivity disruptions in the networks analyzed – or may be the result of changes occurring in visual processing regions, also seen to be involved. Future studies specifically analyzing visual networks might help clarify this issue.

Importantly, there's accumulating evidence that parieto-occipital cortical changes underlie cognitive impairments that herald worse cognitive prognosis in PD patients [Bohnen et al., 2011; Williams-Gray et al., 2007; Williams-Gray et al., 2009]. In *study 3*, this predominantly posterior cortical pattern of atrophy in MCI was confirmed, and also seen to be related to the severity of overall cognitive impairment. Of note, the connectivity 'increments' described in *study 1* were seen even after controlling for GM atrophy, which may suggest that they are not merely a result of structural degeneration; instead, the same pathological mechanisms that lead to the supposed neuronal death underlying cortical thinning may also be responsible for neuronal dysfunction, which in turn leads to the connectivity changes we observed. Future longitudinal studies assessing cognitively-normal PD patients could be useful to clarify whether posterior cortical functional changes antecede structural atrophy, and whether they can be used to predict future cognitive decline. Furthermore, radiotracer or pathological studies could investigate whether parieto-occipital cortical changes, associated with cognitive impairment and dementia in PD, are related to cortical Alzheimer's type pathology and/or cortical synucleinopathy.

PD-MCI is associated with posterior cortical structural and functional changes that are accompanied clinically by the occurrence of visuospatial/visuoperceptual deficits

PD patients with MCI have specific changes in posterior, temporo-occipito-parietal cortical regions that merit further investigation. These regions undergo a functional disruption process characterized by disconnection from their 'original' networks (such as the DAN), with subsequent loss of the anticorrelated pattern between said networks and the DMN. This process is accompanied by structural degeneration and is associated with visuospatial/visuoperceptual deficits. Future studies should investigate the pathological bases of these changes and their value as prognostic markers.

NETWORK ANALYSIS, GRAPH-THEORY PARAMETERS AND COGNITIVE IMPAIRMENT

The analysis of the global connectivity architecture of the brain (*study 2*) revealed that PD patients with MCI had functional connectivity reductions, mainly affecting long-range, interlobar connections, alongside a smaller number of shorter-range connectivity increments. A key methodological aspect differentiates this analysis from the approach used in *study 1*: while the *ICA/dual regression* and the *seed-based connectivity* techniques (*study 1*) take into account correlations and anticorrelations (essential for the analysis of ICN interaction), the global network approach used in *study 2* only considers positive correlations. As a result, in *study 1* the number of connectivity decreases in PD-MCI detected in seed-based analyses was roughly similar to the number of increases; in this case, the loss of an anticorrelation, which is actually the *weakening* of a correlation, is considered as an *increment*. The subsequent analysis of the pattern of changes allows interpreting them under the perspective of correlated and anticorrelated ICNs. In contrast, since the neurobiological interpretation of individual negative correlations is not straightforward, in *study 2* the purpose was to equate *connectivity increases* or *decreases* with *increased* or *decreased connectivity strength*, respectively; as a result, it became evident that in PD-MCI the predominant effect was that of reduced connectivity.

In *studies 1* and *2*, we have identified significant functional connectivity changes associated with the presence of cognitive deficits in PD. In *study 4*, we have found evidence that microstructural WM changes also contribute to the occurrence of cognitive impairment in patients with PD. Future studies combining functional and structural connectivity should be performed to investigate the contribution of WM changes to the global functional changes described in this thesis.

In *study 6*, although patients were relatively young and had, on average, mild cognitive deficits, longitudinal analysis revealed the progressive weakening of long-range, frontoparietal connections; shorter frontofrontal connections that displayed progressive weakening in HC remained stable in PD patients. The observed effect might correspond to the incipient changes that, in time, lead to the ones found in MCI patients in *study 2* – *i.e.*, long-range connectivity loss with increased local interconnectivity. This observation, however, is merely speculative since only a limited circuitry was assessed in *study 6*; more comprehensive longitudinal global connectivity analyses should be performed to evaluate this hypothesis.

The topological analysis in *study 2* revealed no global differences between PD-NMCI patients and HC. The functional connectomes of PD-MCI patients, in turn, showed increased modularity and *small-worldness*, as well as increased clustering coefficients at strict sparsity thresholding. Correlation analyses revealed that these measures – modularity, small-world and clustering coefficients – were negatively associated with memory and visuospatial/visuoperceptual performance. These findings suggest that the functional brain networks of PD-MCI patients are reorganized, with increased interconnectivity inside network modules. It is difficult to establish, however, whether such changes are of a compensatory nature – perhaps due to the loss of long-range connections; or whether they correspond instead to a process of anomalous plasticity (perhaps due to cortical

synucleinopathy or Alzheimer's type pathology) and have a causal role in the deficits they correlate with. Interestingly, a recent study using a similar approach to assess age-related cognitive decline in healthy subjects found that older subjects had long-range connectivity reductions associated with increased clustering – and, as in *study 2*, clustering coefficients correlated with memory performance [Sala-Llonch et al., 2014]. Age-related changes, however, were also characterized by a marked reduction in network integration, a finding not present in our PD subgroups.

Importantly, attention/executive deficits did not correlate with global network measures; the analysis of regional parameters, on the other hand, revealed that performance in this cognitive domain was associated with nodal measures mainly in frontal regions. Future longitudinal studies should assess whether global network measures such as small-world, modularity or clustering coefficients can be helpful in predicting cognitive decline in PD. Further analyses (see Figure 5.1) show that, in PD patients, the clustering coefficients obtained in *study 2* correlate significantly with the posterior cortical connectivity 'increases' described in *study 1*. This observation suggests they may be related processes; it is likely that the connectivity reductions between posterior cortical regions and anterior DAN/FPN nodes (*study 1*) are part of the long-range connectivity reductions seen in *studies 2* and *6*. As a consequence of these long-range disruptions, possibly compensatory increases in local interconnectivity as seen in *study 2* could account for the increased tendency to form clusters.

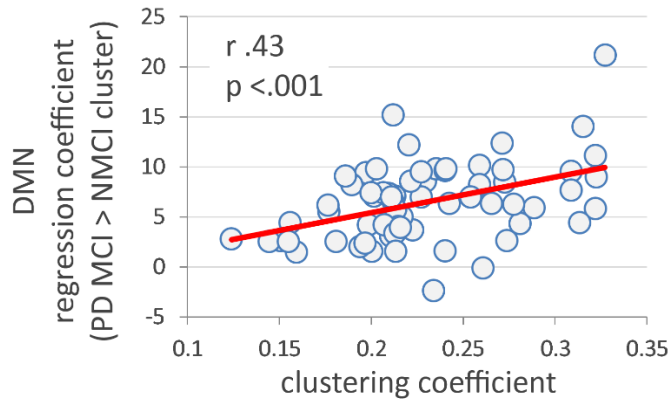

Figure 5.1. Correlation between parieto-occipital connectivity increases (*study 1*) and global clustering coefficients (*study 2*).

Functional network changes have additionally been seen in *study 2* to be associated with changes in the centrality of network nodes. Nodes that normally display high centrality (*network hubs*) tend to lose centrality; nodes that are normally less central, on the other hand, tend to become more so. This process may be part of the global network reorganization – *e.g.*, the strengthening of alternative paths to compensate for the loss of long-range connections. It may, alternatively, reflect the preferential involvement of network hubs in the neurodegenerative process, as has been described in several neurodegenerative diseases [Crossley et al., 2014]. Future studies investigating the preferential degeneration of hub brain regions in PD patients with cognitive decline could help clarify this issue.

Studies 1 and *2* indicate that attention/executive deficits are associated with changes in ICN connectivity as well as with nodal graph-theory measures in frontal regions, whereas

visuospatial/visuoperceptual deficits correlated with parieto-occipital connectivity and structural changes. Memory impairments, on the other hand, did not yield a clear pattern of associated changes. These deficits correlated with the same global graph-theory measures that were associated with visuospatial/visuoperceptual impairments. No correlations, however, were found for intra or inter-ICN connectivity, although memory deficits were common in PD patients. This is somewhat unexpected considering previous evidence that memory deficits in PD have hippocampal structural GM neuroimaging substrates [Beyer et al., 2013; Carlesimo et al., 2012; Pereira et al., 2013; Weintraub et al., 2011] – and that the hippocampi are part of the DMN [Spreng et al., 2013]. In *study 6* and in previous work using similar methodology [Ibarretxe-Bilbao et al., 2011], however, the directed analysis of specific task-related networks was able to reveal functional correlates for the less prevalent recognition memory deficits, even in early-PD patients. Future studies addressing specific networks related to episodic memory performance might shed light on the functional bases of deficits in this function.

NEUROPSYCHIATRIC AND EMOTION PROCESSING DEFICITS

In *studies 4* and *5* we have performed directed analyses of structures and circuits theorized to be related to the impairments of interest, in order to answer specific study questions. In the case of the basal ganglia, this directed approach is essential – given the complex functional neuroanatomy of their subcomponents –, and also problematic considering the low spatial resolution of usual fMRI acquisitions and lack of image contrast to define the boundaries of functional striatal subdivisions. In *study 5*, through the parcellation of the frontostriatal pathways into specific circuits, we were able to demonstrate that apathy in PD is characterized by reduced connectivity, mainly affecting the ventral striatum and orbitofrontal cortex – the so-called limbic subdivision of the frontostriatal loops – especially in the left hemisphere. Specifically, these changes were characterized by a shift in frontostriatal connections from positive correlations in non-apathetic PD patients to negative correlations in apathetic patients; frontofrontal connections, on the other hand, were seen to be positive in non-apathetic patients and to approach zero in those with increasing severity of apathy. The orbitofrontal cortex and the ventral striatum integrate the affective value of a stimulus into behavior in a dopamine-dependent mechanism [Levy and Dubois, 2006; Pessiglione et al., 2007; Sinha et al., 2013], acting as the *limbic-motor* interface [Mogenson et al., 1980]. The changes seen in *study 5* may therefore represent a functional counterpart of the impairment in generating spontaneous behavior directed at external stimuli, related to an impaired capacity of evaluating their affective context [Levy and Dubois, 2006].

Although apathy in PD is theorized to be related to dopamine imbalances, future studies assessing the contribution of WM microstructural changes to the frontostriatal connectivity changes found in *study 5* could provide useful information. Indeed, in *study 4* we have found that FA – an MRI marker of microstructural integrity – was reduced in long-range associative WM tracts in PD patients with relatively preserved cognitive status, and that this reduction was associated with facial emotion recognition performance. Alongside recent evidence of WM degeneration associated with cognitive deficits in PD [Agosta et al., 2013; Melzer et al., 2013], our findings indicate that *structural disconnection* plays a relevant part in the neural substrates of non-motor deficits in PD.

In *study 4*, we have found that PD patients have specific deficits in the identification of negative emotions in facial expressions. The results of this study may further indicate that

GM and WM changes are differentially associated with cognitive deficits in PD: although the correlation between the identification of sad facial expressions and FA was the only one to reach whole-brain statistical significance, GM analysis was able to detect correlates for a wider range of deficits.

Although knowledge about the pathological bases of WM microstructural changes is currently very limited, there's some evidence to indicate that it may be directly related to the synucleinopathy [Orimo et al., 2005; Orimo et al., 2008]. Both synucleinopathy and AD-type pathology, in turn, are thought to be related to the GM changes underlying cognitive decline in PD [Clinton et al., 2010; Compta et al., 2011; Lashley et al., 2008; Tsuboi et al., 2007]. It is therefore licit to speculate that they progress independently. Studies assessing the differential contributions and prognostic values of GM and WM changes to different types of PD-related cognitive decline – as well as pathological studies to clarify the origins of the observed neuroimaging effects – are necessary to better characterize these relevant processes.

PATTERN OF GRAY MATTER LOSS

In *study 3*, a common pattern of cortical thinning was observed for neuropsychological tests across the domains evaluated, including attention/executive functions. As pointed out above, patients in our sample tended to have multiple-domain MCI, and neuropsychological test scores were highly intercorrelated. It cannot be excluded that the observed correlation between attention/executive tests and posterior cortical thinning was driven by the relationship between these impairments and deficits with posterior cortical substrates.

Study 7, performed with a different subject sample, might help clarify this issue. In this longitudinal study, early-PD patients at baseline performed significantly worse than HC, primarily in attention/executive tests – yet there were no intergroup differences in CTh. Longitudinal analysis revealed that PD patients had progressive worsening in attention tests and progressive cortical thinning, both more marked than in the HC group. The pattern of thinning predominated in frontotemporal areas – *i.e.*, did not correspond to the pattern associated with MCI in *studies 1* and *3*. Importantly, the degree of thinning in these regions did not correlate with the observed cognitive deficits. Analyzed together, results obtained from *studies 1*, *3* and *7* suggest that attention/executive deficits in non-demented PD patients, associated with dopamine-related frontostriatal impairments, have predominantly functional neural substrates.

In early-PD patients with limited, mainly frontostriatal deficits, progressive cortical atrophy is detectable even in the absence of significant cognitive decline. In more advanced disease stages, when other types of cognitive deficit are evident, posterior, temporo-occipito-parietal cortical thinning can be detected.

We have been able to identify the initial pattern of progressive GM loss in early-stage PD patients – mainly involving frontotemporal neocortical and medial temporal regions.

Furthermore, the directed analysis of brain structures involved in functions impaired in PD subjects – such as those related to facial emotion recognition, including mesocortical, allocortical, subcortical and neocortical regions – can reveal GM atrophy even in patients with limited cognitive changes. As more severe cognitive deficits set in, posterior cortical atrophy is evident. Although these data shed light on the pattern of progression of structural GM changes in PD, further longitudinal studies, with longer follow-up periods may prove valuable in characterizing this evolution more accurately. It would be interesting to investigate whether the pattern of disease progression differs between younger- and older-onset PD as has been suggested in neuropathological studies [Halliday et al., 2008]. It may be worth pointing out, at any rate, that like most neuroimaging studies, our findings do not conform to the pattern predicted by the Braak staging, suggesting the existence of underlying causes other than cortical LB/LN pathology in the pathophysiology of these structural changes.

REFERENCES

1. Aarsland D, Brønnick K, Larsen JP, Tysnes OB, Alves G, Norwegian ParkWest Study Group (2009): Cognitive impairment in incident, untreated Parkinson disease: the Norwegian ParkWest study. Neurology 72:1121–1126.
2. Aarsland D, Bronnick K, Williams-Gray C, Weintraub D, Marder K, Kulisevsky J, Burn D, Barone P, Pagonabarraga J, Allcock L, Santangelo G, Foltynie T, Janvin C, Larsen JP, Barker RA, Emre M (2010): Mild cognitive impairment in Parkinson disease: a multicenter pooled analysis. Neurology 75:1062–9.
3. Agosta F, Canu E, Stefanova E, Sarro L, Tomić A, Spica V, Comi G, Kostić VS, Filippi M (2013): Mild cognitive impairment in Parkinson's disease is associated with a distributed pattern of brain white matter damage. Hum Brain Mapp 00.
4. Baggio H-C, Segura B, Sala-Llonch R, Marti M-J, Valldeoriola F, Compta Y, Tolosa E, Junqué C (2014): Cognitive impairment and resting-state network connectivity in Parkinson's disease. Hum Brain Mapp.
5. Beyer MK, Bronnick KS, Hwang KS, Bergsland N, Tysnes OB, Larsen JP, Thompson PM, Somme JH, Apostolova LG (2013): Verbal memory is associated with structural hippocampal changes in newly diagnosed Parkinson's disease. J Neurol Neurosurg Psychiatry 84:23–8.
6. Bohnen NI, Koeppe R a, Minoshima S, Giordani B, Albin RL, Frey KA, Kuhl DE (2011): Cerebral glucose metabolic features of Parkinson disease and incident dementia: longitudinal study. J Nucl Med 52:848–855.
7. Carlesimo GA, Piras F, Assogna F, Pontieri FE, Caltagirone C, Spalletta G (2012): Hippocampal abnormalities and memory deficits in Parkinson disease: a multimodal imaging study. Neurology 78:1939–45.
8. Christopher L, Koshimori Y, Lang AE, Criaud M, Strafella AP (2014a): Uncovering the role of the insula in non-motor symptoms of Parkinson's disease. Brain 137:2143–2154.
9. Christopher L, Marras C, Duff-Canning S, Koshimori Y, Chen R, Boileau I, Segura B, Monchi O, Lang AE, Rusjan P, Houle S, Strafella AP (2014b): Combined insular and striatal dopamine dysfunction are associated with executive deficits in Parkinson's disease with mild cognitive impairment. Brain 137:565–575.
10. Clinton LK, Blurton-Jones M, Myczek K, Trojanowski JQ, LaFerla FM (2010): Synergistic Interactions between Abeta, tau, and alpha-synuclein: acceleration of neuropathology and cognitive decline. J Neurosci 30:7281–9.
11. Compta Y, Parkkinen L, O'Sullivan SS, Vandrovcova J, Holton JL, Collins C, Lashley T, Kallis C, Williams DR, de Silva R, Lees AJ, Revesz T (2011): Lewy- and Alzheimer-type pathologies in Parkinson's disease dementia: which is more important? Brain 134:1493–505.
12. Corbetta M, Patel G, Shulman GL (2008): The reorienting system of the human brain: from environment to theory of mind. Neuron 58:306–24.
13. Dalaker TO, Zivadinov R, Larsen JP, Beyer MK, Cox JL, Alves G, Bronnick K, Tysnes O-B, Antulov R, Dwyer MG, Aarsland D (2010): Gray matter correlations of cognition in incident Parkinson's disease. Mov Disord 25:629–33.
14. Dalaker TO, Zivadinov R, Ramasamy DP, Beyer MK, Alves G, Bronnick KS, Tysnes O-B, Aarsland D, Larsen JP (2011): Ventricular enlargement and mild cognitive impairment in early Parkinson's disease. Mov Disord 26:297–301.
15. Dang LC, O'Neil JP, Jagust WJ (2012): Dopamine supports coupling of attention-related networks. J Neurosci 32:9582–7.
16. Emre M (2003): Dementia associated with Parkinson's disease. Lancet Neurol 2:229–37.
17. Goldman JG, Litvan I (2011): Mild cognitive impairment in Parkinson's disease. Minerva Med 102:441–59.
18. Halliday GM, Hely M, Reid W, Morris J (2008): The progression of pathology in longitudinally followed patients with Parkinson's disease. Acta Neuropathol 115:409–15.
19. Ibarretxe-Bilbao N, Zarei M, Junque C, Marti MJ, Segura B, Vendrell P, Valldeoriola F, Bargallo N, Tolosa E (2011): Dysfunctions of cerebral networks precede recognition memory deficits in early Parkinson's disease. Neuroimage 57:589–97.
20. Janvin CC, Larsen JP, Aarsland D, Hugdahl K (2006): Subtypes of mild cognitive impairment in Parkinson's disease: progression to dementia. Mov Disord 21:1343–9.
21. Lashley T, Holton JL, Gray E, Kirkham K, O'Sullivan SS, Hilbig A, Wood NW, Lees AJ, Revesz T (2008): Cortical alpha-synuclein load is associated with amyloid-beta plaque burden in a subset of Parkinson's disease patients. Acta Neuropathol 115:417–25.
22. Levy R, Dubois B (2006): Apathy and the functional anatomy of the prefrontal cortex-basal ganglia circuits. Cereb Cortex 16:916–28.
23. Litvan I, Aarsland D, Adler CH, Goldman JG, Kulisevsky J, Mollenhauer B, Rodriguez-Oroz MC, Tröster AI, Weintraub D (2011): MDS Task Force on mild cognitive impairment in Parkinson's disease: critical review of PD-MCI. Mov Disord 26:1814–24.
24. Litvan I, Goldman JG, Tröster AI, Schmand B a, Weintraub D, Petersen RC, Mollenhauer B, Adler CH, Marder K, Williams-Gray CH, Aarsland D, Kulisevsky J, Rodriguez-Oroz MC, Burn DJ, Barker R a, Emre M (2012): Diagnostic criteria for mild cognitive impairment in Parkinson's disease: Movement Disorder Society Task Force guidelines. Mov Disord 27:349–56.
25. Melzer TR, Watts R, MacAskill MR, Pitcher TL, Livingston L, Keenan RJ, Dalrymple-Alford JC, Anderson TJ (2013): White matter microstructure deteriorates across cognitive stages in Parkinson disease. Neurology 80:1841–9.
26. Menon V, Uddin LQ (2010): Saliency, switching, attention and control: a network model of insula function. Brain Struct Funct 214:655–67.
27. Mogenson GJ, Jones DL, Yim CHIYIU (1980): From motivation to action: functional interface between the limbic system and the motor system. Prog Neurobiol 14:69–97.

28. Orimo S, Amino T, Itoh Y, Takahashi A, Kojo T, Uchihara T, Tsuchiya K, Mori F, Wakabayashi K, Takahashi H (2005): Cardiac sympathetic denervation precedes neuronal loss in the sympathetic ganglia in Lewy body disease. Acta Neuropathol 109:583–8.
29. Orimo S, Uchihara T, Nakamura A, Mori F, Kakita A, Wakabayashi K, Takahashi H (2008): Axonal alpha-synuclein aggregates herald centripetal degeneration of cardiac sympathetic nerve in Parkinson's disease. Brain 131:642–50.
30. Pereira JB, Junqué C, Bartrés-Faz D, Ramírez-Ruiz B, Marti M-J, Tolosa E (2013): Regional vulnerability of hippocampal subfields and memory deficits in Parkinson's disease. Hippocampus 23:720–8.
31. Pereira JB, Svenningsson P, Weintraub D, Brønnick K, Lebedev A, Westman E, Aarsland D (2014): Initial cognitive decline is associated with cortical thinning in early Parkinson disease. Neurology 82:2017–25.
32. Pessiglione M, Schmidt L, Draganski B, Kalisch R, Lau H, Dolan RJ, Frith CD (2007): How the brain translates money into force: a neuroimaging study of subliminal motivation. Science 316:904–6.
33. Sadaghiani S, D'Esposito M (2014): Functional Characterization of the Cingulo-Opercular Network in the Maintenance of Tonic Alertness. Cereb Cortex.
34. Sadaghiani S, Scheeringa R, Lehongre K, Morillon B, Giraud A-L, D'Esposito M, Kleinschmidt A (2012): α-band phase synchrony is related to activity in the fronto-parietal adaptive control network. J Neurosci 32:14305–10.
35. Sala-Llonch R, Junqué C, Arenaza-Urquijo EM, Vidal-Piñeiro D, Valls-Pedret C, Palacios EM, Domènech S, Salvà A, Bargalló N, Bartrés-Faz D (2014): Changes in whole-brain functional networks and memory performance in aging. Neurobiol Aging 35:2193–202.
36. Seeley WW, Menon V, Schatzberg AF, Keller J, Glover GH, Kenna H, Reiss AL, Greicius MD (2007): Dissociable intrinsic connectivity networks for salience processing and executive control. J Neurosci 27:2349–56.
37. Sinha N, Manohar S, Husain M (2013): Impulsivity and apathy in Parkinson's disease. J Neuropsychol 7:255–83.
38. Spreng RN, Sepulcre J, Turner GR, Stevens WD, Schacter DL (2013): Intrinsic architecture underlying the relations among the default, dorsal attention, and frontoparietal control networks of the human brain. J Cogn Neurosci 25:74–86.
39. Spreng RN, Stevens WD, Chamberlain JP, Gilmore AW, Schacter DL (2010): Default network activity, coupled with the frontoparietal control network, supports goal-directed cognition. Neuroimage 53:303–17.
40. Tsuboi Y, Uchikado H, Dickson DW (2007): Neuropathology of Parkinson's disease dementia and dementia with Lewy bodies with reference to striatal pathology. Parkinsonism Relat Disord 13 Suppl 3:S221–4.
41. Weintraub D, Doshi J, Koka D, Davatzikos C, Siderowf AD, Duda JE, Wolk DA, Moberg PJ, Xie SX, Clark CM (2011): Neurodegeneration across stages of cognitive decline in Parkinson disease. Arch Neurol 68:1562–1568.
42. Williams-Gray CH, Evans JR, Goris A, Foltynie T, Ban M, Robbins TW, Brayne C, Kolachana BS, Weinberger DR, Sawcer SJ, Barker RA (2009): The distinct cognitive syndromes of Parkinson's disease: 5 year follow-up of the CamPaIGN cohort. Brain 132:2958–2969.
43. Williams-Gray CH, Foltynie T, Brayne CEG, Robbins TW, Barker R a (2007): Evolution of cognitive dysfunction in an incident Parkinson's disease cohort. Brain 130:1787–9

chapter 6
CONCLUSIONS

Through the combined analysis of the studies included in this thesis, we can conclude that:

1. Parkinson's disease patients with mild cognitive impairment have altered patterns of resting-state functional connectivity mainly characterized by the weakening of long-range connections and, to a lesser degree, local connectivity increases.

2. Parkinson's disease patients with mild cognitive impairment have structural (gray matter atrophy) and functional changes in posterior cortical regions, associated with the presence of visuospatial/visuoperceptual deficits. These regions show reduced long-range connectivity with anterior brain regions; among such posterior regions, parieto-occipital nodes of the dorsal attention network have reduced connectivity with anterior task-positive nodes and lose their normal pattern of anticorrelation with the default mode network.

3. Parkinson's disease patients with mild cognitive impairment have reduced resting-state functional connectivity between the dorsal attention network and the right anterior insula and adjacent frontal regions. This reduced connectivity is not associated with gray matter atrophy and is accompanied by attention/executive deficits.

4. Parkinson's disease patients with mild cognitive impairment display altered global and local graph-theory parameters. Globally, functional brain networks display higher modularity, *small-worldness* and a tendency to form clusters. These changes, which may reflect network reorganization in response to the loss of long-range connections or a primary mechanism of abnormal plasticity, also correlate with visuospatial/visuoperceptual and memory deficits.

5. At the local level, Parkinson's disease patients with mild cognitive impairment display a reorganization of the hub structure; brain hubs become less central in the resting-state functional network.

6. The presence of apathy in Parkinson's disease is associated with resting-state connectivity reductions involving frontostriatal circuits. The mainly-affected connections are those involving the ventral striatum and the orbitofrontal cortex in the left hemisphere.

7. Parkinson's disease patients frequently have deficits in the identification of facial emotions, specifically negative ones. Impaired identification of sadness is associated with white-matter microstructural changes involving long-range association tracts, suggesting that structural disconnection is involved in cognitive deficits in Parkinson's disease. Atrophy of gray matter structures involved in emotion processing in medial temporal, allocortical and neocortical regions is also involved in facial emotion recognition deficits.

8. Early-stage Parkinson's disease patients have progressive functional connectivity changes in the recognition-memory network, characterized by reduced frontoparietal connectivity and preservation of frontofrontal connections.

9. Detectable progressive gray matter atrophy occurs in the early stages of Parkinson's disease, even before the onset of overt clinical manifestations of cognitive decline.

In summary, we have found strong evidence that different types of cognitive decline in Parkinson's disease are associated with different patterns of resting-state functional connectivity, structural connectivity and gray matter structural changes involving distinct neural systems. Different techniques and different conceptual frameworks can provide useful information in the characterization of the neural bases of cognitive deficits associated with Parkinson's disease.

chapter 7
CONCLUSIONS (CATALÀ)

L'anàlisi conjunta dels estudis inclosos en aquesta tesi ens permet concloure que:

1. Els pacients amb malaltia de Parkinson i deteriorament cognitiu lleu tenen patrons alterats de la connectivitat funcional en repòs, caracteritzats predominantment per l'afebliment de connexions de llarga distància i, en menor grau, pel reforçament de connexions locals.

2. Els pacients amb malaltia de Parkinson i deteriorament cognitiu lleu tenen alteracions estructurals (atròfia de la substància grisa) i funcionals en regions corticals posteriors, associades a la presència de dèficits visuoespacials/visuoperceptius. Aquestes regions presenten una reducció de la connectivitat amb regions cerebrals anteriors. Es troben nodes parieto-occipitals de la xarxa dorsal de l'atenció que presenten reduccions de connectivitat amb nodes anteriors de les xarxes de l'atenció dorsal i frontoparietal, i perden el patró normal d'anticorrelació amb la *default mode network.*

3. Els pacients amb malaltia de Parkinson i deteriorament cognitiu lleu presenten reducció en la connectivitat funcional en repòs entre la xarxa dorsal de l'atenció i l'ínsula anterior i regions frontal adjacents en el hemisferi dret. Aquestes pèrdues de connectivitat no estan relacionades amb atròfia de la substància grisa, i s'acompanyen de dèficits d'atenció/executius.

4. Els pacients amb malaltia de Parkinson i deteriorament cognitiu lleu presenten alteracions dels paràmetres globals i locals de la teoria de grafs. A nivell global, les xarxes cerebrals funcionals tenen augments de modularitat, *small-worldness* i tendència d'organitzar-se en *clústers*. Aquestes alteracions, que poden reflectir una reorganització de la xarxa com a resposta a la pèrdua de connectivitat de llarg abast o a un procés primari de plasticitat anormal, es relacionen amb dèficits de memòria i visuoespacials/visuoperceptius.

5. A nivell local, els pacients amb malaltia de Parkinson i deteriorament cognitiu lleu presenten una reorganització de l'estructura dels nodes centrals (els anomenats *hubs*) de les xarxes cerebrals funcionals; els *hubs* es converteixen en nodes menys centrals en les xarxes cerebrals funcionals en repòs.

6. La presència d'apatia en la malaltia de Parkinson està associada a reduccions de connectivitat en repòs en circuits fronto-estriats. Les connexions més afectades son les que involucren l'estriat ventral i l'escorça prefrontal orbitofrontal de l'hemisferi dret.

7. Els malalts de Parkinson freqüentment presenten dèficits d'identificació d'emocions en expressions facials, sobretot d'emocions negatives. Els dèficits d'identificació de tristesa s'acompanyen d'alteracions de la microestructura de la substància blanca en tractes associatius llargs, la qual cosa suggereix que la desconnexió estructural està involucrada en l'ocurrència de dèficits cognitius en la malaltia de Parkinson. L'atròfia d'estructures de substància grisa relacionades amb el processament emocional en regions temporals medials, allocorticals i neocorticals també està involucrada en els dèficits de reconeixement d'emocions.

8. Els pacients amb malaltia de Parkinson inicial presenten canvis progressius de connectivitat funcional en la xarxa de memòria de reconeixement, que estan caracteritzats per la reducció de la connectivitat frontoparietal i la preservació de les connexions frontofrontals.

9. En les fases inicials de la malaltia de Parkinson, fins i tot abans de l'existència de manifestacions clíniques evidents de deteriorament cognitiu, es pot detectar l'atròfia progressiva de la substància grisa.

En resum, els estudis inclosos en aquesta tesi posen en evidència que els diferents tipus de dèficit cognitiu en la malaltia de Parkinson estan associats a disfuncions en els patrons de connectivitat funcional en repòs, connectivitat estructural i d'alteracions de la substància grisa, que impliquen diferents sistemes neurals. L'ús de distintes tècniques i diferents marcs conceptuals poden proporcionar informació útil per a la caracterització de les bases neurals dels dèficits cognitius, neuropsiquiàtrics i emocionals associats a la malaltia de Parkinson.

chapter 8
ABSTRACT

Parkinson's disease is a neurodegenerative process with several motor and non-motor manifestations. Among non-motor symptoms, cognitive decline is a major cause of disability, and its neural bases are poorly understood. In recent years, multimodal neuroimaging techniques have proven to be useful tools in the investigation of the bases of cognitive impairment related to neurological diseases. The objective of this thesis was to evaluate the neuroimaging substrates of Parkinson's disease-related cognitive and neuropsychiatric manifestations through a network approach, using state-of-the art magnetic resonance imaging techniques to assess associated connectivity and structural changes.

In this work, two samples of Parkinson's disease patients and healthy controls underwent neuropsychological evaluation as well as structural and functional magnetic resonance imaging. One of these samples included 121 Parkinson's disease patients and 49 healthy controls. The data obtained were used in 2 studies addressing the resting-state functional connectivity changes associated with mild cognitive impairment in Parkinson's disease; one using a graph-theory approach, and the second assessing large-scale intrinsic connectivity networks through an independent-component analysis/dual regression approach. A third was performed to assess connectivity disruptions in frontostriatal circuits associated with the presence of apathy in Parkinson's disease. And a fourth study was made assessing cortical thickness changes associated with the presence of mild cognitive impairment in Parkinson's disease. The second sample included the longitudinal evaluation of 17 Parkinson's disease patients and 15 healthy controls, and the data obtained resulted in two studies regarding progressive cortical thickness and subcortical volumes in early-stage Parkinson's disease patients. A seventh study, using subjects from both samples, was performed to evaluate microstructural white matter changes (using diffusion tensor imaging) and gray matter changes (through voxel-based morphometry) related to the presence of facial emotion recognition deficits in Parkinson's disease.

We have found that a high percentage of Parkinson's disease patients had mild cognitive impairment. These patients showed altered patterns of resting-state functional connectivity characterized by the loss of long range connections and strengthening of local connectivity. From a graph-theory perspective, these changes translated as increased small-world coefficients, modularity and clustering coefficients, which correlated with visuospatial/visuoperceptual and memory performance. The study of large-scale networks showed that patients with mild cognitive impairment had reduced connectivity between the dorsal attention network and the right frontoinsular region, and that this reduction was associated with attention/executive deficits. Additionally, parieto-occipital regions that

belong to the dorsal attention network showed reduced connectivity with anterior task-positive regions and loss of the normal anticorrelated pattern with the default mode network; furthermore, these posterior regions showed structural degeneration. Finally, these posterior structural and functional changes were associated with the presence of visuospatial/visuoperceptual deficits. The analysis of Parkinson's disease patients with mild cognitive impairment revealed a pattern of cortical thinning predominating in parieto-occipito-temporal regions.

The longitudinal analysis of progressive structural changes in early Parkinson's disease revealed that these patients had more marked cortical thinning in frontotemporal regions, even before the onset of clinically evident cognitive manifestations. The functional analysis of a recognition memory network likewise showed signs of progressive connectivity changes without overt clinical deterioration.

We conclude that different types of cognitive decline in Parkinson's disease are associated with different patterns of resting-state functional connectivity, structural connectivity and GM structural changes involving distinct neural systems. Different techniques and different conceptual frameworks can provide useful information in the characterization of the neural bases of cognitive deficits associated with Parkinson's disease.

chapter 9
RESUM (CATALÀ)

La malaltia de Parkinson és un procés neurodegeneratiu que té diverses manifestacions motores i no motores. Entre les manifestacions no motores, el deteriorament cognitiu és una causa important i comú de discapacitat; al cap de 20 anys des de l'inici de la malaltia, més de 80% dels pacients desenvolupen demència. Tot i tenir una alta prevalença i representar un factor de pèrdua de qualitat de vida tant pels pacients com per als seus cuidadors, les bases neurals d'aquestes alteracions són poc conegudes. En els últims anys, les tècniques d'imatge multimodals han demostrat ser útils en la investigació de les bases dels dèficits cognitius associats a les malalties neurològiques, i alguns estudis previs han trobat alteracions cerebrals tant estructurals com funcionals en subjectes amb la malaltia de Parkinson.

D'altra banda, el concepte de *deteriorament cognitiu lleu* (DCL), utilitzat per definir la presència d'un rendiment cognitiu inferior al esperat segons l'edat i el nivell educatiu – i un major risc de desenvolupament de demència – s'ha començat a aplicar en el context de la malaltia de Parkinson. A més, en estudis epidemiològics s'ha vist que la presència d'alguns tipus d'alteració cognitiva – concretament, aquells que tenen substrats neurals predominants en regions corticals posteriors, com són dèficits visuoespacials i visuoperceptius – indiquen una major probabilitat de desenvolupar demència. Al contrari, en els dèficits relacionats amb els desequilibris en la neurotransmissió dopaminèrgica (com són els dèficits d'atenció i executius), no s'ha trobat que siguin marcadors de pitjor pronòstic cognitiu.

L'objectiu d'aquesta tesi va ser avaluar els substrats neuroanatòmics i neurofuncionals de les diferents alteracions cognitives i neuropsiquiàtriques relacionades amb la malaltia de Parkinson mitjançant un abordatge de xarxes, tot utilitzant tècniques avançades de ressonància magnètica per estudiar les disfuncions de la connectivitat cerebral.

En aquesta tesi, es van utilitzar dues mostres de pacients amb malaltia de Parkinson i subjectes sans que es van sotmetre a avaluació neuropsicològica i de ressonància magnètica funcional i estructural. La primera d'aquestes mostres va incloure 121 malalts de Parkinson i 49 controls sans. Les dades obtingudes amb aquesta mostra han sigut utilitzades en cinc estudis (*estudis 1, 2, 3, 4* i *5*), tres dels quals van abordar la connectivitat funcional cerebral en repòs i les alteracions estructurals associats a la presència de DCL. Per definir la presència de DCL, en dos estudis (*estudis 1* i *2*) s'han avaluat els dèficits en tres dominis cognitius (atenció/funcions executives, memòria i funcions visuoespacials/visuoperceptives); en l'altre estudi (*estudi 3*), s'ha utilitzat un mètode de classificació d'acord amb les recents directrius proposades per la *Movement Disorder Society Task Force*, que consideren el

rendiment en cinc dominis (atenció/memòria de treball, funcions executives, memòria, llenguatge i funcions visuoespacials/visuoperceptives).

En els *estudis 1* i *2*, es van avaluar 66 pacients i 36 controls utilitzant tècniques d'avaluació de la connectivitat cerebral en repòs i les alteracions corresponents associats a la presència de DCL. Trenta cinc per cent dels pacients amb malaltia de Parkinson van complir criteris de DCL.

Estudi 1: En aquest estudi, s'ha aplicat un abordatge de teoria de grafs per avaluar les alteracions globals de connectivitat. Per tal de reconstruir les xarxes cerebrals, la substància grisa cortical i subcortical s'ha dividit en 90 regions definides amb l'atles *Automated Anatomical Labelling*. Posteriorment, s'ha calculat la correlació temporal de l'activitat entre cada parell de regions, obtenint-se així una matriu representativa de la connectivitat funcional de tot el cervell. En un primer pas, s'han comparat directament aquestes matrius de correlació per tal d'avaluar el patró de reducció o augment de connectivitat en els diferents subgrups de pacients. Aquest anàlisi va revelar que els pacients amb DCL tenien reduccions de connectivitat, sobretot afectant les connexions interlobulars de llarga distància, així com alguns augments de connectivitat, sobretot en connexions més curtes. Posteriorment, s'han utilitzat les matrius de correlació per calcular mesures globals i regionals de teoria de grafs. Concretament, s'han avaluat paràmetres que mesuren la integració (l'eficiència d'intercanvi d'informació entre distintes àrees cerebrals): el *characteristic path length* i l'*eficiència global*; i paràmetres de segregació, que mesuren la interconnectivitat local: el *clustering coefficient* i l'*eficiència local*. També s'ha avaluat el grau de *modularitat* de les xarxes cerebrals, és a dir, quant de bé aquestes xarxes es podien dividir en mòduls o comunitats de nodes densament interconnectats, amb poques connexions entre diferents mòduls. S'ha observat que els pacients amb DCL presentaven augments en les mesures de segregació i de modularitat. Les anàlisis de correlació han revelat que aquestes mesures es correlacionaven amb el rendiment en funcions visuoespacials/visuoperceptives i de memòria. En l'anàlisi de les mesures de *centralitat* dels nodes – és a dir, la importància que tenen en el tràfic d'informació dins de la xarxa –, s'ha observat que els nodes que solen ser més centrals en subjectes sans (els anomenats *hubs* cerebrals) perden centralitat en els pacients amb malaltia de Parkinson. Aquest resultat indica una reorganització d'aquestes xarxes caracteritzat per un augment del flux d'informació neural a través de nodes que en subjectes sans són menys rellevants.

Aquest estudi es va publicar a la revista *Human Brain Mapping* a l'any 2014 (*Cognitive impairment and resting-state network connectivity in Parkinson's disease*).

Estudi 2: s'ha utilitzat la mateixa mostra que en l'*estudi 1*. S'ha utilitzat, però, un altre tipus d'anàlisi amb l'objectiu d'estudiar els patrons de connectivitat dins d'un conjunt de xarxes cerebrals que, segons estudis previs, tenen un paper rellevant en els processos cognitius: la *default mode network*, la xarxa dorsal de l'atenció i la xarxa frontoparietal. Inicialment, s'ha realitzat un anàlisi de components independents amb les dades de ressonància magnètica

funcional en repòs per tal d'identificar les xarxes d'interès a nivell grupal. Posteriorment, s'ha utilitzat la tècnica de *dual regression* per identificar les mateixes xarxes a nivell individual, i que permet comparacions entre els grups. En aquesta anàlisi, s'ha observat que els pacients amb DCL presentaven reduccions de connectivitat entre la xarxa dorsal de l'atenció i l'ínsula anterior i regions adjacents del lòbul frontal dret. En el grup de pacients, el nivell de connectivitat en aquestes regions es correlacionava amb el rendiment en el domini d'atenció/executiu. A més, s'ha vist que els pacients amb DCL presentaven un augment de connectivitat entre extenses àrees parieto-occipitals i la *default mode network*; aquestes disfuncions de connectivitat també estaven associats a pitjor rendiment cognitiu, però en aquest cas en el domini visuoespacial/visuoperceptiu. Com anàlisi addicional per definir les alteracions locals de connectivitat, es va realitzar una avaluació de les connexions entre els nodes individuals de les xarxes d'interès; per definir aquests nodes, s'han seleccionat a priori les coordenades disponibles en un estudi de referència. Aquesta anàlisi ha demostrat que els augments de connectivitat de regions corticals posteriors amb la *default mode network* en realitat estaven caracteritzats per una pèrdua del patró normal d'anticorrelació amb aquesta xarxa observat en controls sans. A més, s'ha vist que aquestes mateixes regions tenien menys connectivitat amb les altres xarxes avaluades. Finalment, s'han realitzat anàlisis complementaris per avaluar la presència de degeneració estructural de la substància grisa que pogués estar associada a les alteracions funcionals observades. L'anàlisi del gruix cortical va revelar la presència de reduccions en els pacients amb DCL en regions parieto-occipitals; aquestes reduccions estaven associades a les alteracions de connectivitat de la *default mode network* i amb el rendiment visuoespacial/visuoperceptiu.

Aquest estudi es va publicar a la revista *Human Brain Mapping* a l'any 2014 (*Functional brain networks and cognitive deficits in Parkinson's disease*).

Estudi 5: En el tercer estudi en que es va avaluar la connectivitat funcional en repòs, l'objectiu va ser investigar les alteracions en els circuits fronto-estriats en la malaltia de Parkinson amb apatia – un trastorn neuropsiquiàtric molt freqüent en pacients amb aquesta malaltia. Amb aquesta finalitat, es va utilitzar la mateixa mostra que en els dos primers estudis. Es van classificat els subjectes en apàtics o no-apàtics segons la puntuació en l'escala d'apatia de Starkstein. A més, es va tenir en compte la presència de trastorns depressius, que, a més de tenir una alta prevalença en la malaltia de Parkinson, freqüentment coexisteixen amb l'apatia i tenen manifestacions que s'hi solapen. Així doncs, també es va aplicar l'escala de depressió de Beck; la puntuació en els 11 ítems d'aquesta escala que representen els símptomes disfòrics, més específics de la depressió, es va utilitzar com a covariable en totes les anàlisis. Per a realitzar l'anàlisi de connectivitat funcional, es va parcel·lar l'estriat en 3 regions – límbica, executiva i sensorimotora. Així mateix, es va parcel·lar l'escorça frontal en 4 regions – límbica, executiva, rostral motora i caudal motora. Vint pacients (41%) es van classificar com apàtics (puntuació > 13 en l'escala d'apatia). L'anàlisi de connectivitat va revelar que la presència d'apatia estava acompanyada de reduccions, que principalment afectaven les

regions límbiques tant del estriat com de l'escorça prefrontal. Per tal d'avaluar si aquestes alteracions s'acompanyaven de degeneració de les estructures avaluades, es van realitzar anàlisis addicionals amb *voxel-based morphometry* de les estructures corticals i subcorticals, a més de volumetria i *shape analysis* dels nuclis del estriat. No s'han obtingut resultats significatius amb cap d'aquests abordatges.

Aquest estudi està actualment en revisió en una revista indexada.

Estudi 3: En aquest estudi, 90 pacients i 32 controls van ser estudiats mitjançant tècniques d'avaluació del gruix cortical. Trenta dos (52%) pacients van complir criteris de DCL. S'ha observat que el grup de pacients amb DCL presentava reduccions del gruix cortical en regions parieto-temporals, així com augment en mesures d'atròfia global tals com reducció del gruix cortical global i del volum de substància grisa, així com augment del volum ventricular. Les anàlisis de correlació van revelar que el rendiment en totes les proves neuropsicològiques estava associat a la pèrdua de gruix cortical posterior.

Aquest estudi es va publicar a la revista *Movement Disorders* a l'any 2014 (*Cortical thinning associated with mild cognitive impairment in Parkinson's disease*).

Per a la segona mostra de subjectes, es van reclutar 24 pacients amb malaltia de Parkinson inicial i 24 controls sans, els quals es van estudiar mitjançant ressonància magnètica estructural i funcional així com mitjançant exploració neuropsicològica. Disset pacients i 15 controls van ser avaluats longitudinalment, amb una segona avaluació després d'un seguiment mitjà de 35,5 mesos.

Estudi 6: En el primer estudi fet amb aquesta mostra, es van incloure 17 pacients i 13 controls, i l'objectiu va ser estudiar la xarxa de memòria de reconeixement. Per això, es va utilitzar una seqüència de ressonància magnètica funcional amb un paradigma de memòria de reconeixement que consistia en intentar reconèixer les 35 paraules prèviament apreses entre una llista de 70 paraules. Les dades obtingudes van ser avaluades a través de abordatges convencionals o *model-based*, així com a través de tècniques *model-free* (anàlisi de components independents). En la primera anàlisi, es va identificar el patró d'activació associat a la tasca. En l'anàlisi de components independents, també es van identificar els components associats a la tasca; les principals regions activades en la component més associada a la tasca es van utilitzar com a regions d'interès en un anàlisi subsegüent de canvis progressius de connectivitat. Es va trobar una correlació entre la activació de la component independent més associada a la tasca i el rendiment de memòria de reconeixement dels pacients. A més, l'avaluació longitudinal va revelar canvis progressius en la connectivitat entre els principals nodes d'aquesta xarxa, caracteritzats per la pèrdua de connectivitat entre regions frontoparietals i la preservació de la connectivitat frontofrontal (que en els controls sans s'havia reduït).

Aquest estudi es va publicar a la revista *Journal of Neurology, Neurosurgery and Psychiatry* a l'any 2013 (*Progressive changes in a recognition memory network in Parkinson's disease*).

Estudi 7: En aquest segon estudi fet amb la segona mostra, s'ha volgut analitzar el patró d'atròfia progressiva de la substància grisa en la malaltia de Parkinson inicial i la seva relació amb canvis neuropsicològics. Amb aquesta finalitat, les dades de setze pacients i 15 controls van ser avaluades amb tècniques de gruix cortical, volum de substància grisa a través de *voxel-based morphometry* i volumetria cortical i subcortical. Es van trobar reduccions progressives del gruix cortical en regions frontotemporals bilaterals. L'avaluació neuropsicològica va revelar que els pacients tenien pitjor rendiment en proves d'atenció i de velocitat psicomotora, però aquestes variables no es correlacionaven amb els canvis corticals.

Aquest estudi es va publicar a la revista *Movement Disorders* a l'any 2012 (*Progression of cortical thinning in early Parkinson's disease*).

Un últim estudi (*estudi 4*) es va realitzar amb subjectes de la primera i de la segona mostra. Es va seleccionar una submostra de 39 pacients i 23 controls amb la finalitat d'avaluar les alteracions de les substàncies blanca i grisa associats als dèficits de reconeixement d'emocions facials en la malaltia de Parkinson. Es van utilitzar imatges potenciades en difusió per l'estudi d'alteracions microestructurals de la substància blanca en els tractes llargs que connecten les estructures cerebrals involucrades en el processament emocional, mitjançant tècniques de imatge per tensor de difusió. A més, les imatges estructurals es van avaluar a través de *voxel-based morphometry* per estudiar les alteracions de volum de la substància grisa en les estructures cerebrals prèviament descrites com rellevants pel processament d'emocions. El rendiment en el reconeixement d'emocions facials es va mesurar mitjançant la prova d'Ekman. Els pacients amb la malaltia de Parkinson van obtenir un rendiment inferior als controls en la identificació de les emocions negatives (tristesa, ràbia, por i fàstic). L'anàlisi de correlacions va revelar que els dèficits d'identificació de tristesa correlacionaven amb els valors d'anisotropia fraccional – un paràmetre de la microestructura de la substància blanca – sobretot en el fascicle fronto-occipital inferior dret. L'anàlisi de substància grisa, per contra, va revelar que la identificació de tristesa correlacionava amb el volum de l'escorça orbitofrontal dreta, amígdala i gir postcentral; la identificació de ràbia correlacionava amb el volum de substància grisa de l'estriat ventral, escorça infragenual i gir fusiform occipital dret; i la identificació de fàstic correlacionava amb volum de substància grisa en el còrtex cingulat anterior.

Aquest estudi es va publicar a la revista *Neuropsychologia* a l'any 2012 (*Structural correlates of facial emotion recognition deficits in Parkinson's disease patients*).

Tots aquests estudis ens permeten concloure que un alt percentatge de pacients amb malaltia de Parkinson tenen alteracions cognitives i compleixen criteris de DCL. L'anàlisi de neuroimatge mitjançant diferents estratègies demostra que la presència de DCL en la malaltia

de Parkinson s'acompanya d'alteracions estructurals i funcionals. A més, diferents tipus de dèficit cognitiu es relacionen amb diferents patrons d'alteració. A nivell de connectivitat funcional en repòs, els pacients amb malaltia de Parkinson amb DCL presenten un patró predominant de reducció de connectivitat de llarg abast i augment de la connectivitat local, que es tradueix en un augment del caràcter modular i de segregació de les xarxes cerebrals. Així mateix, s'observa una reducció de connectivitat de components de xarxes de connectivitat intrínseca rellevants per al processament cognitiu, que es caracteritza per una reducció de connectivitat d'una xarxa involucrada en processos de l'atenció (xarxa dorsal de l'atenció) i la regió insular anterior dreta. Al mateix temps, s'observa una reducció de connectivitat de regions corticals posteriors amb regions cerebrals anteriors, que s'associa a atròfia cortical posterior i a la presència de dèficits en les funcions visuoespacials/visuoperceptives.

L'anàlisi de la connectivitat funcional en repòs revela també que la presència d'apatia en la malaltia de Parkinson s'acompanya de reduccions en circuits fronto-estriats, que sobretot afecten els components del sistema de recompensa, és a dir, l'estriat ventral i l'escorça orbitofrontal. Els resultats de l'anàlisi d'alteracions microestructurals de la substància blanca associats al pitjor reconeixement d'emocions facials semblen indicar que els dèficits de connectivitat estructural també estan implicats en l'ocurrència dels dèficits cognitius en la malaltia de Parkinson.

Finalment, en pacients amb malaltia de Parkinson inicial, s'han aportat evidències sobre el poder dels mètodes de neuroimatge per a detectar alteracions estructurals (pèrdua de gruix neocortical) i funcional fins i tot abans de l'inici de símptomes cognitius clínicament evidents.

En conclusió, els resultats obtinguts en els diferents estudis d'aquesta tesi ens permeten concloure que distintes tècniques i diferents marcs conceptuals poden proporcionar informació útil per a la caracterització de les bases neurals dels dèficits cognitius i emocionals associats a la malaltia de Parkinson.